© Copyright 1994
Thomas Alexander Brown

Radiocarbon Dating of Pollen by Accelerator Mass Spectrometry

by

Thomas Alexander Brown

A dissertation submitted in partial fulfillment

of the requirements for the degree of

Doctor of Philosophy

University of Washington

1994

Approved by George W Farwell
(Chairperson of Supervisory Committee)

Linda B Buckler

Wm Stuiver

Program Authorized
to Offer Degree Geophysics Program

Date July 29, 1994

In presenting this dissertation in partial fulfillment of the requirements for the Doctoral degree at the University of Washington, I agree that the Library shall make its copies freely available for inspection. I further agree that extensive copying of this dissertation is allowable only for scholarly purposes, consistent with "fair use" as prescribed in the U. S. Copyright Law. Requests for copying or reproduction of this dissertation may be referred to University Microfilms, 1490 Eisenhower Place, P.O. Box 975, Ann Arbor, MI 48106, to whom the author has granted "the right to reproduce and sell (a) copies of the manuscript in microform and/or (b) printed copies of the manuscript made from microform."

Signature _____

Date July 2/1994

University of Washington

Abstract

Radiocarbon Dating of Pollen by Accelerator Mass Spectrometry

by Thomas Alexander Brown

Chairperson of the Supervisory Committee: Professor George W . Farwell
Department of Physics

The central goal of the research presented in this dissertation was the development of procedures and systems necessary to allow the extraction and accelerator mass spectrometry (AMS) ^{14}C dating of pollen from lake sediment and peat samples.

Modifications of the University of Washington AMS ^{14}C measurement system during this research resulted in several performance improvements: (1) preparation and measurement of reliable ~300 μg ion source targets, (2) development of an improved background correction for measured $^{14}C/^{13}C$ ratios, (3) reduction of the non-Poisson contribution to the observed scatter of unnormalized $^{14}C/^{13}C$ ratios to ≤0.3%, (4) elimination of any significant non-Poisson contribution to the observed scatter of normalized $^{14}C/^{13}C$ ratios, and (5) reduction of any systematic inaccuracies in the normalized $^{14}C/^{13}C$ ratios to ≤0.3%. These improvements allow ^{14}C ages of extracted pollen fractions to be routinely determined to ±40–70 year levels of accuracy and precision.

The pollen extraction procedure developed here includes an H_2SO_4 treatment to ensure the removal of cellulosic materials. Application of the procedure to lake sediment and peat cores shows that: (1) pollen fraction AMS ^{14}C dates are more accurate and reliable than traditional TOC ^{14}C dates, (2) Mazama Ash layer ^{14}C ages derived from lake sediment pollen fraction dates are accurate and reliable within the ±40–70 year uncertainties in the ^{14}C dates, (3) depositional/post-depositional processes can introduce biases into the ^{14}C ages of materials associated with an ash layer, (4) AMS ^{14}C dating of pollen fractions eliminates "hard water" dating errors, and (5) significant differences can exist between the ^{14}C ages of macrofossils and pollen within a sediment sample.

Results from the application of the pollen extraction and dating method to an Alaskan lake sediment core demonstrate that essentially pure spruce pollen fractions can be isolated from low-organic-content sediments. The ^{14}C dates obtained for 30<<88 μm pollen fractions allow the ^{14}C ages of the first establishment of white spruce, alder and black spruce in the Lake Minakokosa, Alaska area to be determined as 9.4 ± 0.2 ka BP, 8.5 ± 0.2 ka BP, and 5.4 ± 0.2 ka BP, respectively.

Table of Contents

		Page
List of Figures.		iii
List of Tables.		v
Chapter 1: Introduction.		1
1.1	Motivation for the Development of Pollen Extraction and AMS ^{14}C Dating.	1
1.2	^{14}C Dating of Bulk Lake Sediment and Peat Samples.	2
1.3	Accelerator Mass Spectrometry ^{14}C Dating.	7
1.4	Pollen Extraction and AMS ^{14}C Dating.	9
Chapter 2: The University of Washington Accelerator Mass Spectrometry System.		13
2.1	Overview.	13
2.2	The University of Washington Accelerator Mass Spectrometry System.	13
2.2.1	Preparation of samples.	13
2.2.2	Ion source and low energy section of the AMS ^{14}C system.	16
2.2.2.1	Components and operation.	16
2.2.2.2	System improvements.	17
2.2.3	Van de Graaff accelerator, high energy section of the AMS ^{14}C system, and ^{14}C detector.	20
2.2.3.1	Components and operation.	21
2.2.3.2	System improvements.	23
2.2.4	Operation of the AMS ^{14}C measurement system.	27
2.2.4.1	Typical operating conditions.	27
2.2.4.2	Primary data from our AMS ^{14}C measurements.	31
2.3	Calculation of ^{14}C ages from Experimental Data.	33
2.3.1	Correction of ^{14}C /^{13}C ratios for background contributions.	33
2.3.2	Calculation of ^{14}C ages from background-corrected ^{14}C /^{13}C ratios.	42
2.4	The Accuracy and Precision of Our AMS ^{14}C Measurements.	46
2.4.1	Reproducibility of the Chinese Sucrose Standard ^{14}C /^{13}C ratios.	48
2.4.2	Reproducibility of the unknown and secondary standard samples' ^{14}C /^{13}C ratios.	52
2.4.3	Accuracy of the ^{14}C measurements on secondary standards.	56
2.4.4	Summary of the accuracy and precision of our ^{14}C measurements.	61
2.4.5	Measurement background.	62
2.5	Summary.	69

Chapter 3: The Extraction and AMS ^{14}C Dating of Pollen. 120

3.1 Overview. 120
3.2 Pollen Extraction Method. 121
3.3 Mazama Ash Study: Validation of the Pollen Extraction Method. 127
3.3.1 Introduction. 127
3.3.2 Sampling sites, cores, and AMS ^{14}C dated samples. 134
3.3.3 Processing of prepared samples for AMS ^{14}C dating. 141
3.3.4 Results and discussion. 142
3.3.4.1 Internal consistency of the ^{14}C dates obtained from each core. 143
3.3.4.2 Bioturbation model. 156
3.3.4.3 Comparison of bioturbation model results to observed differences. 164
3.3.4.4 Summary of the results of the internal consistency analyses. 167
3.3.4.5 Comparison to previous ^{14}C dating of the Mazama Ash layer. 169
3.3.4.6 Discussion of the ^{14}C dates obtained for the Crocker Lake samples. 186
3.3.5 Summary of the results obtained in the Mazama Ash study. 190
3.4 Lake Minakokosa Study. 194
3.4.1 Introduction. 194
3.4.2 Study site, cores, and AMS ^{14}C dated samples. 195
3.4.3 Results and discussion. 200
3.4.4 Alder Migration. 206
3.4.5 Spruce Migration. 209
3.4.6 Summary of the Lake Minakokosa study. 213
3.5 Summary of the Extraction and AMS ^{14}C Dating of Pollen. 215

Chapter 4: Conclusions. 268

List of References. 274

List of Figures

Number Page

2.1 The University of Washington AMS ^{14}C System. 73
2.2 The $^{14}C^{4+}$ and $^{13}C^{4+}$ Transmission Profiles. 77
2.3 A Cycle-by-cycle Data Set from a Typical Measurement (25Jan93Run60). 79
2.4 Offline Program Output from a Typical Measurement (25Jan93Run60). 81
2.5 Offline Program Output from an Atypical Measurement (25Jan93Run57). 83
2.6 Percent Difference as a Function of Sample ^{14}C Age. 89
2.7 Percent Difference as a Function of Sample Mass. 91
2.8 Percent Difference as a Function of Contaminant ^{14}C Content. 93
2.9 Measured ^{14}C /^{13}C Ratios for the 25Jan93 Chinese Sucrose Standard Targets. 95
2.10 Measured ^{14}C /^{13}C Ratios for the 05Oct92 Chinese Sucrose Standard Targets. 97
2.11 Target-Set-Averaged Ratios for the 25Jan93 Chinese Sucrose Standards. 99
2.12 Measured ^{14}C /^{13}C Ratios for the QL11658 Secondary Standard Targets. 107
2.13 Measured ^{14}C /^{13}C Ratios for the IAEA C6 Secondary Standard Targets. 111
3.1 Pollen Extraction Procedure. 219
3.2 Microphotographs of Mazama Ash Study >88 μm Fractions. 221
3.3 Microphotographs of Mazama Ash Study 44<<88 μm Fractions. 223
3.4 Microphotographs of Mazama Ash Study 20<<44 μm Fractions. 225
3.5 Microphotographs of Mazama Ash Study β-prep Samples. 227
3.6 Locations of Mazama Ash Study Sites in British Columbia and Washington. 229
3.7 Bioturbation Model: Age Versus Core Depth. 245
3.8 ^{14}C dates Obtained for Six of the Mazama Ash Study Cores. 247
3.9 Locations of Alaskan Study Sites. 249

3.10 Spruce, Birch and Alder Pollen Percentages for the Alaskan Cores. 251

3.11 Microphotographs of Lake Minakokosa 10 <<30 μm Fractions. 255

3.12 Microphotographs of LM1 10 <<30 μm and 30<<88 μm Fractions. 259

3.13 Microphotographs of Lake Minakokosa 30 <<88 μm Fractions. 261

3.14 ^{14}C Dates Obtained for the Lake Minakokosa Study Samples. 265

3.15 Microphotographs of Lake Minakokosa β-prep Samples. 267

List of Tables

Number Page

2.1 Typical Operating Conditions of the AMS ^{14}C System. 75

2.2 Formulae for the Calculation of Background-Corrected ^{14}C /^{13}C Ratios. 85

2.3 Measurement-Period-Averaged Chinese Sucrose ^{14}C /^{13}C Ratios. 101

2.4 Distributions of χ_ν^2 Values from Repeated Measurements of Samples. 103

2.5 Age-corrected $\Delta^{14}C$ Values Obtained for Secondary Standard QL1567. 105

2.6 ^{14}C ages obtained for Secondary Standard QL11658. 109

2.7 pMC Values Obtained for Secondary Standard IAEA C6. 113

2.8 pMC Values Obtained for Secondary Standard IAEA C5. 115

2.9 Results from Measurements of Background Samples. 117

2.10 Comparison of Corrections for Charge-exchanged $^{13}C^{4+}$ Background. 119

3.1 % Carbon Values and Other Data for the Mazama Ash Study Core Samples. 231

3.2 AMS ^{14}C Dates Obtained for Mazama Ash Study Sample Fractions. 237

3.3 Calculation of $^{C14}\Delta_{ex}$ Values and Comparison to Observed Differences. 239

3.4 Calculation of $^{Cal}\Delta_{ex}$ Values and Comparison to Observed Differences. 241

3.5 Comparison of $^{C14}\Delta_{ex}$, $^{Cal}\Delta_{ex}$, and $^{Biot}\Delta_{ex}$, and Calculation of Mazama Ages. 243

3.6 % Carbon Values and Other Data for Lake Minakokosa Study Samples. 253

3.7 AMS ^{14}C Dates Obtained for the Lake Minakokosa Study Sample Fractions. 263

Acknowledgements

I would like to thank George Farwell, my Ph.D. supervisor, for all of the time and effort he has devoted to the research in this dissertation, to the development of a reliable AMS ^{14}C system at the Nuclear Physics Laboratory that is capable of accurate and precise 0.5% (or better) measurements, and to seeing this dissertation finished. The advice, support, guidance and encouragement that George has provided over the years have helped me get through the Ph.D. process and over academic and personal hurdles that arose in the course of my studies at UW. I especially appreciate the tolerance George has displayed towards my pursuits of time-consuming (and occasionally unproductive) developmental work, and the freedom I have enjoyed to pursue ideas that were interesting to me (but, not always to George). I hope that George has derived as much satisfaction as I have from our group's development of the UW AMS system over the last years and the various earth sciences projects we have undertaken during that time.

I thank Piet Grootes for his contributions to the development and operation of the UW AMS system, for his calm and reasoned approach to science, for his patience with my sometimes impatient actions, and for the long nights he spent running the system during our measurement periods (which often allowed me to catch up on some badly needed sleep). I hope to have the opportunity to visit Piet's new AMS facility at Kiel and see how AMS ^{14}C is done with the "new and improved" HVEE tandetrons.

I would like to express my sadness that I am unable to thank Fred Schmidt in person for his contributions to the development of the UW AMS ^{14}C system, and to the results presented in this dissertation. I have great respect for the time and energy that Fred devoted to the UW AMS system, and for his efforts to develop an unusual measurement system with equipment that was not up to the task. I will remember Fred for his unceasing willingness to take time to answer questions, explain concepts, and teach, and for the wonderful variety of interests and ideas that always seemed to be a part of conversations with Fred.

I thank Minze Stuiver for allowing me to use the facilities of the Quaternary Isotope Laboratory, for providing most of the standard and secondary standard materials used in this research, and for the time he spent discussing ^{14}C systematics and answering the multitude of questions that I have asked.

I thank Linda Brubaker for having taken such an interest in the development and application of the pollen extraction methods, for providing the Crocker Lake samples which permitted one of the advantages of the pollen extraction method to be clearly demonstrated, and for having read

the drafts of this dissertation so thoroughly.

I would also like to thank Pat Anderson for providing the Lake Minakokosa core and her unpublished pollen data, and for many discussions concerning the Alaskan sites, palynology, and paleoecology.

I would like to express my appreciation of those of the UW NPL community who have supported the AMS program since its inception in the late 70's and during the period of my studies at UW. John Luke, Brian McLain, and Jeff Bierman have shown remarkable tolerance of a sometimes quirky officemate. Louis Geissel showed me the proper way to machine various pieces on mills and lathes, and in those cases in which real machining was required, demonstrated considerable wisdom by doing the machining himself. Greg Harper constantly offered reasonable approaches to solving the many problems encountered in trying to improve the AMS system, and almost all of his ideas probably would have worked if I had listened better. The support of the NPL accelerator, computers, and electronics provided by Carl Linder, Dick Seymour, Tim Van Wechel, Don Leach, Rod Stowell, and Mark Howe was much appreciated and the AMS program benefited greatly from their work, advice and expertise. The guidance in administrative matters provided by Maria Ramirez and Karin Hendrickson was much needed and greatly appreciated. I thank the director of the Nuclear Physics Laboratory, Derek Storm, for the support he has given to the AMS program in general (including the acquisition of the large diameter solid state detector), and to my studies in particular (including support of travel to conferences).

I thank Dave Balsley for helping me get started in the AMS program at NPL, for introducing me to his favorite Seattle haunts, for trying to introduce me to the cultural side of Seattle, for his support through some of the roughest months, and for his continued friendship.

I would like to thank Steve Porter and the Quaternary Research Center for making the fumehood, microscopes, and rooms required for the pollen extraction work available. I especially thank Terry Swanson for the opportunity to collect cores with him, and discuss various graduate student matters over beers at the end of long field days. I thank Travis Saling of the Quaternary Isotope Laboratory for graphitizing almost all of the samples measured during this research, and he and Paula Reimer for their help, advice and humour in dealing with Hg diffusion pumps, glass vacuum systems, and IBM clones (when I absolutely could not avoid it).

I thank the UW Geophysics Program for providing an ideal base for my earth sciences studies. With only minor exceptions, I found the environment, courses, and seminars of the program to be challenging and of exceptionally high quality. I thank John Booker for introducing me to the program, and Connie Wright for making me feel I had a home base in the program. I

would like to thank Von Walden for his friendship and company through most of the courses, the qualifying exam, and the following years of research.

I would like to thank Erle Nelson, John Southon, and John Vogel, with whom I did my M.Sc., for their efforts in the initial pollen extraction study (which we started while I was at SFU and finished after I had entered UW), for their continued interest in my research and the AMS activities at UW, and for their continued friendship. Together with Erle, John, and John, I would like to thank Jay Davis and Ivan Proctor for the opportunity to pursue post-doctoral research at the Center for AMS at the Lawrence Livermore National Laboratory.

Finally, I thank my family for their continued support through the many years of post-secondary education that I am now completing. I thank my mother, Juliet Brown, and my father, Samuel Alexander Brown, for the years of unquestioning support they have given me (probably while wondering if I would ever stop going to school). I thank my sister, Marj, and brother-in-law, Allan, for tolerating my frequent visits and helping me through the roughest periods of my Ph.D. studies (probably while thinking that even if he does finish, he will never get a job). I thank my brother, Dan, and sister-in-law, Vicki, who, though far away could always be reached on the phone.

And lastly, I thank my wife Catherine for her love, for her support, and for tolerating the hours I have been working with such calmness and grace. I hope this all seems worth it to you ten years from now.

Chapter 1: Introduction.

1.1 Motivation for the Development of Pollen Extraction and AMS ^{14}C Dating.

Studies of the variations of the Earth's climate over the last hundred thousand years have contributed to the development of our current knowledge of the forces and processes that determine the climatic conditions under which we presently live, and to the use of such knowledge in attempting to predict climatic changes that may occur in the future. In general, the paleoclimatic information produced in such studies is inferred from measurements of proxy-climate indicators that are related to particular components of the earth system and particular aspects of climate, and whose variations over time have been recorded in a suitable natural deposit (e.g., the various climate proxies discussed in Wright, 1983; Hansen and Takahashi, 1984; Sundquist and Broecker, 1985; Ruddiman and Wright, 1987; and Swart *et al.*, 1993).

The predominant proxy-climate indicator used in the reconstruction of continental paleoclimates has been pollen that was deposited and preserved in lake sediments and peat deposits. The records of local and regional vegetation that can be inferred from the study of pollen in such deposits provide information on the past variations of environmental conditions in the regions of the deposits, and much of the current knowledge of continental paleo-environments and climates has been derived from the combined reconstructions from numerous such palynological studies.

While the changes in the distributions of different pollen types (e.g., spruce, pine, alder, etc.) with depth in a deposit provide the basis for inferring past variations in climate and environment at the site of the deposit, the determination of the age at which a particular change occurred depends on the establishment of an independent, accurate and trustworthy chronology for the sedimentary record. Equally importantly, the establishment of an accurate and trustworthy chronology for each study site is necessary to allow the meaningful correlation of similar changes between records from different sites (e.g., regional deglaciations), to allow the detailed study of short duration/transitional events (e.g., the Younger Dryas event), and/or to allow distinctions to be made between environmental/vegetational changes that may be time-transgressive over a significant region (e.g., tree species migrations) as opposed to synchronous.

Radiocarbon dating has been, and remains, the predominant technique used in the establishment of chronologies for lake sediment and peat records in palynological studies of latest Pleistocene and Holocene environments and climates. The traditional, and currently ubiquitous, method used to obtain ^{14}C dates for sedimentary records involves the ^{14}C decay/β-counting of the total-organic-carbon (TOC) fraction from bulk lake sediment or peat samples.

While the majority of the ^{14}C dates obtained in the past using the TOC/β-counting ^{14}C dating method have been satisfactory for the purposes of the studies for which they were obtained, current palynological and paleoclimatological studies tend to emphasize the dynamics of rapid climate change and/or the patterns of environmental variations over large areas. These types of studies require higher degrees of accuracy and reliability in the ^{14}C dates used to establish the chronologies for the paleoclimatic records to ensure that the rates of climate change and/or the temporal patterns of environmental variation are not distorted by inaccurate chronologies. Unfortunately, numerous studies have demonstrated that ^{14}C dates obtained on the TOC fraction from bulk lake sediment and peat samples are subject to a variety of potential dating errors, which frequently raise significant questions concerning the accuracy and trustworthiness of the ^{14}C dates, and hence, of the chronologies being established for the sedimentary records.

The basic goal of the research undertaken for this dissertation was the development of procedures and measurement systems necessary to allow the isolation and accelerator mass spectrometry (AMS) ^{14}C dating of essentially pure pollen fractions from lake sediment and peat samples. These pollen extraction and dating methods were intended to allow the direct ^{14}C dating of the proxy-climate indicator used in palynological studies, and thereby, eliminate questions concerning the association of the materials being ^{14}C dated with the proxy-climate indicator, and eliminate the sources of potential dating errors that plague TOC ^{14}C dating of bulk lake sediment and peat samples. The pollen extraction procedures that have been developed are relatively simple and straightforward, and are appropriate for routine use by palynologists (and other paleoclimatologists) in studies involving lake sediment and peat samples. It is hoped that subsequent, routine application of these pollen extraction and ^{14}C dating methods in palynological studies will significantly improve the accuracy and reliability of ^{14}C dates that are routinely obtained for lake sediment and peat samples, and hence, will improve the accuracy and reliability of the chronologies that allow meaningful intercomparison of paleoclimate records obtained from different sites.

1.2 ^{14}C Dating of Bulk Lake Sediment and Peat Samples.

As implied above, one of the principal motivations for the development of the pollen extraction and AMS ^{14}C dating method was the existing evidence that there were a disturbing number of commonly-encountered causes of significant dating errors in ^{14}C dates obtained using the traditional TOC/β-counting methods for ^{14}C dating bulk lake sediment and peat samples. Some of these causes of error have been known since the earliest years of ^{14}C measurements

(e.g., Deevey *et al.*, 1954), and considerable effort has been expended in attempts to develop methodologies that would either eliminate or allow correction for such dating errors. Unfortunately, these efforts have not been successful, and inconsistencies and inaccuracies in ^{14}C dates obtained for bulk lake sediment and peat samples using the traditional TOC method are still routinely attributed to the same causes of dating errors (e.g., Brugam, 1978; Andree *et al.*, 1986; MacDonald *et al.*, 1987; Lowe *et al.*, 1988). Although a detailed discussion of the many potential causes of errors in TOC ^{14}C dates is beyond the scope of this introduction, the nature of several of these causes will be discussed briefly because they are the most commonly encountered, and because description of these causes here will facilitate later discussion of the impact of the pollen extraction methods on these causes of dating errors. (Succinct and relatively complete summaries of the many potential causes of dating errors encountered in attempting to obtain ^{14}C dates from lake sediment and peat samples have been given by MacDonald *et al.* (1991), and Hedges (1992).)

The most commonly cited cause of "erroneously" old ^{14}C dates obtained for bulk lake sediment samples by TOC ^{14}C dating is the "hard water" effect (Deevey *et al.*, 1954). The overall cause of this effect is the transfer of old (i.e., ^{14}C-depleted) carbon from geological carbonates into the sedimentary deposits. The "hard water" process under which this transfer occurs is basically as follows: (1) the dissolution of ^{14}C-depleted geological carbonates into ground waters causes the dissolved carbon species in the ground waters (carbonate, bicarbonate and carbon dioxide) to be depleted of ^{14}C relative to the prevailing atmosphere, (2) the movement of these ground waters into lakes or bogs causes the dissolved carbonate species in the waters of the lakes or bogs to also be depleted of ^{14}C, (3) the incorporation of the dissolved carbon species by aquatic plants leads to the aquatic plants' and animals' being depleted of ^{14}C, and finally, (4) the incorporation of the remains of these aquatic plants and animals into the sediment or peat causes freshly-deposited sedimentary material to be ^{14}C-depleted relative to the prevailing atmosphere (and relative to terrestrial plants and animals which grew at the same time but derived the carbon in their systems from sources related to atmospheric CO_2). In lakes and bogs that are subject to this "hard water" effect, the relative ^{14}C-depletion of the aquatic materials in the sediments can cause freshly-deposited sedimentary materials to have apparent ^{14}C ages of several hundred years (or, in some cases, as much as several thousand years) (e.g., Deevey and Stuiver 1964; Andree *et al.*, 1986; MacDonald *et al.*, 1987).

(The adjective "erroneously" has been used in quotes in the above because the designation of a particular ^{14}C date as an erroneously old (or young) date is often based on criteria that are,

at least in part, subjective; e.g., the "erroneous" date is the date that is inconsistent with dates obtained for other samples from the same lake sediment or peat core, or all of the dates obtained for a particular core are "erroneous" because they are inconsistent with previously established chronologies for paleoclimatic records from the region, or the date is "erroneous" because it is inconsistent with previously constructed theoretical frameworks. Unfortunately, since essentially all dates involved in paleoclimatic studies based on lake sediments or peats are ^{14}C dates obtained from TOC fractions, and since all of the TOC ^{14}C dates are subject to the same potential causes of dating errors, there is an aspect of circularity in the designation of particular ^{14}C dates, or sets of dates, as being "erroneous" based on the above criteria. In the following discussions, the term erroneous will be used to designate those ^{14}C dates that would be deemed to be "in error" based on the criteria described above, but the use of surrounding quotes will be curtailed.)

In the case of erroneously young ^{14}C dates obtained for bulk lake sediment and peat samples by TOC ^{14}C dating, the dating errors are often attributed to one of two common causes. For peats, erroneously young ^{14}C dates are commonly attributed to the effects of vertical penetration by roots from active growth layers at the surface into deeper and older peat layers below. The inclusion within the bulk peat samples used for TOC ^{14}C dating of the relatively young carbon brought into older peat layers by the root growth (either as intact root/rootlet components or as humic degradation products of the roots) implies that the ^{14}C dates obtained reflect the carbon contributions from both the originally-deposited, older peat and the younger root growth. Studies of this effect in peats suggest that, under some circumstances, the apparent ^{14}C ages of bulk peat samples including roots can be several hundred years younger than the ^{14}C ages of the sedimentary materials remaining after the removal of the roots (e.g., Tornqvist *et al.* (1992), and references therein).

For lake sediments, a more likely cause of erroneously young ^{14}C dates from TOC ^{14}C dating of bulk lake sediment samples appears to be the downward movement within the sediments of relatively mobile, organic humification products (e.g., humic and fulvic acids). This leads to the presence of organic compounds derived from the decay/humification of organic materials in relatively young sediments within sediments at greater depths, which contain immobile materials and compounds whose ^{14}C ages are somewhat older. Unusually young ^{14}C ages obtained in several studies of the close of the lateglacial period in Scotland have been attributed to this effect (Lowe and Walker (1980), and references therein). Unfortunately, as Hedges (1992) has pointed out, very little research effort has been devoted to ^{14}C studies of the different chemical fractions of lake sediments even though the dating of lake sediments is a

major activity in ^{14}C dating. In one of the very few studies in which the ^{14}C ages of various chemical fractions in lake sediment samples have been compared, Fowler *et al.* (1986) showed that in all six of the lakes and peat bogs they studied, age differences of several hundreds of years existed between various chemical fractions within their lake sediment and peat samples. While interpretation of the results obtained for all six of Fowler *et al.*'s lakes is not straightforward, the results suggest that the movement of organic compounds within the sediments and peats may, in some cases, be the cause of significant age differences between various chemical fractions within lake sediment and peats, and hence, is a potential cause of erroneously young TOC ^{14}C dates. (The movement of relatively mobile, organic humification products is also often cited as a cause of erroneously young ^{14}C dates obtained for peat samples by TOC ^{14}C dating.)

The final commonly-cited cause of erroneous TOC ^{14}C dates that will be discussed here is the incorporation of relatively old, reworked materials into the sediments at the time of deposition. The variety of reworked materials that have been invoked in various studies as causes of erroneous TOC ^{14}C dates is considerable, ranging from "unweathered glacial rock flour" (very fine, carbon-containing material eroded from rock by glacial action; e.g., Sutherland, 1980), to "inert carbonaceous geological materials such as graphite and coal" (which may be eroded from geological deposits; e.g., Olsson, 1979; Olsson, 1991), to "previously deposited microfossils and organic debris" (the presence of significant amounts of reworked pre-Quaternary organic debris in some sediments has been inferred from the presence of identifiable pre-Quaternary palynomorphs, e.g., Nambudiri *et al.*, 1980). In essentially all cases in which erroneous ^{14}C dates are attributed to reworked materials, either the ^{14}C age of the reworked materials or the fraction of the carbon in the TOC ^{14}C dating samples that was contributed by reworked materials cannot be determined with any certainty (in many cases neither can be determined). Hence, quantification of the ^{14}C dating errors caused by reworked materials is almost always impossible.

While the preceding discussion has centered on several examples of previously identified causes of significant dating errors in TOC ^{14}C dates, there are three other points concerning the traditional TOC/β-counting method for ^{14}C dating bulk lake sediment and peat samples that are related to the contamination issues that are the root of the causes of dating errors discussed above, and provide further arguments that TOC fractions from lake sediment and peat samples are far from ideal as sources of carbon for the establishment of chronologies in palynological studies by ^{14}C dating.

First, while ^{14}C dates can be obtained for bulk lake sediment and peat samples following the traditional TOC/β-counting ^{14}C dating method, the actual age of interest in paleoclimatological

studies is the age of the proxy-climate indicator from which paleoclimatic information is to be inferred. In the case of palynological studies, the ^{14}C age of true interest is that of the pollen in sediment or peat samples, not the ^{14}C age of the TOC fraction of the sediments or peats. The use of ^{14}C dates obtained on TOC fractions from bulk lake sediment or peat samples to establish a chronology for a pollen-based paleoclimatic record requires the assumption that the ^{14}C ages of the TOC fractions are representative of the ^{14}C ages of the pollen in the sediment samples. However, the great variety of compounds and materials that may be found in lake sediments and peats, and the evidence of significant differences among the ^{14}C ages of various fractions within sediment and peat samples discussed above, argue that the general validity of such an assumption is open to question.

In terms that are more commonly used in radiocarbon dating discussions, the questions concerning the validity of the assumption are essentially questions concerning the association of the material being ^{14}C dated with the event of interest in the study, i.e., the association of the TOC fractions with the ^{14}C age at which the climate signal provided by the proxy-climate indicator was recorded. Even though the physical association of the TOC fractions with the pollen is effectively unquestionable (since they can both be obtained from the same lake sediment or peat sample), the evidence of significant differences among the ^{14}C ages of various fractions within sediment and peat samples implies that there is considerable uncertainty in the association of the ^{14}C age of the carbon in the TOC fraction of a lake sediment or peat sample with the ^{14}C age of the pollen in the same sample.

Second, lake sediment and peat samples prepared for ^{14}C dating following the traditional TOC method invariably contain a great variety of compounds and materials, most of which are either unidentifiable (in any meaningful sense) or are identifiable only in terms of their present state (e.g., humic and/or fulvic acids), and not in terms of their state when they originally incorporated carbon. Hence, microscopic examinations of TOC fractions generally yield little useful information concerning the presence of contaminants in the TOC fractions (the only significant exception being the presence of undecomposed roots in peat samples), and generally do not provide a basis for meaningful discussions concerning potential causes or magnitudes of ^{14}C dating errors for particular TOC fractions.

Finally, as was noted above, several of the commonly-encountered causes of significant dating errors in ^{14}C dates obtained using the traditional TOC ^{14}C dating methods have been known (or suspected) since the earliest years of ^{14}C measurements. While there have been many efforts to develop methods that would either eliminate or allow correction for such dating errors, the potential methodologies that could be considered in these efforts were subject to one

particularly limiting requirement: the ~1 g of carbon sample size requirement for β-counting ^{14}C dating. This requirement precluded the development of highly specific sample preparation techniques that would isolate identifiable and particularly desirable, but tiny, fractions from lake sediment and/or peat samples. In general, the fact that the rejection of significant amounts of the carbon in the available lake sediment or peat samples would not leave sufficient carbon to allow ^{14}C dating has meant that sample preparation methods used in the β-counting ^{14}C dating of lake sediments and peats could not be particularly rigorous selection/isolation processes.

1.3 Accelerator Mass Spectrometry ^{14}C Dating.

In the late 1970's, the first experimental results were published showing that ^{14}C could be measured at natural abundance levels using tandem Van de Graaff accelerators as ultrasensitive mass spectrometers (Nelson *et al.*, 1977; Bennett *et al.*, 1977). In the years since those initial ^{14}C measurements, the AMS field has grown to encompass many isotopes, and to be utilized as a measurement technique in a great variety of research fields (see, for example, Gove *et al.*, 1987; Yiou and Raisbeck, 1990).

While a detailed discussion of AMS is beyond the scope of this introduction, the main feature of the technique in ^{14}C measurements is that the combination of several factors (e.g., the instability of negative nitrogen ions, the breakup of molecular ions in the two-stage acceleration process, the high mass-resolution of the accelerator systems, and the 10's of MeV energies of the ^{14}C ions after acceleration) allow the direct detection and counting of individual ^{14}C ions from samples. This direct detection of ^{14}C ions using AMS techniques increases the sensitivity of ^{14}C measurements by a factor of ~10^6 over that achieved in traditional β-counting ^{14}C methods, in which only those ^{14}C atoms which radioactively decay are detected and counted. While this increased sensitivity could, in theory, result in significant improvements in ^{14}C measurement precision (if various reproducibility difficulties could be overcome), in practice, the increased sensitivity has been used to decrease both the time taken for a ^{14}C measurement and the size of sample required for measurement.

In many fields of study, the decrease in the required sample size by about three orders of magnitude (from ~1 g of carbon for β-counting ^{14}C techniques to ~1 mg for AMS ^{14}C) has been the most significant effect of the development of AMS as a method for the measurement of ^{14}C in natural samples. This small-sample capability has been exploited to measure samples and study processes that would have been difficult (if not impossible) to measure or study using β-counting techniques. (Examples of such studies range from the dating of iron artifacts based on

the extraction of carbon that was incorporated during manufacture (Cresswell, 1992), to the determination of the ^{14}C age of last glacial deep waters through measurements of the ^{14}C contents of monospecific planktonic and benthic foraminifera samples (Shackleton *et al.*, 1988), to the measurement of surface exposure ages of terrestrial rocks through the extraction of ^{14}C produced *in situ* by cosmic ray interactions (Jull *et al.*, 1992).) In a few specific fields of research, highly-selective sample preparation techniques that were designed to isolate pure fractions of unambiguously identifiable materials from samples under study have been developed. (Two examples of such techniques are the isolation of specific tripeptides (van Klinken and Hedges, 1992) and of specific carbon atoms (Nelson, 1991) from the remnants of collagen proteins in archeological bones.)

In palynology (and other paleoclimatological studies involving lake sediments and peats), two methods which attempt to utilize the small sample capability provided by AMS ^{14}C measurement systems have developed. In the less desirable of these methods, the traditional TOC preparation treatment has been used to prepare lake sediment or peat samples for AMS ^{14}C dating; these samples are smaller than, but otherwise essentially indistinguishable from, the traditional TOC samples that are commonly produced for β-counting ^{14}C dating. These "mini-TOC" samples suffer from the same variety of potential dating errors that have been demonstrated in numerous studies to afflict TOC/β-counting ^{14}C dates.

In the second of these methods, the small sample capability of AMS ^{14}C dating has made possible the measurement of preserved macrofossils that can, in some instances, be found in samples of the lake sediments or peats. Unfortunately, this approach to the establishment of accurate and reliable chronologies for sedimentary records suffers from two significant deficiencies: (1) the occurrence of such macrofossils is haphazard and, in most cases, the dating of macrofossils is not possible because macrofossils are not present in the available lake sediments or peats, and (2) in palynological studies, macrofossils are not the proxy-climate indicator under study, and the use of ^{14}C dates obtained on macrofossils to establish a chronology for the palynological record requires the assumption that the ^{14}C ages of macrofossils in particular lake sediment or peat samples are not significantly different from the ^{14}C age of the pollen in the same samples (effectively, the same question of association that arose in the discussions above concerning the ^{14}C dating of TOC fractions). In practice, while the second of these deficiencies is of some concern, the general paucity of macrofossils in most lake sediment and peat samples severely limits the applicability of macrofossil AMS ^{14}C dating, and relatively few macrofossil AMS ^{14}C dates have been used in the establishment of sedimentary chronologies in palynological studies. (It should be noted that in some paleoclimate

studies, particular macrofossils are the proxy-climate indicator of interest; in such studies, AMS ^{14}C dating of the macrofossils of interest is highly desirable, and questions of association between the material ^{14}C dated and the event of interest do not arise if the macrofossils themselves are AMS ^{14}C dated.)

As was stated above, the basic goal of the research undertaken for this dissertation was the development of procedures and measurement systems necessary to allow the isolation and AMS ^{14}C dating of essentially pure pollen fractions from lake sediment and peat samples. Given the ~1 g sample size requirement of β-counting ^{14}C dating, and the extremely small amounts of pollen that are typically in lake sediments and peats (~1 mg or less in typical samples for AMS ^{14}C dating), such pollen extraction procedures were clearly not a viable approach to the ^{14}C dating of lake sediment and peat samples before the development of AMS ^{14}C measurement systems. In the research undertaken for this dissertation, the intention was to develop the methods necessary to isolate essentially pure pollen fractions from lake sediment and peat samples, and then to exploit the small sample capabilities of AMS ^{14}C measurement systems in dating the extracted pollen fractions.

1.4 Pollen Extraction and AMS ^{14}C Dating.

The research undertaken for this dissertation consisted of two main parts: (1) the refinement of the AMS ^{14}C measurement system at the University of Washington's Nuclear Physics Laboratory to allow the measurement of small pollen fraction samples to the required degree of accuracy and precision, and (2) the development, validation, and application of procedures that would allow the isolation of essentially pure pollen fractions from lake sediment and peat samples.

From the discussions above, it is clear that the isolation and AMS ^{14}C dating of pollen fractions from lake sediment and peat samples has several important advantages over the traditional TOC/β-counting method for dating such samples. First, the selection of pollen for ^{14}C dating eliminates essentially all questions concerning the association of the material being ^{14}C dated with the proxy-climate indicator from which paleoclimatic information is being derived; i.e., in palynological studies, the isolation and ^{14}C dating of pollen would mean that pollen was both the paleoclimate proxy and the material being ^{14}C dated. Second, the isolation and ^{14}C dating of pollen from lake sediment and peat samples eliminates essentially all of the commonly-encountered causes of erroneous ^{14}C dates. The highly-selective and rigorous procedure developed to isolate essentially pure pollen fractions eliminates essentially all of the

contaminants that are commonly responsible for the ^{14}C dating errors, e.g., aquatic plant and animal remains ("hard water" effect), intrusive plant components (downward growth of roots in peats), humic and fulvic acids (mobile organic compounds), and fine graphite and/or coal (reworked material from geologic deposits). Third, the highly-selective and rigorous procedure used to isolate essentially pure pollen fractions eliminates essentially all nonpollen components of the lake sediment or peat samples and produces fractions for ^{14}C dating that can be examined microscopically for contaminants. The limited types of material that can survive the pollen extraction procedure imply that the major components of the fractions can usually be identified during microscopic examination, and an evaluation of the potential for significant dating errors can be made before the sample is actually AMS ^{14}C dated. In addition to showing that the extraction and ^{14}C dating of pollen from lake sediment and peat samples has several significant advantages over the traditional TOC/β-counting method, the discussions above also show that the extracted pollen fractions have the basic properties of an ideal ^{14}C dating material for the establishment of ^{14}C chronologies for the paleoclimate records contained in the lake sediments and peats; i.e., the material being ^{14}C dated is unquestionably associated with the event of interest, the material is clearly identifiable, and the presence of contaminants in the material being dated can be determined before the material is dated by microscopic examination. (In the above discussion of the pollen extraction procedure's ability to eliminate all probable causes of ^{14}C dating errors the only significant potential cause that was not discussed was the possible incorporation of reworked pollen into the lake sediment or peat deposits. In those cases where contamination with reworked pollen appears to be a possibility, the ability to microscopically examine the extracted pollen fractions combined with the expertise of palynologists may allow evaluation of the amounts of reworked pollen in the pollen fractions and the probable significance of any reworked pollen in terms of ^{14}C dating.)

In the first part of the research undertaken for this dissertation, the UW AMS ^{14}C measurement system was studied in detail, and the necessary modifications were made to the AMS system to allow the measurement of the pollen fractions that were to be isolated from lake sediment or peat samples. The University of Washington (UW) AMS ^{14}C measurement system had been developed in an ongoing program that had originally begun in the late 1970's (Farwell *et al.*, 1981). At the time of the initiation of the pollen extraction and AMS ^{14}C dating project, the UW AMS system was capable of making ^{14}C measurements on samples containing 2–4 mg of carbon (Balsley *et al.*, 1987) with total accuracy and precision uncertainties of 1–3% (e.g., Grootes *et al.*, 1989). The undertaking of the pollen project required the improvement of the UW AMS ^{14}C system in two major areas. First, because the pollen fractions extracted from typical

lake sediment and peat samples were expected to contain ~1 mg of carbon, the equipment and procedures used to produce and measure carbon samples with the AMS system had to be either modified or replaced to allow samples containing ~1 mg (or less) of carbon to be processed and measured. Second, because most of the commonly-encountered causes of ^{14}C dating errors, if present, were expected to cause differences of 100-1000 years between the ^{14}C ages of extracted pollen fractions and those of TOC fractions from the same lake sediment or peat samples, the accuracy and precision uncertainties of measurements made with the UW AMS ^{14}C system had to be reduced to 0.5–0.8% (equivalent to ^{14}C age uncertainties of ~40–60 years). The reduction of the total uncertainties of the ^{14}C measurements to ±40–60 years (from the ±80–200 year uncertainties at the beginning of the project) would allow statistical scatter within the uncertainties in the measurements to be eliminated as a reasonable cause of any differences larger than ~150 years that might be observed between the ^{14}C ages obtained for various fractions from the lake sediment and peat samples. The research undertaken to achieve these necessary improvements of the UW AMS ^{14}C system is described in detail in the second chapter of this dissertation.

The second part of the research undertaken for this dissertation consisted of three sections. In the first section, the techniques and procedures necessary to isolate essentially pure pollen fractions from lake sediment and peat samples were developed. The pollen extraction procedure developed as a part of the research presented in this dissertation was based on the procedure used in the initial study in which pollen fractions were extracted from lake sediment samples and AMS ^{14}C dated (Brown *et al.*, 1989) (as were the procedures used in two other studies (Brown *et al.*, 1992; Regnell, 1992)). The development of the pollen extraction procedure undertaken for this dissertation was centered on the improvement of several steps in the procedure used in the initial study to expand the range of applicability of the procedure and allow the isolation of essentially pure pollen fractions from sedimentary materials ranging from high-organic-content gyttia or peat to very low-organic-content silty and/or clayey lake sediments.

In the second section, a study was undertaken in which the ^{14}C ages of pollen fractions and TOC-equivalent samples from sedimentary materials associated with a particular volcanic ash layer in several lake sediment and peat deposits were determined. This study was intended to provide more extensive evidence of the effectiveness of the pollen extraction procedure in isolating essentially pure pollen fractions from lake sediment and peat samples, and of the improved accuracy and precision that could be obtained from the AMS ^{14}C dating of pollen fractions (as opposed to TOC fractions). The Mazama Ash layer used in this study has been the subject of numerous previous studies, and the multitude of ^{14}C dates obtained on various

materials associated with the ash layer in these studies allowed the ^{14}C dates obtained for pollen fractions and TOC-equivalent samples in this study to be evaluated in terms of external accuracy as well as internal consistency.

In the final section, the pollen extraction procedure was applied to samples from a low-organic-content Alaskan lake sediment core that was a part of an ongoing paleoclimate study. The application of the procedure to samples from this core was intended to demonstrate that the procedure could isolate essentially pure pollen fractions from such low-organic-content lake sediments, and to assist in establishing an accurate and trustworthy chronology for the palynological record that had been obtained from the lake sediment core. The ^{14}C AMS dating of pollen fractions from this core was also intended to provide accurate dates for the first establishment of spruce and alder in the region of the lake, and hence, provide dates of arrival that could be used in conjunction with such dates from other sites to study the migrations of those tree species across Alaska in the early Holocene.

The research undertaken in these three sections is described in detail in the third chapter of this dissertation.

As a final note before proceeding to the main chapters of this dissertation, it is convenient to state here that all ^{14}C dates and related expressions of ^{14}C concentrations given in this dissertation have been calculated following the conventions of Stuiver and Polach (1977) and of the international journal RADIOCARBON. The ^{14}C dates are expressed in radiocarbon years before present (BP) (or in some cases in thousands of radiocarbon years before present (ka BP)); the uncertainties given with the dates represent the 1σ uncertainty in the dates. In those cases in which calibrated (effectively solar year) dates have been determined, the calibrated dates were obtained using the radiocarbon calibration program CALIB 3.03 Macintosh version (Stuiver and Reimer, 1993), and have been expressed in calibrated years before present (cal BP).

Chapter 2: The University of Washington Accelerator Mass Spectrometry System.

2.1 Overview.

The High Voltage Engineering Corporation (HVEC) Model FN tandem Van de Graaff accelerator at the University of Washington (UW) Nuclear Physics Laboratory (NPL) is the heart of our AMS ^{14}C measurement system. The overall layout of the major components of our system is shown in figure 2.1. Descriptions of these components and the operation of the AMS system have been published previously (Farwell, 1984; Farwell *et al.*, 1984; Grootes *et al.*, 1986; Brown *et al.*, 1990; Schmidt *et al.*, 1990; and most recently by Brown *et al.*, 1994 (in press)).

The process of making a ^{14}C measurement using our AMS system consists of three basic steps: 1) the preparation of an appropriate subsample from the sample material of interest and its conversion into a form that is suitable for insertion into our ion source, 2) the AMS measurement of the ^{14}C in the prepared subsample, and 3) the calculation of the ^{14}C concentration of the sample from the measurement data. In the following sections the major steps in the measurement process and the components of our AMS ^{14}C system will be discussed, with emphasis on the changes that have been made to improve the system over the course of the research presented in this dissertation. In the final section of this chapter, the current level of performance of the AMS ^{14}C system will be discussed in detail.

2.2 The University of Washington Accelerator Mass Spectrometry System.

2.2.1 Preparation of samples.

In general, the preparation of a sample for measurement by AMS ^{14}C involves a number of steps leading from the raw sample to a final "target" suitable for insertion into the ion source. The initial steps (sample pretreatment) are intended to remove carbon-containing contaminants from the raw sample and produce a "purified" sample for the more generally applicable steps leading from the pretreated sample to the ion source target (the term ion source target is used to distinguish a subsample that has been fully prepared for insertion into the ion source from the parent raw or pretreated sample from which several separate targets may be prepared). Pretreatment procedures vary considerably with sample type (e.g., bone, wood, ocean water, lake sediments, etc.) and are of considerable interest to the radiocarbon dating community in their own right. In the following chapter, the development of pretreatment procedures for the extraction and concentration of pollen from lake sediments and peat samples will be discussed in

detail as one of the major components of the research presented in this dissertation. In this section, however, discussion will be limited to the procedures we have used to produce ion source targets from pretreated samples as these procedures are directly related to the performance of our ion source targets, and hence, to the performance of our AMS ^{14}C measurement system.

The procedures used in preparing pretreated carbon samples for measurement in the AMS ^{14}C system consisted of these steps: 1) conversion of the carbon in the pretreated sample to CO_2, 2) reduction of the CO_2 to graphite powder, and 3) conversion of the graphite powder to a solid graphite pellet. The first two steps were accomplished using well established methods that are used routinely in AMS laboratories throughout the world. The Ta-encapsulation techniques used for the third step were developed by the AMS group at the University of Washington over many years of research and are unique to our AMS ^{14}C system.

Conversion of pretreated sample carbon to CO_2.

For most samples prepared for AMS ^{14}C measurement the conversion of the carbon in the pretreated samples to CO_2 was accomplished by high temperature oxidation. Each sample was loaded into a quartz tube with one sealed end and CuO powder was added on top of the sample. The loaded tube was then evacuated and sealed. The sealed tubes were heated to 900°C for one hour and allowed to cool slowly in the furnace overnight. Previous studies have shown this procedure to be essentially 100% effective in converting the carbon in the samples to CO_2 (Stuiver *et al.*, 1984).

For the relatively small number of carbonate samples prepared for measurement, HCl was used to convert the carbonate to CO_2. In this procedure, the carbonate sample was dissolved in 0.7 N HCl under flowing nitrogen gas, and the evolved CO_2 was trapped in a liquid N_2 (LN_2) cold trap. This procedure is commonly used in the routine preparation of carbonate samples in oceanographic and other isotope-based research and is effective in extracting and collecting the carbon in the carbonates as CO_2.

Conversion of CO_2 to filamentous graphite.

The method used for the second step in the preparation of carbon samples for measurement was based on the method first published by Vogel *et al.* (1984). In this method the sample CO_2 is reduced to graphite powder by the catalytic reaction of CO_2 over iron at ~650°C in the presence of excess hydrogen gas. The graphite powder produced under these reaction conditions is in the form of comparatively long 0.1–0.5 μm diameter filaments and, hence, has been referred to as filamentous graphite (Vogel *et al.*, 1987a). The low thermal conductivity of these filaments

makes this graphite powder, by itself, unsuitable for use as an ion source target material.

Vogel *et al.* (1987a) showed that, when an appropriate amount of catalyst is used in the reduction step, the catalyst can act as a high thermal conductivity matrix for the sample when it is pressed into the ion source target holder, and a sample suitable for use in an ion source can be produced. They determined that a ratio of 4–10 mg of iron (or cobalt) catalyst per mg of sample carbon produced the most suitable samples and this ratio is used as a general guide by most laboratories using this catalytic reduction method.

In reducing our sample CO_2 to graphite powder, however, we used only 0.2–0.8 mg iron catalyst per mg of sample carbon. This amount of catalyst was sufficient to allow the reduction of sample CO_2 in a reasonable time and, because the filamentous graphite was converted into a solid graphite plug having sufficiently high thermal conductivity in the next step of our sample preparation procedure, the larger amounts of iron catalyst were not required to provide a high thermal conductivity matrix. In addition, the lower amounts of iron catalyst avoided possible target inhomogeneities that might be introduced by the larger amounts of catalyst.

Conversion of filamentous graphite to an ion source target.

The final step in the preparation of samples for measurement in our AMS ^{14}C system was the conversion of the filamentous graphite into a Ta-encased solid graphite plug. The methods used to achieve this conversion were developed by the University of Washington AMS group and are detailed in a sequence of publications beginning in the mid–1980's (Farwell *et al.*, 1984; Balsley *et al.*, 1987; Brown *et al.*, 1990). These techniques involve the encapsulation of the filamentous sample graphite in Ta, followed by compression of the graphite to ~14 kbar and heating to ~2500 °C. Under these high temperature/high pressure conditions the graphite undergoes a phase transition from the filamentous form to a solid graphite structure which has a relatively high thermal conductivity.

Improvements to the sample preparation methods.

During the course of the research presented in this dissertation, our AMS group devoted considerable effort towards reducing the size of, and improving the consistency and reliability of, routine carbon samples prepared using these techniques. The Ta-encapsulation equipment discussed in Balsley *et al.* (1987) was completely redesigned by Prof. Fred Schmidt in 1988 to allow the Ta encapsulation of 0.7 mm diameter samples. The components of the new encapsulation system were machined by Bob Cooper and Hank Simons (UW NPL instrument makers); Jac Caggiano and Nancy Mar (UW undergraduate students) worked from 1988 to 1991 to develop the techniques necessary to routinely produce consistent and reliable ion source

targets using the new encapsulation system.

Over the last three years (1991-1994), significant modifications have been made to several components of the encapsulation apparatus, several new steps have been introduced into the encapsulation procedure, and the 2500 °C graphite–tube vacuum furnace that is used to heat the Ta-encapsulated samples has been redesigned and rebuilt. With these changes, we have been able to routinely produce reliable and consistent Ta-encapsulated 0.7 mm diameter ion source targets that contained about 300 μg of carbon. Under our normal ion source operating conditions, these ion source targets typically produced the equivalent of 15–25 μA $^{12}C^-$ current and had a useful lifetime of ~1 h (i.e., the targets produced ~20 μA h of $^{12}C^-$ ions). The targets were well-behaved in the ion source and the rate of target failure to produce desired C^- ion beam output levels was essentially zero.

The development of the capability to prepare reliable 300 μg ion source targets was of importance to the pollen dating research presented in this dissertation because the amount of carbon contained in many of the pollen extract samples was significantly less than was required to prepare a single target under the earlier Ta-encapsulation system described by Balsley *et al.* (1987). In addition to the work on the equipment and procedures required to produce the 0.7 mm diameter targets, the utilization of these targets required alterations to our target holder disks and ion source to ensure consistent positioning of the targets relative to the sputtering Cs^+ ion spot. These alterations and the performance of the 300 μg targets under normal ion source operating conditions will be discussed below.

2.2.2 Ion source and low energy section of the AMS ^{14}C system.

The ion source and the important components of the low energy (LE) section of our AMS ^{14}C system are shown in the left third of figure 2.1.

2.2.2.1 Components and operation.

Our ion source is a modified UNIS-type sputter source which is operated in the multiple-beam reflection mode (Schmidt and Farwell, 1979) and has a remotely controlled 20-sample wheel. Amongst other modifications, a four-quadrant sectored einzel lens has been inserted between the Cs ionizer and the sample wheel; this lens allows focusing and steering of the Cs^+ beam to help produce a properly located and focused reflected-Cs^+ sputtering spot on the ion source targets. The C^- ions produced by the sputtering action of the Cs^+ ions impinging on the carbon target are accelerated downstream towards the inflection magnet by the –26 kV potential of the target wheel. The C^- ions pass through an asymmetrical einzel lens at the end of the ion source

and between horizontal and vertical electrostatic steering plates, and are then accelerated to 85 keV by the –59 kV elevation potential of the ion source frame as they exit the ion source system.

The transport of the 85 keV C^- ions from the exit of the ion source system to the entrance of the tandem accelerator is relatively straightforward. The ions are mass analyzed by the NMR-regulated 45° inflection magnet, pass through a set of vertical electrostatic steerer plates at the exit of the inflection magnet, then through a set of horizontal and vertical electrostatic steerer plates, an electrostatic quadrupole lens triplet, and another set of electrostatic steerer plates, and then enter the tandem accelerator. The NMR-regulated 45° inflection magnet is used to select either mass 13 or mass 14 ions for injection into the accelerator; during automated measurement cycling the mass setting of the inflection magnet is alternated between masses 13 and 14 under the control of our AMS sequencing program that is resident in one of the NPL's Texas Instruments 5TI controllers. The quadrupole triplet is used to focus the beam of selected ions onto the stripper foil in the accelerator terminal; this lens and the two sets of steerer plates are adjusted to maximize beam current measured on the Faraday cup at the exit of the accelerator (high energy (HE) cup), i.e., to maximize transmission of the mass-selected ions through the accelerator.

2.2.2.2 System improvements.

During the course of the research undertaken for this dissertation three sets of important modifications were made to the ion source and LE section of our AMS ^{14}C system.

The ion source.

The first set of modifications was intended to improve the stability and reliability of the ion source over the 7 to 12 day periods of essentially continuous operation during which our AMS ^{14}C measurements were made. First, the ion source vacuum system was reorganized by Prof. Fred Schmidt and Jac Caggiano to allow the addition of a LN_2 trap. This LN_2 trap significantly improved the normal operating vacuum of the ion source and decreased the time required for the ion source vacuum to return to operating levels after target set changes.

Second, the home-built voltage supply that provided the bias voltages to each of the four quadrants of the sectored einzel lens that focused and steered the Cs^+ beam was completely rebuilt. This supply had been vulnerable to catastrophic failure of its commercial isolation transformer and/or its heliopot bias voltage resistors due to sparks between the sectored einzel lens (at about –7 kV) and the nearby components at the target wheel potential (–26 kV). During the rebuild the commercial transformer was replaced by a home-built isolation transformer that was

capable of operating at much higher DC voltage differentials, the heliopot resistors were protected by an array of transorb voltage shunts, and the vulnerable sections of the supply were protected by resistor chains and spark gap shunts.

Third, the 15–20% porosity tungsten ionizer frit that had been used in the ion source to produce the Cs^+ ion beam by thermal ionization was replaced with a 25–30% porosity frit. Together, these modifications improved the stability of the modified UNIS-type ion source and significantly reduced the maintenance time required to ensure reliable operation of the source; over the last two AMS ^{14}C measurement periods, the ion source provided desired ion beam intensities from sample targets for a total of 21 days of measurements without requiring disassembly and cleaning of the source during or between the measurement periods.

Target holders and internal ion source alignment.

The second set of modifications to the ion source and LE section of our AMS ^{14}C system was required to allow the 0.7 mm diameter targets to perform properly in the ion source. As was mentioned above, the reduced diameter of these targets placed stringent requirements on the reproducibility of the positioning of the carbon targets relative to the location of the sputtering Cs^+ beam spot. Microscopic examination of several series of sputtered targets from several measurement periods in 1989 and 1990 showed disturbingly large variations (up to ±0.4 mm) in the position of the 0.7 mm diameter carbon targets relative to the sputtering spot. These variations were found to be mainly from two sources.

First, detailed study of the position of the 0.7 mm target well relative to locating edges during Ta encapsulation and target mounting steps showed that a major contributor to the variations in the positioning of the target relative to the Cs^+ spot was inconsistencies in the machining of the target holder disks into which the Ta capsules were mounted for insertion into the source. The location of the central hole in the Al target holder disks (into which the Ta target-capsules were pressed) relative to the outer edge of the holder disks (which position the assembled targets disks in the ion source target wheel) varied by up to ~0.6 mm. These inconsistencies were eliminated by providing the commercial machine shop which produced the Al target holder disks with modified and detailed drawings of the desired disks and by vigilant quality monitoring of the disks received from the commercial machine shop.

Second, examination of the ion source components during routine (and often frequent) disassembly, cleaning, and reassembly of the ion source showed that there was significant play between several structural components of the source; in this state, the alignment of these components (most importantly, the Cs^+ reflection electrode and the target wheel electrode)

could not be ensured during reassembly of the source. Rearrangement of several of the insulator/structural-spacers of the source and precise machining of the alignment faces of a few of these insulator/spacers to match their corresponding electrodes eliminated the play between the important electrodes. As a result, the alignment of the important internal components of the source now seems to be reproducible to within ±0.1–0.2 mm following disassembly and reassembly of the source during routine maintenance and cleaning.

With the elimination of both of these sources of inconsistency, the variations in the position of the 0.7 mm diameter carbon targets relative to the location of the sputtering Cs^+ beam spot were reduced to less than ±0.2 mm and the 0.7 mm diameter targets performed consistently and reliably in the ion source.

The transport of C^- ions through the LE section.

The third set of important modifications to the ion source and LE section of our AMS ^{14}C system was intended to improve the transport of the C^- ions from the ion source into the accelerator. Before these modifications the optical elements of the LE section had been adjusted to maximize the beam current at the HE cup in the following manner: 1) the asymmetric einzel lens at the exit of the ion source, the elevation potential of the ion source system, and vertical electrostatic steerers immediately after the 45° inflection magnet were adjusted to maximize the current of C^- ions transported through a 3.91 mm diameter aperture at the image position of the double-focusing 45° inflection magnet to the Faraday cup just before the accelerator entrance (LE cup), and then 2) the LE electrostatic quadrupole triplet lens, and the sets of electrostatic steerers before and after the lens, were adjusted to maximize the transport of the beam through a grounded fine wire grid at the beam tube entrance and the accelerator itself to the HE cup. The 3.91 mm diameter aperture at the image position of the inflection magnet was intended to limit the transmitted ion beam to match the acceptance of the accelerator and had been a component of the UW AMS ^{14}C system from the earliest measurements (Farwell *et al.*, 1981).

During various ion source tests involving the 0.7 mm targets indications had been seen that the C^- beam current measured at the LE cup could be increased by removing the 3.91 mm diameter aperture and readjusting the ion source einzel lens. In December 1992 we conducted a series of tests of the LE beam transport system with and without the 3.91 mm diameter aperture and the fine wire beam tube entrance grid. We found that, with the 3.91 mm diameter aperture removed and the source einzel adjusted to maximize ion current to the LE cup, ~35% more ion current was transmitted from the ion source to the LE cup than with the aperture in place and appropriate adjustment of the source einzel lens. We also found that, with the aperture removed,

the range over which the ion source vertical and horizontal steerers could be varied without appreciable decrease in the ion current at the LE cup was larger when the source einzel was adjusted to the "no aperture" setting than when it was adjusted to the setting at which the maximum beam transmission through the aperture had been obtained. Further, we found that, with or without the beam tube entrance grid, adjustment of the LE electrostatic quadrupole triplet lens allowed the "no aperture" ion beam to be transmitted through the accelerator with the same efficiency as under the LE beam transport setup which included the aperture (the ~10% loss of ions on the wires of the beam tube entrance grid was taken into account in these transmission efficiency calculations).

These results suggested that, when the source einzel lens was adjusted to maximize ion transmission through the aperture, the optics of the rest of the beam transport system forced the ion beam to be so large at the entrance to or in the inflection magnet vacuum box that part of the beam was lost on the walls of the box. After the removal of the aperture (which had forced an ion beam waist at the image position of the inflection magnet), the readjustment of the source einzel lens to maximize beam current at the LE cup produced an ion beam that was small enough in the inflection magnet box to avoid losses on the walls. Based on these results we discontinued the use of the 3.91 mm diameter aperture at the image position of the inflection magnet and the fine wire beam tube entrance grid. As a result of these modifications to the transport of the ion beam through the LE section of our AMS ^{14}C system the efficiency of the transport of ions from the ion source to the HE cup was increased by ~50% and the sensitivity of ion transmission to small changes in beam trajectory (such as those that can be caused by sample-to-sample variations) was significantly reduced.

These modifications to the ion source components and the transport of the ion beam through the LE section of our AMS ^{14}C system resulted in a significant improvement in the performance of the ion source and in the consistency of the measured $^{14}C/^{13}C$ ratios obtained from our Chinese Sucrose Standard targets. The evidence for significant improvement in the consistency of the Chinese Sucrose $^{14}C/^{13}C$ ratios will be discussed below during analyses of the accuracy and precision of ^{14}C measurements made on our AMS ^{14}C system (section 2.4.1).

2.2.3 Van de Graaff accelerator, high energy section of the AMS ^{14}C system, and ^{14}C detector.

The tandem Van de Graaff accelerator, the important components of the high energy (HE) section of our AMS ^{14}C system, and our ^{14}C detector are shown in the right half of figure 2.1. With the exception of the new ^{14}C detector, these components have been described previously

(Farwell *et al.*,1984; Grootes *et al.*, 1986; Schmidt *et al.*, 1990) and will be discussed only briefly here. The new ^{14}C detector was designed and constructed within the last two years and will be described near the end of this section.

2.2.3.1 Components and operation.

The primary components of the HVEC Model FN tandem Van de Graaff accelerator at NPL are the central, high-voltage terminal, the LE and HE column structures which support and insulate the terminal, and the high vacuum LE and HE beam tubes through which the ion beam travels to and from the terminal. While a lengthy discussion of these components is beyond the scope of this section, there are two points that are worth mentioning: 1) the potential gradient in the beam tubes is maintained by the current flow from the terminal to tank ground through the resistor strings that connect the planes of the LE and HE columns, 2) almost all of the beam tube planes have slotted apertures (only the first 25 of the first LE beam tube section have circular apertures) and many of these planes are inclined relative to vertical by varying amounts as part of the electron cascade suppression design of the HVEC vertical inclined beam tubes.

The C^- ions injected into the accelerator from the LE section of the AMS ^{14}C system are accelerated towards the 7.0 MV terminal by the potential gradient in the LE beam tubes. In operation, the LE electrostatic quadrupole triplet is adjusted so that the characteristics of the injected C^- ion beam are compatible with the accelerating, steering, and focusing characteristics of the potential gradient and apertures of the LE beam tubes. Under these conditions, the C^- ions are transported from the accelerator entrance to, and are focused on, the terminal stripper foil.

The C^- ions arrive at the stripper foil with an energy of about 7 MeV and lose several electrons as they pass through the thin carbon stripper foil (about 2 $\mu g/cm^2$). The efficiency of the stripping process in removing electrons from the C^- ions is dependent on the energy of the incident C^- ions; at the 7.0 MV terminal voltage chosen for our AMS ^{14}C measurements about 50–60% of the incident C^- ions are stripped of 5 electrons to produce C^{4+} ions while the remainder of the C^- ions are stripped predominantly into charge state +3 or +5.

The positive ions produced by the stripping process then pass between vertical and horizontal electrostatic terminal steerer plates and enter the HE beam tube sections. The positive ions are accelerated towards the accelerator exit (and steered and focused) by the potential gradient in the HE beam tubes. With a terminal voltage of 7.0 MV, the C^{4+} ions exit the accelerator with an energy of about 35 MeV.

After exiting the accelerator, the positive ions are focused and steered to the object position

of the NMR-regulated, double-focusing, 40-inch radius 90° analyzing magnet by the HE electromagnetic quadrupole triplet; the current supply circuitry for this quadrupole allows the dipolar biasing of the fields so that the quadrupole can steer as well as focus the positive ion beam. The ion beam then passes through the analyzing magnet to form an ion beam waist at the image position of the magnet. With the withdrawal of the Faraday cup at the image position (Image cup), the ion beam passes through the switching magnet (which is set to direct the beam down the 30° Right beamline during AMS measurements), the beamline quadrupole doublet, and the Wien filter (velocity selector; crossed E and B fields) to the detector position.

Under our normal procedures for setting up the HE section of the AMS ^{14}C system, the ~35–MeV $^{13}C^{4+}$ ion beam from the accelerator was used to optimize the settings of the elements of the HE beam transport system. The terminal voltage and the analyzing magnet field were set to transport the $^{13}C^{4+}$ ions to the image position of the analyzing magnet and the electromagnetic HE quadrupole triplet was adjusted to optimize the $^{13}C^{4+}$ ion beam to the Image cup. Then the Image cup was withdrawn and the switching magnet, beamline quadrupole doublet, and the Wien filter were adjusted to optimize the $^{13}C^{4+}$ ion beam to the Faraday cup at the position of our detector (Detector cup). Once the transport of $^{13}C^{4+}$ ions through the HE section of the system was optimized, the settings of those components downstream of the Image cup (the switching magnet, beamline quadrupole doublet, and Wien filter) were scaled to mathematically appropriate settings for $^{14}C^{4+}$ ions with the same energy as the $^{13}C^{4+}$ ions, and the ^{14}C detector was positioned just in front of the Detector cup in preparation for automated $^{14}C/^{13}C$ measurements. Under our measurement cycling system, the HE quadrupole and the 90° analyzing magnet were alternated automatically between settings for $^{13}C^{4+}$ and $^{14}C^{4+}$ ions; $^{13}C^{4+}$ ion currents were measured on the Image cup under the $^{13}C^{4+}$ settings and $^{14}C^{4+}$ ions were counted in the ^{14}C detector under the $^{14}C^{4+}$ settings.

The ^{14}C detector consisted of a gas ionization detector followed by a solid state Si detector. The gas ionization detector produced a ΔE signal that was proportional to the rate of energy loss of each ion transversing the gas cell, and hence, was related to the nuclear charge, Z, and mass, M, of each ion. The solid state Si detector produced an E_{res} signal that was proportional to the remaining (residual) energy of each ion after transversing the gas cell. The sum of the ΔE and E_{res} signals gave an E_{tot} signal that was related to the total energy of each ion, and hence, to the mass of each ion. The ΔE and E_{tot} signals were amplified, shaped, amplified again, and then gated to allow the ions with the characteristics of 35-MeV $^{14}C^{4+}$ ions to be distinguished from ions of other isotopes of carbon and of other elements present in relatively small numbers, e.g., N

and O.

2.2.3.2 System improvements.

During the course of the research undertaken for this dissertation considerable effort was devoted to understanding the transport of the ion beam through the accelerator and HE section to the detector, and several significant modifications were made to the HE section to improve the performance of the AMS ^{14}C system. Operational experience had suggested that the performance of our measurement system was particularly sensitive to terminal voltage instabilities. Hence, the primary goal of the work on the accelerator and HE section was to eliminate this sensitivity, either by eliminating the instabilities in the terminal voltage or by removing the apertures in the HE section of the system that were obstructing the ion beam during terminal voltage fluctuations, thereby eliminating the sensitivity of ion beam transmission to the instabilities in the terminal voltage.

The terminal voltage instabilities were studied using the Generating Voltmeter (GVM) and Slit Difference terminal voltage sensing systems coupled with the Corona and/or Stripper voltage regulation systems. These studies indicated that there were two main sources of the instabilities when the terminal voltage was regulated by the GVM-Corona system (the combination that was used during AMS measurements). The first of these sources was variations in the delivery of charge to the terminal due to charge distribution inhomogeneities on the surface of the accelerator's charging belt that were related to physical imperfections of the belt (Trainor, 1989). The terminal voltage fluctuations caused by these imperfections occurred at frequencies that were harmonics of the belt cycle frequency (2.4 Hz) and were, for the most part, at frequencies higher than the frequency response range of the GVM-Corona terminal voltage regulation system. The second source of the instabilities was the GVM itself. The output voltage of the GVM system showed fast variations related to the rotational frequency of the GVM's rotor (58 Hz) and slow drifts of several parts in 10^4 over tens to hundreds of seconds that were probably due to mechanical and/or electronic drifts in the GVM system.

While possible methods for eliminating the terminal voltage fluctuations from these sources were being considered, concurrent studies of the beam-limiting apertures in the HE section of the system suggested that the sensitivity of the measurement system to terminal voltage fluctuations could be eliminated by removing the limiting apertures without actually having to eliminate the terminal voltage fluctuations.

Three different methods were used to determine the location and nature of the beam limiting apertures in the HE section of our AMS ^{14}C system: 1) the visual determination of the position

and inside dimensions of constricting apertures in the beamline, 2) the detection of gamma radiation produced by $^{13}C^{4+}$ ions striking limiting apertures, and 3) the movement and changes in shape of a $^{13}C^{4+}$ ion beam at the detector position in response to changes of the settings of upstream components.

Visual examination.

The visual examination of the apertures was conducted using the NPL's alignment telescope and various preexisting and/or purpose-built alignment tools and mounts. The examination suggested that, with only one exception, the apertures in the HE beamline were not sufficiently misplaced, misaligned, or restrictive so as to obstruct the ion beam under normal conditions (e.g., with typical terminal voltage fluctuations). The exception was that the vertical slits at the object position of the 90° analyzing magnet were seriously misaligned. This misalignment was the probable cause of the difficulties that had been encountered in attempting to minimize the vertical steering required to transport the ion beam through the HE beamline to the detector position; the alignment of slits was corrected during the examination of that section of the HE beamline.

Detection of gamma radiation.

The second method was to search for gamma radiation produced by $^{13}C^{4+}$ ions striking the apertures at terminal voltages slightly above and below the 7.0 MV terminal voltage at which the transport of the $^{13}C^{4+}$ ion beam had been optimized. These searches failed to produce any evidence that there were previously unaccounted for apertures upstream of the detector that would obstruct the ion beam during typical terminal voltage fluctuations. The searches also failed to produce any evidence that the beam was being obstructed in its passage through the beamline quadrupole doublet (as had been thought would be the case prior to these searches). The searches did, however, produce evidence that the primary horizontally limiting aperture in the HE section was the horizontal width of the 2.5-cm diameter entrance window of the ^{14}C detector in use at that time (the 2.5-cm detector).

Observations of the luminescence pattern on a quartz slide.

In order to confirm these results a third method was used; a quartz slide (3 cm vertical by 6 cm horizontal) was mounted perpendicularly to the ion beam direction at the detector position and the movement and changes in shape of the luminescence pattern produced by a 35-MeV $^{13}C^{4+}$ ion beam striking the quartz slide were studied as a function of terminal voltage and the settings of other upstream components of the HE section. With the slits at the image position of the 90°

analyzing magnet withdrawn to the edges of the 1.27 cm diameter fixed entrance aperture of the slit box, variation of the terminal voltage showed that the range of unobstructed horizontal motion of the ion beam across the quartz slide was about 5 cm. This observation confirmed that the entrance window of the 2.5-cm detector was the primary horizontally limiting aperture of the HE beam transport system.

Further study of the luminescence pattern showed that: 1) the terminal voltage fluctuations related to the charging belt and the GVM discussed above were evident in the horizontal movement of the ion beam as a fast jitter superimposed on slow drift of the central position of the ion beam, 2) the cross-sectional shape of the ion beam was distorted from the expected circle to a significantly elongated ellipse with its long axis tilted ~30° from horizontal, and 3) the ion beam moved upwards as well as horizontally across the quartz slide when the terminal voltage was increased above the voltage setting at which the HE transport system had been adjusted to direct the ion beam to the center of the quartz slide (i.e., the position at which the center of the detector would be located).

The extended horizontal width of the distorted ion beam and the horizontal motion of the ion beam at the detector position caused by terminal voltage variations (fast jitter plus slow drift) implied that the ion beam would, over times much shorter than the time required for normal measurements, occupy essentially all of the horizontal width of the 2.5-cm detector entrance window and occasionally be obstructed by the window boundaries. The limited acceptance of the 2.5-cm detector implied that small drifts and/or shifts in the GVM-Corona terminal voltage regulation system or the HE ion beam transport system would have had a significant effect on the transmission of $^{14}C^{4+}$ ions from the accelerator into the detector, and hence, would have introduced inconsistencies into our ^{14}C measurements.

The 5-cm ^{14}C detector.

Based on our observation that the horizontal range of motion at the detector position over which the ion beam, in the absence of obstructions, could move in response to terminal voltage variations was about twice the diameter of the 2.5-cm detector window, the decision was made to construct a ^{14}C detector which would allow the full width of the HE beamline transmission window to be utilized. The 5-cm diameter window of the new detector (the 5-cm detector) was expected to provide sufficient horizontal width to allow the full transmission of the ion beam through the HE beamline into the detector over a range of terminal voltages that was much larger than the range of the typical fluctuations, and hence, to eliminate the sensitivity of our AMS ^{14}C measurement system to the terminal voltage fluctuations introduced by the charging belt and the GVM-Corona

regulation system.

The 5-cm detector was designed and constructed by Prof. George Farwell and machined by Louis Geissel (UW NPL instrument maker). The detector was housed in a 12-cm inner diameter Al cylinder with a 5-cm diameter 400 $\mu g/cm^2$ aluminized mylar entrance window. The gas ionization cell ΔE detector was operated at gas pressure of about 200 Torr of 90 % Ar/10% CH_4 counting gas and had a sensitive region which was about 5.6 cm in diameter and about 4.3 cm deep. The electron collection space of the gas ionization cell was defined by a ground plate and a curved (radius about 7.5 cm) Frisch grid and collector plate pair (which were operated at +500 V and +900 V, respectively). The solid state E_{res} detector was a 2000 mm^2 Series CAM PIPS detector obtained commercially from Canberra Industries, Inc.

After some modifications to the detector electronics to optimize signal-to-noise ratios and eliminate ground loop pick-up noise, the resolution of the 5-cm detector for 35-MeV $^{14}C^{4+}$ ions was determined to be as follows: 1) ΔE peak FWHM of 0.28 MeV (about 7% of the 7 MeV deposited in the ΔE detector), 2) E_{res} peak FWHM of 0.40 MeV (about 1.5% of the 28 MeV deposited in the E_{res} detector), and 3) E_{tot} peak FWHM of 0.28 MeV (about 0.8% of the 35 MeV total energy of the $^{14}C^{4+}$ ions). The width of the ΔE peak can be largely attributed to variations in the energy deposited in the ΔE detector due to variations in the ionization path length of the ions caused by the outward bulge of the mylar window under the 200 Torr counting gas pressure. The width of the E_{res} peak can be attributed to the variations in energy deposited in the E_{res} detector caused by the variations in the energy lost by the ions in the ΔE detector and the finite width of the E peak from the solid state CAM PIPS detector. Hence, the decreased width of the E_{tot} peak (sum of the ΔE and E_{res} signals) relative to the E_{res} peak shows that the ΔE and E_{res} signals are anti-correlated, i.e., extra energy detected in the ΔE detector results in the detection of less energy in the E_{res} detector, so that the E_{tot} signal remains essentially the same for all the ions.

The Wien filter magnetic field.

The second and third observations from the luminescence patterns produced by the $^{13}C^{4+}$ ion beam on the quartz slide (the distortion and tilting of the ion beam shape and the vertical movement of the ion beam), were attributed to inhomogeneities in the magnet field created by the permanent magnets of the Wien filter. Under Prof. George Farwell's direction, David Balsley (UW NPL Research Scientist) measured the magnet field to prove the existence of the inhomogeneities, constructed iron shims to correct the field, and then measured the shimmed field to demonstrate that the new magnet field had the desired, smoothed profile. This modification to the Wien filter's magnetic field eliminated the vertical motion of the ion beam in

response to terminal voltage increases and significantly decreased the ellipsoidal distortion of the ion beam.

These modifications to the ion beam transport elements of the HE section of our AMS ^{14}C system and the introduction of the 5-cm ^{14}C detector significantly decreased the sensitivity of ion beam transmission to minor fluctuations in terminal voltage (and other components of the system) and resulted in a significant improvement in the stability of the measurement system. The present insensitivity of our AMS ^{14}C system to variations in terminal voltage (and evidence of the sensitivity of the system before the introduction of the 5-cm ^{14}C detector) will be mentioned below during a discussion of the normal conditions under which the AMS ^{14}C system was operated (section 2.2.4.1).

2.2.4 Operation of the AMS ^{14}C measurement system.

The performance of an AMS ^{14}C system can be evaluated in terms of a wide variety of parameters. Some measures of system performance are directly related to the capabilities of the components of the system, e.g., ion source output, efficiency of utilization of carbon sample, ion transmission efficiency through the system, ^{14}C count rate, and overall sample throughput of the system. In the following sections data will be presented which describe typical operating conditions and performance of our AMS ^{14}C system. In addition, the form of the primary data obtained during the measurement of an unknown or secondary standard sample under our routine operating conditions will be discussed.

2.2.4.1 Typical operating conditions.

Typical operating conditions for the AMS ^{14}C system during our measurements are given in table 2.1. In general, these operating conditions were established during the 1–2 day setup/checkout period at the beginning of each 7 to 12 day AMS measurement period and then maintained, with only minor adjustments, throughout the remainder of the measurement period. The initial operating conditions at the beginning of each 1–2 day setup/checkout period were based on past experience and the settings of the LE and HE ion beam transport systems were then adjusted to optimize ion transport following the procedures outlined above. In the following, several aspects of our typical operating conditions will be discussed in detail with emphasis on their impact on the overall performance of the AMS ^{14}C system.

The ion source.

The ion source was operated conservatively at 15–20 μA $^{12}C^-$ output (measured at the LE cup) in order to ensure stable and reliable long-term operation of the source over the 7 to 12 days

of essentially continuous operation during a measurement period. This low to moderate output operation of the ion source was also required to ensure that the lifetime of the stripper foils was reasonably long compared to the time required to measure a sample; at the 15–20 μA $^{12}C^-$ output level, the stripper foil lifetime was ~5 h/foil while samples were measured in 30-45 min.

On several occasions, the ability of the ion source to operate at higher output levels was tested; under high output operating conditions the ion source was shown to be capable of producing 50–80 μA $^{12}C^-$ from our 0.7 mm diameter, 300 μg targets. However, the operation of the ion source at the high output levels was considered to be unacceptable for routine measurements for two reasons: 1) under high output conditions, the ion source seemed to be considerably less stable, and the reliable operational lifetime of the source seemed to be considerably shorter, than under low/moderate output operation, and 2) the injection of the large mass 13 beams produced under the high output conditions (on the order of 1 μA of $^{13}C^-$ and $^{12}CH^-$ ions) into the accelerator was considered to be detrimental to the overall performance of the measurement system.

One significant aspect of the conditions under which the ion source was normally operated was the adjustment of the Cs^+ reflection potential to slightly defocus the Cs^+ sputtering spot on the surface of the sample (Brown *et al.*, 1990). Although this resulted in an ~10% decrease in the output from the source relative to the output obtained from a sharply focused Cs^+ spot, the defocusing of the Cs^+ spot significantly improved the sample utilization efficiency of the source and reduced the sensitivity of the system to small misalignments of the samples by spreading the Cs^+ ions more evenly over the surface of the targets.

Tests of our targets in the ion source showed that the sample utilization efficiency of sputtering in the ion source was ~80% (i.e., ~80% of the volume of the target could be sputtered to produce usable C^- ions before the produced C^- current fell to negligible levels). The tests also showed that ~4% of the carbon in the target was converted to C^- ions and transported to the LE cup under the "no aperture" LE beamline setup; this implied that C^- production efficiency of the Cs^+ sputtering process in our ion source was about 5%.

The LE and HE ion beam transport systems.

The operating conditions for the LE and HE ion beam transport systems were established following the procedures outlined in the previous sections. In general, once the beam transport systems had been optimized using the mass 13 and $^{13}C^{4+}$ ion beams, the ratio of the HE cup to LE cup currents was about 3.0–3.3, about 45–50% of the HE current was transported to the Image cup as $^{13}C^{4+}$, and essentially 100% of the ion beam at the Image cup was transported to

the Detector cup. Taken together, with some attempt to account for the contributions of $^{12}CH^-$ ions to the mass 13 LE current injected into the accelerator, these values implied that the total transport efficiency of ^{13}C (and presumably ^{14}C) ions from the LE cup to the detector of our AMS system was about 40% (including the stripping efficiency to the 4+ charge state of 50–60%). These results implied that there was some loss of C ions during transit through our AMS system in addition to the expected loss due to stripping efficiency.

Tests of our Ta-encapsulated 300 μg targets using the FN tandem Van de Graaff accelerator at the Center for AMS at the Lawrence Livermore National Laboratory (CAMS) showed that the current on the HE cup per μA of injected mass 13 beam was 25–30% higher for the CAMS accelerator than was observed at NPL; i.e., the HE cup to LE cup current ratio was ~4 at CAMS (cf., 3.0–3.3 at NPL). The discrepancy between the CAMS and NPL results was attributed to beam loss on the slotted apertures of the HE sections of the vertical inclined field beam tubes of our accelerator; the CAMS accelerator was equipped with new spiral inclined field beam tubes with circular apertures that were designed to provide sufficient clearance to ensure the unobstructed transmission of most ion beams through the beam tubes.

Combined with the C^- production efficiency of the sputtering process in our ion source of about 5%, the 40% total transmission efficiency of our AMS system implied that the overall efficiency of the AMS ^{14}C system (carbon ions detected per carbon atom in an ion source target) was about 2%.

In establishing the operating conditions of the system during the setup/checkout period at the beginning of each measurement period, the transmission of the ion beam through the HE section as a function of terminal voltage was determined in detail in order to ensure that the transmission of the ion beam through the HE section would be insensitive to the typical terminal voltage fluctuations discussed above. The transmission profiles obtained at the beginning of the 26May93 AMS measurement period are shown in figure 2.2; these profiles were obtained under operating conditions that were optimized for the 5-cm detector. The profiles obtained for the $^{13}C^{4+}$ ions at the Image and Detector cups indicate that, under these operating conditions, the transmission limiting aperture in the HE section was the 1.27 cm diameter aperture at the entrance to the image slit vacuum box.

The profile obtained for the $^{14}C^{4+}$ ions with the 5-cm detector has essentially the same width as the $^{13}C^{4+}$ profiles (~32 kV) but is offset by 3–4 kV towards higher terminal voltages. This offset may have been due to nonlinearities in the scaling of the analyzing and/or switching magnets from the optimized settings for $^{13}C^{4+}$ ions to settings for $^{14}C^{4+}$ ions. However,

because of the very wide transmission plateaux under operating conditions optimized for the 5–cm detector, the offset did not have a significant impact on the insensitivity of the measurement system to typical terminal voltage fluctuations. (Prior to the introduction of the 5-cm detector, the transmission plateaux obtained under operating conditions established for the 2.5–cm detector were 4–8 kV wide; clearly, an offset of 3–4 kV between the terminal voltage of the actual center of the $^{14}C^{4+}$ transmission plateau and the expected terminal voltage based on scaling from $^{14}C^{4+}$ settings of the analyzing and switching magnets would have caused the measurement system to be quite sensitive to typical terminal voltage fluctuations.) The ~32 kV wide transmission plateaux under the 5-cm detector operating conditions show that the introduction of the 5-cm detector and associated modifications to the HE section made the transmission of $^{13}C^{4+}$ and $^{14}C^{4+}$ ions through the HE section of the system insensitive to typical terminal voltage fluctuations.

Automated measurement cycling.

Our ^{14}C measurements were made under an automated measurement cycling system that controlled the settings of the HE quadrupole and the 45° inflection and 90° analyzing magnets, the position of the Image cup, and the sample changer. Under our unique cycling scheme the automated system alternated between two adjacent targets in the sample wheel as well as between settings that allowed the measurement of $^{13}C^{4+}$ currents on the Image cup and settings that allowed the counting of $^{14}C^{4+}$ ions in the E–ΔE detector. During a routine measurement under this cycling scheme the $^{13}C^{4+}$ currents from an unknown sample target and then an adjacent Chinese Sucrose Standard target were measured, then the $^{14}C^{4+}$ ions from the unknown sample target and adjacent Chinese Sucrose Standard target were measured; this measurement cycle, which took about 3 min to complete, was repeated until the desired counting statistics uncertainty for the measurement had been reached. (The two targets involved in a routine measurement under this cycling scheme, the unknown sample and adjacent Chinese Sucrose Standard targets, are referred to as a measurement pair in discussions below.)

The ^{14}C concentration of the unknown sample was determined by normalization of the measured $^{14}C/^{13}C$ ratio of the unknown sample target to that of the Chinese Sucrose Standard target. Under our automated cycling scheme this normalization took place with each 3 minute measurement cycle, and thus, minor drifts of the measurement system that took place on longer time scales were corrected for by normalization to the Chinese Sucrose Standard. (i.e., slow drifts in any of many difficult-to-determine target-independent instrumental factors (such as isotopic fractionation in the ion source, fractionation effects in the stripper foil, and small transmission

differences between isotopes) over the 30–45 minutes required to measure a sample may introduce small variations in the $^{14}C/^{13}C$ ratios of the unknown and Chinese Sucrose targets over the course of a measurement, but the normalization of the $^{14}C/^{13}C$ ratio of the unknown target to the "concurrently" measured $^{14}C/^{13}C$ ratio of the Chinese Sucrose target would correct for the effects of these slow drifts).

Our method of "concurrent standard sample measurement" has the advantage of relatively short-timescale normalization compared to the measurement cycling schemes used in most AMS ^{14}C laboratories (in which the $^{14}C/^{13}C$ ratio of each target is measured separately, with each determination typically taking 200–500 s, and a standard target is measured between sets of 5–10 unknown samples (i.e., a standard sample is measured every 15–60 min)). However, our method has the disadvantage of requiring that each unknown target have at least one adjacent standard target in the target wheel.

In practice, each of our routine target sets consisted of 6–8 unknown targets, 7–9 Chinese Sucrose Standard targets, and several secondary standard targets to fill the 20 target capacity of the sample changer wheel. Under our cycling scheme, measurements on a target set containing 6–8 unknown targets required 16–20 h (during these measurements, each secondary standard and unknown target was measured at least twice (once against each of the adjacent Chinese Sucrose Standard targets) and often 3–4 times). The replacement of a measured target set with a new set required 4–6 h. (The ion source had to be cooled before the replacement and then restarted afterwards; the accelerator system stood idle but not shut down during this period.) Thus, a target set containing 6–8 unknown targets could be measured in ~24 h and the total sample throughput of the system over a 10 day measurement period was about 75 unknown targets.

2.2.4.2 Primary data from our AMS ^{14}C measurements.

Under our method of isotope and sample cycling, data collection during a routine sample measurement followed this sequence: 1) the $^{13}C^{4+}$ beam current from the first target of the measurement pair was integrated for 30 sec., 2) the automated cycling system shifted to the second sample of the measurement pair and the $^{13}C^{4+}$ beam current from the second target was integrated for 30 sec., 3) the system shifted to $^{14}C^{4+}$ settings and back to the first sample of the measurement pair and the $^{14}C^{4+}$ ions reaching the detector from the first target were counted for 30 sec., 4) the system shifted to the second sample of the measurement pair and the $^{14}C^{4+}$ ions from the second target were counted for 30 sec., and 5) the system shifted back to $^{13}C^{4+}$ settings and the first sample of the measurement pair and repeated the sequence. After

sufficient $^{14}C^{4+}$ counts had been obtained for the unknown sample, a final set of 30 sec-integrated $^{13}C^{4+}$ beam currents was obtained to complete the routine measurement data set. Figure 2.3 shows a typical cycle-by-cycle data set (25Jan93Run60).

The measurement data set produced was then input to an offline program which calculated $^{14}C/^{13}C$ ratios for each of the measurement pair samples and the normalized $^{14}C/^{13}C$ ratio of the unknown sample (i.e., the ratio of the unknown sample $^{14}C/^{13}C$ ratio to that of the standard sample). The offline program calculated these ratios in the following manner. First, the raw 30-sec-integrated $^{13}C^{4+}$ beam currents and the 30–sec $^{14}C^{4+}$ ion counts were converted to currents and count rates by dividing by the measured cycle period; in some cases the cycle period varied by one or two tenths of a second because of data collection interruptions due to tank sparks, etc. Then $^{14}C/^{13}C$ ratios for each of the measurement pair samples were calculated for each measurement cycle by dividing the $^{14}C^{4+}$ count rate for the *i*th cycle by the average of the $^{13}C^{4+}$ beam currents for the *i*th and the (*i*+1)th cycles. This averaging of the "before and after" $^{13}C^{4+}$ beam currents was primarily intended to correct for slow variations of the ion source output from targets during measurement cycling. The normalized $^{14}C/^{13}C$ ratio for the unknown sample was calculated for each cycle from the corresponding $^{14}C/^{13}C$ ratios for the unknown and standard in the measurement pair. Finally, the calculated ratios were averaged over the measurement cycles to produce unweighted and weighted mean values for the $^{14}C/^{13}C$ ratios of each of the measurement pair samples and the normalized $^{14}C/^{13}C$ ratio of the unknown sample.

Figure 2.4(25Jan93Run60) shows the cycle-by-cycle plots and final mean values produced by the offline program for the typical measurement data set presented in figure 2.3(25Jan93Run60). For the unweighted means, the quoted 1σ uncertainties in the means represent: (1) scatter — calculated from the scatter of the individual cycle ratios (i.e., standard deviation of cycle values divided by (number of cycles)$^{1/2}$), and (2) counts — calculated by standard error-propagation of the individual cycle counting statistics uncertainties. For the weighted means, the quoted 1σ uncertainties in the means represent the calculated weighted error based on the individual cycle counting statistics uncertainties.

To demonstrate the effectiveness of the "before and after" averaging of the $^{13}C^{4+}$ beam currents in correcting for slow changes of the ion source output of an ion source target, the offline program products for a not-so-routine measurement of an unknown sample are shown in figure 2.5(25Jan93Run57). During the course of this measurement the ion source output of the unknown sample dropped by more than 30% while the output of the standard sample remained constant to within ±3%. Despite this significant decline in output, neither the $^{14}C/^{13}C$ ratios for

the unknown sample nor the normalized $^{14}C/^{13}C$ ratios for the unknown/standard measurement pair obtained during the measurement show any evidence of a significant correlated trend, and the cycle-to-cycle variations in the ratios are within the scatter expected on the basis of the counting statistics estimates of the uncertainties in the ratios.

The normalized $^{14}C/^{13}C$ ratio for the unknown sample and associated 1σ uncertainties produced by the offline program were used in subsequent calculations leading to the ^{14}C ages of the unknown samples.

2.3 Calculation of ^{14}C Ages from Experimental Data.

In this section the methods used to calculate ^{14}C concentrations and corresponding ^{14}C ages from the normalized $^{14}C/^{13}C$ ratios obtained for unknown and secondary standard samples from the offline program will be described in detail. In these calculations the normalized $^{14}C/^{13}C$ ratios are first corrected for measurement background contributions and then converted to specific ^{14}C activity ratios, from which ^{14}C ages (and related measures of ^{14}C concentration) can be calculated. In the first part of this section, the background correction expression used in this study will be derived and then compared to other expressions currently used at other laboratories in correcting AMS measured ^{14}C ratios for measurement background contributions. The results of this comparison show that the expression obtained in this dissertation provides a more accurate correction for background contributions to the measured $^{14}C/^{13}C$ ratios than other, currently used expressions. In the second part of this section, the expression used to convert the background-corrected normalized $^{14}C/^{13}C$ ratios to specific ^{14}C activity ratios will be derived. Comparison of the expression obtained in this dissertation to expressions used in other studies will show that the expressions are essentially equivalent. And, finally, the expression used to calculated of ^{14}C ages from the specific ^{14}C activity ratios following the conventions of Stuiver and Polach (1977) will be given.

2.3.1 Correction of $^{14}C/^{13}C$ ratios for background contributions.

In calculating ^{14}C concentrations and corresponding ^{14}C ages for unknown samples from the normalized $^{14}C/^{13}C$ ratios, it is necessary to apply a correction for background contributions to the ratios. In previous studies of background levels in AMS ^{14}C measurements (Vogel *et al.*, 1986; Vogel *et al.* 1987b; Donahue *et al.*, 1990a), the dependence of the background on the mass of processed carbon sample has been shown to be consistent with the introduction of a constant mass of modern carbon during sample processing, e.g. Vogel *et al.* (1987b) found that

sample processing introduced the equivalent of 2.2 ±1.1 μg of modern carbon contaminant into their samples. Based on this model of the source of the background in our measurements I have derived a background correction formula for our measurements as follows:

Derivation of our background correction expression.

The contribution of a mass of carbon contaminant to the sample during processing can be described as the two-component mixing of one material with a particular $^{14}C/^{13}C$ ratio (the sample carbon) with another material with its own $^{14}C/^{13}C$ ratio (the contaminant carbon) and can be expressed as

$$\left(\frac{14}{13}\right)_x^M = \left(\frac{14}{13}\right)_x^A \left(1 - R_{cx}\right) + \left(\frac{14}{13}\right)_c R_{cx} \qquad (2.1)$$

where the superscript M denotes the $^{14}C/^{13}C$ ratio of the measured processed sample, the superscript A denotes the actual $^{14}C/^{13}C$ ratio of the sample, the subscript x denotes the unknown sample, the subscript c denotes the contaminant carbon, and R_c is the mass mixing ratio of the contaminant carbon in the processed sample. Since the source of the measurement background has been shown to be consistent with the addition of a constant mass of contaminant, then R_c will vary with processed sample size, increasing as the sample size decreases. Solving equation 2.1 for the actual $^{14}C/^{13}C$ ratio of the unknown sample gives

$$\left(\frac{14}{13}\right)_x^A = \left(\frac{14}{13}\right)_x^M \left[1 - \left(\frac{\left(\frac{14}{13}\right)_c}{\left(\frac{14}{13}\right)_x^M}\right) R_{cx}\right] \frac{1}{\left(1 - R_{cx}\right)} \qquad (2.2)$$

If a similar equation is derived for the standard sample in the measurement pair, the two equations can be combined and the background-corrected (actual) normalized $^{14}C/^{13}C$ ratio for the unknown sample can be expressed as

$$\frac{\left(\frac{14}{13}\right)_x^A}{\left(\frac{14}{13}\right)_s^A} = \frac{\left(\frac{14}{13}\right)_x^M}{\left(\frac{14}{13}\right)_s^M} \left[1 - \left(\frac{\left(\frac{14}{13}\right)_c}{\left(\frac{14}{13}\right)_x^M}\right) R_{cx}\right] \left[1 - \left(\frac{\left(\frac{14}{13}\right)_c}{\left(\frac{14}{13}\right)_s^M}\right) R_{cs}\right]^{-1} \frac{\left(1 - R_{cs}\right)}{\left(1 - R_{cx}\right)} \qquad (2.3)$$

where the subscript s denotes the standard sample. In order to proceed further, expressions for the mixing ratios in terms of measurable quantities are required.

The mixing ratio of the contaminant carbon in a processed sample can be determined through AMS ^{14}C measurements on processed subsamples of a ^{14}C-free (or at least of very low ^{14}C concentration) material and a secondary standard. Following equation 2.1, the two-component mixing of the ^{14}C-free material with the contaminant carbon can be expressed as

$$\left(\frac{14}{13}\right)_b^M = \left(\frac{14}{13}\right)_b^A \left(1 - R_{cb}\right) + \left(\frac{14}{13}\right)_c R_{cb} \qquad (2.4)$$

where the subscript b denotes the ^{14}C-free material. Using a similar expression for the two-component mixing of standard material and contaminant carbon and the fact that the $^{14}C/^{13}C$ ratio of the ^{14}C-free material is equal to zero, the ratio of the measured $^{14}C/^{13}C$ ratios for the background and standard samples can be expressed as

$$\frac{\left(\frac{14}{13}\right)_b^M}{\left(\frac{14}{13}\right)_s^M} = \frac{\left(\frac{14}{13}\right)_c R_{cb}}{\left(\frac{14}{13}\right)_s^A \left(1 - R_{cs}\right) + \left(\frac{14}{13}\right)_c R_{cs}} \qquad (2.5)$$

Since the amount of contaminant carbon sample introduced during sample processing is on the order of 1 to 5 μg of modern carbon equivalent, then for large standard samples (say 10 to 20 mg of carbon) R_{cs} will be very much less than one. Hence, equation 2.5 can be approximated as

$$\frac{\left(\frac{14}{13}\right)_b^M}{\left(\frac{14}{13}\right)_{s(L)}^M} = \frac{\left(\frac{14}{13}\right)_c}{\left(\frac{14}{13}\right)_s^A} R_{cb} \qquad (2.6)$$

where the subscript s(L) denotes a large standard sample.

In the same manner, the normalized $^{14}C/^{13}C$ ratio of the secondary standard can be expressed as

$$\frac{\left(\frac{14}{13}\right)_z^M}{\left(\frac{14}{13}\right)_{s(L)}^M} = \frac{\left(\frac{14}{13}\right)_z^A \left(1 - R_{cz}\right) + \left(\frac{14}{13}\right)_c R_{cz}}{\left(\frac{14}{13}\right)_s^A} \qquad (2.7)$$

where z denotes the secondary standard.

If the processed ^{14}C-free material and secondary standard samples are the same size, then R_{cz} is equal to R_{cb}, and solving both equation 2.6 and equation 2.7 for $(^{14}C/^{13}C)_c$ and equating the two expressions leads to

$$\frac{\left(\frac{14}{13}\right)_b^M \left(\frac{14}{13}\right)_s^A}{\left(\frac{14}{13}\right)_{s(L)}^M} = \frac{\left(\frac{14}{13}\right)_z^M \left(\frac{14}{13}\right)_s^A}{\left(\frac{14}{13}\right)_{s(L)}^M} - \left(\frac{14}{13}\right)_z^A (1 - R_c) \qquad (2.8)$$

This expression can be rearranged to give

$$R_c = 1 - \frac{\left(\frac{14}{13}\right)_s^A}{\left(\frac{14}{13}\right)_z^A} \left(\frac{\left(\frac{14}{13}\right)_z^M}{\left(\frac{14}{13}\right)_{s(L)}^M} - \frac{\left(\frac{14}{13}\right)_b^M}{\left(\frac{14}{13}\right)_{s(L)}^M} \right) \qquad (2.9)$$

If the secondary standard is now chosen to be equal to the standard (z was used as a convenience to help clarify the derivation), R_c can be expressed in terms of measurable quantities as

$$R_c(m) = 1 - \left(\frac{\left(\frac{14}{13}\right)_s^M (m)}{\left(\frac{14}{13}\right)_{s(L)}^M} - \frac{\left(\frac{14}{13}\right)_b^M (m)}{\left(\frac{14}{13}\right)_{s(L)}^M} \right) \qquad (2.10)$$

where (m) indicates that R_c and the measured $^{14}C/^{13}C$ ratios of the ^{14}C-free background material and the standard are functions of processed sample mass.

Similarly, setting R_{cz} equal to R_{cb} in equations 2.6 and 2.7, solving for R_c, and then equating the two expressions leads to the following expression for the $^{14}C/^{13}C$ ratio of the contaminant carbon normalized to that of the standard material:

$$\frac{\left(\frac{14}{13}\right)_c}{\left(\frac{14}{13}\right)_s^A} = \left[1 + \left(\left(1 - \frac{\left(\frac{14}{13}\right)_s^M (m)}{\left(\frac{14}{13}\right)_{s(L)}^M} \right) \left(\frac{\left(\frac{14}{13}\right)_b^M (m)}{\left(\frac{14}{13}\right)_{s(L)}^M} \right)^{-1} \right) \right]^{-1} \qquad (2.11)$$

Thus, $R_c(m)$ and the normalized $^{14}C/^{13}C$ ratio of the contaminant carbon can be determined from measurable quantities.

If $h_b(m)$ is defined to be the ratio of the measured $^{14}C/^{13}C$ ratio of a processed sample of ^{14}C–free material of mass m to the measured $^{14}C/^{13}C$ ratio of a large processed standard sample, then equation 2.6 can be reexpressed to give

$$h_b(m) \equiv \frac{\left(\frac{14}{13}\right)_b^M (m)}{\left(\frac{14}{13}\right)_{s(L)}^M} = \frac{\left(\frac{14}{13}\right)_c}{\left(\frac{14}{13}\right)_s^A} R_c(m) = C^{-1} R_c(m) \qquad (2.12)$$

where C^{-1} denotes the $^{14}C/^{13}C$ ratio of the contaminant carbon normalized to that of the standard material.

Using equation 2.12 and some algebraic manipulation, equation 2.3 can be rewritten as

$$\frac{\left(\frac{14}{13}\right)_x^A}{\left(\frac{14}{13}\right)_s^A} = \frac{\left(\frac{14}{13}\right)_x^M}{\left(\frac{14}{13}\right)_s^M} \left[1 - \left(\frac{\left(\frac{14}{13}\right)_c}{\left(\frac{14}{13}\right)_s^M} \right) \left(\frac{\left(\frac{14}{13}\right)_x^M}{\left(\frac{14}{13}\right)_s^M} \right)^{-1} Ch_{b_x} \right] \left[1 - \left(\frac{\left(\frac{14}{13}\right)_c}{\left(\frac{14}{13}\right)_s^M} \right) Ch_{b_s} \right]^{-1} \frac{(1-Ch_{b_s})}{(1-Ch_{b_x})} \qquad (2.13)$$

If equation 2.2 is rewritten for the standard sample and rearranged to give

$$\frac{\left(\frac{14}{13}\right)_s^A}{\left(\frac{14}{13}\right)_s^M} = \left(1 - \frac{\left(\frac{14}{13}\right)_c}{\left(\frac{14}{13}\right)_s^M} R_{cs} \right) (1 - R_{cs})^{-1} \qquad (2.14)$$

then equation 2.12 allows the measured $^{14}C/^{13}C$ ratio of the standard sample to be expressed as

$$\left(\frac{14}{13}\right)_s^M = \left(\frac{14}{13}\right)_s^A (1 - h_{b_s} (C - 1)) \qquad (2.15)$$

Substituting this expression into equation 2.13 and using equation 2.12 allows the background-corrected normalized $^{14}C/^{13}C$ ratio of the unknown sample to be expressed as

$$\frac{\left(\frac{14}{13}\right)_x^A}{\left(\frac{14}{13}\right)_s^A} = \frac{\left(\frac{14}{13}\right)_x^M}{\left(\frac{14}{13}\right)_s^M} \frac{\left[1 - \left(\frac{h_{b_x}}{(1- h_{b_s} (C - 1))} \right) \left(\frac{\left(\frac{14}{13}\right)_x^M}{\left(\frac{14}{13}\right)_s^M} \right)^{-1} \right]}{\left[1- \left(\frac{h_{b_s}}{(1- h_{b_s} (C - 1))} \right) \right]} \frac{(1 - Ch_{b_s})}{(1 - Ch_{b_x})} \qquad (2.16)$$

Thus, by measuring the normalized $^{14}C/^{13}C$ ratios of samples prepared from a ^{14}C-free material and a standard to determine h as a function of sample mass, the measured normalized $^{14}C/^{13}C$ ratios of unknown samples can be corrected for background contributions caused by

contamination introduced during sample processing.

Comparison to other background correction expressions.

Previously published background correction formulae fall into two basic groups. The simplest expressions involve the simple subtraction of measured $^{14}C/^{13}C$ ratios of presumably ^{14}C-free material from the measured $^{14}C/^{13}C$ ratio obtained for the unknown samples (e.g., Elmore *et al.* ,1984; Thomsen, 1990). As the end product of an extensive derivation, Donahue *et al.* (1990b) published a more complicated background correction expression,

$$F = F_m (1 + f) - f \qquad (2.17)$$

where F denotes the background corrected fraction modern carbon of the sample, F_m denotes the measured fraction modern carbon of the sample, and f denotes the ratio of the measured $^{14}C/^{13}C$ ratio of presumably ^{14}C-free material (Donahue *et al.* used "dead" graphite from NBS) to the $^{14}C/^{13}C$ ratio of the defined modern standard. Simple rearrangement of an expression given earlier by Gillespie and Hedges (1984) shows that it is essentially equivalent to Donahue *et al.* 's expression. Interestingly, if the measured $^{14}C/^{13}C$ ratio of a sample is equal to that obtained from ^{14}C-free material (i.e., $F_m = f$), then Donahue *et al.* 's expression gives a nonzero value for the background corrected fraction modern of the sample (i.e., $F = f^2$) even though the measured $^{14}C/^{13}C$ ratio provides no evidence of $^{14}C/^{13}C$ above background contamination levels.

In deriving their background correction expression, Donahue *et al.* (1990b) chose to normalize the measured $^{14}C/^{13}C$ ratios of the samples to the $^{14}C/^{13}C$ ratio of the defined modern standard and assumed that the $^{14}C/^{13}C$ ratio of contaminant carbon was equal to the $^{14}C/^{13}C$ ratio of the defined modern standard. If these conditions are applied to equation 2.16, then $(^{14}C/^{13}C)_c = (^{14}C/^{13}C)_s = (^{14}C/^{13}C)_{1950}$ implies that C = 1, and we obtain

$$\frac{\left(\frac{14}{13}\right)_x^A}{\left(\frac{14}{13}\right)_{1950}^A} = \frac{\left(\frac{14}{13}\right)_x^M}{\left(\frac{14}{13}\right)_{1950}} \frac{\left[1 - h_{b_x}\left(\frac{\left(\frac{14}{13}\right)_x^M}{\left(\frac{14}{13}\right)_{1950}}\right)^{-1}\right]}{\left(1 - h_{b_x}\right)} \qquad (2.18)$$

where the measured $^{14}C/^{13}C$ ratio of ^{14}C-free material has been normalized to $(^{14}C/^{13}C)_{1950}$ in determining h_x. Using the approximation $(1+h)^y \cong (1+yh)$ for $|h|<<1$ and the symbol definitions for equation 2.17 (i.e., $f = h_b$), equation 2.18 can be rewritten as

$$F = (F_m - f)(1 + f) = F_m(1 + f) - f - f^2 \qquad (2.19)$$

when $f<<1$. Hence, by dropping the $-f^2$ term, Donahue *et al.* 's expression can be obtained as an approximation to the two-component mixing expression derived above. Clearly, equation 2.19 and the two-component mixing expression give zero for the background corrected fraction modern of a sample whose measured $^{14}C/^{13}C$ ratio is equal to that obtained from ^{14}C-free material (i.e., F=0 for $F_m = f$).

In order to evaluate the consistency and reliability of these background correction expressions (the simple subtraction expressions, Donahue *et al.*'s expression, and the expression derived above), a set of "measured" $^{14}C/^{13}C$ ratios for unknown samples was generated using the two-component mixing model of the contamination process. The background correction expressions were then applied to these "measured" ratios to calculate "actual" $^{14}C/^{13}C$ ratios for the unknown samples, and these "actual" values were compared to the known $^{14}C/^{13}C$ ratios of the initial, uncontaminated materials that were used to generate the "measured" samples.

The "measured" $^{14}C/^{13}C$ ratios for the samples were generated by first assigning $^{14}C/^{13}C$ ratios to uncontaminated standard and "unknown" materials and to the contaminant material. Then, the amount of contaminant material to be mixed into the samples during processing was set (4 µg of contaminant material was used for the calculations presented here), mixing ratios were calculated for various processed sample sizes, and the two-component mixing model (i.e., equation 2.1) was used to calculate the "measured" $^{14}C/^{13}C$ ratios for the processed samples. This method was used to calculate "measured" $^{14}C/^{13}C$ ratios for processed samples which ranged in size from 10 mg to 10 µg, from 1.5 to 0.005 times the $^{14}C/^{13}C$ ratio of the standard material (if the standard is the defined modern standard, this is equivalent to radiocarbon ages ranging from about -3.3 ka BP to 43 ka BP), and over C values which ranged from 0.758 to 136 (using the defined modern standard, the C values represent contaminant carbon having $^{14}C/^{13}C$ ratios ranging from about 130 pMC to about 0.7 pMC (equivalent to a ^{14}C age of about 38 ka BP)).

The "actual" $^{14}C/^{13}C$ ratios were calculated from the modeled "measured" $^{14}C/^{13}C$ ratios using background correction expressions from the three basic groups discussed above: the simple subtraction expressions, Donahue *et al.* 's expression, and the two-component mixing expression derived above. The "actual" $^{14}C/^{13}C$ ratios were also calculated using an expanded version of Donahue *et al.* 's expression, in which the second order terms in the $(1+x)^y$ expansion were retained. (This expanded version was used to check for "truncated expansion" errors in the calculated "actual" $^{14}C/^{13}C$ ratios obtained from Donahue *et al.* 's expression.) For each of these

expressions, "actual" $^{14}C/^{13}C$ ratios were calculated using at least two variants of the expressions to reflect two normalization options that could be used in making routine AMS ^{14}C measurements. The specific formulae used in these calculations are given in table 2.2. The "actual" $^{14}C/^{13}C$ ratios calculated from the "measured" ratios using these expressions are compared to the known $^{14}C/^{13}C$ ratios of the initial, uncontaminated materials in figures 2.6 through 2.8.

Figure 2.6 shows the % difference of the calculated "actual" $^{14}C/^{13}C$ ratios obtained from the $^{14}C/^{13}C$ ratios of the initial, uncontaminated materials as a function of the $^{14}C/^{13}C$ ratio of the unknown sample for 1 mg and 100 μg samples with C = 1. Clearly, the significant offset of the values calculated by method 1b indicates that this method does not provide an acceptable background correction. The increasing difference with increasing unknown sample age for methods 2a and 2b and the lack of this increasing difference for methods 2aa and 2bb indicate that methods 2a and 2b suffer from errors introduced by the use of a truncated expansion, i.e., in methods 2a and 2b, $(1-f)^{-1} \cong (1+f)$ was used as the expansion and the $-f^2$ term was dropped; in methods 2aa and 2bb, another order was included in the expansion to give $(1-f)^{-1} \cong (1+f+f^2)$ and all terms were retained.

Figure 2.7 shows the % difference of the calculated "actual" $^{14}C/^{13}C$ ratios obtained from the $^{14}C/^{13}C$ ratios of the initial, uncontaminated materials as a function of the size of the unknown sample for samples with $^{14}C/^{13}C$ ratios equal to 1.0 and 0.1 times the $^{14}C/^{13}C$ ratio of the standard (i.e., modern and about 18.5 ka BP samples if the defined modern standard is used) and with C = 1. Again, method 1b does not provide an acceptable background correction and, for the 18.5 ka BP unknown sample, methods 2a and 2b suffer from truncated expansion errors that increase as the unknown sample size decreases. Methods 2aa and 2bb show possible evidence of truncated expansion error but this is only significant for the 10 μg sample.

Figure 2.8 shows the % difference of the calculated "actual" 14/13 ratios obtained from the $^{14}C/^{13}C$ ratios of the initial, uncontaminated materials as a function of C for 1) a 1 mg unknown sample with a $^{14}C/^{13}C$ ratio equal to 1.0 times the $^{14}C/^{13}C$ ratio of the standard (i.e., modern, if the defined modern standard is used), and for 2) a 100 μg unknown sample with a $^{14}C/^{13}C$ ratio equal to 0.1 times the $^{14}C/^{13}C$ ratio of the standard (i.e., about 18.5 ka BP, if the defined modern standard is used). The dependence of the background correction errors on C shown by methods 1b, 2b, and 2bb (all of which use a large standard sample for normalization), and the lack of such dependence for the corresponding "a" methods (which used a standard sample which was the same size as the unknown sample), suggest that these "b" methods do not correctly account for

the mass of contaminant carbon added to the unknown and standard samples during processing. That is to say that, while the subtraction and/or addition of $^{14}C/^{13}C$ ratios obtained for processed ^{14}C-free samples from the ratios obtained for the unknown and standard samples involved in methods 1 and 2 correctly account for the number of ^{14}C atoms per ^{13}C atom added to the sample during processing, these subtractions and/or additions do not correctly account for the total mass of added contaminant ^{13}C (and hence, the total mass of added contaminant carbon). The 4% difference (equivalent to an error of about 300 years) found for a 100 μg 18.5 ka BP sample under method 2b when the $^{14}C/^{13}C$ ratio of the contaminant carbon differed from that of the standard by only 30% suggests that errors introduced by using background correction equations based on the assumption that C=1 can be significant.

The above comparisons of the various background correction equations show that several of the methods produce estimates of the original $^{14}C/^{13}C$ ratios of the "unknown" samples that differ significantly from the known initial $^{14}C/^{13}C$ ratios of the samples. In terms of general use in routine AMS ^{14}C measurements, another important consideration in evaluating these methods is the amount of sample preparation and measurement time required to use the method; i.e., a background correction method that allows one to normalize the $^{14}C/^{13}C$ ratios obtained from many unknown samples to $^{14}C/^{13}C$ ratios obtained from standard targets that have been prepared from a single large standard sample is much more desirable than to have to measure a processed standard sample that is approximately the same size as each processed unknown sample that is measured. In fact, large processed standard samples are routinely used for normalization purposes in several AMS ^{14}C facilities, and methods similar to methods 1b and 2b above are used to correct for background contamination.

In the above comparisons of the background correction equations, method 3b was the only method based on normalization to large processed standard samples that produced estimates of the original $^{14}C/^{13}C$ ratios of the "unknown" samples that did not differ significantly from the known initial $^{14}C/^{13}C$ ratios of the "unknown" samples for any of the calculations. This suggests that the two-component mixing expression derived above is more appropriate for background correction of $^{14}C/^{13}C$ ratio measurements made by AMS than the expressions in general use at this time. The two-component mixing expression was used in correcting the measured $^{14}C/^{13}C$ ratios of the unknown and secondary standard samples in this research for background contamination during sample processing.

(The derivation of our background correction expression given above (which gave methods 3a and 3b) was constructed in terms of the measured $^{14}C/^{13}C$ ratios obtained from our AMS ^{14}C

system. An equivalent background correction expression for the measured $^{14}C/^{12}C$ ratios produced from some other AMS ^{14}C systems can be obtained following the same derivation with the trivial substitution of $^{14}C/^{12}C$ ratios for the $^{14}C/^{13}C$ ratios in the above derivation.)

Measurement background from charge-exchanged ions.

There is one other potential source of background in our measurements which we have not accounted for in these calculations; the erroneous identification and counting of charge-exchanged $^{13}C^{4+}$ ions as $^{14}C^{4+}$ ions (i.e. charge-exchanged $^{13}C^{4+}$ ions may produce E_{res} and ΔE signals that are indistinguishable from those of real $^{14}C^{4+}$ ions). In general, this source of background did not introduce significant error into the measured $^{14}C/^{13}C$ ratios for the samples in this study. The nature of this background and a method for correcting for it will be discussed in the section below concerning very low ^{14}C concentration materials that we have measured to determine the contribution of our measurement background to the $^{14}C/^{13}C$ ratios obtained for our samples.

2.3.2 Calculation of ^{14}C ages from background-corrected $^{14}C/^{13}C$ ratios.

The final step in obtaining ^{14}C ages from the measured $^{14}C/^{13}C$ ratios involves the conversion of the background-corrected $^{14}C/^{13}C$ ratios into the equivalent of the specific activity ratios that are appropriate for ^{14}C age calculations using the equation that defines the ^{14}C timescale (e.g., Stuiver and Polach, 1977).

In general, our measurements and background correction procedures have produced a $^{14}C/^{13}C$ ratio for an unknown sample, x, normalized to the $^{14}C/^{13}C$ ratio obtained for a standard sample, s. In addition, separate stable isotope measurements have produced $\delta^{13}C$ values for the unknown and standard samples of δ_x and δ_s per mil respectively. (The $\delta^{13}C$ values express the ^{13}C contents of the samples as fractional differences from the reference standard PDB under the standard definition of $\delta^{13}C$ values (e.g., Faure, 1986).) In the following I derive an expression which relates the normalized ratio we obtained for an unknown sample to the ratio of the ^{14}C specific activity of the unknown sample (normalized to $\delta^{13}C = -25$ per mil wrt PDB) and 0.95 times the ^{14}C specific activity of the NBS oxalic acid ^{14}C reference standard (normalized to $\delta^{13}C = -19$ per mil wrt PDB); ^{14}C ages are defined in terms of this ratio of specific activities.

The first step in this derivation is the conversion of the $^{14}C/^{13}C$ ratios to $^{14}C/^{12}C$ ratios, i.e.,

$$\left(\frac{14}{12}\right)^{A}_{x\,(\delta_x)} = \left(\frac{14}{13}\right)^{A}_{x\,(\delta_x)}\left(\frac{13}{12}\right)_{x\,(\delta_x)} = \left(\frac{14}{13}\right)^{A}_{x\,(\delta_x)}\left(1+\frac{\delta_x}{1000}\right)\left(\frac{13}{12}\right)_{PDB} \qquad (2.20)$$

where we have used the standard definition of the $\delta^{13}C$ expression (e.g, Faure, 1986), and the

PDB reference standard. This expression and a similar expression for the standard sample can be rearranged and combined to give

$$\frac{\left(\frac{14}{13}\right)^{A}_{x\,(\delta_x)}}{\left(\frac{14}{13}\right)^{A}_{s\,(\delta_s)}} = \frac{\left(\frac{14}{12}\right)^{A}_{x\,(\delta_x)}}{\left(\frac{14}{12}\right)^{A}_{s\,(\delta_s)}}\,\frac{\left(1+\frac{\delta_s}{1000}\right)}{\left(1+\frac{\delta_x}{1000}\right)} \qquad (2.21)$$

Since about 1% of natural carbon is ^{13}C and the range of variation in the $\delta^{13}C$ values of natural materials is about 0 to −70 per mil wrt PDB, the ratio of the $^{14}C/^{12}C$ ratios in equation 2.21 can be approximated to a few parts in 10^4 as

$$\frac{\left(\frac{14}{12}\right)^{A}_{x\,(\delta_x)}}{\left(\frac{14}{12}\right)^{A}_{s\,(\delta_s)}} \cong \frac{\left(\frac{14}{12+13}\right)^{A}_{x\,(\delta_x)}}{\left(\frac{14}{12+13}\right)^{A}_{s\,(\delta_s)}} \qquad (2.22)$$

The specific activity of a sample is proportional to the ratio of the number of ^{14}C atoms per gram of the sample to the total number of carbon atoms per gram of the sample. Hence, the $^{14}C/(^{12}C + ^{13}C)$ ratios in equation 2.22 are proportional to the specific activities of the samples and equation 2.21 can be rewritten as

$$\frac{\left(\frac{14}{13}\right)^{A}_{x\,(\delta_x)}}{\left(\frac{14}{13}\right)^{A}_{s\,(\delta_s)}} = \frac{A_{x\,(\delta_x)}}{A_{s\,(\delta_s)}}\,\frac{\left(1+\frac{\delta_s}{1000}\right)}{\left(1+\frac{\delta_x}{1000}\right)} \qquad (2.23)$$

where $A_{x(\delta x)}$ denotes the specific activity of the unknown sample with a $\delta^{13}C$ value of δ_x and $A_{s(\delta s)}$ denotes the specific activity of the standard sample with a $\delta^{13}C$ value of δ_s.

Following Stuiver and Polach (1977), the ^{14}C specific activity of the unknown sample normalized to a $\delta^{13}C$ value of –25 per mil is given by

$$A_x(-25) = A_x(\delta_x)\left[\frac{\left(1+\frac{-25}{1000}\right)}{\left(1+\frac{\delta_x}{1000}\right)}\right]^2 \qquad (2.24)$$

and the ^{14}C specific activity of the standard sample normalized to a $\delta^{13}C$ value of –19 per mil is given by

$$A_S(-19) = A_S(\delta_S)\left[\frac{\left(1+\frac{-19}{1000}\right)}{\left(1+\frac{\delta_S}{1000}\right)}\right]^2 \qquad (2.25)$$

Hence equation 2.23 can be rewritten as

$$\frac{\left(\frac{14}{13}\right)^A_X(\delta_X)}{\left(\frac{14}{13}\right)^A_S(\delta_S)} = \frac{A_X(-25)}{A_S(-19)}\left[\frac{0.981}{0.975}\right]^2\frac{\left(1+\frac{\delta_X}{1000}\right)}{\left(1+\frac{\delta_S}{1000}\right)} \qquad (2.26)$$

The only remaining part of this derivation is to relate the specific activity of the working standard, s, to the specific activity of the NBS oxalic acid ^{14}C reference standard (which is normalized to a $\delta^{13}C$ value of –19 per mil). In normal practice, the relationship between the specific activities of the working standards in common use and the oxalic acid standard have been established by previous high precision β-counting measurements, e.g.,

$$0.95\,A_{OX}(-19) = 0.7459\,A_{NOX}(-25) = B\,A_S(-19) \qquad (2.27)$$

where the subscript OX refers to the oxalic acid ^{14}C standard, the subscript NOX refers to the new oxalic acid ^{14}C standard, and B is the proportionality constant that relates a generalized working standard, s, to the oxalic acid ^{14}C standard. The relationship between the specific activities of the old and new oxalic acid standards was presented by Stuiver (1983).

Substituting an expression for $A_{S(-19)}$ in terms of $A_{OX(-19)}$ from equation 2.27 into equation 2.26 gives

$$\frac{\left(\frac{14}{13}\right)^A_X(\delta_X)}{\left(\frac{14}{13}\right)^A_S(\delta_S)} = B\,\frac{A_X(-25)}{0.95\,A_{OX}(-19)}\left[\frac{0.981}{0.975}\right]^2\frac{\left(1+\frac{\delta_X}{1000}\right)}{\left(1+\frac{\delta_S}{1000}\right)} \qquad (2.28)$$

and, hence, the normalized $^{14}C/^{13}C$ ratios for unknown samples obtained from the measurements and background correction procedures can be converted into the specific activities ratios needed to calculate ^{14}C ages using the expression

$$\frac{A_X(-25)}{0.95\,A_{OX}(-19)} = B^{-1}\left[\frac{0.975}{0.981}\right]^2\left[\frac{\left(1+\frac{\delta_S}{1000}\right)}{\left(1+\frac{\delta_X}{1000}\right)}\right]\frac{\left(\frac{14}{13}\right)^A_X(\delta_X)}{\left(\frac{14}{13}\right)^A_S(\delta_S)} \qquad (2.29)$$

This expression is essentially identical to an expression obtained by Thomsen (1990) via a very different derivation.

If the standard is chosen to be the NBS oxalic acid standard with $\delta^{13}C = -19$ per mil, then B = 0.95 and equation 2.29 can be rearranged to give the expression obtained by Donahue *et al.* (1990b) in an extensive derivation, i.e.,

$$\frac{A_X(-25)}{0.95\,A_{OX}(-19)} = \left[\frac{\frac{0.975}{\left(1+\frac{\delta_X}{1000}\right)}\left(\frac{14}{13}\right)^A_X(\delta_X)}{0.9558\,\left(\frac{14}{13}\right)^A_{OX}(-19)}\right] \qquad (2.30)$$

The value of B for the Chinese Sucrose working standard used for routine AMS ^{14}C measurements at the UW AMS ^{14}C facility can be calculated from previous high precision β-counting results obtained at the Quaternary Isotope Laboratory at the University of Washington (M. Stuiver, personal communication). From these results and $\delta^{13}C$ measurements, B = (0.95/1.3045) and $\delta_s = -19.25$ per mil for our Chinese Sucrose Standard.

The ^{14}C age of a sample can be calculated from the specific activities ratio in equation 2.29 using an expression derived from Stuiver and Polach (1977):

$$^{14}C\ \text{Age} = -8033\ \ln\left[\frac{A_X(-25)}{0.95\,A_{OX}(-19)}\right] \qquad (2.31)$$

The ^{14}C ages reported in this research were calculated using the following expression:

$$^{14}C\ \text{Age} = -8033\ \ln\left[1.3303\left(1+\frac{\delta_X}{1000}\right)^{-1}\frac{\left(\frac{14}{13}\right)^A_X(\delta_X)}{\left(\frac{14}{13}\right)^A_S(-19.25)}\right] \qquad (2.32)$$

which was obtained by substituting the specific activities ratio expression in equation 2.29 into equation 2.31. Related measures of the ^{14}C content of a sample, such as age-corrected $\Delta^{14}C$ and pMC, were calculated using the expression for the specific activities ratio in

equation 2.29 and the definitions and equations given by Stuiver and Polach (1977).

2.4 The Accuracy and Precision of Our AMS ^{14}C Measurements.

As mentioned above, the performance of an AMS ^{14}C system can be evaluated in terms of a wide variety of parameters. In addition to the performance measures related to the capabilities of the components of the system discussed above, other (and perhaps more fundamental) measures of system performance provide information on the reliability of the measurements made with the system. Clearly, the primary measure of the performance of a ^{14}C measurement system is the accuracy and precision to which one is able to measure the ^{14}C concentration of an unknown sample. In the following sections data will be presented which allow the measurement performance that has been attained with our AMS ^{14}C system to be evaluated.

During the period in which the samples for the research reported in this dissertation were measured several data sets were produced as a part of our ongoing program to evaluate the accuracy and precision of our AMS ^{14}C measurements. In particular, the measured $^{14}C/^{13}C$ ratio of our Chinese Sucrose Standard was monitored throughout the unknown measurements and repeated measurements were made on several secondary standards of "known" ^{14}C concentration. In addition, two or more ion source targets were measured for all secondary standards and almost all unknown samples. Following a brief discussion of the types of uncertainties in our AMS ^{14}C measurements, the data obtained from these sets of measurements will be used to evaluate the performance of the AMS ^{14}C system during this period.

In general, the precision of a measurement reflects the exactness to which the result has been determined and is normally indicated by an estimate of uncertainty given with the result (ideally, this estimate of uncertainty will also reflect the accuracy of the measurement). For our AMS ^{14}C measurements, we have used two methods of estimating the precision of the ^{14}C concentration determinations (these methods were mentioned briefly in section 2.2.4.2 above). The first method is based on normal error propagation of counting statistics estimates of the uncertainty in each measurement cycle to give estimated uncertainties for the $^{14}C/^{13}C$ ratios obtained for the samples. These counting statistics estimates are based on the discrete sampling of events that are randomly distributed in time ($^{14}C^{4+}$ ions being detected in the gas ionization detector) and, for our purposes, can be described by the Poisson probability distribution. These estimates will accurately describe the scatter in a series of measurements if the statistical fluctuations caused by the discrete sampling are the only source of uncertainty in the data.

Unfortunately, while such estimates are relatively easy to calculate for each measurement directly from the data obtained during that measurement, the counting statistics estimates may not reflect the true uncertainty in the measurements if variations are being introduced by other (non-Poisson) sources.

The second method for estimating the precision of the ^{14}C concentration determinations is based on the scatter in a series of repeated measurements of a sample, i.e., the standard deviation estimate of the uncertainty calculated from a series of $^{14}C/^{13}C$ ratios obtained for a sample. The standard deviation estimate is a measure of the actual scatter of the repeated measurements and, hence, provides an estimate of the total precision uncertainty in the result that includes the counting statistics contributions to the uncertainty as well as contributions from non-Poisson sources. Unfortunately, while the standard deviation estimate provides a measure of the true precision uncertainty in the results, it is not feasible to measure several targets of each unknown sample several times in order to obtain a statistically significant number of measurements for a standard deviation calculation for each unknown sample. Thus, the precision of the ^{14}C measurements is fundamentally limited by the counting statistics component of the uncertainty in the measurements, but the true uncertainty in the measurements may be larger than the counting statistics estimate because of contributions to the uncertainty from non-Poisson sources. Hence, evaluation of the precision of our ^{14}C measurements amounts to attempting to quantify the non-Poisson contributions to the uncertainty of the measurements and to showing that, if these contributions are significant, appropriate estimates that incorporate the non-Poisson contributions can be obtained for the true precision uncertainty in the measurements.

While counting statistics and standard deviation uncertainties provide estimates of the precision of our measurements, these uncertainties do not provide information on the accuracy of the results, i.e., counting statistics and standard deviation uncertainties provide information on the exactness of a measurement but not on how close a measured ^{14}C concentration is to the "true" ^{14}C concentration of the sample. The most straightforward method for evaluating the accuracy of the measurements is to measure the ^{14}C concentrations of secondary standards with "known" ^{14}C concentrations. Comparison of the measured and "known" ^{14}C concentrations allows limits to be placed on the magnitude of the inaccuracies in our results that may be introduced by systematic effects in our total measurement process. The final uncertainties that are assigned to individual results should reflect both the precision of the measurements and any systematic inaccuracies found in our measurements of "known" secondary standards.

2.4.1 Reproducibility of the Chinese Sucrose Standard $^{14}C/^{13}C$ ratios.

Operationally, one of the most easily accessible levels at which the performance of a AMS ^{14}C system can be evaluated is the reproducibility of the $^{14}C/^{13}C$ ratio of the standard used in the normalization of the measured $^{14}C/^{13}C$ ratios of the unknown targets. Under our cycling scheme the $^{14}C/^{13}C$ ratio of the Chinese Sucrose Standard was measured during the routine course of each unknown target measurement. Hence, the measured $^{14}C/^{13}C$ ratios of our Chinese Sucrose Standard provide an essentially continuous monitor of the consistency of the measurement system over the periods in which targets were measured.

The series of $^{14}C/^{13}C$ ratios obtained for the Chinese Sucrose Standard during the 12-day AMS ^{14}C measurement period which started on 25Jan93 is shown in figure 2.9. These 216 measurements were obtained from a total of 102 Chinese Sucrose Standard targets contained in 12 ion-source-target sets. Under our normal operating procedures the settings of the ion source and the accelerator system were checked at the beginning of measurements on each new target set, and adjusted when deemed appropriate to try to maintain optimum operating conditions. Since these adjustments may have caused subtle changes in ion production efficiencies, ion transmission efficiencies, etc., slight variations in the measured $^{14}C/^{13}C$ ratio for the Chinese Sucrose Standard targets would not be unexpected between target sets. Hence, the $^{14}C/^{13}C$ ratios in the series were divided into 12 subsets for independent statistical analysis; each subset consisted of the $^{14}C/^{13}C$ values obtained for a particular target set.

Two estimates of the uncertainty in a single $^{14}C/^{13}C$ ratio determination were calculated for each subset (as discussed above). The first was derived from the counting statistics estimates of the uncertainties in the individual $^{14}C/^{13}C$ ratio determinations. The second estimate was derived from the scatter of the individual $^{14}C/^{13}C$ ratio determinations in each subset, i.e., the standard deviation of the $^{14}C/^{13}C$ ratios in each subset. The values obtained for these two estimates are shown in figure 2.9 for a typical target set (Wheel #7).

When averaged over the 12 subsets, the typical 1σ counting statistics uncertainty of a single $^{14}C/^{13}C$ ratio determination in the subsets was 0.64% and the typical standard deviation estimate of the 1σ uncertainty in a single $^{14}C/^{13}C$ ratio determination was 0.69%. These values imply that counting statistics uncertainties account for almost all of the scatter in the measured Chinese Sucrose $^{14}C/^{13}C$ ratios from the 25Jan93 period; only 0.26% of the scatter could not be accounted for by counting statistics uncertainties (i.e., $0.069^2 - 0.064^2 = 0.026^2$).

Similar statistical analysis of the series of 148 $^{14}C/^{13}C$ ratios obtained from a total of 74 Chinese Sucrose Standard targets during the 9-day AMS ^{14}C measurement period which

started on 26May93 yielded an average 1σ counting statistics uncertainty for a single $^{14}C/^{13}C$ ratio determination of 0.59% and an average standard deviation estimate of the 1σ uncertainty in a typical single $^{14}C/^{13}C$ ratio determination of 0.67%. These values imply that about 0.32% of the scatter in our measured Chinese Sucrose $^{14}C/^{13}C$ ratios from the 26May93 period could not be accounted for by counting statistics uncertainties.

In considering the significance of these results, there are several aspects of our AMS ^{14}C measurement process that should be taken into account. First, each of the 8 to 10 Chinese Sucrose targets in each target set was generally measured at least twice to produce the 16 to 22 $^{14}C/^{13}C$ values in each subset. Therefore, any variations introduced by target to target differences contributed to the observed scatter of the $^{14}C/^{13}C$ values within a subset. Second, during routine operation of our measurement system the carbon stripper foils in the accelerator terminal had a useful measurement lifetime of 4–6 hours and were changed 3–5 times during the measurement of each target set. Therefore, any variations introduced by differences between stripper foils also contributed to the observed scatter of the $^{14}C/^{13}C$ values within a subset. Third, each of these $^{14}C/^{13}C$ values for the Chinese Sucrose Standard was obtained during routine measurement cycling at the same time as an unknown or secondary standard target was being measured. Thus, the variations of the $^{14}C/^{13}C$ values within these subsets are expected to be representative of the variations that would be found in unnormalized $^{14}C/^{13}C$ values obtained during routine measurements of unknown or secondary standard targets. For example, if the unnormalized $^{14}C/^{13}C$ ratio of an unknown sample were repeatedly determined to a counting statistics uncertainty of about 0.6%, the measured unnormalized $^{14}C/^{13}C$ values would scatter by about 0.67% ($(0.006^2 + 0.003^2)^{1/2}$).

As was discussed above, the four AMS ^{14}C measurement periods during which the unknown samples reported here were measured spanned a time during which significant modifications were made to our AMS ^{14}C system. One of the most important modifications during that time was the removal of the LE aperture at the image point of the 45° inflection magnet and the adjustment of the ion source einzel lens to maximize the C^- ion current at the LE cup. This modification was tested between the 05Oct92 and 25Jan93 AMS ^{14}C measurement periods and first used in routine measurements during the 25Jan93 period. The modification significantly increased the amount of C^- ion beam that could be transported from the ion source through the 45° inflection magnet and injected into the accelerator; the modification also significantly decreased the sensitivity of the C^- ion beam being injected into the accelerator to small changes in ion beam trajectory between the ion source and the accelerator entrance.

The effect of this modification on the $^{14}C/^{13}C$ ratios obtained for the Chinese Sucrose Standard can be seen clearly by comparing the data series obtained before the modification during the 10-day AMS ^{14}C measurement period which started on 05Oct92 (figure 2.10) to the data series obtained after the modification during the 25Jan93 period (figure 2.9). The 128 measurements obtained during the 05Oct92 period were from a total of 62 Chinese Sucrose Standard target in 7 target sets. Application of the same statistical analysis as used above for the 25Jan93 and 26May93 data series to the 7 target sets of the series obtained during the 05Oct92 period yielded an average 1σ counting statistics uncertainty for a single $^{14}C/^{13}C$ ratio determination of about 0.9% and an average standard deviation estimate of the 1σ uncertainty in a typical single $^{14}C/^{13}C$ ratio determination of about 1.2%. These values imply that about 0.8% of the scatter in the measured unnormalized Chinese Sucrose $^{14}C/^{13}C$ ratios from the 05Oct92 period cannot be accounted for by counting statistics uncertainties. Similar analysis of the 109 $^{14}C/^{13}C$ ratios obtained from a total of 53 Chinese Sucrose Standard targets during the 9-day AMS ^{14}C measurement period which started on 19Mar92 yielded results essentially identical to those obtained for the 05Oct92 period.

These results show that, before the modification of the ion beam transport from the ion source to the accelerator, the contribution of the non-Poisson component to the observed scatter of the $^{14}C/^{13}C$ ratios obtained for the Chinese Sucrose Standard was quite significant. In fact, for targets measured to a counting statistics uncertainty of about 0.9%, the uncertainty introduced by the non-Poisson component was almost as large as the counting statistics uncertainty. Clearly, the addition of a 0.8% non-Poisson component for each target in a measurement pair to the counting statistics estimates of the uncertainty in the normalized $^{14}C/^{13}C$ ratios obtained for the unknown and secondary standard targets measured during the 19Mar92 and 05Oct92 periods would contribute significantly to the estimated total uncertainty of the normalized $^{14}C/^{13}C$ ratios; e.g., if a normalized $^{14}C/^{13}C$ ratio with a counting statistics uncertainty of 1.2% was obtained for an unknown target, then the addition of a 0.8% non-Poisson component for each target in the measurement pair to the counting statistics uncertainty would produce a total uncertainty estimate for the normalized $^{14}C/^{13}C$ ratio of 1.6%.

However, as will be shown below during discussion of the normalized $^{14}C/^{13}C$ ratios obtained for multiple targets prepared from the unknown and secondary standard samples, there is evidence that a significant fraction (if not all) of the 0.8% non-Poisson component of the scatter in the unnormalized $^{14}C/^{13}C$ ratios must be correlated between targets in a measurement pair and, hence, that most of the 0.8% non-Poisson scatter component can be removed from the $^{14}C/^{13}C$

ratios for the unknown and secondary standard targets measured during the 19Mar92 and 05Oct92 periods by normalization of the $^{14}C/^{13}C$ ratio obtained for the unknown or secondary standard target to that obtained for the Chinese Sucrose Standard target in the measurement pair.

Information on the consistency of our AMS ^{14}C measurement system can also be obtained by examining the variations of the target-set-averaged $^{14}C/^{13}C$ values obtained for the Chinese Sucrose Standard over the course of an AMS ^{14}C measurement period. Figure 2.11 shows the 12 target-set-averaged $^{14}C/^{13}C$ values obtained for the Chinese Sucrose Standard during the 25Jan93 period. The standard deviation estimate of the uncertainty in an individual target-set-averaged $^{14}C/^{13}C$ value calculated from these data is 0.28% and the counting statistics estimate of the uncertainty in a typical target-set-averaged $^{14}C/^{13}C$ value is 0.17%. These uncertainty estimates imply that about 0.23% of the scatter in the target-set-averaged $^{14}C/^{13}C$ values from the 25Jan93 period cannot be accounted for by counting statistics uncertainties. Similar analysis of the target-set-averaged $^{14}C/^{13}C$ values obtained for the Chinese Sucrose Standard during the 26May93 period yielded essentially identical estimates of the uncertainty components.

Application of the same statistical analysis to the target-set-averaged $^{14}C/^{13}C$ values obtained for the Chinese Sucrose Standard during the 05Oct92 period (before the modification to the LE ion transport system) yielded a standard deviation estimate of the uncertainty in an individual target-set-averaged $^{14}C/^{13}C$ value of 0.82% and a counting statistics estimate of the uncertainty in a typical target-set-averaged $^{14}C/^{13}C$ value of 0.21%. These uncertainty estimates imply that about 0.79% of the scatter in the target-set-averaged $^{14}C/^{13}C$ values from the 05Oct92 period cannot be accounted for by counting statistics uncertainties. Similar analysis of the target-set-averaged $^{14}C/^{13}C$ values obtained for the Chinese Sucrose Standard during the 19Mar92 period (also before the modification to the LE ion transport system) yielded essentially identical estimates of the uncertainty components.

For all four periods, the magnitude of the non-Poisson component of the observed scatter in the target-set-averaged $^{14}C/^{13}C$ values was about the same as that of the non-Poisson component of the observed scatter within the target sets, i.e., about 0.8% for the 19Mar92 and 05Oct92 periods and about 0.3% for the 25Jan93 and 26May93 periods. As has been mentioned above, adjustments of the ion source and accelerator settings between target sets may have introduced some of the non-Poisson variations of the target-set-averaged $^{14}C/^{13}C$ values obtained for the Chinese Sucrose Standard during the periods. However, it is unclear why the target-set-averages of the 16–22 Chinese Sucrose $^{14}C/^{13}C$ values in each target set should

show the same amount of non-Poisson scatter as the Chinese Sucrose $^{14}C/^{13}C$ values within the target sets (especially with the substantial drop in the non-Poisson scatter within the target sets after the modification of the LE ion beam transport).

The averaging of the $^{14}C/^{13}C$ values obtained for the Chinese Sucrose Standard over each measurement period can also provide information on the long-term consistency of our AMS ^{14}C measurement system. The four AMS ^{14}C measurement periods during which the results reported in this dissertation were obtained spanned more than a year and were separated by months of accelerator use by other research groups. Hence, comparison of measurement-period-averaged $^{14}C/^{13}C$ values can provide information on the effects of these long periods of non-AMS use of the accelerator on the consistency of the AMS ^{14}C measurement system.

The measurement-period-averaged Chinese Sucrose $^{14}C/^{13}C$ values obtained for the four periods are given in table 2.3 along with standard deviation and counting statistic estimates of the uncertainty in these means. There are two prominent features of these data. First, the measurement-period-averaged $^{14}C/^{13}C$ values for the two periods after the modification to the LE ion beam transport are significantly (about 1.2%) higher than the values for the two periods before the modification. One possible explanation for this difference is that, with the modification of the LE ion beam transport, the characteristics of the ion beam injected into the accelerator better matched the acceptance characteristics of the rest of the transport system, resulting in improved transmission of $^{14}C^{4+}$ ions to the gas ionization detector. Second, the standard deviation scatter-based estimates of the uncertainty in the means dropped by a factor of 3–4 in going from the periods before the modification of the LE ion beam transport to the periods after the modification. This drop is in keeping with the decreases in the non-Poisson component of the observed scatter of the Chinese Sucrose $^{14}C/^{13}C$ values within target sets and between target sets discussed above.

Clearly, the effects of the modification of the LE ion beam transport system dominate the variations of the measurement-period-averaged Chinese Sucrose $^{14}C/^{13}C$ values over these four measurement periods. These effects effectively divide the four measurement periods into two sections each containing only two values and, hence, preclude any useful conclusions being drawn from statistical analysis of these measurement-period-averaged data.

2.4.2 Reproducibility of the unknown and secondary standard samples' $^{14}C/^{13}C$ ratios.

A second, and perhaps more important, level at which the precision of the measurements can be evaluated is the reproducibility of the normalized $^{14}C/^{13}C$ ratios obtained for unknown and secondary standard samples. The scatter of the normalized $^{14}C/^{13}C$ ratios obtained through

repeated measurement of targets prepared from a single sample reflects the total precision uncertainty in the final normalized $^{14}C/^{13}C$ ratios that will be used in subsequent ^{14}C age calculations. During the course of the four measurements periods, repeated measurements were made of each secondary standard and unknown target and, in most cases, more than one target was measured for each sample. Following a brief discussion of the methods used to extract information on the precision of our results from these repeated measurements, the data obtained for each of the four measurements periods will be used to evaluate the performance of our AMS ^{14}C system over the periods in which the unknown samples were measured.

The relationship between the expected scatter in a series of measurements that are thought to be governed by a particular probability distribution and the observed scatter in the measurements is quantified by the reduced chi-square statistic, χ_ν^2, which can be expressed as

$$\chi_\nu^2 = \frac{1}{(n-1)} \sum \left[\frac{(x_i - \bar{x})^2}{\sigma_i^2} \right]$$

where n denotes the number of measurements in the series, x_i denotes the value of the ith measurement, $\bar{x}$ denotes the mean of the measurements in the series, and σ_i denotes the estimated uncertainty assigned to the ith measurement under the particular probability distribution. The properties of the reduced chi-square statistic have been described previously (e.g., Bevington, 1969).

For the purposes of our analyses, the reduced chi-square statistic has been constructed to compare the observed scatter of the measurements with the expected scatter in the measurements based on counting statistics and non-Poisson estimates of the uncertainty in the measurements. Clearly, if the uncertainty estimates are based on counting statistics and $\chi_\nu^2 \cong 1$ then the observed scatter of the data is accurately described by the counting statistics estimates of the uncertainty in the measurements. If χ_ν^2 is consistently greater than one then the observed scatter in the measurements may be greater than expected from counting statistics, suggesting that the true uncertainty in the measurements contains a significant non-Poisson component. Alternatively, if an estimated non-Poisson component is added to the counting statistics estimates to give larger values for the σ_i's and the subsequently calculated values of χ_ν^2 are found to be consistently and significantly less than one, then the added non-Poisson component has led to values for the expected uncertainty in the measurements that are larger than is consistent with the observed scatter in the measurements.

In the following analysis the χ_ν^2 statistic will be used to evaluate the appropriateness of

counting statistics estimates of the uncertainty to describe the true precision of our measurements and, if necessary, to estimate the magnitude of any non-Poisson component that must be added to the counting statistics uncertainties to produce total uncertainty estimates that accurately describe the precision of the measurements.

Within each of the four measurement periods, at least two separate determinations were made of the normalized $^{14}C/^{13}C$ ratio of each measured secondary standard and unknown target, and two or more targets were measured for most samples. This repeated measurement of multiple targets for each sample produced 120 sets of measurements which each contained at least two (and more often 4–8) determinations of the normalized $^{14}C/^{13}C$ ratio of a secondary standard or unknown sample. (Since the secondary standard QL1567 was used as a system setup/checkout sample at the beginning of measurements on each target set, the data obtained for QL1567 have not been used in this analysis because of concerns that the scatter of the QL1567 values might also include variations caused by the initial adjustments of the AMS system settings made routinely at the beginning of measurements on each new target set.)

χ_ν^2 values were calculated for the normalized $^{14}C/^{13}C$ ratios in each of these measurement sets using two different estimates of the uncertainty, σ_i, in a given measurement. In one case the χ_ν^2 values were calculated using counting statistics estimates of the uncertainties in the ratios (χ_ν^2–cts). In the other case, the uncertainty estimates consisted of the counting statistics component of the uncertainty plus the non-Poisson uncertainty components determined above in the analysis of the observed variations of the unnormalized $^{14}C/^{13}C$ ratios during the four measurement periods (χ_ν^2–non-Poisson); a 0.8% non-Poisson component was added to the counting statistics estimates for each target in the measurement pairs of the 19Mar92 and 05Oct92 periods, and a 0.3% non-Poisson component was added for the 25Jan93 and 26May93 periods.

Each χ_ν^2 value was then used to determine the probability, P, that, if the measurements in a set were repeated, a χ_ν^2 value would be obtained that was larger than the value calculated from the original normalized $^{14}C/^{13}C$ ratios, i.e., the probability that repeating the measurements in a set would produce a set of normalized $^{14}C/^{13}C$ ratios that scattered more than the original set of ratios. Using these probabilities, the measurements sets from each period were divided into three groups: 1) $P \geq 32\%$, 2) $5\% \leq P < 32\%$, and 3) $P \leq 5\%$. The numbers of measurement sets falling into each of these groups in each measurement period for the χ_ν^2–cts and the χ_ν^2–non-Poisson values are given in table 2.4 along with overall totals for each of the three groups and the expected distribution of the overall totals.

The distribution of the overall totals of the probabilities derived from the χ_ν^2–cts values is reasonably consistent with the expected distribution of the totals, indicating that the scatter of the measurements within the measurement sets is, on average, consistent with the expected scatter in the measurements based on the counting statistics estimates of the uncertainty in the measurements. The distribution of the overall totals of the χ_ν^2–non-Poisson based probabilities shows that, on average, the measurements in a measurement set scatter less than would be expected based on the non-Poisson augmented estimates of the uncertainty in the measurements. While the limited number of measurement sets available for each of the measurement periods limit the certainty of conclusions based on these data, the distributions of the χ_ν^2–non-Poisson based probabilities obtained for the individual measurement periods suggest that the addition of a non-Poisson contribution of 0.8% to the counting statistics estimates of the uncertainties in the measurements of the 19Mar92 and 05Oct92 periods and 0.3% to the counting statistics estimates of the uncertainties in the measurements of the 25Jan93 period produced estimates of the total uncertainty in the measurements which are considerably larger than necessary to account for the observed scatter in the measurements.

If the numbers of measurement sets assigned to the probability groups for the 19Mar92 and 05Oct92 periods are totaled separately from those of the 25Jan93 and 26May93 periods then the following distributions can be obtained: 1) for the 51 measurement sets from the 19Mar92 and 05Oct92 periods the distribution of the χ_ν^2–cts derived probabilities in the three groups ($P \geq 32\%, 5\% \leq P < 32\%, P < 5\%$) is (65%,27%,8%) and the distribution of the χ_ν^2–0.8% non-Poisson probabilities is (84%,12%,4%), and 2) for the 69 measurement sets from the 25Jan93 and 26May93 periods the distribution of the χ_ν^2–cts derived probabilities is (64%,32%,4%) and the distribution of the χ_ν^2–0.3% non-Poisson probabilities is (72%,25%,3%).

Comparison of these results to the expected (68%,27%,5%) distribution clearly indicates that the addition of a 0.8% non-Poisson component to the counting statistics uncertainty estimates produces total uncertainty estimates for the combined 19Mar92 and 05Oct92 measurements which are larger than necessary to account for the actual scatter in the measurements. This implies that a significant fraction (if not all) of the 0.8% non-Poisson component of the scatter in the unnormalized $^{14}C/^{13}C$ ratios must be correlated between targets in each measurement pair, and hence, that most of the 0.8% non-Poisson scatter component is removed from the normalized $^{14}C/^{13}C$ ratios for the unknown and secondary standard targets by the normalization of the $^{14}C/^{13}C$ ratio obtained for the unknown or secondary standard target to the ratio obtained for the Chinese Sucrose Standard target in each measurement pair.

The results obtained for the combined 25Jan93 and 26May93 periods suggest that counting statistics uncertainty estimates are slightly smaller than necessary to account for the actual scatter in the measurements and that the addition of a 0.3% non-Poisson component to the counting statistics uncertainty estimates produces total uncertainty estimates that are slightly larger than necessary to account for the actual scatter in the measurements. Recalculation of the χ_ν^2–non-Poisson values for the measurements set of the 19Mar92 and 05Oct92 periods using a 0.3% non-Poisson uncertainty component (rather than the 0.8% component used above) produced a probabilities distribution (74%, 18%, 8%) which also suggests that the addition of a 0.3% non-Poisson component to the counting statistics uncertainty estimates produces total uncertainty estimates that are slightly larger than necessary to account for the actual scatter in the measurements.

Based on these results, and the data presented above concerning the variations in the unnormalized $^{14}C/^{13}C$ ratios obtained for the Chinese Sucrose Standard targets, a 0.3% non-Poisson component has been added to the counting statistics uncertainty estimate of each measurement pair target in deriving the total uncertainty estimates assigned to the normalized $^{14}C/^{13}C$ ratios obtained for our unknown and secondary standard targets. In adding this 0.3% uncertainty component for each of the targets in the measurement pair, the assumption has been made that the 0.3% non-Poisson uncertainty component for the unknown target was independent of the 0.3% component for the Chinese Sucrose Standard target; i.e., the effects that are causing the 0.3% non-Poisson component of the scatter in the observed unnormalized $^{14}C/^{13}C$ ratios are not correlated between targets in a measurement pair and, hence, the 0.3% non-Poisson scatter component would not be removed by the unknown/standard normalization. While the results above suggest that the non-Poisson contribution to the total uncertainty may be somewhat less than 0.3%, the 0.3% augmented uncertainty estimates provide an appropriately conservative estimate of the precision uncertainty of our measurements and are used as the total uncertainty estimates for all of the measurements on pollen extract samples presented in the following chapter.

2.4.3 Accuracy of the ^{14}C measurements on secondary standards.

As was mentioned above, the primary measure of the performance of a AMS ^{14}C measurement system is the accuracy and precision to which one is able to determine the ^{14}C concentration of an unknown sample. In order to further evaluate the accuracy and precision of our ^{14}C concentration measurements, repeated measurements were made of four secondary standard materials during the periods in which the unknown samples for the research reported in

this dissertation were measured. The ^{14}C concentration of two of these secondary standards had been previously measured by high-precision β-counting at the University of Washington Quaternary Isotope Laboratory. The other two secondary standards were part of the International Atomic Energy Agency ^{14}C Quality Assurance Program; consensus values for the ^{14}C concentrations of these materials obtained from measurements by many ^{14}C laboratories have been published (Rozanski *et al.*, 1992). In the following, the data obtained for each of the secondary standard samples will be presented and the results will be used to evaluate the performance of our AMS ^{14}C system over the periods in which the unknown samples were measured.

Secondary standard QL1567: 1964 A.D. growth-ring tree wood.

The secondary standard QL1567 was obtained from M. Stuiver as about 1.6 g of carbon as high purity CO_2 gas whose ^{14}C concentration had been determined by β-counting at the Quaternary Isotope Laboratory. The QL1567 gas was initially used as a working standard during early measurements with the UW NPL AMS ^{14}C system (before the research described in this dissertation began) but was relegated to the role of a secondary standard when the Chinese Sucrose working standard became available from the Quaternary Isotope Laboratory. The β–counting measurements yielded an age-corrected $\Delta^{14}C$ value (as defined by Stuiver and Polach (1977)) of 870 ± 10 per mil for the ^{14}C concentration of QL1567. The sample QL1567 was used extensively both as a secondary standard and as an ion source and accelerator system setup/checkout sample during all four of the periods in which the unknown samples for this research were measured. Typically, one or two subsamples of the QL1567 gas, each containing 10–25 mg of carbon, were reduced to graphite powder before each AMS ^{14}C measurement period and 20–50 QL1567 targets were made from the graphite powder for use during each period. At least one QL1567 target was included in every target set measured during the four periods, and at least one measurement (usually several measurements) of the normalized $^{14}C/^{13}C$ ratio of the QL1567 secondary standard was made during the measurement of each target set.

The age-corrected $\Delta^{14}C$ values obtained for the QL1567 secondary standard in the four measurement periods are given in table 2.5. All four of these age-corrected $\Delta^{14}C$ values agree with the value obtained by β-counting within the one sigma uncertainty of the β-counting value. The weighted mean of the four age-corrected $\Delta^{14}C$ values is 869.4 ± 2.4, which is

indistinguishable from the β-counting result (given above). The fractional uncertainty in the specific activities ratio of the QL1567 secondary standard corresponding to the uncertainty in the weighted mean $\Delta^{14}C$ value is 0.13%.

Reduced chi-square values for the normalized $^{14}C/^{13}C$ ratios obtained for QL1567 within each measurement period are also given in table 2.5. One set of the χ_ν^2 values has been calculated using counting statistics estimates of the uncertainty in each normalized $^{14}C/^{13}C$ ratio. These values show that the observed scatter in the normalized $^{14}C/^{13}C$ ratios is generally consistent the counting statistics estimates of the uncertainty in the measurements. The second set of χ_ν^2 values has been calculated using uncertainty estimates that incorporate non-Poisson components from the analysis of the variations of the unnormalized $^{14}C/^{13}C$ Chinese Sucrose ratios for each period above, i.e., a 0.8% non-Poisson component for each target in a measurement pair was added to the counting statistics estimates of the uncertainty in the normalized $^{14}C/^{13}C$ ratios obtained for the unknown targets for the 19Mar92 and 05Oct92 periods, and a 0.3% non-Poisson component for each target in a measurement pair was added for the 25Jan93 and 26May93 periods. The χ_ν^2 values obtained for the 19Mar92 and 05Oct92 periods indicate that the uncertainty estimates incorporating the 0.8% non-Poisson component for each target in a measurement pair are significantly larger than necessary to account for the observed scatter in the measurements. The χ_ν^2 values obtained for the 25Jan93 and 26May93 periods suggest that the uncertainty estimates incorporating the 0.3% non-Poisson component are somewhat larger than necessary to account for the observed scatter in the measurements. These χ_ν^2 results are in general agreement with the results obtained above from the evaluation of the reproducibility of the normalized $^{14}C/^{13}C$ ratios obtained for unknown and secondary standard targets.

Secondary standard QL11658: 5050-5060 B.C. growth-ring tree wood.

The secondary standard QL11658 was obtained from M. Stuiver as about 3.8 g of carbon as high purity CO_2 gas whose ^{14}C concentration had been determined by high precision β-counting at the Quaternary Isotope Laboratory during studies of past variation of the ^{14}C content of the atmosphere and establishment of a decadal calibration of the radiocarbon time scale (Stuiver and Becker, 1993 (page 64, 5055 BC sample)). The high precision β-counting measurements yielded a conventional ^{14}C age of 6120 ± 30 BP for QL11658. The sample QL11658 was measured during three of the periods in which the unknown samples for this research were measured. Typically, one or two 1–4 milligram subsamples of the QL11658 CO_2 gas were

reduced to graphite powder before each AMS ^{14}C measurement period and 6–20 QL11658 targets were made from the graphite powder for use during each period. The QL11658 targets were included in target sets during the three periods at convenient and opportune intervals, which were chosen to mix the measurements of the secondary standards throughout each measurement period.

The normalized $^{14}C/^{13}C$ ratios obtained for the QL11658 targets measured during the 05Oct92, 25Jan93 and 26May93 periods are shown in figure 2.12 and the conventional ^{14}C ages calculated from these data for each of the periods are given in table 2.6. All three of these conventional ^{14}C ages agree with the value obtained by high precision β-counting within one sigma uncertainties. The weighted mean of the three conventional ^{14}C ages is 6142 ± 29 BP, which is indistinguishable from the high precision β-counting result (given above). The fractional uncertainty in the specific activity ratio of the QL11658 secondary standard corresponding to the uncertainty in the weighted mean conventional ^{14}C age is 0.35%.

Reduced chi-square values for the normalized $^{14}C/^{13}C$ ratios obtained for QL11658 within each measurement period are also given in table 2.6. The set of χ_ν^2 values calculated using counting statistics estimates of the uncertainty in each normalized $^{14}C/^{13}C$ ratio shows that the observed scatter in the normalized $^{14}C/^{13}C$ ratios is consistent with the counting statistics estimates of the uncertainty in the measurements. The second set of χ_ν^2 values, which were calculated using uncertainty estimates that incorporate non-Poisson components from the analysis of the variations of the unnormalized $^{14}C/^{13}C$ Chinese Sucrose ratios for each period given above, shows that the observed scatter in the normalized $^{14}C/^{13}C$ ratios is not inconsistent with the augmented estimates of the uncertainty in the measurements. While these results do not provide any evidence that the scatter in the measurements is inconsistent with either set of total uncertainty estimates, the limited number of measurements of QL11658 in each of the measurement periods implies that caution must be used in attempting to draw conclusions based on these χ_ν^2 results.

Secondary standard IAEA C6: ANU Sucrose Secondary Standard.

The secondary standard IAEA C6 was obtained from M. Stuiver as about 25 g of purified sucrose granules. The sample was one of six intercomparison materials of the IAEA's ^{14}C Quality Assurance Program and consisted of the ANU Sucrose Secondary Standard (Currie and Polach, 1980). During the course of the IAEA ^{14}C Intercomparison Exercise 1990, the six intercomparison materials were distributed to many laboratories worldwide for measurement. The results of these measurements

were used to derive consensus values for the six intercomparison materials (Rozanski *et al.*, 1992). The consensus value obtained for the IAEA C6 intercomparison material from the 22 independent measurements that were accepted for inclusion in the consensus value calculation (17 reported measurements were rejected in the analysis of the submitted results) was 150.61±0.11 pMC (percent Modern Carbon as defined by Stuiver and Polach (1977)). The IAEA C6 sample was measured during two of the periods in which the unknown samples for this research were measured. Typically, one or two approximately 2 milligram subsamples of the IAEA C6 sucrose granules were oxidized to CO_2 by combustion and then reduced to graphite powder before each AMS ^{14}C measurement period and 2–6 IAEA C6 targets were made from the graphite powder for use during each period. The IAEA C6 targets were mixed into the target sets of the 25Jan93 and 26May93 periods at convenient and opportune intervals.

The normalized $^{14}C/^{13}C$ ratios obtained for the IAEA C6 targets measured during the 25Jan93 and 26May93 periods are shown in figure 2.13 and the pMC values calculated from these data for each of the periods are given in table 2.7. Both of these pMC values agree with the consensus value obtained for the IAEA C6 intercomparison material within the one sigma uncertainties. The weighted mean of the two pMC values is 150.88 ± 0.54, which is indistinguishable from the consensus value (given above). The fractional uncertainty in the specific activity ratio of the IAEA C6 secondary standard corresponding to the uncertainty in the weighted mean conventional ^{14}C age is 0.36%.

Reduced chi-square values for the normalized $^{14}C/^{13}C$ ratios obtained for IAEA C6 within each measurement period are also given in table 2.7. As above, the limited number within each period implies that caution must be used in attempting to draw conclusions based on these χ_ν^2 results. In this case, the two sets of χ_ν^2 values (counting statistics based or counting statistics plus non-Poisson based) do not provide any reliable evidence that the observed scatter in the normalized $^{14}C/^{13}C$ ratios is inconsistent with either set of uncertainty estimates.

Secondary standard IAEA C5: Subfossil wood.

The secondary standard IAEA C5 was obtained from M. Stuiver as about 15 g of preprocessed wood. The sample was another intercomparison material from the IAEA's ^{14}C Quality Assurance Program and consisted of subfossil wood from a buried bed forest in eastern Wisconsin, USA (Rozanski *et al.*, 1992). The consensus

value obtained for the IAEA C5 intercomparison material from the 49 independent measurements that were accepted for inclusion in the consensus value calculation (26 reported measurements were rejected in the analysis of the submitted results) was 23.05±0.02 pMC. The IAEA C5 sample was measured during the 25Jan93 and 26May93 periods. Subsamples of IAEA C5 wood were processed in the same manner as the IAEA C6 sucrose granules.

The pMC values calculated from the normalized $^{14}C/^{13}C$ ratios obtained for the IAEA C5 targets measured during the 25Jan93 and 26May93 periods are given in table 2.8. One of these pMC values agrees within the one sigma uncertainties with the consensus value for the IAEA C6 intercomparison material while the uncertainties of other value and the consensus value only overlap at the two sigma level. The weighted mean of the two pMC values is 22.79± 0.13 which overlaps the uncertainties in the consensus value at the two sigma level. The fractional uncertainty in the specific activity ratio of the IAEA C5 secondary standard corresponding to the uncertainty in the weighted mean conventional ^{14}C age is 0.57%.

Reduced chi-square values for the normalized $^{14}C/^{13}C$ ratios obtained for IAEA C5 within each measurement period are also given in table 2.8. Again, the limited number within each period implies that caution must be used in attempting to draw conclusions based on these χ_ν^2 results, and the two sets of χ_ν^2 values do not provide any reliable evidence that the observed scatter in the normalized $^{14}C/^{13}C$ ratios is inconsistent with either set of uncertainty estimates.

2.4.4 Summary of the accuracy and precision of our ^{14}C measurements.

Analyses of the reproducibility of the $^{14}C/^{13}C$ ratios obtained for the Chinese Sucrose Standard and the normalized $^{14}C/^{13}C$ ratios obtained for secondary standards and unknown samples show that counting statistics estimates of the precision uncertainty in our measurements account for almost all of the scatter in the measurements. These analyses show that non-Poisson sources contribute ≤0.3% to the scatter in the measured $^{14}C/^{13}C$ ratios. Based on these results, the total precision uncertainties in the normalized $^{14}C/^{13}C$ ratios obtained from our AMS ^{14}C measurements have been derived by the addition in quadrature of a 0.3% non-Poisson contribution to the counting statistics estimates of the uncertainties in each of the measured $^{14}C/^{13}C$ ratios. While analysis of the reproducibility of the normalized $^{14}C/^{13}C$ ratios obtained for secondary standards and unknown samples suggests that such augmented uncertainty estimates may slightly overestimate the actual precision uncertainty in the normalized $^{14}C/^{13}C$ ratios, these 0.3% augmented uncertainty estimates were used as appropriately conservative estimates of the precision uncertainty for all of the measurements on secondary standards

discussed above and for the samples obtained from the pollen extraction procedure presented in the following chapter.

Comparison of the ^{14}C results obtained in this study for four secondary standards to the results that had been obtained in previous measurements (high-precision β–counting or intercomparison consensus values) shows that our AMS ^{14}C measurements are accurate within the total precision uncertainty estimates discussed above. For three of the four samples, the ^{14}C result obtained in our measurements differ from the previously obtained results by less than the 1σ uncertainties in the measurements (which range from 0.36% to 0.13%); for the fourth sample, the ^{14}C result obtained in our measurements differs from the previously obtained result by just less than the 2σ uncertainty in the difference between our result and the previously obtained value. The scatter of the normalized $^{14}C/^{13}C$ ratios obtained for each of these secondary standards was not inconsistent with the expected scatter based on the total precision uncertainty estimates discussed above. These results show that inaccuracies in our AMS ^{14}C measurements amount to ≤0.3% and that the total precision uncertainty estimates discussed above provide accurate (if not somewhat conservative) estimates of the uncertainty in both the accuracy and the precision of our AMS ^{14}C measurements.

2.4.5 Measurement Background.

The $^{14}C/^{13}C$ ratio obtained for a target measured in our AMS ^{14}C system reflects not only the $^{14}C/^{13}C$ ratio of the unknown or standard material being measured but also the ^{14}C and ^{13}C contributed to the measured $^{14}C/^{13}C$ ratio by background sources such as sample contamination during processing, erroneous identification of $^{13}C^{4+}$ ions as $^{14}C^{4+}$ ions, ion source memory effects, etc. The calculation of accurate and precise ^{14}C concentrations and ages from measured $^{14}C/^{13}C$ ratios requires that the magnitude of the measurement background contribution to the ratios be determined and, if the measurement background is found to be significant, that the measured $^{14}C/^{13}C$ ratios be corrected to remove its contribution.

The method most commonly used to determine the magnitude of the measurement background has been the measurement of the $^{14}C/^{13}C$ ratios of targets prepared from ^{14}C-free (or at least very low ^{14}C concentration) materials (e.g., Grootes *et al.*, 1986; Vogel *et al.* 1986; Donahue *et al.*, 1990a). The $^{14}C/^{13}C$ ratios obtained from such targets provide a measure of the total ^{14}C and ^{13}C contributed by the various measurement background sources during the steps required to prepare and measure a sample by ^{14}C AMS.

Over the four measurement periods during which the samples for the research reported in this dissertation were measured, the $^{14}C/^{13}C$ ratios of targets prepared from five different

samples that were thought to have very low ^{14}C concentrations (i.e., were thought to be very old) were measured to determine the magnitude of the measurement background for our AMS ^{14}C measurement system. While these measurements were important in determining the magnitude of the measurement background of the system, it is worth noting here that an extensive study of the measurement background was not conducted for the research presented in this dissertation because the contribution of the measurement background to the relatively high $^{14}C/^{13}C$ ratios of the relatively young unknown samples measured for this research was almost negligible.

In a preceding section, I derived an expression which allows the correction of measured $^{14}C/^{13}C$ ratios for the contaminant carbon introduced during the processing steps required to produce an ion source target from a raw sample. The data obtained during the limited number of measurements of background samples during this dissertation research do not allow the full implementation of this expression; most of the background measurements were made on samples containing 1-4 mg of carbon and were not sufficient to determine the $^{14}C/^{13}C$ ratios of the standard and background material as functions of sample mass, and hence, did not allow the determination of $R_c(m)$ and C (see equations 2.10 and 2.11).

The measured $^{14}C/^{13}C$ ratios obtained for the secondary standards discussed above and for the unknown samples discussed in the following chapter were corrected for measurement background contributions by using the expression derived above (equation 2.16) with two assumptions: 1) that the $^{14}C/^{13}C$ ratio of the contaminant carbon was equal to that of the defined modern standard, and 2) that, given the almost negligible impact of the background correction on the results and the fact that almost all of the unknown samples contained 1–4 mg carbon, the values of h_b obtained from the measurements of 1–4 mg background samples during each of the periods could be averaged appropriately and used for both of the h_b values required to correct the normalized $^{14}C/^{13}C$ ratios obtained for the unknown samples (i.e., h_{bx} for the unknown sample and h_{bs} for the Chinese Sucrose Standard).

The five samples measured to determine the measurement background of our AMS ^{14}C system were:

Background Sample QL1428gas.

This background sample was obtained from M. Stuiver as about 5.7 grams of carbon as high purity CO_2 gas whose ^{14}C concentration had been previously determined by high precision β-counting at the Quaternary Isotope Laboratory by M. Stuiver. The high precision β-counting measurements yielded an upper limit on the ^{14}C concentration of the QL1428gas sample of <0.11 pMC (equivalent to a >55,000 BP

^{14}C age) (M. Stuiver, personal communication). During the measurement periods which preceded the four periods in which the results presented in this dissertation were obtained the QL1428gas sample had been used as our routine background sample; typically, one or more subsamples of the QL1428gas, each containing either ~1 mg or 15–25 mg of carbon, were reduced to graphite powder before each AMS ^{14}C measurement period and either 1–2 or 4–10 targets were made from the graphite powder produced from these samples, respectively, for use during each period. During the four measurement periods in which the results presented in this dissertation were obtained, the QL1428gas background sample was measured only during the 05Oct92 period; the QL1428gas sample was replaced as our routine measurement background sample with the QL1428wood sample (described below) because the preparation of the wood sample included the high temperature/CuO oxidation step that was expected to contribute significantly to the measurement background (e.g., Vogel *et al.* 1986) and was not required for the QL1428gas sample. For the 05Oct92 measurement period, a 1.2 mg carbon (as CO_2) subsample of the QL1428gas background sample was reduced by Fe/H_2 catalytic reduction and one target was prepared from the resulting graphite powder and measured during the period.

Background Sample QL1428wood.

The background sample QL1428wood was obtained from M. Stuiver as about 5 g of small wood fragments (1–4 mm long, ~1 mm wide and deep). This wood was a subsample of the parent, alkali-treated sample from which the QL1428gas subsample discussed above had been prepared. The QL1428wood sample was expected to have the same very low ^{14}C concentration as the QL1428gas sample (i.e., <0.11 pMC; equivalent to >55,000 BP). Typically, one or more 1–6 mg subsamples of the QL1428wood were converted to CO_2 by high temperature/CuO oxidation before each AMS ^{14}C measurement period; the 0.5–3 mg of carbon as CO_2 produced was reduced by Fe/H_2 catalytic reduction and 2–8 QL1428wood targets were made from the resulting graphite powder for use during each period.

Background Sample IAEA C1: carbonate (Carrara marble).

The background sample IAEA C1 was obtained from M. Stuiver as about 6 g of milled (dust-free 1.6–5.0 mm fraction) Carrara marble (carbonate). The sample was one of

the intercomparison material from the IAEA's ^{14}C Quality Assurance Program (Rozanski *et al.*, 1992). The consensus value obtained for the IAEA C1 intercomparison material from the 36 independent measurements that were accepted for inclusion in the consensus value calculation (37 reported measurements were rejected in the analysis of the submitted results) was 0.02±0.02 pMC. The IAEA C1 background sample was prepared for only the 26May93 measurement period; the 116.7 mg subsample of the IAEA C1 sample was converted to CO_2 by dissolution in 0.7 N HCl, the first half of the evolved CO_2 was collected and stored, the second half of the evolved CO_2 was collected (6.4 mg carbon as CO_2) and about half of this CO_2 (3.4 mg carbon) was converted to graphite powder by Fe/H_2 catalytic reduction. Two targets were made from the IAEA C1 graphite powder for use during the 26May93 measurement period.

Background Sample IAEA C4: subfossil wood.

The background sample IAEA C4 was obtained from M. Stuiver as about 10 g of preprocessed wood. The sample was another intercomparison material from the IAEA's ^{14}C Quality Assurance Program and consisted of subfossil wood excavated from peat bogs near Waikato on the North Island of New Zealand (Rozanski *et al.*, 1992). The consensus value obtained for the IAEA C4 intercomparison material from the 36 independent measurements that were accepted for inclusion in the consensus value calculation (43 reported measurements were rejected in the analysis of the submitted results) was 0.20–0.44 pMC (inconsistencies in the results obtained led Rozanski *et al.* (1992) to quote a 95% confidence interval for the sample rather than a weighted mean). The IAEA C4 background sample was prepared for only the 19Mar92 measurement period; a 2.2 mg subsample of the IAEA C4 sample was converted to CO_2 by high temperature/CuO oxidation and the CO_2 produced was converted to graphite powder by Fe/H_2 catalytic reduction. IAEA C4 targets were made from the graphite powder and one of the targets was measured during the 19Mar92 measurement period.

Background Sample Salmon Springs Peat.

The Salmon Springs Peat background sample was obtained from Prof. D. J. Huntley (Physics, Simon Fraser University) as several hundred grams of hard, dry peat. The sample had been taken from a hill-side exposure of a preserved peat layer in hills just

to the northeast of Sumner, Washington (47° 30′ N, 122° W) (Divigalpitiya, 1982). Previous carbon dating of the peat layer by thermal diffusion enrichment followed by β-counting gave a ^{14}C age of 71.5 (+1.7 –1.4) ka BP (QL110, Stuiver *et al.*, 1978). This ^{14}C age corresponds to a ^{14}C concentration of the Salmon Springs Peat sample of ~0.014 pMC. The Salmon Springs Peat sample was obtained for this study because it offered the opportunity of being able to prepare a true "chemical blank" background sample; i.e., the Salmon Springs Peat provided a pollen-rich, very old sample that should contain essentially no ^{14}C and from which pollen extract samples could be obtained following the same pollen extraction, oxidation and reduction steps that were used to prepare the pollen extracts from the samples of interest for the research presented in this dissertation. The pollen extraction procedures that will be discussed in the following chapter were used to extract two pollen fractions from a 40 g subsample of the Salmon Springs Peat. The carbon in subsamples of the 44<<88 μm and 20<<44 μm pollen extract fractions was converted to CO_2 by high temperature/CuO oxidation (producing 3.91 mg and 2.30 mg of carbon as CO_2, respectively) and then reduced to graphite powder; several targets were produced from the graphite powder for measurement during the 26May93 period.

The results obtained from the measurement of these samples during the four measurement periods are given in table 2.9. In general, the results obtained for the first three measurement periods are consistent with a measurement background of 0.2–0.5 pMC; the results obtained for the 26May93 period were affected by instrumental factors peculiar to that period and will be discussed separately below.

As was noted above, the ^{14}C concentration of the IAEA C4 sample was determined to be in the range 0.20–0.44 pMC under the IAEA's ^{14}C Quality Assurance Program. While the pMC value obtained in the 19Mar92 period, if corrected for a measurement background of ~0.35 pMC (about the middle of the 0.2-0.5 pMC range), would not be inconsistent with the quoted IAEA range, the measurable level of ^{14}C in the sample implies that deriving an estimate of the measurement background of our system from the value obtained for this sample requires that the contribution of the actual ^{14}C concentration of the sample (which is poorly known) be separated from the measurement background contribution. Hence, the value obtained for the IAEA C4 sample during the 19Mar92 period was not used in determining the measurement background of our system.

The 05Oct92 result for the QL1428gas background sample is consistent with the values of

about 0.21 ± 0.08 pMC (± 1 standard deviation) obtained during measurement periods prior to 19Mar92.

The higher values obtained for some of the QL1428wood targets suggest that the high temperature/CuO oxidation step did contribute significantly to the measurement background and that the contribution of this step (and/or some other factors) was somewhat variable during the 05Oct92 and 25Jan93 periods, resulting in significant variation in the pMC values obtained for various QL1428wood targets. Based on these results, the average of the values obtained for the QL1428wood targets during the 05Oct92 and 25Jan93 periods of 0.40 ± 0.15 pMC was used as the measurement background contribution in correcting the measurements on secondary standards discussed above and on unknown samples discussed in the following chapter. This measurement background corresponds to a background ^{14}C age of 44200 ± 3100 BP.

Measurement background from charge-exchanged $^{13}C^{4+}$ ions.

As was mentioned above, one of the potential sources of the measurement background in AMS ^{14}C measurements is the erroneous identification of charge-exchanged $^{13}C^{4+}$ ions as $^{14}C^{4+}$ ions. These charge-exchanged $^{13}C^{4+}$ ions are ions that were stripped to charge state 5+ in the terminal, and then, while being accelerated in the HE beamtube, picked up an electron through an interaction with a residual gas molecule in the beam tube to become $^{13}C^{4+}$ ions. If this charge-exchange interaction occurred at a particular point within the HE beam tube, the acceleration of the $^{13}C^{4+}$ ions through the remainder of the HE beamtube produces $^{13}C^{4+}$ ions which have the same magnetic rigidity as $^{14}C^{4+}$ ions that were stripped to the 4+ charge state in the terminal and transported unaltered to the detector.

The transport of these charge-exchanged $^{13}C^{4+}$ ions and the $^{14}C^{4+}$ ions through the purely magnetic elements of the HE beamline is identical; only the Wien filter (crossed E and B fields velocity selector) discriminates against the $^{13}C^{4+}$ ions (by deflecting them vertically upwards so that almost all of the charge-exchanged $^{13}C^{4+}$ ions strike an aperture plate, preventing them from entering enter the detector). However, a small fraction of the charge-exchanged $^{13}C^{4+}$ ions are not deflected sufficiently and do enter the detector; most of these ions have a higher total energy than the $^{14}C^{4+}$ ions and are clearly separable based on their E_{res} and ΔE signals. Unfortunately, a very small fraction of the charge-exchanged $^{13}C^{4+}$ ions can produce E_{res} and ΔE signals that are indistinguishable from those produced by the $^{14}C^{4+}$ ions.

Under our normal operating conditions the contribution of these ions to the measurement background of our system was small compared to the background of true $^{14}C^{4+}$ ions introduced by contamination during sample processing. However, during the 26May93 measurement period

the HE high vacuum cryopump at the exit of the accelerator did not operate properly (the pump essentially failed by the end of the period) and the pressure in the HE beamline and beamtube sections was 3–7 times the pressures that were observed when the pump was operating properly. Since the probability that a $^{13}C^{5+}$ ion will interact with a residual gas molecule in the HE beamtubes increases with the residual gas pressure in the beamtubes, the much higher pressures in the beamtubes due to the pump failure resulted in a significantly larger contribution of charge-exchanged $^{13}C^{4+}$ ions to the measurement background during the 26May93 period. This larger contribution is reflected in the higher measurement background values obtained during the 26May93 period, which have an average of 0.74 ± 0.13 pMC (equivalent to 39400 ± 1400 BP), compared to the background for the previous three periods discussed above (0.40 ± 0.15 pMC).

The data available through the NPL data acquisition system, which is used to identify and count the $^{14}C^{4+}$ ions entering the detector, can permit the number of erroneously identified $^{13}C^{4+}$ ions that have been counted as $^{14}C^{4+}$ ions to be estimated for a particular measurement if the appropriate data are recorded. Using such estimates, the measured $^{14}C/^{13}C$ ratios for three of the four background samples measured during the 26May93 period have been corrected for the contributions of the erroneously identified $^{13}C^{4+}$ ions and the resulting values are given in table 2.9 ("adjusted 26May93"). The average of these values is 0.36 ± 0.11 pMC (equivalent to 45200 ± 2400 BP) which is less than half of the measurement background before correction and is indistinguishable from the measurement background obtained above for the other three measurement periods.

Unfortunately, the data necessary to correct all of the measurements during the 26May93 period were not recorded. In order to properly correct a measured $^{14}C/^{13}C$ ratio of an unknown or secondary standard sample for both the charge-exchanged $^{13}C^{4+}$ and the sample processing contributions to the measurement background, the appropriate data have to be available for both the unknown or secondary standard and the background sample measurements; such data were recorded for only five of the unknown samples and three of the background samples measured during the period. Fortunately, however, the data on these eight samples do allow a comparison of the ^{14}C ages calculated for the unknown samples by either: 1) correcting the $^{14}C/^{13}C$ ratios from the unknown and background samples for the charge-exchanged $^{13}C^{4+}$ contributions and then using these charge-exchanged $^{13}C^{4+}$ corrected values in the calculating the ^{14}C age, or 2) not correcting the unknown or measurement background $^{14}C/^{13}C$ ratios for the charge-exchanged $^{13}C^{4+}$ contributions and using these uncorrected ratios in calculating the ^{14}C age.

(In the first calculation the correction for the charge-exchanged $^{13}C^{4+}$ contributions is explicit; in the second calculation the correction for the charge-exchanged $^{13}C^{4+}$ contributions is implicit.)

The ^{14}C ages obtained for the five unknown samples by these two methods are given in table 2.10. In all cases the difference between the ages obtained by the two calculational methods for each sample is not significant (in fact, for all of the pairs the difference between the ages is less than 1σ). This agreement between the ages obtained by the two methods implies that explicit correction of the measured $^{14}C/^{13}C$ ratios from the 26May93 period for the charge-exchanged $^{13}C^{4+}$ contributions to the measurement background is not required (nor is it possible since not all of the necessary data were recorded), and that the inclusion of the charge-exchanged $^{13}C^{4+}$ contributions in the formalism of correcting for measurement background contributions from contamination introduced during sample processing does not introduce significant errors in the calculated dates.

Based on these results, the average of the values obtained for the background sample targets measured during the 26May93 period of 0.74 ± 0.13 pMC (equivalent to 39400 ± 1400 BP) was used as the measurement background in correcting the measured $^{14}C/^{13}C$ ratios obtained from the secondary standards discussed above and from the unknown samples discussed in the following chapter.

The results obtained for the 44< <88 μm and 20< <44 μm pollen fractions from the Salmon Springs peat sample do not show any evidence of the introduction of significant amounts of ^{14}C during the pollen extraction procedure. The average of the results obtained for the QL1428wood and IAEA C1 samples is not statistically distinguishable from the average of the results for the two pollen fractions. Given the significant background determination difficulties during the 26May93 measurement period, there remains the possibility that some small amount of ^{14}C may have been introduced during the procedure, but the available data indicate that the amount introduced (if any) was certainly less than 30% of the ^{14}C introduced during the oxidation and reduction sample preparation steps. These results, obtained on a true "chemical blank" background sample for the pollen extraction procedure, show that the procedure is essentially "^{14}C clean" and that any ^{14}C introduced during the pollen extraction procedure will not have a significant impact on the ^{14}C ages obtained for the products of the pollen extraction procedure that will be discussed in the following chapter.

2.5 Summary.

Over the course of the research undertaken for this dissertation significant improvements

were made by our research group to many of the components of the AMS ^{14}C system at the University of Washington Nuclear Physics Laboratory. The most significant of these improvements were:

1) The development of Ta encapsulation equipment and procedures which allowed the preparation of consistent and reliable ion source sample targets that contained ~300 μg of sample carbon.

2) The reorganization of the transport of C^- ions through the LE section of the system which improved the overall transmission of the system by ~50% and eliminated the sensitivity of the system to small differences in ion beam trajectory between the ion source and the accelerator stripper foil for different ion source targets.

3) The construction and use of a 5-cm diameter ^{14}C detector (and associated adjustments to the HE ion transport system) which eliminated the sensitivity of ion transmission through the HE section of the AMS ^{14}C system to small fluctuations in the terminal voltage.

These improvements were directed towards (and were successful in) increasing the long-term stability and reliability of the measurement system and increasing the precision and accuracy of our ^{14}C measurements.

In conjunction with the improvements to the measurement system, the methods used to calculate ^{14}C ages from the $^{14}C/^{13}C$ ratios obtained in our measurements were examined in detail. In particular, consideration of the apparent source of the measurement background in our ^{14}C measurements (and in those made at other AMS ^{14}C laboratories) led to the derivation of a new background correction expression. Intercomparison of model results obtained using this expression and several background correction expressions that are currently used in other AMS ^{14}C laboratories showed that the expression derived here corrected for measurement background contributions from contaminants more accurately than the other, routinely used expressions.

Analyses of the scatter of the $^{14}C/^{13}C$ ratios obtained for the hundreds of Chinese Sucrose Standard, secondary standard, and unknown sample ion source targets measured over the course of the research presented in this dissertation showed that the estimates of the uncertainties in our ^{14}C measurements accurately described the true uncertainty in the measurements. These analyses showed that ≤0.3% of the scatter in the measurements could not be accounted for by (Poisson) counting statistics estimates of the precision uncertainties in our measurements (i.e., that non-Poisson sources of scatter contributed ≤0.3% to the observed

scatter in the measurements). In addition, the analyses of the results obtained on secondary standards allowed an upper limit of ~0.3% to be placed on any systematic inaccuracies in our measurements.

On the basis of these results, a 0.3% non-Poisson contribution was added to the counting statistics estimates of the uncertainties to provide somewhat conservative estimates of the total uncertainties in our measurements. Thus, for our typical $^{14}C/^{13}C$ measurements of approximately modern samples with ~0.6% counting statistics uncertainties, the inclusion of the 0.3% contribution from non-Poisson sources of scatter led to ~0.7% estimates of the total uncertainty in these measurements. In terms of ^{14}C ages obtained from our measurements, these results implied that our routine sets of four ~1.2% counting statistics uncertainty measurements on each ~6000 BP pollen fraction sample produced ^{14}C dates that had total uncertainties of ±50–60 years (which is equivalent to ~0.6–0.7%).

Study of $^{14}C/^{13}C$ ratios obtained for targets prepared from "^{14}C-free" materials showed that the measurement background of our AMS ^{14}C system for targets prepared from ~1 mg processed samples was equivalent to 0.40±0.15 pMC (equivalent to a measurement background ^{14}C age of 44200±3100 BP). While the contribution of this measurement background to the $^{14}C/^{13}C$ ratios obtained for standard and unknown sample targets was corrected for using the background correction expression derived in this dissertation, the fact that almost all of the samples measured in this research were ~1 mg carbon samples and were relatively young (< 10 ka BP) implied that such corrections were essentially negligible compared to the counting statistics uncertainties in the ^{14}C dates.

Taken together, the improvements made to our AMS ^{14}C system over the course of the research undertaken for this dissertation have resulted in significant improvements in the long-term stability and reliability of our measurement system and in the precision and accuracy of our ^{14}C measurements. These improvements were of particular significance to the results presented in the second half of this dissertation in that the decrease in the size of the sample required for AMS ^{14}C measurement and the improvements in the precision and accuracy of the measurements were necessary for the studies undertaken during the development, testing, and application of the pollen extraction and ^{14}C dating techniques described in the following chapter.

Figure 2.1 The University of Washington AMS ^{14}C System.

The layout of the primary components of the University of Washington AMS ^{14}C system is shown schematically. The roles of the various components in the production and transport of carbon ions from the ion source to the Faraday cups and ^{14}C detector are discussed in the text. (The ion source and LE components are discussed in section 2.2.2 and the accelerator, HE and ^{14}C detector components are discussed in section 2.2.3.) The figure indicates the general layout of the various components but is not to scale.

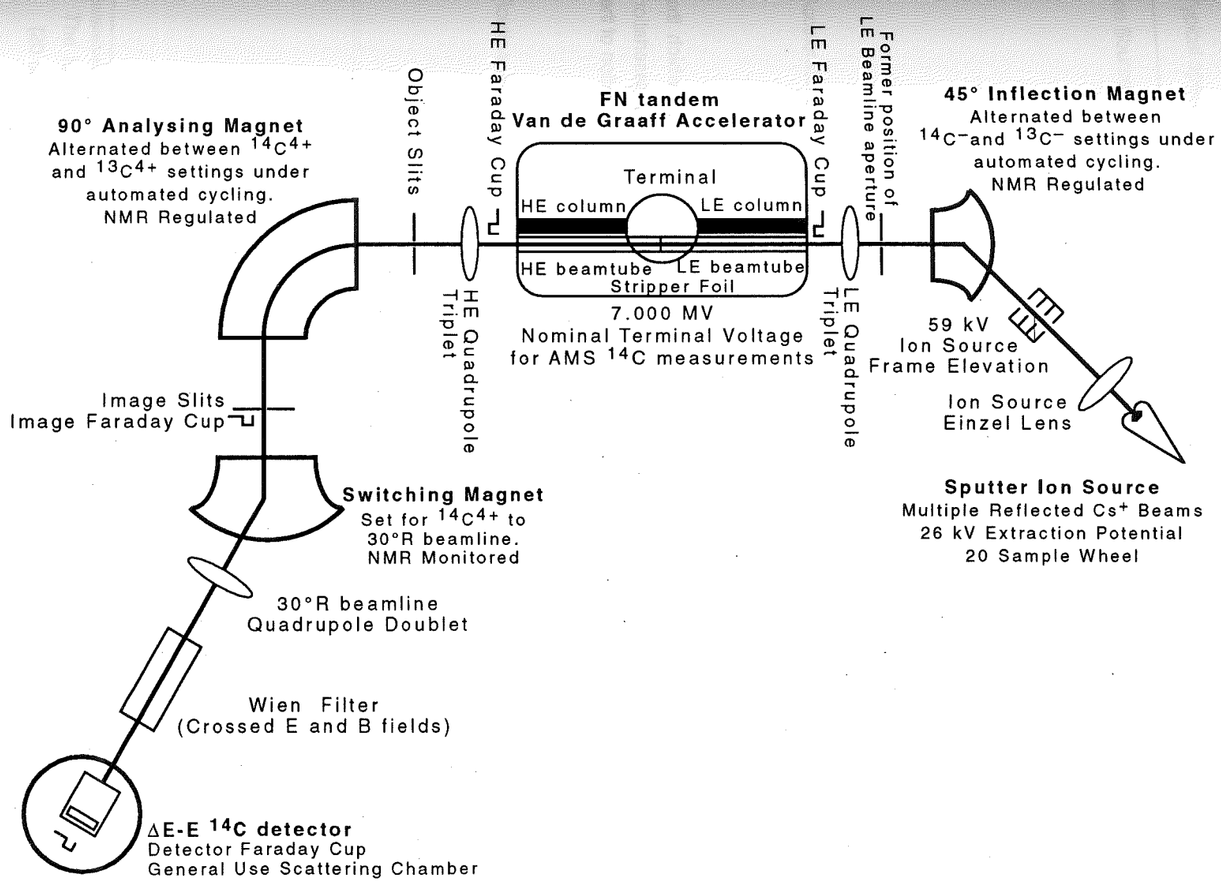

Table 2.1. Typical Operating Conditions of the AMS ^{14}C System.

The provided data are representative of the operating conditions under which the ^{14}C measurements of secondary standards and unknown samples discussed in this dissertation were obtained. Various aspects of the establishment of these conditions and the operation of the AMS ^{14}C system are discussed in the text (sections 2.2.2, 2.2.3 and 2.2.4).

Typical operating conditions of the University of Washington AMS ^{14}C system

Ion Source:	
Extraction potential	26 kV
Extraction current	0.6-0.8 mA
Elevation potential	59 kV
Ion beam output[1]	15-25 μA $^{12}C^-$
Sample size	~350 μg carbon
C^- ion production efficiency	about 5%
Accelerator and HE section:	
Terminal Potential	7.000 ± 0.003 MV
Stripper foil	carbon (2 μg/cm^2)
$^{13}C^{4+}$ current	300-500 nA
Modern carbon $^{14}C^{4+}$ count rate	45-75 cps
Transport efficiency (includes stripping loss)	about 40%
Routine unknown sample measurement:	
Measurement time	30-45 minutes
Repeated cycles	10-15
$^{14}C^{4+}$ counts for an approx. modern unknown	1.5 – 3.5 X10^4
$^{14}C^{4+}$ counts for Chinese Sucrose Standard	2 - 4 X10^4
Typical counting statistics uncertainty in a single measurement of an approx. modern unknown	8 - 9 ‰

[1] The ion source is purposely operated at low to medium output levels to ensure long-term (20 day), continuous, stable operation.

Figure 2.2 The $^{14}C^{4+}$ and $^{13}C^{4+}$ Transmission Profiles.

The transmission of $^{14}C^{4+}$ and $^{13}C^{4+}$ ions through the HE section of the AMS system is shown as a function of terminal voltage. The ion currents for the $^{13}C^{4+}$ profiles were measured using (open circles) the Image cup (a Faraday cup at the image position of the 90° analyzing magnet; the position at which $^{13}C^{4+}$ currents are measured during routine sample measurements) and (crosses) the Detector cup (a Faraday cup at the position of the ΔE-E ^{14}C detector). The vertical error bars on the $^{13}C^{4+}$ current data indicate the range of variation of the $^{13}C^{4+}$ current observed during the short period (~10 s) during which each datum was obtained. The $^{14}C^{4+}$ profile was obtained using our new 5-cm ΔE-E detector (I symbols; the height of the symbol indicates the counting statistics uncertainty (1σ) in the measured count rate). During routine measurements a suitable terminal voltage was selected and a data acceptance window of ±0.003 MV around that voltage was set.

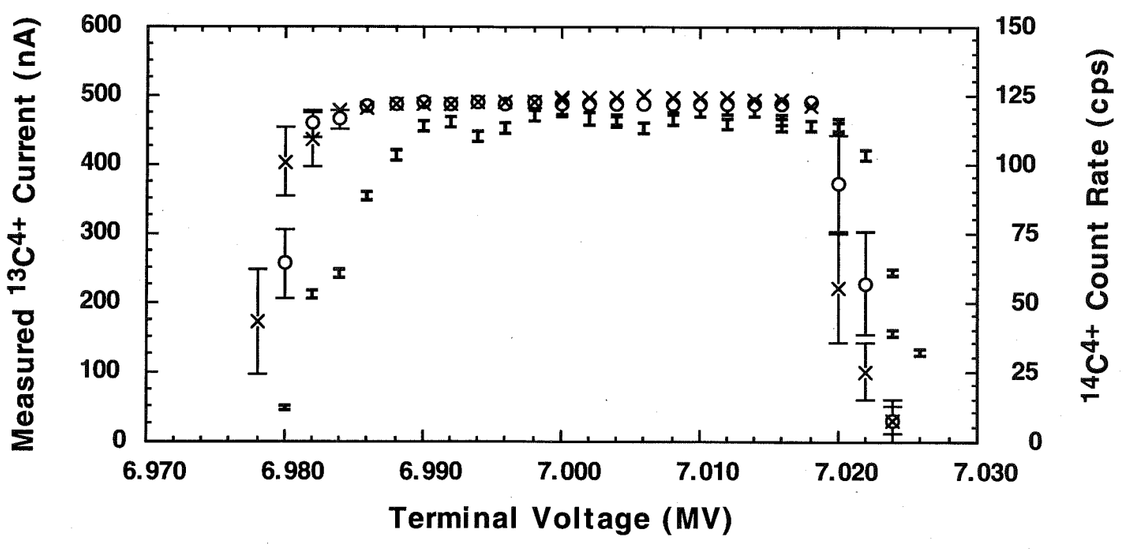

Figure 2.3. A Cycle-By-Cycle Data Set from a Typical Measurement (25Jan93Run60).

The primary data obtained during routine measurement cycling are shown for the pair of samples measured in the 60th run during the 25Jan93 measurement period. The upper two plots show the 30-sec-integrated $^{13}C^{4+}$ currents obtained for the unknown sample (TAB8GRL5) and the Chinese Sucrose Standard sample during each of the measurement cycles. The lower two plots show the numbers of $^{14}C^{4+}$ ions counted for the unknown and Chinese Sucrose Standard samples during each of the 30-sec measurement periods in each measurement cycle.

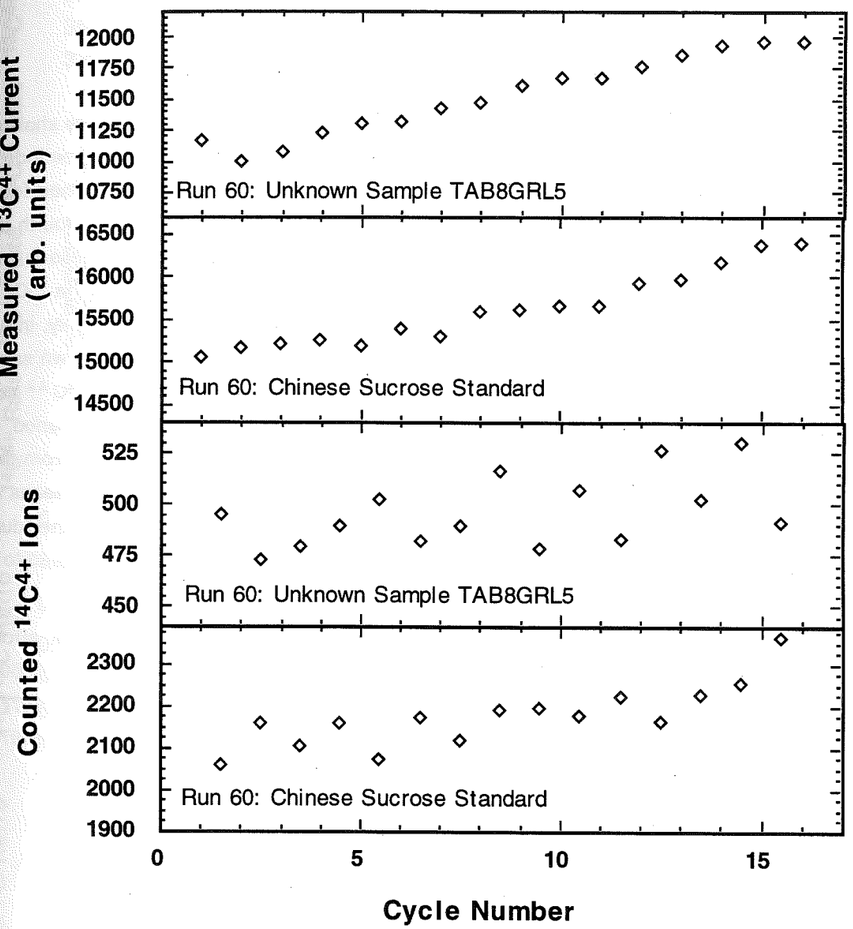

Figure 2.4. Offline Program Output from a Typical Measurement (25Jan93Run60).

The output obtained from the offline program (discussed in section 2.2.4.2) are shown for the pair of samples measured in the 60th run during the 25Jan93 measurement period. The upper two plots show the average $^{13}C^{4+}$ currents and $^{14}C^{4+}$ count rates obtained for the unknown sample (TAB8GRL5) in each 30-sec measurement cycle. The third and fourth plots show the average $^{13}C^{4+}$ currents and $^{14}C^{4+}$ ion count rates obtained for the Chinese Sucrose Standard sample in each 30-sec measurement cycle. The fifth and sixth plots show the $^{14}C/^{13}C$ ratios obtained for the unknown and Chinese Sucrose Standard samples, respectively, in each cycle. The final plot shows the normalized $^{14}C/^{13}C$ ratios obtained for the unknown sample during the 15 measurement cycles of the 60th run. The error bars for each of the $^{14}C^{4+}$ count rates are derived from the total number of $^{14}C^{4+}$ ions counted in the relevant 30-sec period. The error bars for the $^{14}C/^{13}C$ ratios and the normalized $^{14}C/^{13}C$ ratios are derived from these counting statistics estimates of the uncertainties in the $^{14}C^{4+}$ count rates. The means and uncertainties in the means for the unnormalized and normalized $^{14}C/^{13}C$ ratios obtained during the 60th run are as follows (the data are expressed in arbitrary units that are related to the $^{14}C^{4+}$ count rates and the $^{13}C^{4+}$ currents):

Sample	Unweighted Mean	±scatter	±counts	Weighted Mean	±Wtd error
Unknown	0.04309	0.00034	0.00050	0.04304	0.00050
Chinese Sucrose	0.13929	0.00067	0.00077	0.13926	0.00077
Normalized ratio	0.30953	0.00354	0.00398	0.30856	0.00397

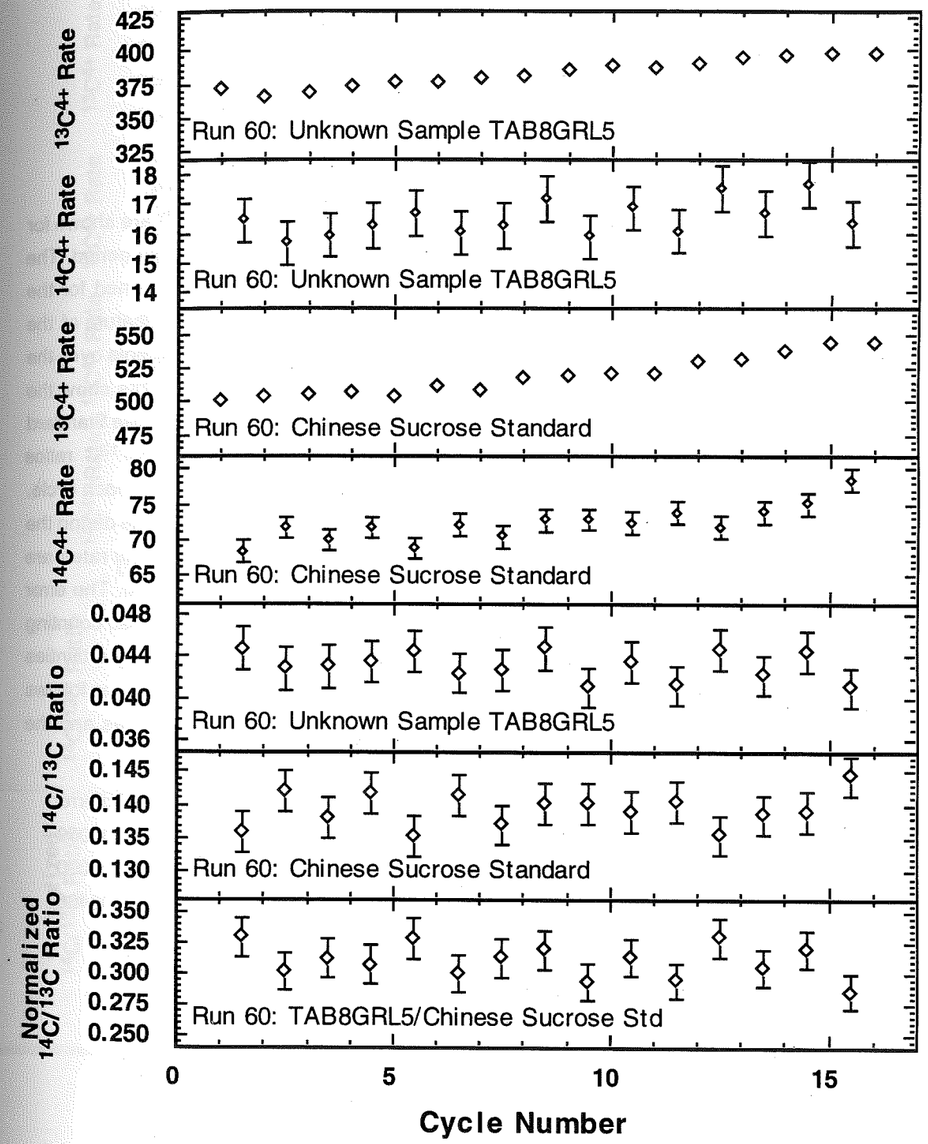

Figure 2.5: Offline Program Output from an Atypical Measurement (25Jan93Run57).

The output obtained from the offline program (discussed in section 2.2.4.2) are shown for the pair of samples measured in the 57th run during the 25Jan93 measurement period. The upper two plots show the average $^{13}C^{4+}$ currents and $^{14}C^{4+}$ count rates obtained for the unknown sample (TABRARB3) in each 30-sec measurement cycle. The atypical nature of the 57th run is indicated by the ~30% decrease in the output from the unknown sample over the course of the 13 measurements cycles of the 57th run. The third and fourth plots show the average $^{13}C^{4+}$ currents and $^{14}C^{4+}$ ion count rates obtained for the Chinese Sucrose Standard sample in each 30-sec measurement cycle. The fifth and sixth plots show the $^{14}C/^{13}C$ ratios obtained for the unknown and Chinese Sucrose Standard samples, respectively, in each cycle. The final plot shows the normalized $^{14}C/^{13}C$ ratios obtained for the unknown sample during the 13 measurement cycles of the 57th run. The error bars for each of the $^{14}C^{4+}$ count rates are derived from the total number of $^{14}C^{4+}$ ions counted in the relevant 30-sec period. The error bars for the $^{14}C/^{13}C$ ratios and the normalized $^{14}C/^{13}C$ ratios are derived from these counting statistics estimates of the uncertainties in the $^{14}C^{4+}$ count rates. The means and uncertainties for the unnormalized and normalized $^{14}C/^{13}C$ ratios obtained during the 57th run are as follows (the data are expressed in arbitrary units that are related to the $^{14}C^{4+}$ count rates and the $^{13}C^{4+}$ currents):

Sample	Unweighted Mean	±scatter	±counts	Weighted Mean	±Wtd error
Unknown	0.04928	0.00046	0.00059	0.04931	0.00059
Chinese Sucrose	0.13836	0.00060	0.00090	0.13833	0.00090
Normalized ratio	0.35623	0.00337	0.00488	0.35630	0.00486

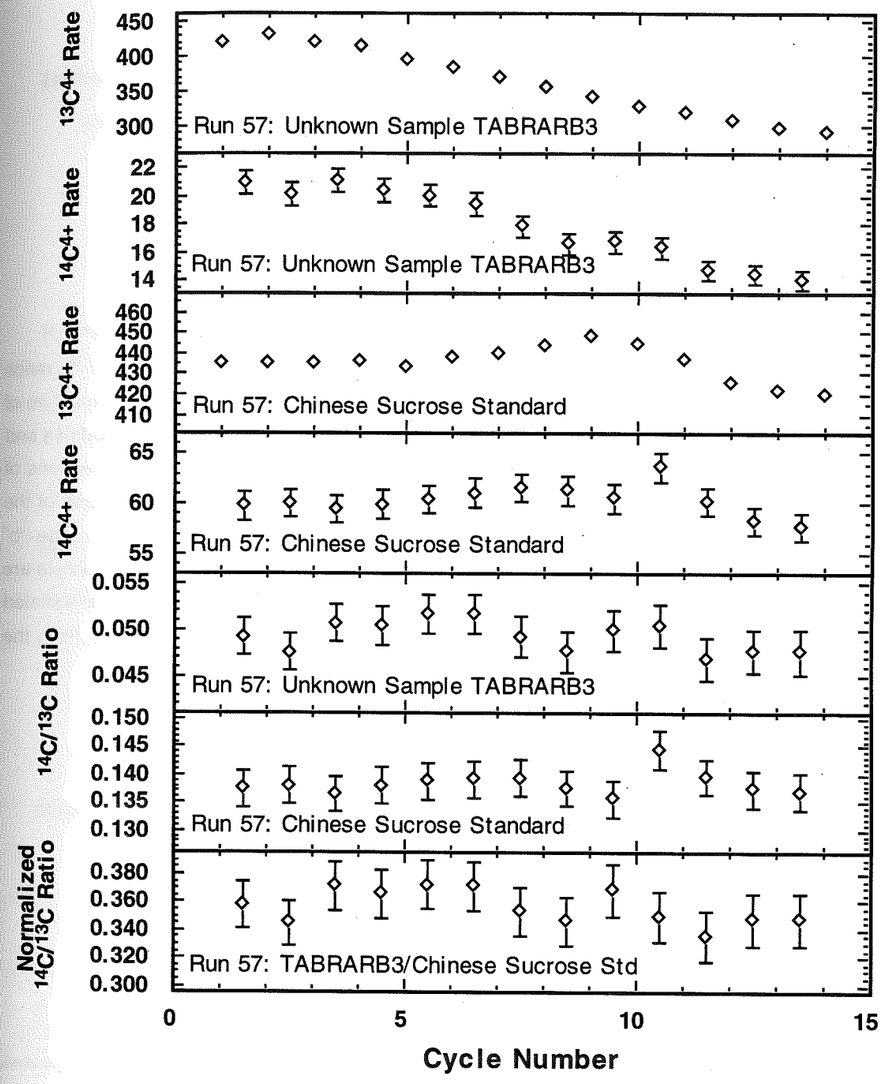

Table 2.2. Formulae for the Calculation of Background-Corrected $^{14}C/^{13}C$ Ratios.

Four of the background correction expressions used to calculate "actual" $^{14}C/^{13}C$ ratios from the modeled "measured" $^{14}C/^{13}C$ ratios are shown. These four expressions are from two of the three basic groups of such expressions discussed in the text. The first two (Methods 1a and 1b) are simple subtraction expressions. The second two (Methods 2a and 2b) are versions of Donahue *et al.*'s (1991) expression. In the "a" versions of methods 1 and 2 the masses of the unknown, standard and associated ^{14}C-free background samples are all equal. In the "b" versions of these methods the standard sample and associated ^{14}C-free background sample are large (10-20 mg) and of equal mass, while the mass of the unknown sample (and its associated ^{14}C-free background sample) is smaller (i.e., ~1 mg or less). The results obtained from the calculations involving these expressions are discussed in the text (section 2.3.1).

Method 1a. Simple subtraction with a standard sample which is the same size as the unknown sample.

$$\frac{\left(\frac{14}{13}\right)^{A}_{x}}{\left(\frac{14}{13}\right)^{A}_{s}} = \frac{\left(\frac{14}{13}\right)^{M}_{x}(m) - \left(\frac{14}{13}\right)^{M}_{b}(m)}{\left(\frac{14}{13}\right)^{M}_{s}(m) - \left(\frac{14}{13}\right)^{M}_{b}(m)}$$

Method 1b. Simple subtraction with a large standard sample.

$$\frac{\left(\frac{14}{13}\right)^{A}_{x}}{\left(\frac{14}{13}\right)^{A}_{s}} = \frac{\left(\frac{14}{13}\right)^{M}_{x}(m) - \left(\frac{14}{13}\right)^{M}_{b}(m)}{\left(\frac{14}{13}\right)^{M}_{s(L)} - \left(\frac{14}{13}\right)^{M}_{b(L)}}$$

Method 2a. Donahue *et al.*'s expression with a standard sample which is the same size as the unknown sample.

$$\frac{\left(\frac{14}{13}\right)^{A}_{x}}{\left(\frac{14}{13}\right)^{A}_{s}} = \frac{\left(\frac{14}{13}\right)^{M}_{x}(m)}{\left(\frac{14}{13}\right)^{M}_{s}(m)}(1+f) - f \; ; \; f = \frac{\left(\frac{14}{13}\right)^{M}_{b}(m)}{\left(\frac{14}{13}\right)^{M}_{s}(m)}$$

Method 2b. Donahue *et al.*'s expression with a large standard sample.

$$\frac{\left(\frac{14}{13}\right)^{A}_{x}}{\left(\frac{14}{13}\right)^{A}_{s}} = \frac{\left(\frac{14}{13}\right)^{M}_{x}(m)}{\left(\frac{14}{13}\right)^{M}_{s(L)}}(1+f) - f \; ; \; f = \frac{\left(\frac{14}{13}\right)^{M}_{b}(m)}{\left(\frac{14}{13}\right)^{M}_{s(L)}}$$

Table 2.2. (Continued) Formulae for the Calculation of Background-Corrected $^{14}C/^{13}C$ Ratios.

Four of the background correction expressions used to calculate "actual" $^{14}C/^{13}C$ ratios from the modeled "measured" $^{14}C/^{13}C$ ratios are shown. These four expressions are from two of the three basic groups of such expressions discussed in the text. The first two (Methods 2aa and 2bb) are expanded versions of Donahue *et al.*'s (1991) expression, in which the second order terms in the $(1+x)^y$ expansion were retained (discussed in section 2.3.1). The second two (Methods 3a and 3b) are versions of the background correction expression derived in section 2.3.1. In methods 2aa and 3a the masses of the unknown, standard and associated ^{14}C-free background samples are all equal. In methods 2bb and 3b the standard sample and associated ^{14}C-free background sample are large (10-20 mg) and of equal mass, while the masses of the unknown sample and its associated ^{14}C-free background sample are smaller (i.e., ~1 mg or less). The results obtained from the calculations involving these expressions are discussed in the text (section 2.3.1).

Method 2aa. An expanded version of Donahue *et al.*'s expression with a standard sample which is the same size as the unknown sample.

$$\frac{\left(\frac{14}{13}\right)^{A}_{x}}{\left(\frac{14}{13}\right)^{A}_{s}} = \frac{\left(\frac{14}{13}\right)^{M}_{x}(m)}{\left(\frac{14}{13}\right)^{M}_{s}(m)}\left(1+f+f^2\right) - f\left(1+f+f^2\right) \; ; \; f = \frac{\left(\frac{14}{13}\right)^{M}_{b}(m)}{\left(\frac{14}{13}\right)^{M}_{s}(m)}$$

Method 2bb. An expanded version of Donahue *et al.*'s expression with a large standard sample.

$$\frac{\left(\frac{14}{13}\right)^{A}_{x}}{\left(\frac{14}{13}\right)^{A}_{s}} = \frac{\left(\frac{14}{13}\right)^{M}_{x}(m)}{\left(\frac{14}{13}\right)^{M}_{s(L)}}\left(1+f+f^2\right) - f\left(1+f+f^2\right) \; ; \; f = \frac{\left(\frac{14}{13}\right)^{M}_{b}(m)}{\left(\frac{14}{13}\right)^{M}_{s(L)}}$$

Method 3a. Two component mixing expression with a standard sample which is the same size as the unknown sample.

$$\text{Equation 2.16 with } h_{b_x} = h_{b_s} = \frac{\left(\frac{14}{13}\right)^{M}_{b}(m)}{\left(\frac{14}{13}\right)^{M}_{s(L)}}$$

(The standard measured for the normalization of the $^{14}C/^{13}C$ ratio obtained from the unknown sample was the same size as the unknown sample, but the standard used in determining the appropriate h_b value for these samples was large (i.e., s(L)).)

Method 3b. Two component mixing expression with a large standard sample.

$$\text{Equation 2.16 with } h_{b_x} = \frac{\left(\frac{14}{13}\right)^{M}_{b}(m)}{\left(\frac{14}{13}\right)^{M}_{s(L)}} \text{ and } h_{b_s} = \frac{\left(\frac{14}{13}\right)^{M}_{b(L)}(m)}{\left(\frac{14}{13}\right)^{M}_{s(L)}}$$

Figure 2.6. Percent Difference as a Function of Sample ^{14}C Age.

The percent differences between the "actual" $^{14}C/^{13}C$ ratios calculated for the modeled samples using the various background correction expressions (table 2.2) and the initial, uncontaminated $^{14}C/^{13}C$ ratios of the model materials are shown as a function of sample ^{14}C age for (a) a 1.0 mg sample, and (b) a 0.1 mg sample. The $^{14}C/^{13}C$ ratio of the contaminant carbon was set equal to that of the standard for these calculations (i.e., C=1). The data symbols mark the points at which the percent differences were calculated; the lines between data points are drawn to indicate the trends of the data points obtained from each of the 8 background correction methods discussed in the text. The background correction method used to produce each set of percent difference data is indicated by the method designators from table 2.2 associated with each of the curves (e.g., 1b).

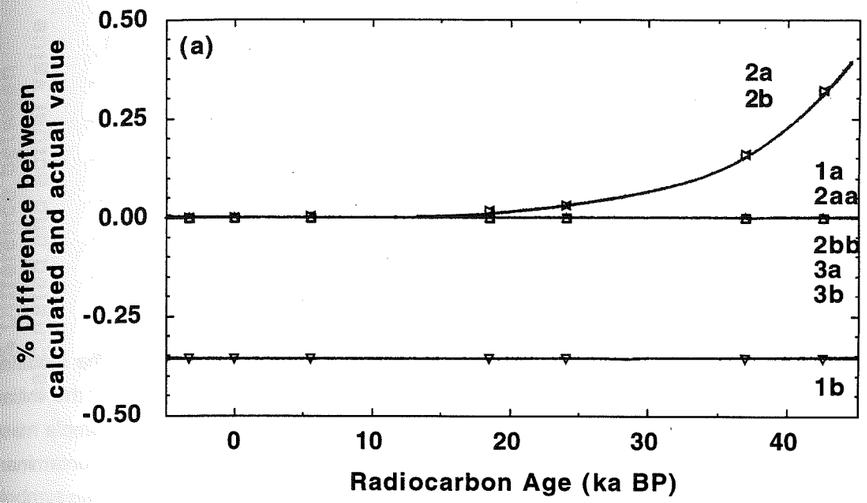

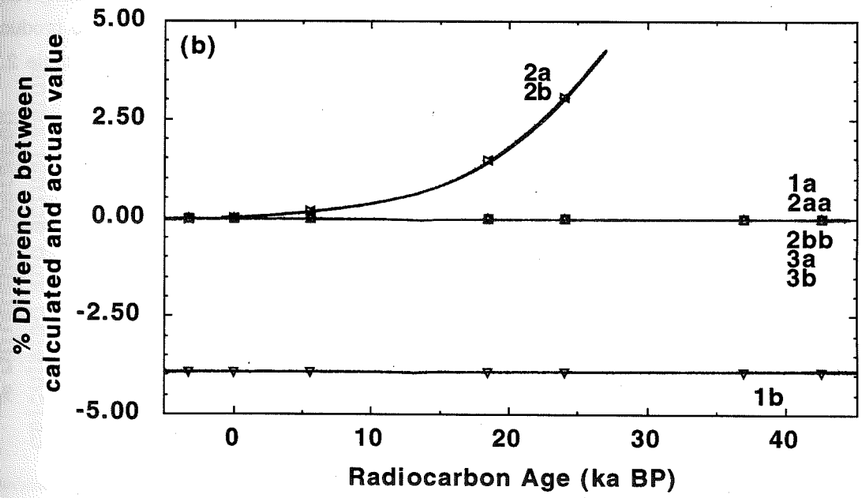

Figure 2.7. Percent Difference as a Function of Sample Mass.

The percent differences between the "actual" $^{14}C/^{13}C$ ratios calculated for the modeled samples using the various background correction expressions (table 2.2) and the initial, uncontaminated $^{14}C/^{13}C$ ratios of the model materials are shown as a function of sample mass for (a) a modern sample, and (b) an 18.5 ka BP sample. The $^{14}C/^{13}C$ ratio of the contaminant carbon was set equal to that of the standard for these calculations (i.e., C=1). The data symbols mark the points at which the percent differences were calculated; the lines between data points are drawn to indicate the trends of the data points obtained from each of the 8 background correction methods discussed in the text. The background correction method used to produce each set of percent difference data is indicated by the method designators from table 2.2 associated with each of the curves (e.g., 1b).

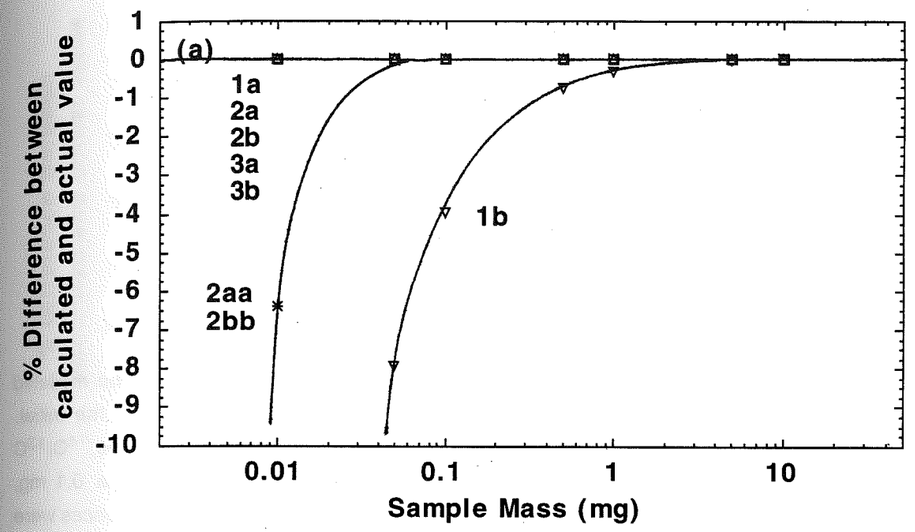

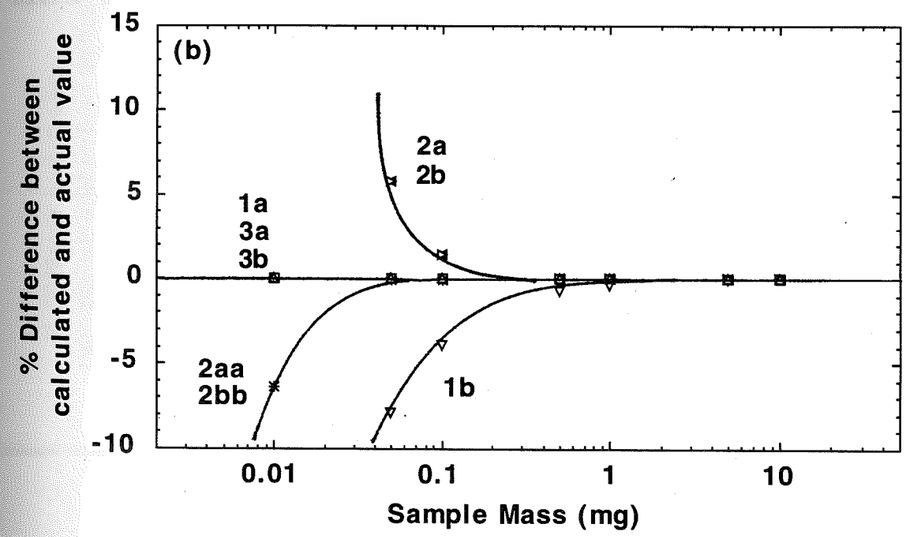

Figure 2.8. Percent Difference as a Function of Contaminant ^{14}C Content.

The percent differences between the "actual" $^{14}C/^{13}C$ ratios calculated for the modeled samples using the various background correction expressions (table 2.2) and the initial, uncontaminated $^{14}C/^{13}C$ ratios of the model materials are shown as a function of the $^{14}C/^{13}C$ ratio of the contaminant carbon, C, for (a) a 1.0 mg, modern sample, and (b) a 0.1 mg, 18.5 ka BP sample. The data symbols mark the points at which the percent differences were calculated; the lines between data points are drawn to indicate the trends of the data points obtained from each of the 8 background correction methods discussed in the text. The background correction method used to produce each set of percent difference data is indicated by the method designators from table 2.2 associated with each of the curves (e.g., 1b).

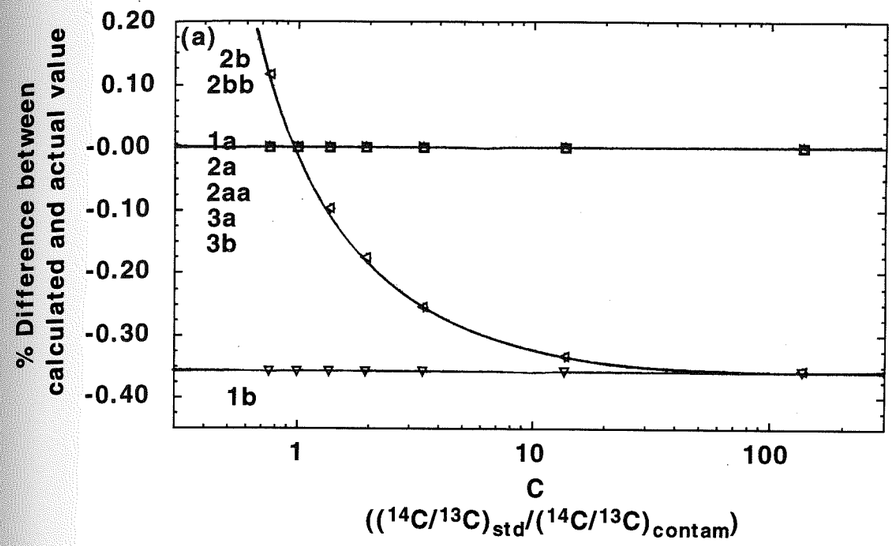

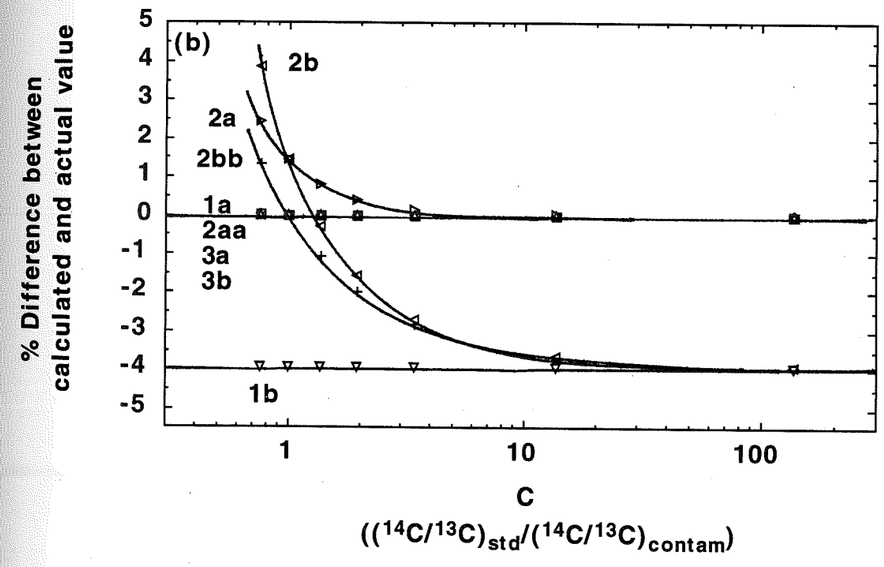

Figure 2.9 Measured $^{14}C/^{13}C$ Ratios for the 25Jan93 Chinese Sucrose Standard Targets.

The $^{14}C/^{13}C$ ratios obtained for the Chinese Sucrose Standard targets measured during the 25Jan93 measurement period are shown. The various data symbols are used to distinguish among the$^{14}C/^{13}C$ ratios obtained for the 12 target sets measured during the 25Jan93 period. The vertical error bars indicate the counting statistics estimates of the uncertainty (1σ) in the measured ratios. The $^{14}C/^{13}C$ ratios between measurement numbers 111 and129 (indicated by the vertical lines) were obtained for the Chinese Sucrose Standard targets in the 7th target set. The mean of the ratios, and the uncertainties in the mean and in a typical single measurement, obtained for the 7th target set are shown in the lower half of the figure. The six initial ratios were obtained during the period in which the measurement system was being setup and tested at the beginning of the measurement period; these six data have not been included in the calculations of the mean and standard deviation of the ratios obtained for the first target set.

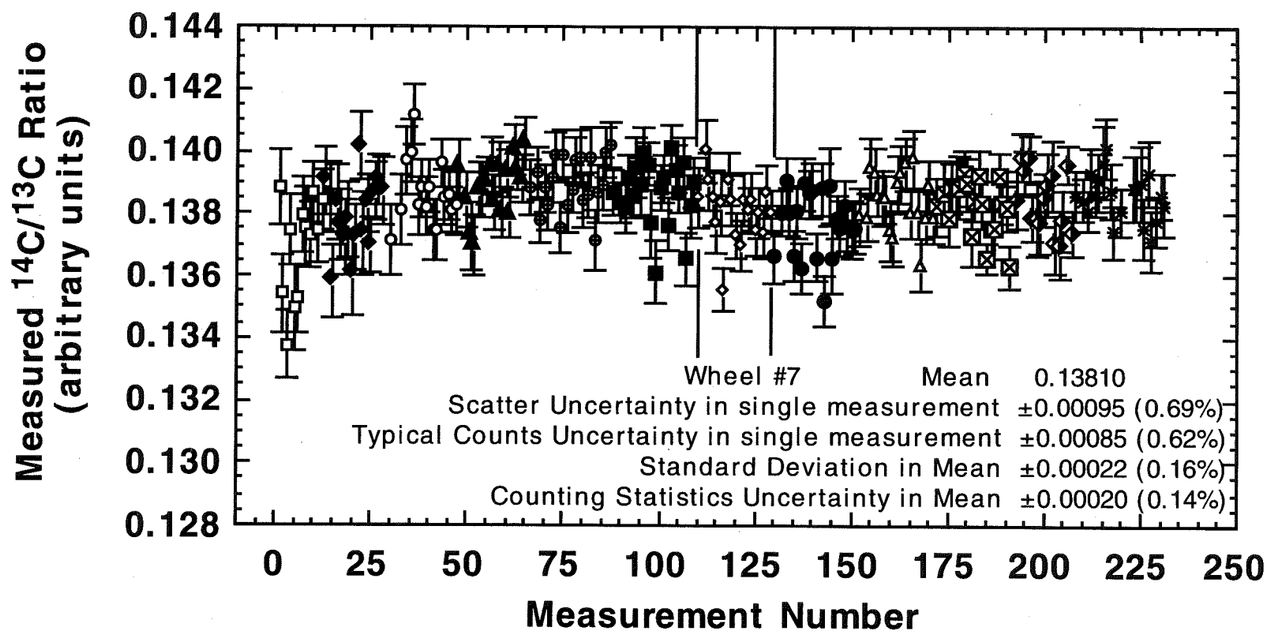

Figure 2.10 Measured $^{14}C/^{13}C$ Ratios for the 05Oct92 Chinese Sucrose Standard Targets.

The $^{14}C/^{13}C$ ratios obtained for the Chinese Sucrose Standard targets measured during the 05Oct92 measurement period are shown. The various data symbols are used to distinguish amoung the $^{14}C/^{13}C$ ratios obtained for the 7 target sets measured during the 05Oct92 period. The vertical error bars indicate the counting statistics estimates of the uncertainty (1σ) in the measured ratios. As discussed in the text, the $^{14}C/^{13}C$ ratios obtained for the Chinese Sucrose Standard targets measured during the 05Oct92 measurement period scatter significantly more than those from the 25Jan93 period (figure 2.9).

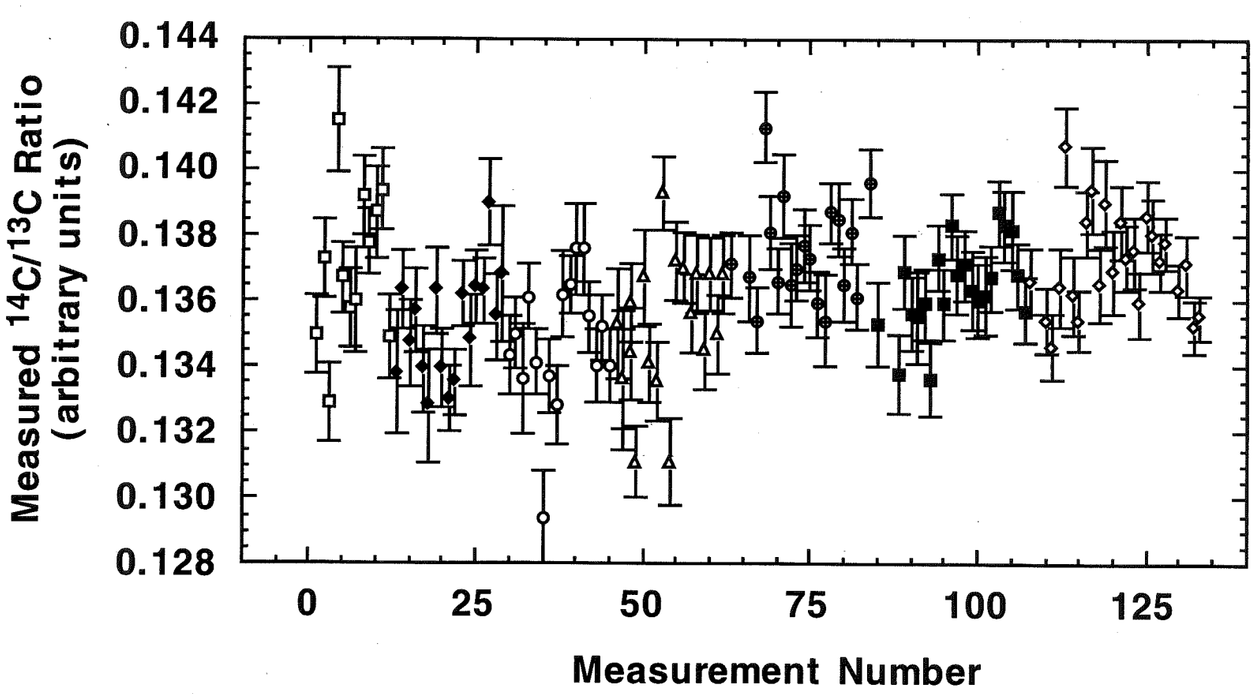

Figure 2.11 Target-Set-Averaged $^{14}C/^{13}C$ Ratios for the 25Jan93 Chinese Sucrose Standards.

The target-set-averaged $^{14}C/^{13}C$ ratios for the Chinese Sucrose Standard targets in the 12 target sets measured during the 25Jan93 measurement period are shown. The vertical error bars indicate the counting statistics estimates of the uncertainty (1σ) in the target-set-averaged $^{14}C/^{13}C$ ratios, which were derived from the counting statistics estimates of the uncertainty in each $^{14}C/^{13}C$ ratio. As discussed in the text, the scatter of these target-set-averaged ratios is larger than expected from the counting statistics estimates of the uncertainties in the ratios.

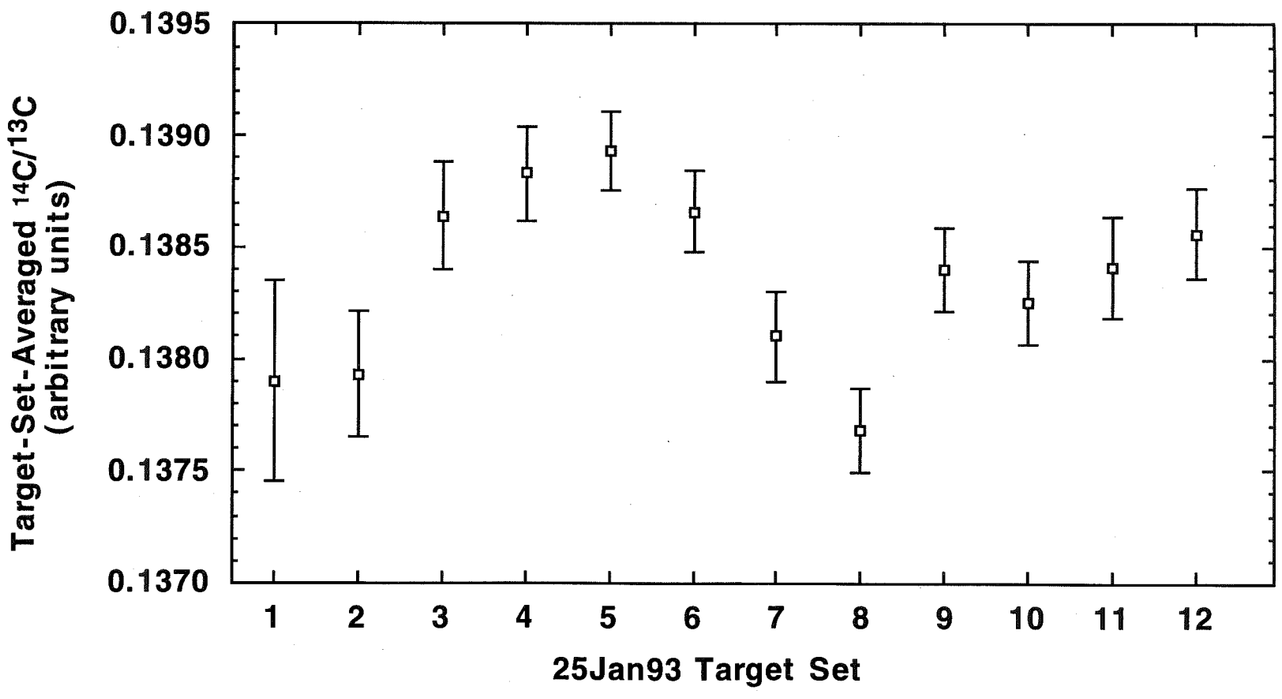

Table 2.3 Measurement-Period-Averaged Chinese Sucrose $^{14}C/^{13}C$ Ratios.

The measurement-period-averaged $^{14}C/^{13}C$ ratios for the Chinese Sucrose Standard targets measured during each of the 4 measurement periods in which the samples discussed in this dissertation were measured are given. The counting statistics estimates of the uncertainties in the mean $^{14}C/^{13}C$ ratios were calculated from the counting statistics estimates of the uncertainty in the measured $^{14}C/^{13}C$ ratios. The scatter based estimates of the uncertainties in the mean $^{14}C/^{13}C$ ratios were obtained from the scatter of the target-set-averaged $^{14}C/^{13}C$ ratios within each measurement period.

Measurement Period	Mean $^{14}C/^{13}C$ of Chinese Sucrose over period (arbitrary units)	Counting statistics based estimate of uncertainty in mean	Scatter based estimate of uncertainty in mean
19Mar92	0.13647	0.00010 (0.076%)	0.00054 (0.40%)
05Oct92	0.13617	0.00011 (0.080%)	0.00042 (0.31%)
25Jan93	0.13836	0.00007 (0.050%)	0.00011 (0.08%)
26May93	0.13773	0.00009 (0.064%)	0.00014 (0.10%)

Table 2.4 Distributions of χ_ν^2 Values from Repeated Measurements of Samples.

The distributions of the probabilities derived from the χ_ν^2 values calculated for the 120 sets of repeated measurements on unknown and secondary standard samples discussed in the text are shown. One of the shown sets of probabilities (designated by "cts") was derived from χ_ν^2 values obtained using counting statistics uncertainties. The other set of probabilities (designated by "cts+non-P") was derived using the non-Poisson augmented uncertainties. The methods by which the "cts" and the "cts+non-P" uncertainties were obtained are discussed in detail in the text (section 2.4.2). The numbers of measurement sets whose derived probabilities fell within the three probability groups, $P \geq 32\%$, $5\% \leq P < 32\%$, and $P < 5\%$, are shown separately for each of the four measurement periods and for the measurement sets in total (the fraction of the total number of measurement sets in each period that fell within each group are expressed as a percentage below each entry). The expected distribution of the 120 measurement sets in this analysis among the three probability groups is also shown.

Measurement Period	19Mar92 cts	19Mar92 cts + non-P	05Oct92 cts	05Oct92 cts + non-P	25Jan93 cts	25Jan93 cts + non-P	26May93 cts	26May93 cts + non-P	Overall Totals cts	Overall Totals cts + non-P	Expected distribution
$P \geq 32\%$	16	24	17	19	29	33	15	17	77	93	82
	(59%)	(89%)	(71%)	(79%)	(73%)	(83%)	(52%)	(59%)	(64%)	(78%)	(68%)
$5\% \leq P < 32\%$	9	2	5	4	9	6	13	11	36	23	32
	(33%)	(7%)	(21%)	(17%)	(23%)	(15%)	(45%)	(38%)	(30%)	(19%)	(27%)
$P < 5\%$	2	1	2	1	2	1	1	1	7	4	6
	(7%)	(4%)	(8%)	(4%)	(5%)	(3%)	(3%)	(3%)	(6%)	(3%)	(5%)
Number of Measurement Sets in Distribution.	27	27	24	24	40	40	29	29	120	120	120

Table 2.5 Age-corrected $\Delta^{14}C$ Values Obtained for Secondary Standard QL1567.

The age-corrected $\Delta^{14}C$ values obtained for the secondary standard QL1567 in each of the four measurement periods are shown along with the weighted mean of these $\Delta^{14}C$ values and the $\Delta^{14}C$ value obtained in previous β-counting measurements. The reduced chi-square values obtained from the measurements in each period and the statistical probability that a larger χ_ν^2 value would be obtained if the set of measurements was repeated are also shown. The "cts" and "cts+non-P" χ_ν^2 values were calculated using counting statistics only and augmented counting statistics estimates, respectively, of the uncertainties in the individual measurements. (The calculation of these χ_ν^2 values and associated probabilities is discussed in the introductory paragraphs of section 2.4.2.) As discussed in the text, the large probabilities obtained for the "cts+non-P" values indicate that the augmented uncertainties over-estimate the true precision uncertainty in the measurements.

Measurement Period	Number of individual measurements	$\Delta^{14}C$ (per mil)	Fractional uncertainty in the measured $^{14}C/^{13}C$ ratio (%)	χ_ν^2 cts	χ_ν^2 cts + non-P
19Mar92	19	862.8±5.2	0.25	0.84 (65%)	0.41 (99%)
05Oct92	20	870.7±5.1	0.23	1.03 (42%)	0.45 (98%)
25Jan93	20	877.0±4.7	0.21	0.84 (65%)	0.70 (82%)
26May93	31	866.9±4.0	0.15	0.87 (67%)	0.71 (88%)
Weighted Mean	90	869.4±2.4	0.13[1]		
β-counting determination		870±10	0.54[1]		

[1] These are the fractional uncertainties in the specific activities ratios from which the age-corrected $\Delta^{14}C$ values were calculated (expressed as percentages). These uncertainties include the additional contributions from the uncertainties in the $\delta^{13}C$ and background correction factors used in the calculation of the $\Delta^{14}C$ values.

Figure 2.12 Measured $^{14}C/^{13}C$ Ratios for the QL11658 Secondary Standard Targets.

The $^{14}C/^{13}C$ ratios obtained for the secondary standard QL11658 targets measured during the 05Oct92, 25Jan93 and 26May93 measurement periods are shown. The vertical error bars indicate the counting statistics estimates of the uncertainty (1σ) in the measured $^{14}C/^{13}C$ ratios. The mean of the measured ratios is indicated by the solid line and the dashed lines indicate the $\pm 1\sigma$ uncertainty in the mean derived from the counting statistics estimates of the uncertainties in the individual measurements.

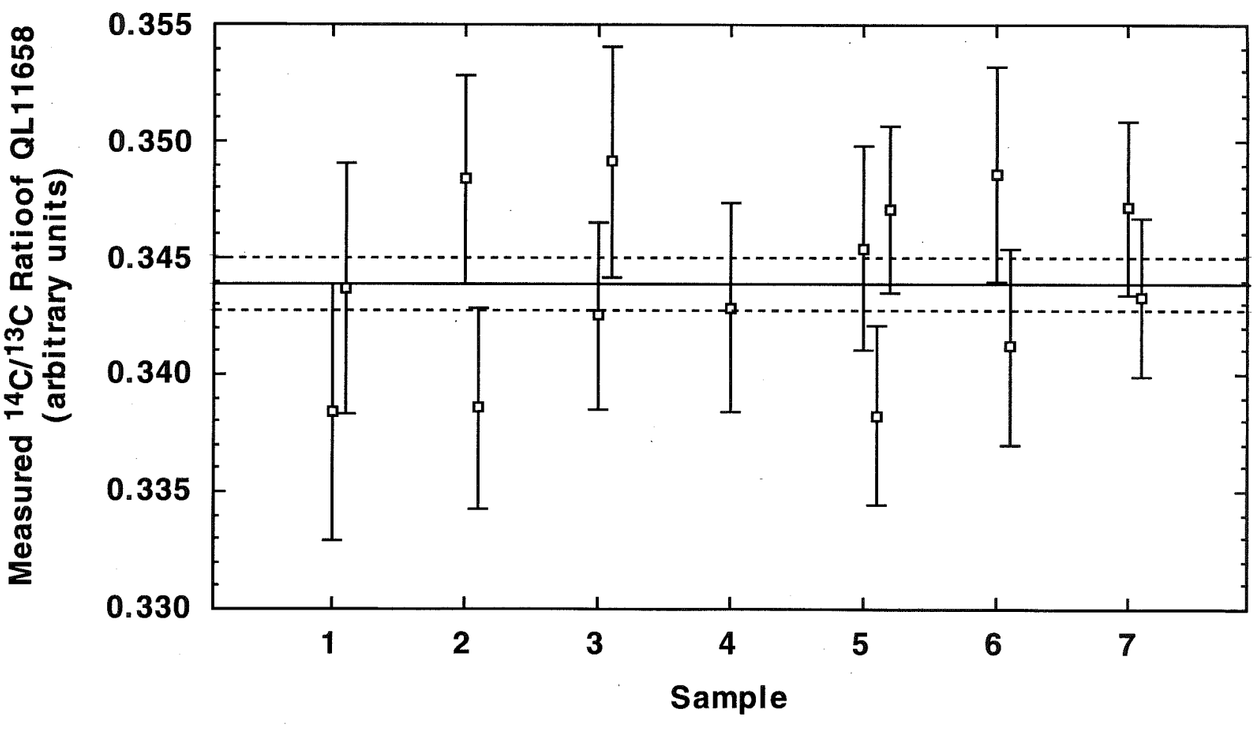

Table 2.6 ^{14}C ages obtained for Secondary Standard QL11658.

The conventional ^{14}C ages calculated from the $^{14}C/^{13}C$ ratios obtained for the secondary standard QL11658 targets measured during the 05Oct92, 25Jan93 and 26May93 measurement periods are shown along with the weighted mean of these ^{14}C ages and the ^{14}C age obtained in previous β-counting measurements. The quoted uncertainties are the augmented counting statistics estimates of the uncertainty (1σ) in the measured $^{14}C/^{13}C$ ratios (as discussed in the text). The reduced chi-square values obtained from the measurements in each period and the statistical probability that a larger χ_ν^2 value would be obtained if the set of measurements was repeated are also shown. The "cts" and "cts+non-P" χ_ν^2 values were calculated using counting statistics only and augmented counting statistics estimates, respectively, of the uncertainties in the individual measurements. (The calculation of these χ_ν^2 values and associated probabilities are discussed in the introductory paragraphs of section 2.4.2.) As discussed in the text, the probabilities obtained from the "cts" and "cts+non-P" χ_ν^2 values indicate that the scatter of the measurements in each period is consistent with both the counting-statistics-alone and the augmented-counting-statistics estimates of the uncertainties in the measurements.

Measurement Period	Number of individual measurements	^{14}C age (BP)	Fractional uncertainty in the measured $^{14}C/^{13}C$ ratio (%)	χ_ν^2 cts	χ_ν^2 cts + nonP
05Oct92	2	6182±92	1.13	0.47 (50%)	0.31 (58%)
25Jan93	5	6120±49	0.58	0.96 (43%)	0.87 (48%)
26May93	7	6148±39	0.44	0.87 (52%)	0.77 (59%)
Weighted Mean	14	6142±29	0.35[1]		
β-counting determination		6120±30	0.37[1]		

[1] These are the fractional uncertainties in the specific activities ratios from which the age-corrected $\Delta^{14}C$ values were calculated (expressed as percentages). These uncertainties include the additional contributions from the uncertainties in the $\delta^{13}C$ and background correction factors used in the calculation of the $\Delta^{14}C$ values.

Figure 2.13 Measured $^{14}C/^{13}C$ Ratios for the IAEA C6 Secondary Standard Targets.

The $^{14}C/^{13}C$ ratios obtained for the secondary standard IAEA C6 targets measured during the 25Jan93 and 26May93 measurement periods are shown. The vertical error bars indicate the counting statistics estimates of the uncertainty (1σ) in the measured $^{14}C/^{13}C$ ratios. The mean of the measured ratios is indicated by the solid line and the dashed lines indicate the $\pm 1\sigma$ uncertainty in the mean derived from the counting statistics estimates of the uncertainties in the individual measurements.

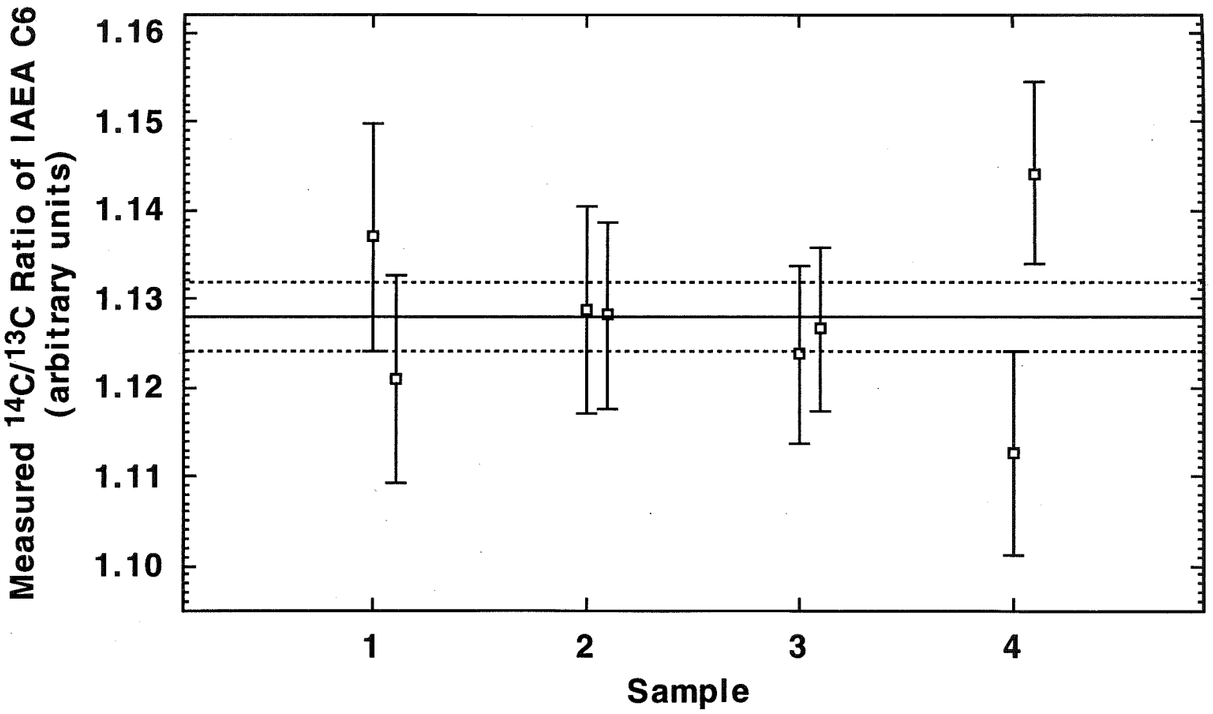

Table 2.7 pMC Values Obtained for Secondary Standard IAEA C6.

The pMC values calculated from the $^{14}C/^{13}C$ ratios obtained for the secondary standard IAEA C6 targets measured during the 25Jan93 and 26May93 measurement periods are shown along with the weighted mean of these pMC values and the consensus pMC value given by Rozanski *et al* (1922). The quoted uncertainties are the augmented counting statistics estimates of the uncertainty (1σ) in the measured $^{14}C/^{13}C$ ratios (as discussed in the text). The reduced chi-square values obtained from the measurements in each period and the statistical probability that a larger χ_ν^2 value would be obtained if the set of measurements was repeated are also shown. The "cts" and "cts+non-P" χ_ν^2 values were calculated using counting-statistics-only and augmented-counting-statistics estimates, respectively, of the uncertainties in the individual measurements. (The calculation of these χ_ν^2 values and associated probabilities are discussed in the introductory paragraphs of section 2.4.2.) As discussed in the text, the inconsistencies of the probabilities obtained from these "cts" and "cts+non-P" χ_ν^2 values for the two measurement periods do not allow meaningful conclusions to be drawn from the probabilities.

Measurement Period	Number of individual measurements	pMC	Fractional uncertainty in the measured $^{14}C/^{13}C$ ratio (%)	χ_ν^2 cts	χ_ν^2 cts + nonP
25Jan93	4	150.96±0.81	0.52	0.29 (83%)	0.25 (86%)
26May93	4	150.82±0.72	0.45	1.50 (21%)	1.25 (29%)
Weighted Mean	8	150.88±0.54	0.36[1]		
Consensus value		150.61±0.11			

[1] This is the fractional uncertainty in the specific activities ratio from which the age-corrected $\Delta^{14}C$ value was calculated (expressed as a percentage). This uncertainty includes the additional contributions from the uncertainties in the $\delta^{13}C$ and background correction factors used in the calculation of the $\Delta^{14}C$ value.

Table 2.8 pMC Values Obtained for Secondary Standard IAEA C5.

The pMC values calculated from the $^{14}C/^{13}C$ ratios obtained for the secondary standard IAEA C5 targets measured during the 25Jan93 and 26May93 measurement periods are shown along with the weighted mean of these pMC values and the consensus pMC value given by Rozanski *et al* (1922). The quoted uncertainties are the augmented counting statistics estimates of the uncertainty (1σ) in the measured $^{14}C/^{13}C$ ratios (as discussed in the text). The reduced chi-square values obtained from the measurements in each period and the statistical probability that a larger χ_ν^2 value would be obtained if the set of measurements was repeated are also shown. The "cts" and "cts+non-P" χ_ν^2 values were calculated using counting-statistics-only and augmented-counting-statistics estimates, respectively, of the uncertainties in the individual measurements. (The calculation of these χ_ν^2 values and associated probabilities are discussed in the introductory paragraphs of section 2.4.2.) As discussed in the text, the probabilities obtained from the "cts" and "cts+non-P" χ_ν^2 values indicate that the scatter of the measurements in each period is consistent with both the counting-statistics-alone and the augmented-counting-statistics estimates of the uncertainties in the measurements.

Measurement Period	Number of individual measurements	pMC	Fractional uncertainty in the measured $^{14}C/^{13}C$ ratio (%)	χ_ν^2 cts	χ_ν^2 cts + nonP
25Jan93	6	22.72±0.15	0.59	0.99 (42%)	0.91 (48%)
26May93	2	22.96±0.23	0.93	0.61 (43%)	0.55 (46%)
Weighted Mean	8	22.79±0.13	0.57[1]		
Consensus value		23.05±0.02			

[1] This is the fractional uncertainty in the specific activities ratio from which the age-corrected $\Delta^{14}C$ value was calculated (expressed as a percentage). This uncertainty includes the additional contributions from the uncertainties in the $\delta^{13}C$ and background correction factors used in the calculation of the $\Delta^{14}C$ value.

Table 2.9 Results from Measurements of Background Samples.

The pMC values and equivalent ^{14}C ages calculated from the $^{14}C/^{13}C$ ratios obtained for the background sample targets measured during the four measurement periods are shown. The quoted uncertainties are the augmented counting statistics estimates of the uncertainty (1σ) in the measured $^{14}C/^{13}C$ ratios (as discussed in the text). The significance of the differences between the results obtained for the different samples and between the results from the 26May93 period and the other three periods is discussed in the text. The results obtained for the SS1 (44<<88 μm) and the SS1 (20<<44 μm) samples show that the pollen extraction methods developed in the following chapter do not contribute significantly to the measurement background.

Measurement Period	Sample	pMC	Equivalent ^{14}C age(BP)
19Mar92	IAEA C4 (#1)	0.535±0.048	41970 ± 720
05Oct92	QL1428gas	0.204±0.027	49710 ±1070
	QL1428wood (#10)	0.221±0.026	49090 ± 940
	QL1428wood (#11)	0.551±0.049	41730 ± 710
25Jan93	QL1428wood (#16)	0.255±0.025	47940 ± 770
	QL1428wood (#18)	0.485±0.023	42770 ± 380
	QL1428wood (#19)	0.508±0.038	42390 ± 600
26May93	QL1428wood (#20)	0.640±0.026	40540 ± 330
	IAEA C1 (C1B))	0.762±0.029	39130 ± 300
	SS1 (44<<88 μm)	0.655±0.026	40350 ± 310
	SS1 (20<<44 μm)	0.910±0.082	37710 ± 720
adjusted 26May93	QL1428wood (#20)	0.395±0.061	44420 ±1250
	IAEA C1 (C1B))	0.238±0.047	48500 ±1600
	SS1 (44<<88 μm)	0.448±0.038	43400 ± 680

Table 2.10 Comparison of Corrections for Charge-exchanged $^{13}C^{4+}$ Background.

The ^{14}C ages obtained from the two background correction calculations discussed in the text (section 2.4.5) are given for the five samples for which sufficient data were recorded to allow both calculations. The first set of ^{14}C ages (uncorrected background) were calculated using $^{14}C/^{13}C$ ratios for the unknown, standard, and background targets which had not been corrected for the contributions of charge-exchanged $^{13}C^{4+}$ to the ratios. The second set of ^{14}C ages (corrected background) were calculated using $^{14}C/^{13}C$ ratios for the unknown, standard, and background targets which had been corrected for the contributions of charge-exchanged $^{13}C^{4+}$ to the ratios. As discussed in the text, the implicit correction for the charge-exchanged $^{13}C^{4+}$ background during the ^{14}C age calculations using the uncorrected $^{14}C/^{13}C$ ratios yields ^{14}C ages which are not significantly different from the ages obtained from the explicit correction calculations using the corrected $^{14}C/^{13}C$ ratios.

Sample designation	^{14}C age uncorrected background (BP)	^{14}C age corrected background (BP)
TAB1GLM2	8836±97	8865±98
TWSPC01B	13098±121	13020±116
TAB1GLM5	15653±159	15768±164
TAB1OLM1	21160±257	21259±263
TAB8OLM1	21801±200	21858±209

Chapter 3: The Extraction and AMS ^{14}C Dating of Pollen.

3.1 Overview.

The basic goal of the research described in the second half of this dissertation was the development of reliable methods that would allow the isolation and AMS ^{14}C dating of pollen fractions from lake sediment and/or peat samples. As discussed above in the introduction, the extracted pollen fractions should provide a nearly ideal material for the establishment of ^{14}C chronologies for the paleoclimate records contained in the lake sediments and peats because the pollen is unambiguously identifiable, is almost entirely of terrestrial (as opposed to aquatic) origin, and is directly associated with the paleoclimate proxy under study in palynological research (i.e., pollen). The development of the pollen extraction procedures during this research was guided by the intention of providing a relatively simple procedure that could be used routinely by palynologists (and other paleoclimatologists) in the preparation of pollen fractions from lake sediment and peat samples for AMS ^{14}C dating.

In the following sections, the research undertaken to develop, test, and apply the pollen extraction and AMS ^{14}C dating procedures will be described. In the first section, the pollen extraction procedure will be presented and the various steps in the procedure will be discussed in detail. In the second section, a study undertaken to validate the pollen extraction and AMS ^{14}C dating procedures will be presented and the results obtained will be discussed. In this study the pollen extraction and dating procedures were applied to samples that were associated with a chronostratigraphic marker of known age, the Mazama Ash layer, in 9 lake sediment and peat cores from sites in the Pacific Northwest. The study was designed to demonstrate the accuracy and reliability of ^{14}C dates obtained from pollen fractions extracted from lake sediment and peat samples and to allow the direct comparison of the pollen fraction AMS ^{14}C dates with the ^{14}C dates that would have been obtained for the same samples following the traditional total-organic-carbon (TOC) sample preparation methods commonly used in β-counting ^{14}C dating of lake sediment and peat samples. In the final section, the results obtained from the application of the extraction and AMS ^{14}C dating procedures to samples from a low-organic-content lake sediment core from Lake Minakokosa, south-central Brooks Range, Alaska, will be discussed. The Lake Minakokosa study was undertaken in an effort to provide a reliable ^{14}C chronology for the palynological record contained in the core and, hence, to contribute to the understanding of the migrations of alder and spruce across Alaska in the early Holocene.

3.2 Pollen Extraction Method.

The initial method developed to extract pollen for AMS ^{14}C dating from samples of interest in paleoclimate studies was based on techniques used routinely in the preparation of samples for palynological studies (e.g., Faegri and Iversen, 1975) and was adequate for the separation of pollen concentrate fractions from subsamples of an organic-rich lake sediment core from a site in southwestern British Columbia, Canada (Brown *et al.*, 1989). Application of this method to peat samples in the initial stages of the research presented in this dissertation showed that the method was incapable of adequate rejection of the high levels of non-pollen organic material in peat samples, and the method was altered to improve the rejection of the non-pollen materials (Brown *et al.*, 1992). Subsequently, the extraction method was modified further with the aim of developing a more generally applicable methodological framework within which essentially pure pollen fractions could be obtained from peat and organic-poor lake sediments as well as from organic-rich lake sediments.

The procedure used in preparing almost all of the pollen extracts that were AMS ^{14}C dated as a part of the research presented in this dissertation is given in figure 3.1. This pollen extraction procedure evolved from the earlier versions mentioned above as results obtained following various changes to the methods were studied; some of the initial samples in this study were processed following slight variants of the procedure given in figure 3.1.

Removal of humic and fulvic acids.

The initial steps of repeated treatment with 1.6 N KOH in a hot water bath followed by a single treatment with 1 N HCl served to remove the majority of humic and fulvic acids and carbonates from the samples. The second set of repeated treatments with 1.6 N KOH followed by 1 N HCl (on the smaller size fraction obtained after sieving at 88 μm) was found to be necessary to ensure the removal of humic and fulvic acids from the <88 μm fractions obtained from some peat and lake sediment samples. These steps were used routinely in the preparation of most of the peat and lake sediment samples, even those for which the initial KOH treatments appeared to have removed all of the humic and fulvic acids.

Physical separation by sieving.

Sieving of the samples served to isolate particular size fractions that contained the pollen of interest for AMS ^{14}C dating from the considerable amounts of non-pollen components of the samples that did not match the size selection criteria. Sieving with an 88 μm-opening nylon monofilament mesh separated the pollen-containing <88 μm fraction from larger organic and non-organic fragments in the sample. Microphotographs of the >88 μm fractions obtained from

several samples are shown in figure 3.2. For peat samples and some lake sediment samples the >88 μm fraction was composed predominantly of plant debris and/or macrofossils (figure 3.2(a)). For some organic-poor/silty lake sediment samples the >88 μm fraction contained significant quantities of crystalline minerals as well as plant debris and/or macrofossils (figures 3.2(b) and (c)). For some organic-poor/silty lake sediment samples only a very small >88 μm fraction was recovered as essentially all of the material in the samples was <88 μm in size. Microscopic examination showed that almost all of the >88 μm fractions were essentially devoid of pollen (i.e., all of the pollen in the samples were in the <88 μm size fraction). The only pollen observed in any of the >88 μm fractions were a few large Douglas-fir pollen grains in the fractions extracted from the core samples from Heal Lake in southwestern British Columbia. (The sites from which the lake sediment cores used in this research were obtained will be described below during the presentation of the specific studies for which the cores were obtained.)

Following the application of several chemical treatments, the 44<<88 μm and 20<<44 μm size fractions were isolated from the <88 μm fraction by sieving at 44 μm and then 20 μm; the <20 μm size fraction was not used in AMS ^{14}C dating and was normally discarded. The 20<<44 μm and 44<<88 μm size fractions were selected from the peat and organic-rich lake sediment samples for two reasons. First, microscopic examination of the products of several initial pollen extracts showed that while essentially all non-pollen contaminants larger than ~30 μm were rejected by the pollen extraction procedures, the ability of the procedures to discriminate between pollen and other organic materials seemed to decrease with the size of the particles being separated, especially for particles less than 10-15 μm in size. Since the peat and organic-rich lake sediment samples contained sufficient amounts of >20 μm pollen, the extracted samples were sieved at 20 μm to remove the <20 μm particles from the pollen extracts and minimize the amount of non-pollen material in the samples for AMS ^{14}C dating. Second, the pollen in the peat and organic-rich lake sediment samples were, in general, from a mixture of coniferous and deciduous trees. The separation of the pollen in the 20–88 μm size range into 20<<44 μm and 44<<88 μm size fractions produced one fraction in which the larger coniferous pollen were concentrated (44<<88 μm), and a second fraction in which the deciduous pollen were concentrated (20<<44 μm). (However, if significant quantities of pine (*Pinus*) pollen were present in the sample, then the 20<<44 μm fraction would also contain significant numbers of pine pollen that were small enough to pass through the 44 μm sieve.) Thus, in most circumstances, two pollen extraction fractions that contained significantly different pollen distributions could be obtained from each peat and lake sediment sample. The AMS ^{14}C dating of both pollen extract fractions provided an additional level at which the effectiveness of the pollen extraction method could be

evaluated; i.e., a significant difference between the ^{14}C ages obtained for the two pollen extraction fractions from a single core sample would suggest that a significant level of some contaminant may have been left in at least one of the fractions by the pollen extraction method.

In considering the general utility of sieving in the extraction of pollen for AMS ^{14}C dating, the selection of particular size range fractions has to be based on the types and sizes of the pollen preserved in the samples that are of interest for the particular research being undertaken. The application of sieving methods to the separation of pollen fractions from samples deposited under different paleoenvironmental conditions may require significant adjustment of the size range limits used to isolate appropriate fractions for AMS ^{14}C dating. Thus, the selection of the 20<<44 μm and 44<<88 μm fractions, while appropriate and advantageous in the case of the peat and organic-rich lake sediment samples analyzed in this research, may not be suitable for the extraction of pollen for AMS ^{14}C dating from samples that were deposited under different paleovegetational conditions such as tundra or grassland environments. The adjustment of the size fraction ranges will be discussed below in the context of the extraction of pollen for AMS ^{14}C dating from the organic-poor/pollen-poor sediments from Lake Minakokosa.

While the relatively simple method of size fraction selection by sieving was the only physical separation method chosen for use in the pollen extraction procedure in this research, relative density differences have been used in the preparation of samples for palynological study to separate pollen from non-pollen materials. In particular, the relative density differences between mineral fragments (relative density >2) and pollen and other organic materials (relative density ≤1.7) have been exploited in procedures involving the use of bromoform/ethanol or zinc chloride/water heavy liquid solutions to remove the mineral fragments from the organic materials in the samples (Faegri and Iversen, 1975). Since the selection of specific size fractions by sieving was found to be an adequate physical separation method for the peat and organic-rich lake sediments, such relative density separation methods were not pursued during the development of the pollen extraction method used in this research.

Removal of silicates.

The standard palynological method for the removal of siliceous materials (sand, clay, etc.) involving treatment with 29 N HF followed by 1 N HCl (both in a hot water bath; figure 3.1) was used to dissolve and remove siliceous materials from the peat and lake sediment samples; the use of hot 1 N HCl after dissolution of the siliceous materials in hot HF was required to ensure the removal of SiO_2 and silicofluorides from the sample solutions (Faegri and Iversen, 1975).

Deflocculation and oxidation of organic detritus.

The bleaching of the samples with 2-3% NaOCl for ~5 min periods both before and after sieving served to deflocculate and oxidize organic detritus that was evident to varying degrees in all of the samples. In general, the use of oxidizing reagents such as NaOCl in preparing pollen samples for palynological study has not been considered part of routine sample preparation methods; the pollen wall material (sporopollenin polymers (Heslop-Harrison, 1968)) seems to be much less resistant to oxidation than to the chemical treatments discussed above, and the use of oxidants in preparing samples for palynological study has been considered undesirable and to be avoided if at all possible (Faegri and Iversen, 1975). In initial studies of possible chemical methods for use in the extraction procedure (Brown *et al.*, 1989), it was found that the standard procedures routinely used to prepare samples for palynological study, which included KOH, HCl, HF and acetolysis, commonly left considerable amounts of organic detritus in the samples in the form of numerous pollen-sized amorphous lumps. Subsequent studies showed that short treatments of samples with 2-3% NaOCl not only reduced the amount of cellulose evident in the final products (and hence performed part of the function of the acetolysis treatment in the standard procedures), but also was very effective in breaking up the amorphous lumps of organic detritus, allowing the detritus to be removed from the sample in subsequent preparation steps.

The general reluctance to use oxidizing agents in the preparation of palynological samples has been based on the potential for preferential loss of particular pollen types during the oxidation step (such preferential loss could introduce significant bias into the observed relative percentages of pollen types within the samples, and hence, introduce significant errors into the paleoclimatological information derived from the pollen data). However, as the loss of minor numbers of pollen grains during the preparation of samples for AMS ^{14}C dating was not as important as ensuring the removal of all possible contaminants from the prepared pollen extracts, the ~5 min treatments with 2-3% NaOCl were incorporated into the pollen extraction method because of the significant improvements in the rejection of non-pollen contaminants that resulted from the use of the bleaching steps.

Removal of cellulose.

The treatment of the separated fractions with H_2SO_4 was designed to ensure the complete removal of cellulosic materials from the pollen fractions intended for AMS ^{14}C dating. The acetolysis procedure normally used in standard palynological preparation methods to try to remove cellulose was replaced with the H_2SO_4 treatment in order to eliminate the use of carbon-containing reagents in the pollen extraction method, and to ensure that all cellulose in the

samples could be removed without requiring excessive use of NaOCl. (NaOCl can be used to oxidize cellulose, but it also oxidizes the pollen wall material, as noted above.) The H_2SO_4 treatment procedure was adapted from the techniques used in the quantitative determination of the neutral monosaccharide constituents of natural samples (Cowie and Hedges, 1984). The first step in these determinations was the decomposition of the complex polysaccharides in the natural samples into their constituent monosaccharides by acid hydrolysis.

In developing their method, Cowie and Hedges (1984) studied the conditions necessary to ensure the maximum yield of the constituent monosaccharides from a number of natural and artificial samples, including wood and pure cellulose. Their studies showed that optimal hydrolysis yields were obtained from the complex polysaccharides using a two-step procedure in which the samples were first allowed to soak in 72% wt% H_2SO_4 (12 M) for 2 h; the acid was then diluted to 1.2 M H_2SO_4 with distilled water and the sample solutions were heated in a boiling water bath for 3 h with frequent stirring. While Cowie and Hedges' motivation for decomposing the complex polysaccharides into their constituent monosaccharides was not related to the development of a pollen extraction method, the complete decomposition of the cellulose-based materials in the pollen fractions into monosaccharide molecular units using the procedures they developed provided a relatively simple and effective method for the removal of the cellulose-based materials from the pollen fractions.

The two-stage H_2SO_4 procedure was applied to the 20<<44 µm and 44<<88 µm pollen fractions produced by the preceding steps of the extraction method in the following manner: 1) The pollen fractions (0.3-0.8 ml of solids in the bottom of 15 ml Pyrex centrifuge tubes) were suspended in 1.5-2 ml 12 M H_2SO_4 for 2 h with frequent agitation (the solids tended to float in the H_2SO_4 due to the relatively high density of the acid). 2) The solutions were diluted to 15 ml with distilled water (~1.2 M H_2SO_4) and the centrifuge tubes were placed in a boiling water bath for 3 h with frequent stirring. (Again the solids floated in the solution, but in this case, the floating seemed to be due to the formation of tiny gas bubbles on the surfaces of the solid particles of the pollen fraction.) 3) The pollen fractions were centrifuged, the ~1.2 M H_2SO_4 was decanted, and the residues were washed several times with 0.01 N HCl.

Microscopic examination of the pollen fractions produced by the above-described pollen extraction method (which included this H_2SO_4 treatment) showed that the method was effective in removing all recognizably cellulosic material from the pollen fractions.

Microscopic examination of the pollen fractions.

In general, the 44<<88 µm pollen fractions produced by the pollen extraction procedure were

composed of essentially pure pollen. Microscopic examination of these fractions showed the presence of Douglas-fir (*Pseudotsuga menziesii*), western hemlock (*Tsuga heterophylla*), fir (*Abies*), and pine in various pollen fractions. The presence or absence of particular pollen types in particular 44<<88 μm pollen fractions was generally in agreement with the palynological results obtained in previous studies of lake sediment and peat cores from sites within the regions of the sites from which the samples studied here were obtained (discussed below as part of the Mazama Ash study). Microphotographs of the 44<<88 μm pollen fractions from three of the core samples taken for the Mazama Ash study are shown in figure 3.3.

The 20<<44 μm pollen fractions produced by the pollen extraction procedure were composed predominantly of pollen (intact grains and numerous fragments of larger pollen grains), but also contained relatively small numbers of fragments that could not be identified. Microscopic examination of these fractions showed the presence of pine, alder (*Alnus*), and sedge (*Cyperaceae*) in various pollen fractions. Again, the presence or absence of particular pollen types (or fragments of larger pollen types) in the 20<<44 μm pollen fractions was consistent with previous palynological studies within the areas of the sites from which these samples were obtained. The presence of the unidentifiable fragments (perhaps degraded fragments of plants or possibly badly-degraded pollen fragments) demonstrates the decreasing ability of the pollen extraction procedure to discriminate between pollen and other organic materials with decreasing particles size mentioned above. Microphotographs of the 20<<44 μm pollen fractions from three of the core samples taken for the Mazama Ash study are shown in figure 3.4.

Bulk (TOC) samples.

As a part of the Mazama Ash study validation of the pollen extraction and AMS ^{14}C dating method, subsamples of all peat and lake sediment samples were also prepared for AMS ^{14}C dating following the procedure normally used in preparing bulk peat or sediment samples for β-counting ^{14}C dating. (This procedure is now often used in preparing "bulk carbon" samples from lake sediments and peat for AMS ^{14}C dating.) The normal procedure consists of the single step of treating the bulk sample with ~1 N HCl to ensure the removal of carbonates and leaving the TOC fraction for combustion to CO_2 and subsequent ^{14}C measurement (samples prepared for AMS ^{14}C dating by this treatment as a part of the research presented here are referred to as "β-prep" samples in the following).

Microscopic examination of the β-prep samples prepared in this research from peat and organic-rich lake sediments showed that they were composed of unidentifiable plant fragments, amorphous lumps of unconsolidated organic material, and/or consolidated lumps of dark,

unidentifiable material. The β-prep samples prepared from organic-poor lake sediment samples did not contain large amounts of plant fragments and/or debris but rather were composed predominantly of very finely divided unidentifiable materials that appeared to be a combination of clayey silts and organic material. These β-prep samples also contained significant numbers of amorphous lumps of partially consolidated organic material, and consolidated lumps of dark, unidentifiable material. On rare occasions, individual pollen grains could be located in the β-prep samples. Microphotographs of the β-prep samples from three lake sediment and peat samples are shown in figure 3.5.

3.3 Mazama Ash Study:Validation of the Pollen Extraction Method.

3.3.1 Introduction.

The central purpose of the Mazama Ash study was to test the pollen extraction procedure that had been developed by extracting and AMS ^{14}C dating pollen fractions from samples of known age. The study was designed to demonstrate the accuracy and reliability of AMS ^{14}C dates obtained from pollen fractions extracted from lake sediment and peat samples through the application of the extraction procedure to several sets of samples associated with a well-known chronostratigraphic marker in cores from lake sediment and peat deposits. In this study, samples for AMS ^{14}C dating were also prepared following the β-prep procedures described above to allow the direct comparison of the pollen fraction AMS ^{14}C dates to the ^{14}C dates that would have been obtained for the same lake sediment and peat samples by the traditional total-organic-carbon (TOC) sample preparation method commonly used in preparing samples for β-counting or AMS ^{14}C dating (the samples prepared by this method are commonly referred to as "bulk" sediment or peat samples).

The Mazama Ash layer.

The chronostratigraphic marker chosen for this study was the volcanic ash layer that was deposited over much of the western United States and Canada as a result of the climactic eruption of Mount Mazama that formed Crater Lake, Oregon at ~6800 BP. The Mazama Ash layer provided a nearly ideal chronostratigraphic marker for evaluating the accuracy and precision of ^{14}C dates obtained following the pollen extraction and ^{14}C dating methods developed in this research because of the ash's production and wide-spread dispersal in a relatively short-term event and because of the numerous ^{14}C dates on samples associated with the Mount Mazama eruptive event and/or ash layer available from previous studies.

The determination of the age of the Mazama Ash layer has been a part of innumerable ^{14}C dating studies that include some of the first ^{14}C determinations (Arnold and Libby, 1951; Broecker *et al.*, 1956). On the basis of a number of these early ^{14}C dates (Libby, 1952; Rubin and Alexander, 1960), Fryxell (1965) reached the commonly cited conclusion that the age of the Mazama eruptive event/ash layer was "about 6600 years". In a subsequent summary of selected early ^{14}C dates on materials found in stratigraphic association with the ash layer (such as charcoal, rat dung, and peat), Kittleman (1973) showed that the then available ^{14}C dates ranged from ~6000 BP to ~7000 BP (with 1σ uncertainties of 250-500 years) and concluded that two dates of 7010±120 BP and 6940±120 BP were accurate estimates of the age of the eruptive event.

Since that time a large number of ^{14}C dates pertaining to the age of the Mazama eruptive event/ash layer have been obtained in a multitude of studies. In these studies β-counting ^{14}C dating techniques were applied to a variety of carbon-containing materials found in association with the Mazama Ash in various types of deposits. In general, the ^{14}C dates obtained in these studies ranged widely relative to the uncertainties in the dates but tended to group between ~6500 BP and ~7100 BP (see, for example, Mullineaux, 1974; Mehringer *et al.*, 1977; Mack *et al.*, 1979; Clague, 1980; Barnosky, 1981; Leopold *et al.*, 1982). More recently, Sarna-Wojcicki *et al.* (1983) reviewed the current knowledge of Holocene volcanism in the conterminous United States and summarized the state of ^{14}C dating of the Mazama eruptive event/ash layer as follows: 1) several ~6700 BP dates with 100-200 year uncertainties had been recently obtained from peat and organic material samples taken from immediately above or within the ash layer, 2) several ~7000 BP dates with 100-200 year uncertainties had been recently obtained from peat and charcoal samples taken from immediately beneath or within the ash layer, and 3) an age of 6840±50 BP has been assigned to the climactic eruption of Mount Mazama based on the weighted mean of four ^{14}C dates on burnt twigs found in close association with ash deposits in the vicinity of Mount Mazama by D. R. Crandell (Bacon, 1983).

In general, the overall range of variation of the ^{14}C dates obtained in the more recent studies has also been somewhat larger than is consistent with the quoted uncertainties in the dates. This has led to questions concerning the temporal association of many of these materials with the actual eruptive event. (For example, dates obtained on pieces of burnt logs found in proximal ash flows may be older than the actual date of the eruption because the source tree had died several tens of years before the eruptive event and/or because the outer rings of the log had been burned off in the ash flow and the remaining outer layers grew several tens of years before the eruptive event.) This has resulted in significant uncertainty as to the actual age of the eruptive

event within the 6700±100 BP to 7000±100 BP range.

In light of this uncertainty, the accuracy and precision of the ^{14}C dates obtained for the pollen fractions and β-prep samples extracted from the lake sediment and peat samples in this study will be compared to the age of the Mazama eruption/ash layer in two ways. First, the individual ^{14}C dates will be compared to the normal 6600 BP to 7100 BP range of the ^{14}C dates that have been obtained in previous studies involving the β-counting ^{14}C dating of the TOC fraction from lake sediment, peat, charcoal, and other types of carbon-containing samples. Second, the age of the Mazama Ash layer derived from the set of ^{14}C dates obtained for the samples from each lake sediment or peat core will be compared to a "consensus" age of the Mazama Ash layer. For the purposes of these comparisons the ^{14}C date obtained by Bacon (1983) of 6840±50 BP for the climactic eruption of Mount Mazama will be used as the "consensus" age of the Mazama Ash layer.

Given the considerable range of the ^{14}C dates that have been obtained in previous studies the choice of this particular date as the "consensus" age of the Mazama Ash layer is somewhat arbitrary, but the date does have two significant attributes: (1) the sources of the carbon that was ^{14}C dated were clearly defined and essentially unambiguous (burnt twigs found within pyroclastic flows near the eruptive site), and (2) the date falls at about the middle of the normal 6600 BP to 7100 BP range of dates that have been obtained in previous studies on samples associated with the Mazama Ash layer in a variety of deposits. Notwithstanding these attributes, the wide range of dates obtained in previous studies strongly suggests that the actual age of the Mazama eruptive event/ash layer is not known with certainty to better than ±100-200 years, and that this uncertainty will have to be considered in the comparisons of the Mazama ages obtained in this study to the ^{14}C dates obtained in previous studies. (Based on the ^{14}C-to-calibrated year (effectively solar year) calibration program CALIB 3.03 Macintosh version (Stuiver and Reimer, 1993), the 6840±50 BP date for the Mount Mazama eruption corresponds to a calibrated year (cal year) age of 7633 (7665–7579) cal BP or, equivalently, 5684 (5715– 5629) cal BC (method A intercept and 1σ range).)

The minimum areal distribution of the ash deposited as a result of the climactic eruption of Mount Mazama has been mapped by Mullineaux (1974) based on the locations of sites at which the ash has been identified in deposits under study. The ash from the eruption has been identified at sites throughout most of Oregon, Washington and Idaho, and the outer limits of the ash dispersal are defined by its presence at sites in northeastern California and northern Nevada and Utah, in northwestern Wyoming and western Montana, and, in Canada, in southwestern Saskatchewan, central Alberta and southern British Columbia. The widespread dispersal of the

ash was of significance for the purposes of this study in that it implied that lake sediment and peat cores from almost any sites in the Pacific Northwest would probably contain a Mazama Ash layer and, hence, that the selection of coring sites could be dictated by convenience and opportunity rather than by requirements imposed by the limited dispersal of the ash.

Selection of study sites.

The nine sites from which the lake sediment and peat cores used in this study were obtained were all from the western side of the Mazama Ash dispersal area; two of the sites were located on southern Vancouver Island, British Columbia, two sites were located in the Puget Lowlands, Washington, four sites were located on the eastern side of the southern North Cascade Range, Washington (the locations of the British Columbia and Washington sites are shown in figure 3.6), and one site was located in the central Sierra Nevada, California (just beyond the southern limit of the mapped ash distribution). The selection of these cores for use in this study was based on timely opportunity and the convenience of obtaining samples associated with the Mazama Ash layer from the lake sediment and peat cores from the sites.

The cores were obtained as parts of other ongoing paleoclimatological studies and were not obtained specifically for the purposes of this study. Eight of the nine cores were selected without any specific prior knowledge of the quality of the lake sediments or peat deposits at the sites nor of the physical state (nor, in most cases, even the presence) of the Mazama Ash layer in the cores. In the one case in which prior knowledge of the lake sediments and ash layer was made available (Crocker Lake, Washington), the information indicated that significant errors had been encountered in ^{14}C dating the sediments using the TOC/β-counting methods.

The cores used in this study were selected in this manner for two reasons: 1) the diversity of sites, core materials, and physical states of the ash layers was intended to provide a representation of circumstances likely to be encountered by palynologists and other paleoecologists in attempting to utilize the pollen extraction procedure under normal field and laboratory conditions (at least in the Pacific Northwest), and 2) the avoidance of any screening of the cores to select cores with "ideal" ash layers and sediments was intended to preclude arguments that the data obtained in this study were a result of the selection of special lake sediment and peat cores and were not representative of the data that would be obtained from the routine application of the pollen extraction and AMS ^{14}C dating procedures in palynological (and other paleoclimatological) studies involving typical lake sediment or peat cores.

Paleovegetational context of the study sites.

In general, palynological studies indicate that extensive forests existed in the areas of the

coring sites in British Columbia, Washington and California at the time of the Mazama eruptive event/ash layer deposition. The forests at the lower elevation sites in the Puget Lowlands and on southern Vancouver Island were characterized by Douglas-fir and alder at that time (Mathewes, 1973; Leopold *et al.*, 1982; Allen and Hebda,1993). These, and other (e.g., Mathewes and Heusser,1981), studies show that the forests were then in a process of transition in response to a climatological change from a regime that was warmer and drier than today towards a cooler and wetter regime that was more similar to the present. These studies indicate that the composition of the forests changed over a relatively long period (several hundred to a couple of thousand years) from the Douglas-fir/alder forest of the warmer/drier times to a western hemlock/western red cedar (*Thuja plicata*) forest in the later cooler/wetter times.

Unfortunately, the reconstruction of paleoenvironmental conditions at higher elevation in the region of the four sites on the eastern side of the southern North Cascade Range has not been the subject of as many studies as the vegetation history of the lowland areas of western Washington and southwestern British Columbia. In fact, there appears to be only one palynological record from the southern North Cascade Range in the available literature. That record was obtained from a 4-m long core from a small bog near the south end of Lake Kachess by Hansen (1947). Hansen's Lake Kachess site is located near the center of the region of the higher elevation sites in this study (in fact, one of the cores used in this study may have come from the same bog as Hansen's core). Fortuitously, Hansen's record provides reasonable information on the forest composition in the region at the time of the Mazama eruptive event/ash layer deposition (the presence of a (probably Mazama) volcanic ash layer at 3.2 m depth in the core was reported by Hansen (1947)). Based of this single palynological record, the forests at the higher elevation sites on the eastern side of the southern North Cascade Range in this study were characterized by the presence of Douglas-fir, western white pine (*Pinus monticola*), lodgepole pine (*Pinus contorta*), and fir at the time of the Mazama eruptive event/ash layer deposition. As with the lowlands sites, the forests were in a process of transition at the time of ash layer deposition with Douglas-fir and lodgepole pine declining and western white pine and western hemlock increasing over a period of perhaps 2-3 thousand years around the time of ash layer deposition (since ^{14}C dating did not exist at the time of Hansen's (1947) study there are no ^{14}C dates available for the record; the period of time over which the transition took place mentioned above was estimated from the depth of the ash layer in the core and the (now known) age of the (Mazama) ash layer).

The Holocene forests in the region of the one site in this study that was located in the central Sierra Nevada, California have been reconstructed in a recent palynological and macrofossil

study by Anderson (1990). One of the lakes studied by Anderson, Barrett Lake, is located ~30 km northwest of the site in this study and is at about the same elevation and position relative to the Sierra Nevada Crest (~2800 m elevation and just to the east). Given the similarities in the location, elevation, etc., the reconstructed forests obtained by Anderson (1990) should be representative of the forests at the site in this study. At the time of the climactic eruption of Mount Mazama, the forests in the Barrett lake region were characterized by limber pine (*Pinus flexilis*), lodgepole pine (*Pinus murrayana*), mountain hemlock (*Tsuga mertensiana*), and shrub oak species (probably huckleberry oak (*Quercus vaccinifolia*)). As in the forest and climate reconstructions for western Washington and southern British Columbia discussed above, the forests at higher elevation in the central Sierra Nevada appear to have been in the midst of a transition from a warmer/drier regime towards a cooler and effectively wetter regime at the time of the Mount Mazama eruption. Anderson (1990) found that the pollen percentages of fir and mountain hemlock increased in the Barrett Lake record from ~7000 BP to ~4000 BP and inferred an increase in effective precipitation and winter snowpack in the central Sierra Nevada over that period.

In terms of their significance to the purposes of the Mazama Ash study, the paleovegetational reconstructions described above show that well-developed forests existed in the areas of the coring sites at the time of the Mazama eruptive event/ash layer deposition. On the basis of these reconstructions, the application of the pollen extraction procedure to samples taken from the cores from the sites in the Puget Lowlands and on southern Vancouver Island was expected to produce 44<<88 μm pollen fractions that were composed predominantly of coniferous pollen grains (Douglas-fir and western hemlock) and 20<<44 μm pollen fractions that were composed of coniferous and deciduous pollen grains (western red cedar, alder, and perhaps oak). The samples taken from the cores from the sites on the eastern side of the southern North Cascade Range were expected to produce 44<<88 μm and 20<<44 μm pollen fractions that were composed predominantly of coniferous pollen grains (Douglas-fir, western hemlock, pine, and fir in the 44<<88 μm fractions and primarily pine in the 20<<44 μm fractions). The samples taken from the core from the site in the central Sierra Nevada were expected to produce 44<<88 μm pollen fractions that were composed predominantly of coniferous pollen grains (pine, fir and mountain hemlock) and 20<<44 μm pollen fractions that were composed of coniferous and deciduous pollen grains (pine and oak). Microscopic examination shows that the samples produced by the pollen extraction procedure are in general agreement with these expectation (see, for example, figures 3.3 and 3.4).

Mount Mazama eruption and pollen fraction AMS ^{14}C dating.

The pollen extraction procedures in this research have been developed to allow the isolation and direct AMS ^{14}C dating of the paleoclimate proxy under study in palynological research with the goal of eliminating several common sources of ^{14}C dating error and improving the accuracy and reliability of ^{14}C chronologies established for paleoclimate records contained in lake sediment and peat deposits. In the Mazama Ash study, the age of central interest is that of the eruption of Mount Mazama and not the age of the pollen in the core samples. Clearly, the pollen that is being extracted from the core samples and ^{14}C dated is only indirectly associated with the actual Mazama eruptive event through the physical association of the pollen-containing core samples with the ash layer that was deposited at the site as a result of the eruption. Thus, as in the case of essentially all previous ^{14}C dating of materials related to the Mount Mazama eruption, questions can be raised concerning the relationship between the ^{14}C ages of pollen in lake sediment and peat samples and the ^{14}C age of the Mount Mazama eruption. In particular, the possibility exists that depositional and/or post-depositional processes within the lakes or bogs could cause the ash layer in the sediments to be surrounded by sedimentary material that contains pollen whose average age is significantly different from that of the ash layer. In such cases, the ^{14}C dates obtained for the pollen fractions could accurately represent the average age of the pollen in the core sample, but could be inaccurate measures of the age of the ash layer.

In the following discussions, the effects of several possible depositional and post-depositional processes will be discussed in detail and, where possible, explicit corrections will be made for the effects. While the lack of direct association of the ^{14}C dates for the pollen fractions from the core samples with that of the event of interest in the Mazama Ash study must be considered in evaluating the accuracy of the ages of the Mount Mazama eruptive event derived from the pollen fraction dates, the question of association does not arise in the use of the pollen extraction and AMS ^{14}C dating procedures in palynological studies. In palynological studies, the pollen extraction and AMS ^{14}C dating procedures allow the direct dating of the proxy climate indicator being studied (pollen), and the association of the material being dated with the material of interest in the study is clear and unambiguous.

Overview of the sections that follow.

In the following sections, the main elements of the Mazama Ash study will be described and the results obtained will be presented and discussed. In the first section, the nine sites from which the lake sediment and peat cores used in this study were obtained, the sections of the

cores that contained the Mazama Ash layer, and the core samples taken for pollen extraction and ^{14}C dating are described. The core samples for pollen extraction were taken from immediately above and below the ash layer from each of the nine cores in order to investigate possible ^{14}C dating offsets introduced by depositional or post-depositional processes. (The core samples from above and below the ash layer will be referred to as the *above* and *below* samples, respectively, throughout this discussion of the Mazama Ash study.) In the second section, the processing of the extracted pollen fractions and prepared β-prep samples for AMS ^{14}C measurement is described. Then, in the final section, the ^{14}C dates obtained for the pollen fractions and β-prep samples will be presented and discussed in detail. In the first part of this discussion, the internal consistency of the dates will be evaluated in terms of the consistency of dates obtained for the two pollen fractions from each core sample and the inconsistencies between the dates obtained for the pollen fractions and β-prep samples from each core sample. As a part of these discussions, the differences observed between the pollen fraction ^{14}C dates obtained for the *above* core samples and those for the *below* core samples in several of the cores will be considered in terms of the possible effects of post-depositional redistribution of pollen in the upper layers of the sediments by bioturbative processes. Then, the ^{14}C dates obtained for the pollen fractions from the core samples, and the Mazama Ash deposition ages calculated from them, will be compared to the range of Mazama Ash ages obtained in previous studies and the "consensus" age of the Mount Mazama eruption discussed above. And finally, the ^{14}C dates obtained for the pollen fractions and β-prep samples from a particular core (Crocker Lake) will be discussed in further detail because the dates demonstrate the ability of the pollen extraction procedure to eliminate one of the common sources of ^{14}C dating error encountered under the traditional TOC sample preparation methods commonly used in β-counting and AMS ^{14}C dating.

3.3.2 Sampling sites, cores, and AMS ^{14}C-dated samples.

Chase Lake.

Chase Lake is a small ~2 ha, ~4.7 m deep lake located ~3 km northwest of Freeland on Whidbey Island, Washington, USA at an elevation of ~60 m (48° 3´ N, 122° 33´ W). The lake is currently surrounded by a Douglas-fir/alder forest, with some western red cedar. There were no streams flowing into or out of the lake at the time the core was obtained. The 5-cm diameter lake sediment core used in this research was obtained from near the center of the lake using a modified Livingstone sampler (Wright, 1967) with the cooperation of Catherine Macoomb (White Rock, B.C.) and Terry Swanson (UW Geology) in the summer of 1992. The total length of the core was ~4 m; the core was composed of brown clayey gyttia to a depth of ~3.2 m, with coarse

brown gyttia between ~3.2 and ~3.8 m core depth, and solid glacial clay below ~3.8 m depth.

A 1-cm thick layer of orange-brown volcanic ash was found in the core between core depths 291 cm and 292 cm. Four samples were taken from the core immediately above and below the ash layer; both of the samples of the first *above/below* pair were ~3 cm long and constituted one-quarter of a cross section (a one-quarter pie-shaped solid piece), including about 0.5 cm of the ash layer in each sample (~15 cm^3). The 20<<44 μm and 44<<88 μm pollen fractions produced from the first two samples, following the pollen extraction procedure given in figure 3.1, were not sufficient for intended studies including AMS ^{14}C dating. Pollen fractions and β-prep samples were prepared from the second pair of samples following the same procedure. The first sample of this pair, CL3, was a 5-cm long by one-quarter cross-section solid piece taken from the core below the ash layer between 292 cm and 297 cm core depth (~25 cm^3); the sample consisted of compacted, clayey brown gyttia. The second sample of the pair, CL4, was a 5-cm long by one-quarter cross-section solid piece taken from the top of the ash layer between 286 cm and 291 cm core depth (~25 cm^3); the sample consisted of compacted, clayey brown gyttia.

Crocker Lake.

Crocker Lake is an ~76 ha, ~5 m deep lake located ~5 km north of Leland Lake on the Olympic Peninsula, Washington, USA at an elevation of ~60 m (47° 56´ N, 122° 52´ W). The lake is currently surrounded by cleared farmland with a young Douglas-fir/alder forest or clear-cut logged areas on the nearby hills. At the present time, Andrews Creek flows into the lake from the south and Snow Creek flows out of the lake to the north. The 5-cm diameter lake sediment core used in this research was obtained using a modified Livingstone sampler by Prof. L. B. Brubaker and J. S. McLachlan (UW Forest Resources) in the summer of 1991. (The site, vegetation, and coring description given above is based on information provided by J. S. McLachlan (personal communication, 1994).) The total length of the core was ~11.8 m; the upper sections of the core were composed of brown gyttia while the lower sections became more silty and gray with less organic material.

A graded, gray volcanic ash layer (with orange oxidation patches) was found in the core between the core depths 613 cm and 614 cm; the ash layer was ~1 cm thick and tilted at an ~17° angle from the horizontal. Two samples were taken from the core immediately above and below the ash layer; pollen fractions and β-prep samples were prepared from them for AMS ^{14}C dating following the usual pollen extraction procedure (figure 3.1). The first sample, CR3, was a 2.5-cm long by one-half cross-section solid piece taken from above the ash layer between 611 cm and 613.5 cm core depth (~25 cm^3); the entire sample was composed of slightly silty soft brown

gyttia. The second sample, CR4, was a 2.5-cm long by one-half cross-section solid piece taken from the core below the ash layer between 614.5 cm and 617 cm core depth (~25 cm^3); the entire sample was also composed of slightly silty soft brown gyttia.

Dead Ice Pond.

Dead Ice Pond (unofficial name) is a small ~0.1 ha area, ~3.6 m deep kettle depression pond located just east of the crest of Snoqualmie Pass in the Wenatchee National Forest at an elevation of ~880 m (47° 25´ N, 121° 24´ W, ~3 km north of Keechelus Lake, Washington, USA). The pond is currently surrounded by a fir (*Abies lasiocarpa*)/western white pine forest. There are no apparent streams flowing into or out of the pond. The 5-cm diameter lake sediment core used in this research was obtained using a modified Livingstone sampler by Terry Swanson and Todd Hurley (UW Geology) in the winter of 1990. (The site, vegetation, and coring description given above is based on information provided by Terry Swanson (personal communication, 1994).) Only the 0.8-1.6 m section of the core was available for examination; this section contained the ash layer and was composed of coarse, dark brown peat with many stringy fragments (roots?) and occasional larger organic fragments.

A 5.7-cm thick layer of fine cream-tan volcanic ash was found in the core between the core depths 112 cm and 117.5 cm; there were numerous brown streaks within the ash layer that appeared to be from decomposed organic matter. Three samples were taken from the core, and pollen fractions and β-prep samples were prepared from two of them for AMS ^{14}C dating. The first sample processed, DP1, was a 3.8-cm long by one-quarter cross-section solid piece taken from the core between 107 cm and 111 cm core depth (~19 cm^3); the sample consisted of matted, dark brown organic material with some rootlet-like fragments. The second sample processed, DP3, was a 3.8-cm long by one-quarter cross-section solid piece taken from the core between 118 cm and 122 cm core depth (~19 cm^3); this sample also consisted of matted dark brown organic material with numerous rootlet-like fragments.

Heal Lake.

Heal Lake was a 40 ha, ~15 m deep lake located ~3 km northwest of Prospect Lake on the Sannich Peninsula, Vancouver Island, British Columbia, Canada at an elevation of ~140 m (48° 32´ N, 123° 28´ W). The lake was recently drained and excavated as part of the development of a refuse disposal site. Richard Hebda (Royal British Columbia Museum, Botany) recognized the potential for recovering paleoclimatic records from the lake sediments and has been studying the various types of materials preserved in the lake sediments as part of an ongoing paleoclimatic research program (Hebda, 1993). The lake is in the Coastal Douglas-fir Biogeoclimatic Zone

(Krajina, 1978) and is currently surrounded by a Douglas-fir dominated forest. The lake sediments were up to 14 m thick in the deepest sections of the lake basin. A 30-cm long, 16-cm wide, and ~12-cm deep sediment section containing a gray-white ash layer was obtained from the Heal Lake site by Paula Reimer (UW, Quaternary Isotope Laboratory) in the summer of 1992. The sediment section was taken from an ~4.6 m lake sediment face exposed during excavation; the section was almost completely composed of relatively dry, compacted, coarse brown gyttia. (The site, vegetation, and sampling description given above is based on information provided by Paula Reimer and Richard Hebda (personal communications, 1994).)

The ash layer was ~2 cm thick and was at a depth of 367 cm relative to the top of the exposure face directly above the sampling site. The top of the ash layer formed a smooth clearly-defined interface with the sediments above; the bottom of the ash layer was a clumpy intermixing over 0.5 cm depth of the ash with the sediments below the layer. Four samples were taken from the sediment section. The first two were used in evaluating modifications to the pollen extraction method. Pollen fractions and β-prep samples were prepared from the second pair of samples for AMS ^{14}C dating. The first of these samples, HL3, was a 5-cm long, 2-cm wide and 3-cm deep solid piece of the sediments taken from the section from just above the ash layer between 362 cm and 367 cm depth (~30 cm^3); the sample consisted of dry, compacted, coarse brown sediments. The second sample, HL4, was also 5 cm long, 2 cm wide and 3 cm deep, and was taken from the section just below the ash layer between 369 cm and 374 cm depth (~30 cm^3); the sample consisted of dry, compacted, coarse brown sediments containing numerous rootlets.

Kachess Bog.

Kachess Bog (unofficial name) is a ~6 ha marsh area impounded behind Domerie moraines (Porter, 1976) located near the south end of Kachess Lake at an elevation of ~710 m (47° 17´ N, 121° 13´ W, ~3 km northwest of the Lake Easton State Park, Washington, USA). The bog was an ~1 m deep frozen-over pond at the time the core was obtained and had, in recent times, been surrounded by a Douglas-fir/fir dominated forest with some western red cedar and western hemlock (and lodgepole pine in disturbed areas). (However, the neighboring forest had been removed by clear-cut logging operations at the time the core was obtained.) While there were no apparent streams flowing directly into or out of the area of the bog from which the core was taken, there was a stream that flowed into the general bog area from the west and an outflow stream from the general bog area to the east. The 5-cm diameter sediment core used in this research was obtained using a modified Livingstone sampler by Terry Swanson in the winter of 1990. (The site, vegetation, and coring description given above is based on information provided

by Terry Swanson (personal communication, 1994).) The total length of the lake sediment core from Kachess Bog was ~5.3 m; the upper ~4.5 m of the core was composed of dark-brown to red-brown fibrous peat, which graded into lacustrine clay at the bottom.

A 6.5-cm thick layer of yellow-tan volcanic ash was found in the core between core depths 166 cm and 172.5 cm; there were numerous brown streaks within the ash layer that appeared to be from decomposed organic matter. Six samples were taken from the core immediately above and below the ash layer. The first four were processed during the studies of the modifications required to improve the rejection of non-pollen materials in the extraction of pollen from peat samples; the results from these studies have been reported previously (Brown *et al.*, 1992). Pollen fractions and β-prep samples were prepared from the last pair of samples for AMS ^{14}C dating. The first sample of this pair, KB7, was a 5-cm long by one-quarter cross-section solid piece taken from the top of the ash layer between 162 cm and 167 cm core depth (~25 cm^3). The upper 3.7 cm consisted of matted, coarse, dark brown organic peat with rootlet-like fragments; the lower 1.3 cm of the sample consisted of the yellow-tan volcanic ash. The second sample of the pair, KB8, was a 5-cm long by one-quarter cross-section solid piece taken from the core below the ash layer between 171 cm and 176 cm core depth (~25 cm^3). The upper third of the sample consisted of the yellow-tan volcanic ash; the lower two thirds of the sample (3.3 cm) consisted of matted, coarse, dark brown organic peat with rootlet-like fragments.

Lizard Lake.

Lizard Lake is a small ~1 ha, ~3 m deep pond located near the crest of Stampede Pass in the Snoqualmie National Forest at an elevation of ~1100 m (47° 17′ N, 121° 21′ W, ~4 km south of Kachess Lake, Washington, USA). The lake is currently surrounded by a western white pine/fir forest. There is one very small, overgrown stream flowing into the lake from the east through a small marsh and there is no apparent outflow stream. The 5-cm diameter lake sediment core used in this research was obtained from near the center of the lake using a modified Livingstone sampler with the cooperation of Terry Swanson (UW Geology) in the summer of 1991. The total length of the core was 3.3 m; the core was almost completely composed of brown to dark-brown gyttia with oxidized angular gravel at the bottom.

A 42-cm thick layer of fine gray-white volcanic ash was found in the core between the core depths 105 cm and 147 cm (depth measured from the top of the core). Two samples were taken from the core and pollen fractions and β-prep samples were prepared from them for AMS ^{14}C dating. The first sample, LZ1, was taken from the core at the top of the ash layer between 102 cm and 106 cm core depth and consisted of a 4–cm long by one-quarter cross-section solid

piece (~20 cm^3). The upper 3 cm of the sample consisted of the dark brown gyttia that was above the ash layer and the lower 1 cm of the sample consisted of the gray-white volcanic ash. The second sample, LZ2, was taken from the core at the bottom of the ash layer between 146 cm and 149 cm core depth and consisted of a 3-cm long by one-third cross-section solid piece (~20 cm^3). The upper 1 cm of the sample consisted of the gray-white volcanic ash, and the lower 2 cm of the sample consisted of the dark brown gyttia that was below the ash layer.

Rhamnus Lake.

Rhamnus Lake (unofficial name) is a small ~2 ha, ~4 m deep pond located ~5 km west of Shawnigan Lake on Vancouver Island, British Columbia, Canada at an elevation of ~320 m (48° 38′ N, 123° 43′ W). The lake is in the Coastal Western Hemlock Biogeoclimatic Zone (Krajina, 1978) but is currently surrounded by a second growth, managed Douglas-fir forest. There were no apparent streams flowing into the lake at the time the core was obtained and there is one intermittent stream flowing out of the lake through the marshy area at the east end of the lake. The 5-cm diameter lake sediment core used in this research was obtained from near the center of the lake using a modified Livingstone sampler with the cooperation of Richard Hebda and Greg Allen (Royal British Columbia Museum, Botany) in the summer of 1991. A lake sediment core with a total length of ~7 m was taken from Rhamnus Lake for palynological study; a second core section which encompassed the core depth of the suspected Mazama Ash layer was obtained specifically for this study (370 cm to 470 cm core depth). The entire core and the secondary core section were composed almost completely of green-brown gyttia.

A fine, pale yellow-white volcanic ash layer was found in the core section between the core depths 417 cm and 419 cm. The ash layer was 0.5 cm thick, with well-defined top and bottom interfaces for about half of the core section width, but was somewhat clumpy and spread over ~2 cm depth in the other half of the core section width. A total of five samples were taken from the core section near the ash layer; the first three samples were processed during the studies of the modifications required to improve the rejection of non-pollen materials in the extraction. Pollen fractions and β-prep samples were prepared from the last pair of samples for AMS ^{14}C dating. This pair of samples were taken from the half section of the core in which the ash layer had well-defined top and bottom interfaces. The first sample of this last pair, RL4, was a 5-cm long by one-half cross-section solid piece taken from immediately above the ash layer between 412 cm and 417 cm core depth (~50 cm^3). The entire sample was composed of soft green-brown gyttia. The second sample of the pair, RL5, was a 5-cm long by one-half cross-section solid piece taken from the core immediately below the ash layer between 418 cm and 423 cm core depth

(~50 cm^3). The entire sample was also composed of soft green-brown gyttia.

Rock Creek Pond.

Rock Creek Pond (unofficial name) is a small ~0.5 ha area, ~4.5 m deep pond which formed as a bedrock basin behind Hilgard terminal moraines (Birman, 1964) and is located near Rock Creek Lake in the John Muir Wilderness at an elevation of ~2850 m (37° 30´ N, 118° 44´ W, ~1 km north of Rock Creek Lake, California, USA). The pond is currently surrounded by a lodgepole pine/limber pine/aspen forest. Rock Creek, a relatively large (~5 m width) stream, flows into Rock Creek Pond from the south and out of the pond to the north. The 5-cm diameter lake sediment core used in this research was obtained using a modified Livingstone sampler by Terry Swanson (UW Geology), Fawn Swanson (Freeland, Washington) and Dan Cutchell (U California, White Mtn. Res. Station) in the summer of 1990. (The site, vegetation, and coring description given above is based on information provided by Terry Swanson (personal communication, 1994).) The total length of the core was ~10.0 m; the core was composed of dark-brown/black gyttia.

A gray volcanic ash layer was found in the 460-558 cm core section between the core depths 531 cm and 533.5 cm; the ash layer was ~2.0 cm thick with a diffuse top and sharply-defined bottom interface. Two samples were taken from the core, and pollen fractions and β-prep samples were prepared from them for AMS ^{14}C dating. The first sample, RC1, was a 5-cm long one quarter cross-sectional area solid piece taken from just above the ash layer between 527 cm and 532 cm core depth (~25 cm^3); the upper 3.8 cm of the sample was composed of dark brown gyttia and the lower 1.2 cm was the gray volcanic ash. The second sample of the pair, RC2, was a 3.8-cm long one quarter cross-sectional area solid piece taken from the core just below the ash layer between 533 cm and 537 cm core depth (~19 cm^3); the entire sample was composed of dark brown gyttia.

Ronald Bog.

Ronald Bog (unofficial name) is an ~2 ha open meadow that is bounded on three sides by the Bullfrog Moraines (Porter, 1976) and is located ~1 km southeast of Ronald, Washington, USA at an elevation of ~700 m (47° 14´ N, 121° 1´ W). The bog is currently surrounded by a ponderosa pine (*Pinus ponderosa*) forest. There were no streams flowing into or out of the bog at the time the core was collected. The 5-cm diameter sediment core used in this research was obtained from near the center of the lowest area of the bog using a modified Livingstone sampler with the cooperation of Terry Swanson (UW Geology) in the summer of 1991. The total length of the core was ~4 m. The upper 15 cm of the core were composed of dark brown, muddy peat; the next

46 cm were composed of light brown silty sediments, and the remainder of the core was composed of a mixture of silty, sandy, and clayey sediments with varying, but relatively small, amounts of organic material throughout.

An orange-yellow ash deposit was found in the core at 39 cm core depth; the ash appeared to be the edge of a lens-shaped deposit that occupied about half of the core cross-section and had a maximum thickness of 2.5 cm. Four samples were taken from the core. The first pair of samples were processed during the studies of the modifications required to improve the rejection of non-pollen materials in the extraction of pollen from peat samples. Pollen fractions and β-prep samples were prepared from the second pair of samples for AMS ^{14}C dating. The first of these two samples, RB3, was taken from the core beside the upper part of the ash lens (33.5 cm to 38.5 cm core depth) and consisted of a 5-cm long by one-third cross-section solid piece (~33 cm^3). The sample was composed entirely of slightly silty, brown gyttia. The second sample, RB4, was taken from the core beside the lower part of the ash lens (39.5 cm to 44.5 cm core depth)and consisted of a 5-cm long by one-third cross-section solid piece (~33 cm^3). The sample was composed entirely of slightly silty, light brown gyttia.

3.3.3 Processing of prepared samples for AMS ^{14}C dating.

In general, the preparation of ion source targets from the pollen fractions and β-prep samples produced under the procedures outlined in figure 3.1 followed the procedures for ion source target preparation discussed in the preceding chapter. While awaiting further processing, the prepared pollen fractions and β-prep samples were stored under 0.01 N HCl solution in plastic-cap sealed vials. In preparation for high temperature oxidation, the desired subfractions of the pollen fractions and β-prep samples were transferred in solution by Pasteur pipette into weighed 4 cm long 4 mm i.d./6 mm o.d. quartz tubes which were sealed at one end. The samples were then dried for 18-24 hr in an 86 °C oven and weighed again to determine the dry weight of the combustion subsamples. After the addition of CuO on top of the subsamples, the subsamples/CuO/quartz tubes were slid inside 10 cm long 7 mm i.d./9 mm o.d. quartz tubes (also sealed at one end) and the combined tubes were evacuated using a Hg diffusion pump; the subsamples inside the two sets of quartz tubes were left on the vacuum system for at least 30 min to reduce the amounts of adsorbed H_2O and CO_2 left on the surfaces of the subsamples and quartz tubes. The outer quartz tubes were then sealed and the evacuated tubes were placed in a 900°C furnace for 1 hr to oxidize the carbon in the subsamples to CO_2. After cooling in the furnace overnight, the tubes were broken open in an evacuated gas handling system, the CO_2 from the samples was transferred cryogenically to a measured volume, and the carbon yield from

the samples was determined manometrically. The subsample CO_2 was then transferred to the reduction-to-graphite system, a fraction of the CO_2 was taken for $\delta^{13}C$ measurement, and the remainder was reduced to graphite powder. Ion source targets were produced from the graphite powder following the Ta encapsulation process discussed above. (These procedures have been discussed in detail in section 2.2.1)

Data obtained during the processing of most of the samples in this part of this research are given in table 3.1. The % carbon values for the β-prep samples range from 2 to 42% with the low values being from silty gyttia samples and the higher values from peat/organic matter samples. The 30-40% carbon values obtained for the peat/organic samples are typical of the carbon content of organic matter (e.g., pure cellulose is 44% carbon by weight) and are consistent with these samples' being composed predominantly of organic matter. For the relatively large and relatively low organic content β-prep samples, the uncertainty in the % carbon values introduced by uncertainties in the manometer readings, etc., is about ±5% of the % carbon value obtained (i.e., 4.3±0.2% or 30.0±1.5%). The rather large differences between the % carbon values obtained for the pairs of β-prep samples for each core (e.g., CL3 and CL4) reflects changes in the composition of the raw sediment or peat rather than the uncertainties in the measurements.

Most of the % carbon values obtained for the pollen fractions lie in the range between 59–68%. Estimates of uncertainties in manometer readings and other steps of the carbon yield determinations suggest that the uncertainty in a typical 63% carbon value is about ±3 for samples containing 1-5 mg carbon (i.e., 63±3%) and about ±5 for samples containing ≤1 mg carbon (i.e., 63±5%). Within these uncertainties, the % carbon values obtained for the pollen fractions are consistent with the 60-66% carbon content of the sporopollenin polymers that compose the walls of the pollen grains (Heslop-Harrison, 1968; Brooks and Shaw, 1971). The high and low outlier % carbon values in the data set were obtained from the three smallest samples (TAB2GCR3, TAB2GCR4, and TAB2GKB8 in table 3.1). This suggests that, for samples containing ~0.5 mg carbon or less, the above estimates of the uncertainties in the measurements may underestimate the true uncertainty in the data, and that % carbon values obtained for such small samples by this method must be treated with some caution.

3.3.4 Results and discussion.

The 57 AMS ^{14}C dates obtained for the pollen fractions and β-prep samples extracted from the 9 lake sediment and peat cores chosen for this method validation study are given in table 3.2. Most of the AMS ^{14}C dates obtained for these samples are consistent with the range of previous dates obtained from samples associated with the Mazama Ash layer (~6.6-7.1 ka BP, as

discussed above). However, several of the dates fall significantly outside this age range. In the following, the dates obtained for the pollen fractions and β-prep samples will first be discussed in terms of the internal consistency of the dates obtained from each lake sediment or peat core (i.e., the reproducibility of the dates obtained from the two pollen fractions extracted from each core sample, the differences between the dates obtained on the pollen fractions and the β-prep sample from each core sample, and the differences between the dates obtained for the *above* and *below* core samples). Then, the dates will be compared to dates previously obtained by others on materials associated with the Mazama eruptive event and ash layer, with particular emphasis on the consistency and accuracy of the pollen fraction dates and the sources of differences between the dates from different cores in this study. Finally, the ^{14}C dates obtained for the pollen fractions and β-prep samples extracted from the Crocker Lake core will be discussed additionally in some detail because these dates provide clear evidence of the effectiveness of the extraction and AMS ^{14}C dating of pollen fractions in eliminating one of the reasonably common sources of ^{14}C dating error encountered in applying the traditional method of dating the TOC fraction from lake sediment samples using β-counting ^{14}C dating techniques.

However, before these discussions are begun there is one aspect of the dates that should be noted. Examination of the dates in table 3.2 shows that the date obtained for the 20<<44 μm pollen fraction from the *above* sample from the Ronald Bog core (9430±70 BP) is anomalous relative to both the other dates obtained for that particular core sample and the dates obtained for all of the other core samples. Unfortunately, the entire 20<<44 μm pollen fraction sample was used in obtaining this anomalous date and it has not been possible to determine whether the date was caused by contaminants in the pollen fraction that were not removed during the pollen extraction procedure or by contamination introduced during the subsequent steps in the preparation of the ion source target. Given the obviously anomalous nature of this date and the lack of opportunity to investigate its cause, the date obtained for the 20<<44 μm pollen fraction from the *above* sample from the Ronald Bog core has been excluded from all of the following analyses of the dates obtained in this study.

3.3.4.1 Internal consistency of the ^{14}C dates obtained from each core.

Internal consistency of pollen fraction ^{14}C dates.

In general, the dates obtained for the 44<<88 μm and 20<<44 μm pollen fractions from each core sample agree within the uncertainties in the measurements (table 3.2). The overall agreement between the dates obtained for the two pollen fractions can be evaluated by constructing a normalized Gaussian statistic as the ratio of the difference between the two pollen

fraction dates for each core sample to the propagated 1σ uncertainty in that difference; i.e., for two dates $x_1 \pm \sigma_1$ and $x_2 \pm \sigma_2$, the normalized Gaussian statistic would be $z = (x_1 - x_2)/((\sigma_1^2 + \sigma_2^2)^{1/2})$. Evaluation of this statistic for the 15 pairs of pollen fraction dates ($|z|_{pp}$ values in table 3.2) shows that $|z|_{pp} \leq 1$ for 12 of the date pairs (i.e., the difference between the dates is less than the propagated 1σ uncertainty in the difference), that $1 < |z|_{pp} \leq 2$ for 2 of the date pairs (i.e., the difference is greater than the 1σ uncertainty, but less than the 2σ uncertainty, in the difference), and that $|z|_{pp} > 2$ for 1 of the date pairs (i.e., in one case the difference is just greater than propagated 2σ uncertainty in the difference). Hence, the $|z|_{pp} \leq 1 : 1 < |z|_{pp} \leq 2 : |z|_{pp} > 2$ distribution of statistic values derived from the date pairs is 12 : 2 : 1.

If the observed differences between the dates in each of the 15 date pairs were due to measurement uncertainties alone (i.e., if, for each core sample, the difference between the actual ^{14}C ages of the two pollen fractions were zero), then the statistically expected $|z|_{pp} \leq 1 : 1 < |z|_{pp} \leq 2 : |z|_{pp} > 2$ distribution of normalized Gaussian statistic values would be 10.2 : 4.0 : 0.8. Thus, the observed differences between the two pollen fraction dates for each core sample are consistent with the actual ^{14}C ages of the two pollen fractions' being identical. These results indicate that the significant differences between the distributions of pollen types in the 44<<88 μm and 20<<44 μm pollen fractions do not introduce significant bias into the measured ^{14}C ages of the two pollen fractions. In addition, in order for the ^{14}C ages of the two pollen fractions to be statistically identical, any significant amounts of carbon-containing non-pollen materials which had not been removed from the pollen fractions, and whose ^{14}C contents differed significantly from that of the pollen, must constitute the same fraction of the total carbon in both of the pollen fractions from each core sample (a seemingly improbable occurrence for all 15 pollen fraction pairs). Hence, these results also indicate that the pollen extraction procedures have removed all significant amounts of carbon-containing contaminants whose ^{14}C contents differed significantly from that of the pollen in the samples.

Based on this analysis, the two dates obtained on the pollen fractions from each core sample have been treated as independent measurements of a single ^{14}C age, and weighted means (and corresponding uncertainties) have been calculated from the date pairs for use in subsequent analyses (table 3.2).

Inconsistencies between pollen fraction and β-prep sample ^{14}C dates.

The dates obtained for the pollen fractions from the various core samples can be compared to the corresponding β-prep samples using the same normalized Gaussian statistic as was used above. In this analysis, the β-prep date for each core sample was compared to the corresponding

weighted mean date calculated from the available pollen fraction dates for the core sample (since 20<<44 μm fractions from the two Crocker Lake core samples were not measured, only the 44<<88 μm dates for these samples were used in the comparison). Evaluation of z, the normalized Gaussian statistic described above, for the 18 pollen-fraction/β-prep date pairs ($|z|_{pb}$ values in table 3.2) shows that the observed $|z|_{pb} \leq 1 : 1 < |z|_{pb} \leq 2 : |z|_{pb} > 2$ distribution of the statistic values derived from the date pairs is 8 : 4 : 6. If the observed differences between the dates in each of the 18 date pairs were due only to measurement uncertainties the statistically expected distribution would be 12.2 : 4.9 : 0.9. Clearly, the observed differences between the pollen fraction and β-prep dates are not consistent with the expected differences derived from the uncertainties in the dates. The larger-than-expected number of statistic values in the $|z|_{pb} > 2$ range indicates that there are significant differences between the ^{14}C ages obtained for some of the β-prep samples and their corresponding pollen fractions.

Examination of the β-prep and pollen fraction (weighted mean) date pairs shows that by far the largest differences are between the dates obtained for the samples from the Crocker Lake core; both of the dates on the β-prep samples are ~1000 years older than the pollen fraction dates (these differences correspond to $|z|_{pb}$ values of ~11). Since the purpose of this analysis is to determine if there are, in general, significant unexplained differences between the β-prep and pollen fraction dates, and since the relatively old dates for the Crocker Lake β-prep samples can be attributed to specific effects in the lake and watershed ("hard water" effects: discussed separately below), the Crocker Lake dates have been excluded from the following more detailed analysis of the differences between the β-prep and pollen fraction dates. This will avoid biasing the results of the analysis with the very large, but explainable, differences between the β-prep and pollen fraction dates obtained from the Crocker Lake core samples.

If the normalized Gaussian analysis used above is applied to the dates obtained from the 8 *below* core samples separately from those obtained from the 8 *above* core samples, the observed $|z|_{pb} \leq 1 : 1 < |z|_{pb} \leq 2 : |z|_{pb} > 2$ distributions of the statistic values are 6 : 2 : 0 for the *below* samples and 2 : 2 : 4 for the *above* samples. If the observed differences between the dates in each of the 8 date pair sets were due only to measurement uncertainties then the statistically expected distribution would be 5.4 : 2.2 : 0.4. Thus, the observed differences between the weighted mean pollen fraction dates for the 8 *below* core samples and the dates obtained for the corresponding β-prep samples are consistent with the actual ^{14}C ages of the pollen fractions and β-prep samples obtained from these samples' being identical. However, the observed differences between the weighted mean pollen fraction dates for the 8 *above* core samples and the dates obtained for the corresponding β-prep samples are not consistent with expected differences

derived from the uncertainties in the dates.

The larger-than-expected number of statistic values in the $|z|_{pb}>2$ range for the 8 *above* core samples indicates that some of the observed differences are significant and cannot be attributed to the statistical uncertainties in the AMS ^{14}C dates. For all 4 of the *above* core samples for which $|z|_{pb}>2$ in the above analysis, the dates obtained from the β-prep samples are younger than the corresponding pollen fraction dates (the Crocker Lake dates have been excluded from this analysis). As a consequence, although the β-prep and pollen fraction dates for the *below* core samples are statistically consistent, the differences between the β-prep dates obtained from corresponding *above* and *below* core samples are larger than the differences between the pollen dates obtained from the same core samples.

Together, the close agreement of dates for pollen fraction pairs, the differences between pollen fraction and β-prep dates, the bias of the *above* β-prep dates towards significantly younger ages, and the larger differences between the β-prep dates from the *above* and *below* core samples than between the corresponding pollen fractions provide significant evidence that the AMS ^{14}C dates obtained from the pollen fractions are more consistent and reliable than the dates obtained from the β-prep samples.

(Given that the possible causes of erroneous TOC ^{14}C dates discussed in the introduction also pertain to the β-prep AMS ^{14}C dates, and that the β-prep samples (and typical TOC samples) consist almost entirely of unidentifiable materials, no attempt will be made to identify the specific causes of the bias of the *above* β-prep dates towards significantly younger ^{14}C ages. From the discussion in the introduction, the two most commonly cited causes of erroneously young TOC ^{14}C dates for lake sediment and peat samples are (1) root growth to depth in peats and (2) mobile organic compounds in the sediment and/or peat deposits; either or both of these may be the cause of the significantly younger ^{14}C dates obtained for the β-prep samples.)

Analysis of differences between ^{14}C dates obtained for *above* and *below* samples.

The third aspect of the internal consistency of the dates obtained for each of the lake sediment and peat cores that will be discussed is the differences between the dates obtained for the *above* and *below* core samples. (Given the evidence obtained above on the internal consistency of the dates obtained from the pollen fraction samples and the significant bias of the dates obtained from the *above* β-prep samples towards younger ^{14}C ages, only the dates obtained from the pollen fractions have been used in the following analysis of these differences.) Examination of the dates shows that for 8 of the 9 date pairs the *above* date is younger than the date from the *below* sample (the Crocker Lake samples are included in this and subsequent

analyses), and in the single case in which the date from the *below* sample is younger, the difference between the dates is not statistically significant (the difference between the dates is only 10 years while the 1σ uncertainty in the difference is ±80 years).

Application of the normalized Gaussian statistic analysis used above to the weighted mean pollen fraction date pairs obtained for these samples (z_{ab} values in table 3.2) yields a $|z|_{ab}\leq 1 : 1<|z|_{ab}\leq 2 : |z|_{ab}>2$ distribution of the statistic values of 2 : 2 : 5, which is clearly not consistent with the 6.1 : 2.4 : 0.5 distribution that would be expected if the differences between the dates for the *above* and *below* samples were only due to the measurement uncertainties. The actual z values for the five date pairs with $|z|_{ab}>2$ are all more negative than -4.0 (recall that $z=(x_1-x_2)/((\sigma_1^2 + \sigma_2^2)^{1/2})$; here x_1 is the *above* date and x_2 is the *below* date). This indicates that the differences between the dates are much larger than statistically expected based on their uncertainties. (The probability of z values more negative than –4.0 for a normalized Gaussian statistic is negligible; $P(z \leq -4.0) < 0.0001$.)

Finding that the dates obtained for the pollen fractions show that the *above* core samples are younger than those from the *below* core samples is, given the stratified nature of the lake sediment and peat deposits, consistent with expectations. However, for five of the nine sets of core samples, the magnitudes of the differences between the dates obtained for the pollen fractions from the *above* and *below* core samples are not consistent with expectations based on estimates derived from the sediment or peat deposition rates for the cores and the lengths of the core samples taken for AMS ^{14}C measurement (see table 3.3). (These crude estimates of the expected differences were calculated from the expression $^{C14}\Delta_{ex} = (l_a/d)/2+(l_b/d)/2$, where l_a and l_b are the lengths of the *above* and *below* core samples, respectively, and d is the sediment or peat deposition rate. The deposition rate was estimated for each core as the core depth at the top of the Mazama Ash layer divided by the ^{14}C age of the pollen fractions from the *above* core sample. The first term in the $^{C14}\Delta_{ex}$ expression gives the length of time taken to deposit half of the *above* core sample and the second term gives the same quantity for the *below* core sample; the sum of these terms gives the expected difference between the measured ages of the two core samples assuming a constant sediment deposition rate.) In the following sections several possible causes of these larger-than-expected differences will be considered in detail.

Possible causes of the larger-than-expected *above/below* ^{14}C date differences: ^{14}C calibration, inaccurate sedimentation rates, and bioturbation.

In the preceding discussion, three factors which could be the cause of the unexpectedly large differences between the ^{14}C dates obtained for the *above* and *below* core sample pair have been

ignored.

First, the observed differences have been calculated as differences between the ^{14}C ages obtained for the *above* and *below* core samples. Measurements of the ^{14}C ages of dendrochronologically dated tree-ring samples have shown that the ^{14}C concentration in the atmosphere has not been constant in the past and that significant variations in the ^{14}C concentration of the atmosphere can occur in relatively short time periods (i.e., <100 years) (see, for example, references in Stuiver *et al.*, 1993). These variations can lead to circumstances in which indistinguishable ^{14}C ages (in radiocarbon years before present (BP)) can be obtained for two samples whose actual ages (in cal years before present (cal BP)) are significantly different and, just as importantly for this discussion, to circumstances in which a relatively large difference between the ^{14}C ages obtained for two samples actually represents a much smaller difference in cal year ages. This second circumstance could be the cause of the larger than expected differences between the ^{14}C ages obtained for the pollen fractions from the *above* and *below* core samples.

In order to ensure that the age differences observed between the *above* and *below* core samples are not artifacts of nonlinearities in the ^{14}C year/cal year relationship, the weighted mean ^{14}C ages obtained for the pollen fractions from each core sample were converted to cal year ages using the CALIB 3.0.3 (Macintosh Version) program (Stuiver and Reimer, 1993). The first step in the conversion of the ^{14}C ages was the calculation of a sediment or peat deposition rate (in cm/cal year) for each core sample from a preliminary calibration of the ^{14}C ages from the *above* samples and the core depth of the ash layer. These deposition rates were combined with the lengths of the core samples to yield estimates of the cal year time spans each core sample represented. Since the ^{14}C age obtained for each core sample represents an average ^{14}C concentration over the time span during which the sediment or peat in the core sample was deposited, the bidecadal ^{14}C-to-cal year calibration curve used in the CALIB program was smoothed by an appropriately long moving average to account for the ^{14}C averaging effect introduced by the incorporation of ^{14}C over the entire time span during which each core sample was deposited. For example, a 5-cm long sample from a core in which the sediments were deposited at a rate of 0.05 cm/year would have been deposited over a time span of 100 years and the ^{14}C concentration in the sample would reflect the average ^{14}C concentration over that time period; hence, in converting the ^{14}C age obtained for this sample to a cal year age, the calibration curve should be smoothed with a 100 year moving average.

The calibrated cal year ages produced by this process for the *above* and *below* pollen fractions are given in table 3.4 along with the moving average time spans used to smooth the

calibration curve for each sample and $^{Cal}\Delta_{ex}$ estimates of the expected *above/below* differences between the dates obtained for the core samples (derived using the cal year ages of the pollen fractions from the *above* core samples in the $^{C14}\Delta_{ex}$ expression given above). The major effect of the conversion of the pollen fraction ^{14}C dates to cal year ages was to add about 800 years to the core sample ages. The effect of the conversion on the magnitudes of the uncertainties in the core sample ages, the differences between the ages of the *above* and *below* core samples, and the magnitudes of the expected *above/below* differences was in all cases small compared to the uncertainties in these quantities, except for the Rock Creek Pond ^{14}C dates. (The expected cal year *above/below* age differences, $^{Cal}\Delta_{ex}$, are shown in table 3.5, column 7. The expected radiocarbon year *above/below* age differences, $^{C14}\Delta_{ex}$, are shown in table 3.5, column 6.)

For the Rock Creek Pond ^{14}C dates, the conversion to cal year ages increased the *above/below* age difference from 198±104 ^{14}C years (table 3.5, column 5) to 318±198 cal years (table 3.5, column 4). Thus, the age difference was increased by just slightly more than the 1σ uncertainty in the ^{14}C age difference, and the uncertainty in the age difference was almost doubled. However, the increased age difference and increased uncertainty in that difference have had no statistically significant effect on the relationship between the observed *above/below* age difference and the corresponding $^{C14/Cal}\Delta_{ex}$ estimate of that difference; i.e., for both sets of dates, the Δ_{ex} estimate of the *above/below* age difference for the Rock Creek Pond core samples is larger than the corresponding observed age difference by about 1.2 times the 1σ uncertainty in the observed age difference.

Thus, the conversion of ^{14}C ages to cal year ages has a minimal effect on the *above/below* age differences for the core samples studied. This shows that the differences cannot be attributed to nonlinearities in the ^{14}C year/cal year relationship, but rather represent significant cal year differences between the ages of the *above* and *below* core samples. In addition, the disagreements between the observed *above/below* age differences for the core samples and the crude estimates of the expected differences were not significantly affected by the conversion of the ^{14}C dates to cal year ages, and hence also cannot be explained as artifacts of a non-linear ^{14}C year/cal year relationship.

The second factor which could be the cause of the larger-than-expected differences between the ^{14}C dates obtained for the *above* and *below* core samples is the inaccurate estimation of the rates of sediment deposition during the periods before and after ash layer deposition. In the calculations of the relatively crude $^{C14}\Delta_{ex}$ estimates given above, the deposition rate for each core was estimated from the core depth at the top of the Mazama Ash layer and the ^{14}C age of the pollen fractions from the *above* core sample. In using these estimates, the assumption was

made that the average sediment deposition rate over the last ~7500 cal years provided a relatively accurate measure of the deposition rate for ~500 year periods both before and after the deposition of the ash layer. Obviously, this assumption would have been unnecessary if several ^{14}C dates which spanned a significant depth range above and below the ash layer had been obtained for each core and used to directly determine the sedimentation rates. However, given the considerable number of ^{14}C dates required by this direct determination method, such an approach was not viable within the resources available for this study. In the following, two lines of indirect evidence will be discussed which suggest that inaccuracies in the sedimentation rate estimates are unlikely to be sufficiently large to explain the observed differences between the ^{14}C dates obtained for several of the *above* and *below* core sample pairs.

The first line of indirect evidence is based on the physical appearance and constancy of composition of the cores in this study and of cores from similar locations in the Pacific Northwest and California. For six of the nine cores in this study, field notes and observations (during the extrusion of the core sections from Livingstone sampler tubes) indicate that there were no significant changes in the physical appearance of the sediments between the ash layers and the tops of the cores (Chase Lake (T. W. Swanson, 1992 Field Notes), Crocker Lake (J. S. McLachlan, 1991 Field Notes, personal communication, 1993; McLachlan, 1994), Heal Lake (P. J. Reimer, 1992 Field Notes, personal communication, 1994), Kachess Bog (T. W. Swanson, 1990 Field Notes, personal communication, 1994), Lizard Lake (T. W. Swanson, 1991 Field Notes), Rhamnus Lake (T. A. Brown, 1991 Field Notes)). While such information was not available for two (Dead Ice Pond and Rock Creek Pond) of the three remaining cores, examination of the sediments in the sections of these two cores from which the *above* and *below* samples were taken showed that there were no significant changes in the character of the sediments above the ash layer within these sections. Similar examinations of the sediments in the relevant core sections from the six cores mentioned above also showed that there were no significant changes in the character of the sediments above the ash layer within those sections. (The core sections were all about 1 m long and the position of the ash layer within each section varied among the sections.) In the one remaining core (Ronald Bog), the sediments between the ash layer and the core top did show significant changes in physical appearance; this core will be discussed separately below.

Information on the constancy of the composition of the sediments deposited at the coring sites over the last ~7500 cal years also provides indirect evidence on the possible inaccuracies in the sedimentation rate estimates. Sediment composition data are available for only one of the nine cores used in this study. Loss-on-ignition data obtained during a study of the Crocker Lake

core show that the composition of the sediments above the ash layer was essentially constant (McLachlan, 1994). (The only significant change in the composition of the sediments above the ash layer appears to have occurred at the same time as European settlement in the Crocker Lake area (~90 cm of sediment was deposited within the last ~100 years); adjustments for this change in sedimentation rate do not have a significant effect on the average sedimentation rate after the deposition of the Mazama Ash layer, and do not impact significantly on the calculated $C14\Delta_{ex}$ values for Crocker Lake.)

While direct data on the composition of the sediments in the other eight cores in this study are not available, some information on the probability of significant changes in sediment composition of these cores can be obtained from studies of other cores in the same regions. In the case of the Rock Creek Pond core, the data obtained by Anderson (1987, 1994) from the lake sediment core from the nearby Barrett Lake site (~30 km from the Rock Creek Pond site) indicate that the composition of the sediments in the Barrett Lake core did not vary appreciably between the ash layer deposition and the present. If the Barrett Lake is a reasonable proxy for the Rock Creek Pond core, Anderson's observations suggest that the composition of the sediments in the Rock Creek Pond core probably did not vary significantly over the same period.

For the other six cores which did not show any evidence of significant changes in the physical appearance of the sediments between the ash layers and the tops of the cores (Chase Lake, Dead Ice Pond, Heal Lake, Kachess Bog, Lizard Lake, and Rhamnus Lake), information on the probability of compositional variations can be inferred from studies of other sites within the Fraser and Puget Lowlands (e.g., Mathewes,1973; Barnosky, 1981; Tsukada *et al.*, 1981; Barnosky, 1985a; Barnosky, 1985b; Wainman and Mathewes, 1987). In the two of these studies in which the physical appearance of the sediments changed between the ash layer and the top of the core (Barnosky, 1981; Barnosky, 1985b), loss-on-ignition data also show significant variations. In the other four studies, there was no evidence of significant changes in the physical appearance of the sediments between the ash layer and the core top, and the loss-on-ignition data did not show any evidence of significant variations. From these studies, the inference can be drawn that the lack of significant changes in the physical appearance of the sediments in the six cores in this study mentioned above indicates that the composition of the sediments (e.g., the loss-on-ignition measure of the organic carbon content) also did not vary significantly.

Thus, for eight of the nine cores used in this study, the available information on the physical appearance and composition of the sediments above the ash layers does not provide any evidence suggesting that significant changes in the rates of sediment deposition occurred at the coring sites during the period between the deposition of the ash layer and the present. While

such indirect evidence does not prove that significant sedimentation rate changes did not occur at one or more of these coring sites, the constancy of the physical appearance and composition of the sediments in these sections of the eight cores does imply that the environmental conditions in the lakes and/or bogs from which these cores were taken have probably remained relatively stable over the time since the deposition of the ash layer, and suggests that dramatic changes in the sedimentation rates are unlikely.

The Ronald Bog core was the only core used in this study in which a significant change in the character of the sediments between the ash layer and the core top was observed. As mentioned in the site/core description above, the ash layer in the Ronald Bog core was contained in the uppermost section of the core; the upper 15 cm of this section was composed of dark brown, muddy peat and the next 46 cm (which contained the ash deposit at 39 cm core depth) was composed of light brown silty sediments. This significant change in the nature of the sediments between the ash deposit and the surface suggests that the rate of sediment deposition at the Ronald Bog coring site has not been constant since the deposition of the ash layer. This suggests that the sedimentation rate estimate derived from the core depth and ^{14}C age of the pollen fractions from the *above* core sample probably does not provide an accurate estimate of the sedimentation rate in the Ronald Bog core during relatively short periods before and after the deposition of the ash layer. The change in the physical appearance of the Ronald Bog sediments (coupled with the "edge of a lens" shape of the ash deposit in the core and the relative closeness of the ash deposit to the sediment surface) also raises significant questions concerning the environmental conditions under which the sediments and the ash were deposited and preserved at the Ronald Bog coring site, and concerning the interpretation of the ^{14}C dates obtained for the pollen fractions and β-prep samples from this core. These questions will be discussed in later sections in the context of an alternative explanation (bioturbation) of the larger-than-expected *above/below* ^{14}C date differences and of comparisons of the ^{14}C dates obtained for the Ronald Bog samples with the "consensus" ^{14}C age of the Mazama Ash layer.

The second line of indirect evidence is based on the measured core depth versus ^{14}C age profiles obtained for one of the sediment cores in this study and for sediment cores from similar locations in the Pacific Northwest and California. The core depth versus ^{14}C age data obtained by McLachlan (1994) for the Crocker Lake core show that the sedimentation rate at that site has been essentially constant over the entire length of the core (~9 m sediment that has been deposited since ~11 ka BP). Linear regression of the ^{14}C dates used by McLachlan yields a sedimentation rate of 0.075 cm/yr for the Crocker Lake core. Comparison to the sedimentation rate of 0.0877 cm/yr calculated from the core depth and ^{14}C age of the top of the ash layer (table

3.3) shows that the method of calculation used in this study produces an estimate of the sedimentation rate that is inaccurate by ~15%. (If adjustments are made for the higher sedimentation rate at the Crocker Lake site attributed to the first European settlements in the Crocker Lake area (~90 cm of sediment appears to have been deposited in the last ~100 years), the sedimentation rate calculated by the method used in this study is indistinguishable from the rate obtained from the linear regression.)

For the other eight cores in this study, core depth versus ^{14}C age data are not available and the probability of significant inaccuracies in the estimated sedimentation rates must be inferred from the studies at other sites within the Fraser and Puget Lowlands and California which were mentioned above. The cores from three of these studies were chosen as examples on the basis of the availability of appropriate core depth versus ^{14}C age data and the lack of any significant changes in the physical appearance of the sediments above the ash layer. The core depth versus ^{14}C age data obtained by Anderson (1987, 1994) for the Barrett Lake core suggests that the sedimentation rate at the site was relatively constant over the period of interest; linear regression of the data yields a sedimentation rate of 0.014 cm/yr. Calculation of the sedimentation rate using only the core depth and ^{14}C age of a sample from just below the ash layer yields a sedimentation rate estimate of 0.016 cm/yr, which is inaccurate by ~12%. Application of the same procedures to the essentially linear core depth versus ^{14}C age data obtained by Mathewes (1973) for the Marion Lake core yields a linear regression sedimentation rate of 0.096 cm/yr, which is ~10% higher than the sedimentation rate calculated from the core depth and ^{14}C age of the top of the ash layer (0.088 cm/yr). The essentially linear core depth versus ^{14}C age data obtained by Barnosky (1985a) for the Battle Ground Lake core yields a linear regression sedimentation rate of 0.067 cm/yr (only the three samples with ^{14}C ages less than 10 ka BP were used in the regression), which is <5% lower than the sedimentation rate calculated from the core depth and ^{14}C age of the sample closest to the ash layer (0.069 cm/yr).

Thus, the core depth versus ^{14}C age data obtained for the Crocker Lake core and for the three cores from the other studies indicate that, for cores in which there are no significant changes in the physical appearance of the sediments between the ash layer and the surface, the inaccuracies in the sedimentation rates calculated from the core depth and ^{14}C age of the top of the ash layer are probably not larger than ~15%. Comparison of the calculated $^{C14}\Delta_{ex}$ values for the nine cores in this study to the observed ^{14}C age differences (table 3.3) shows that the observed differences for four of the nine *above/below* core sample pairs are more than 300% larger than the calculated $^{C14}\Delta_{ex}$ values for the samples. Hence, the two lines of indirect evidence argue strongly that the probable magnitude of any inaccuracies in the sedimentation

rate estimates used in the $^{C14}\Delta_{ex}$ calculations cannot explain the disagreement between the $^{C14}\Delta_{ex}$ values and the large observed differences between the ^{14}C dates obtained for several of the *above* and *below* core sample pairs.

The third factor which could have had a significant impact on the differences between the dates obtained for the *above* and *below* core samples, and which was ignored in the initial discussion of the expected and observed differences, is the possibility of bioturbative mixing of the upper layers of the sediment over some significant core depth/time span following deposition.

In a series of laboratory experiments, Davis (1974) showed that tubificids (worms) obtained from the natural lake sediments commonly burrowed to 12 cm depths in the laboratory sediment columns used in these experiments and that there were sporadic occurrences of burrowing to depths as great as 40 cm. These results were in general agreement with observations of tubificids in sediment cores which were recovered from various sites in several studies that encompassed a variety of limnological conditions, tubificid population densities, and measurement methodologies (Davis, 1967; references cited in Davis (1974)). Davis (1974) also showed that, over the 145 and 260 day durations of the laboratory experiments, the feeding activities of tubificids significantly disturbed the upper layers of the sediment columns used in the study and that measurable mixing of the upper layers of the sediments occurred down to ~9 cm below the sediment surface.

Studies of the distributions of ^{210}Pb and ^{137}Cs in the upper layer of lake sediments under laboratory conditions (Robbins *et al.*, 1977) and natural conditions (Robbins *et al.*, 1979) provided support for the results obtained by Davis (1974) and showed that the bioturbation by tubificids of the upper layers of the sediments used in their laboratory studies effectively mixed the ^{137}Cs-containing tracer material (this material had been initially applied as a <1 mm thick layer on top of the sediments) throughout the upper 7-9 cm of the sediment column over the 173 day period of the experiment.

In relation to the ^{14}C dating of sediment samples, the bioturbative mixing of the upper layers of the sediments has the effect of mixing recently deposited sedimentary material with material that was deposited previously, and, hence, causes the sediments at the surface to have a non-zero apparent age; the surface sediments (and the sediments throughout the bioturbation layer) have an apparent age that is essentially equal to the thickness of the bioturbation layer divided by the deposition rate of the sediments. For example, if the sediments at a particular site in a lake were being deposited at a rate of 0.06 cm yr^{-1} and the bioturbation layer was 12 cm thick at that site, then the ^{14}C concentration in any sediment sample taken from within the bioturbation layer (including samples of the surface sediments) would yield an apparent ^{14}C age of about

200 years (In this simple example, possible variations in the atmospheric ^{14}C concentration have been neglected). Clearly, such bioturbation processes in the upper layers of the sediments could have a significant impact on the observed age differences between *above* and *below* core samples.

In considering the possible impact of bioturbation on the *above/below* age differences observed for the samples in this study, the fact that the depositional environments under which sediments accumulate in lakes are different from those in peat bogs implies that depositional processes that have a significant impact on the deposition of sediments in lake environments may be unimportant in bog environments. In particular, there is evidence from several studies of palynological records in peat bogs that bioturbative processes similar to those described above could not have been active in the peat bogs from which the sediment cores used in those studies were obtained (e.g., Green *et al.*, 1988; Sugita, 1990). As described above in section 3.3.2, seven of the nine cores obtained and sampled for the Mazama Ash study were composed of lake sediments of various types, and only two (Dead Ice Pond and Kachess Bog) were composed of peat. Thus, while particular depositional and/or post-depositional processes in lakes, such as bioturbation, may be considered in attempting to explain the larger-than-expected *above/below* age differences observed for the sample pairs from the seven lake sediment cores, the invocation of the same processes to explain the results obtained from the two peat cores would (in all probability) be inappropriate.

In the final two sections of these internal consistency analyses, the effects of bioturbation on the *above/below* age differences will be considered in detail and the expected *above/below* age differences obtained from a model of the bioturbation effects will be compared to the observed differences. Keeping in mind that the application of the bioturbation model to the peat cores is clearly questionable, the expected *above/below* age differences will be calculated under the bioturbation model for all nine of the cores sampled for the Mazama Ash study and the results will be considered in terms of the possible importance of bioturbation in the environments under which the sediments in the various cores were deposited. Consideration of other depositional and post-depositional processes in lakes and/or bogs, such as sediment resuspension and redeposition within lakes during isothermal conditions (Davis, 1968; Davis, 1973), the growth of roots to depth in peat deposits (Dickinson, 1983), and movement of pollen within peat deposits in response to water movement through the upper layers of the deposits (Clymo and Mackay, 1987), will be postponed until comparisons of the ^{14}C ages obtained for the Mazama Ash layer from the samples in this study to the ^{14}C ages obtained in previous studies (section 3.3.4.5).

3.3.4.2 Bioturbation model.

In order to investigate the combined effects of bioturbative mixing of the upper layers of the lake sediments and the interruption of the normally continuous sediment deposition process by the deposition of the ash layer on the expected age differences between the *above* and *below* core samples, a computer model of the deposition and bioturbation processes was developed. The initial versions of this model were developed by Prof. George Farwell, and the results obtained using these versions provided motivation and guidance for the further development and utilization of the model to obtain the results presented below.

The sediment deposition and bioturbation model is a finite step model in which the sedimentary and bioturbative processes are represented by the incremental deposition of a succession of new sediment layers onto the top of a sediment column. In this model the deposition of each new sediment layer is followed by the homogeneous mixing of the new layer with the several layers of previously deposited sediments within the bioturbation layer. With each new sediment layer added to the total depth of the sediments, one layer at the bottom of the bioturbation layer drops below the bioturbation depth and becomes isolated from the effects of the addition of subsequent new sediment layers. Similar models of sediment deposition and bioturbation have been developed previously in studies of apparent sediment age, radioactive tracer or chemical species versus depth profiles observed in deep sea sediments and lake sediments (e.g., Davis, 1967; Berger and Heath, 1968; Guinasso and Schink, 1975; Robbins and Edgington, 1975; Peng *et al.*, 1979).

The model developed for this study was constructed using generalized time and length units to allow simple scaling of the results for particular circumstances; viz., the generalized length unit in the model is the thickness of the bioturbation layer (this length is commonly referred to as one bioturbation depth) and the generalized time unit is the length of time taken to deposit a layer of sediment that was one bioturbation depth thick (i.e., one generalized time unit equaled the bioturbation depth divided by the sediment deposition rate). In running the model, the length of time represented by each increment was set as 1/25 of the generalized time unit so that the deposition of a sediment layer whose thickness equaled that of the bioturbation layer required 25 model steps; this step size was chosen because it provided sufficient time and depth resolution for the purposes for this study without having the model become cumbersome or having its operation become unduly time-consuming. Tests of the model with a step size of 1/10 of the generalized time unit showed that the results were not significantly sensitive to the step size over the 1/10 to 1/25 step size range.

In applying this finite step model to the circumstances of interest in this study (the interruption

of the continuous and relatively slow deposition of sediments by the essentially instantaneous deposition of an ash layer of significant thickness), the ash layer was assumed to form a barrier that prevented bioturbative mixing of the sediments deposited before the ash layer with the sediments deposited afterwards. Thus, the sediments below the ash layer were "frozen" as a buried set of sediments having the age/depth profile expected of bioturbated surface sediments, and the sediments deposited above the ash layer were free of any influence from the older sediments below the ash layer. The appropriateness of this assumption (and other assumptions concerning the thickness of the bioturbation layer and the determination of the sediment deposition rate) in relation to the physical state of the ash layers and sediments in the lake sediment and peat cores used in this study will be discussed below, as will the use of this model to determine the expected age differences between samples obtained from above and below an ash layer.

Figure 3.7 shows the variation of the apparent age of the sediments immediately above and below an ash layer as a function of sediment depth, as predicted by this generalized model. Comparison of these results (heavy solid line) with the sediment age versus sediment depth relationship expected if the upper layers of the sediments were not subject to bioturbation (heavy dashed line) shows that bioturbation has two significant effects: (1) The sediments throughout a significant layer immediately below the ash layer have a constant apparent age, and this age is older than the age unbioturbated sediments would have at the same depths; the thickness of this layer is equal to one generalized length unit (i.e., the bioturbation depth) and, relative to the time at which the ash layer was deposited, the apparent age of the sediments in the layer is one generalized time unit (i.e., the bioturbation depth divided by the sediment deposition rate). (2) The sediments above the ash layer have apparent ages that are younger than the expected ages of unbioturbated sediments at the same depths. The bioturbated sediments on the surface of the ash layer (i.e., within the first incremental sediment layer deposited in the model) have an apparent age of -0.5 generalized time units relative to the time at which the ash layer was deposited. The difference between the apparent ages of the bioturbated and unbioturbated sediments decreases slowly with decreasing depth, i.e., with increasing distance above the ash layer (the difference between the ages decreases to just less than 1% of the time between the deposition of the ash layer and of the sediment layer of interest within 3 generalized length units of the top the ash layer).

It is evident that the results obtained from this model suggest that the effects of bioturbation would make the age difference between sediment samples from above and below an ash layer considerably larger than would be expected without bioturbation. For example (shown in

figure 3.7), if sediment samples that were 0.5 generalized length units long were taken from above and below the ash layer then, without bioturbation, the sample from above (below) the ash layer would have an apparent age (an average of all ages present in the sample) that was 0.25 generalized time units younger (older) than the time of ash layer deposition. Hence, for unbioturbated sediments, an age difference of 0.50 time units would be expected between the ages obtained for the above and below samples (A in figure 3.7). If the same samples were taken from bioturbated sediments, then the sample from below the ash layer would have an apparent age of 1.00 time units and the sample from above would have an apparent age of -0.63 time units. (The apparent age of the sample from above was determined as the mean of the apparent ages of the 12.5 model sediment layers in the 0.5 length unit long sample.) Thus, the expected difference between the ages of the above and below samples for bioturbated sediments would be 1.63 generalized time units (B in figure 3.7), more than 3 times the age difference expected for unbioturbated sediments.

The calculation of the expected differences between the ages of the *above* and *below* core samples using this bioturbated sediments model required the selection of appropriate values for the bioturbation layer thickness and the sedimentation rate for each core in order to convert the generalized time and length units of the model into physical measurement units (centimeters and years) and allow comparison of the results to the observed age differences and the expected age differences for unbioturbated sediments. Based on the studies of the activities of tubificids in laboratory sediment columns and in natural sediments which were discussed above, and observations during the collection of the cores used in this study, a bioturbation layer thickness of 12 cm was assumed in the calculations of expected age differences. This bioturbation depth, which is somewhat greater than the ~9 cm depths observed in the laboratory studies, was chosen for the following reasons:

(1) The relatively short periods of the laboratory experiments (100-200 days) compared to the lengths of time that sediments typically reside in the surface layers of natural lake sediments (on the order of 100 years for the sediments in this study) may not have been sufficient for less probable mixing events to have produced measurable effects in the laboratory experiments. (For example, the burrowing of the tubificids to depths greater than 10 cm has been observed as a not uncommon occurrence in the natural sediments.)

(2) During the collection of several of the cores used in this study, the upper layers of the sediments (15-30 cm) were observed to consist of unconsolidated, fluid sedimentary material with the sediments gradually becoming more consolidated and relatively firm towards the bottom of the 15-30 cm surface layers. (The sediments below this 15-30 cm surface layer were more

consolidated and sufficiently firm that they held their shape after extrusion from the Livingstone sampler tubes.) The descriptions of the sediment columns used in the laboratory experiments discussed above do not mention a similar, relatively thick, unconsolidated layer at the water/sediment interface of the columns; rather, the descriptions suggest that the laboratory columns were composed entirely of the more consolidated sediments that would lie towards the bottom of, or somewhat below, the fluid, unconsolidated sediment layers observed during the collection of several of the cores used in this study. This suggests that the laboratory sediment columns may not accurately represent natural sediment columns from the coring sites in this study. Specifically, the effect of the layer of unconsolidated, fluid sedimentary material on the activities of the tubificids and the effective depth of bioturbation does not appear to have been accounted for in the laboratory determinations of the bioturbation layer thickness. Hence, the ~9 cm bioturbation depth estimates obtained from the laboratory experiments may be less than the actual bioturbation depths produced by tubificids in natural surface sediments at the coring sites in this study.

(3) The gradual transition from unconsolidated, fluid sediments at the surface to consolidated, relatively firm sediments below 15-30 cm depth observed in several of the sediment cores obtained for this study is primarily caused by the settling and compaction of the sedimentary materials under the weight of overlying sediments. This compaction of the sediments with depth implies that a 1 cm thick layer of consolidated sedimentary material at depth in a core actually represents a significantly greater thickness of unconsolidated sedimentary material when it was freshly-deposited on the surface at some previous time. Quantitative analysis of the effects of compaction on the sediment columns requires data relating to the degree of compaction of the sediments (such as water content and bulk density) as a function of core depth. Unfortunately, such data were not obtained for any of the cores used in this study, and hence, it is not possible to develop a quantitative model of the combined effects of compaction and bioturbation on the age versus depth relationship in the sediment column. However, a general picture of the possible effects of compaction on the sediments can be obtained from a previously developed model of biologically active (i.e., bioturbated) lake sediments (Hakanson and Kallstrom, 1978).

In the model developed by Hakanson and Kallstrom (1978), sediment compaction was expressed as a function of the measured water contents and bulk densities of the sediments at depth and in the upper 1 cm of the sediment column. In applying this model to sediments from two lakes in Sweden, Hakanson and Kallstrom showed that a significant fraction of the sediment compaction that occurs in the sediment column actually occurs in the upper layers of the sediments, e.g., in one of the lakes they studied (which had a surface sediment deposition rate of

0.2 cm/yr), most of the compaction of the sediments occurred in the upper 10 cm of the sediment column. As an example they showed that an ~1 cm thick layer deposited on the surface of the sediments in the 0.2 cm/yr lake (representing ~5 years of deposition) was compacted to a thickness of ~0.5 cm by the time it was buried under 10 cm of subsequently deposited sedimentary material. The 10 cm of sediment overlying the initial layer represented a total of ~90 years of deposition because of the continuing compaction of the sediments deposited after the initial layer. (If the layers on top of the initial layer had not been compacted, the 10 cm of sediment would have represented only 50 years of deposition.)

While the direct application of Hakanson and Kallstrom's (1978) model to the sediments in the cores obtained for this study was not possible because water content and bulk density data were not obtained for the cores, the example from their study presented above suggests that a significant fraction (or most) of the compaction that the sediments undergo within the sediment column occurs within the upper 10-20 cm of the sediments. The effects of this compaction on the expected ^{14}C age differences for the *above/below* sample pairs obtained from the bioturbation model can be derived (at least in a general sense) by considering a sediment core which is "typical" of the cores in this study.

If we assume a surface sedimentation rate of ~0.13 cm/yr at the "typical" coring site, the results obtained by Hakanson and Kallstrom suggest that the compaction of the sediments would occur within the upper ~15 cm of the sediment column and that the sediments at 15 cm depth would be compacted by a factor of ~0.4. Hence, the apparent sedimentation rate of the compacted sediments at depth would be ~0.05 cm/yr, a rate that is typical of the sedimentation rates determined for the cores in this study (table 3.3). If the bioturbation depth in these sediments was ~12 cm, then the sediments at the bottom of the bioturbation layer would be compacted by a factor of ~0.5 and the overlying sediments (which are completely within the bioturbation layer) would represent ~200 years of sediment deposition. Thus, the compaction in the upper layers of the sediments would cause the homogeneously mixed sediments in the bioturbation layer to have an apparent age of ~200 years, rather than ~90 years or ~240 years (the apparent ages that would be expected from the bioturbation layer thickness and the surface sedimentation rate, or the apparent sedimentation rate at depth, respectively).

Subsequently, if (as in the bioturbation model presented above) the deposition of an ash layer effectively isolated the sediments below the ash layer from younger materials and the normal process of sediment deposition continued onto the top to the ash layer, then a bioturbation layer with an apparent age of ~200 year would be trapped, preserved and compacted beneath the ash layer under subsequently deposited sediments. At depth, the preserved bioturbation layer would

have a compacted thickness of ~6 cm and would have an apparent age of ~200 years relative to ash layer deposition (which is considerably larger than the ~90 year age that would be expected if the sediments had not been compacted as well as bioturbated within the bioturbation layer). Similarly, the combined effects of compaction and bioturbation on the age versus depth relationship for the sediments deposited on top of the ash would compress the vertical scale over which bioturbation effects caused significant differences between the apparent ages of bioturbated sediments and the expected ages for unbioturbated sediments, but the differences would have essentially the same magnitudes as in the bioturbation model presented above. Thus, Hakanson and Kallstrom's model suggests that if most of the compaction the sediments undergo occurs within the bioturbation layer, the combined effects of compaction and bioturbation would decrease the expected *above/below* ^{14}C age difference by only a small amount and the bioturbated sediments difference would still be much larger than the difference expected for unbioturbated sediments.

Together these three factors suggest that (1) the use of a 12 cm thick bioturbation layer in the calculations of expected age differences for bioturbated sediments is not unreasonable, and (2) the addition of compaction within the upper layers of the sediment column to the bioturbated sediments model would not significantly alter the *above/below* ^{14}C age differences calculated from the model described above.

In addition to the bioturbation layer thickness, the calculation of expected *above/below* ^{14}C age differences from the bioturbated sediments model results required sedimentation rate estimates for each core. These sedimentation rate estimates were obtained in the same manner as the estimates used in the $^{Cal}\Delta_{ex}$ calculations discussed above (i.e., the core depth of the top of the ash layer divided by the cal year age of the *above* core sample). As was discussed above, the inaccuracies in these sedimentation rates are probably not larger than ~15%. Given that the observed differences for several of the *above/below* core sample pairs are more than 3 times larger than the $^{Cal}\Delta_{ex}$ values for those cores, the uncertainties introduced into the expected *above/below* ^{14}C age differences obtained from the bioturbated sediments model by the ~15% inaccuracies in the sedimentation rate estimates are not of significance. Hence, these sedimentation rate estimates were judged to be sufficiently accurate for the purposes of these calculations.

(As discussed above, the Ronald Bog core was the only core used in this study in which significant changes in the character of the sediments between the ash layer and the core top were observed. This change in the sediments suggests that the rate of sediment deposition at the Ronald Bog coring site has not been constant since the deposition of the ash layer, and that

the estimate of the sedimentation rate derived as described above for the Ronald Bog core may be inaccurate by much more than ~15%. This uncertainty in the sedimentation rate estimate implies that considerable caution must be used in attempting to draw conclusions from the expected *above/below* ^{14}C age difference calculated for the Ronald Bog core from the bioturbated sediments model. In addition to the concerns raised about the accuracy of the sedimentation rate estimate by the change in the Ronald Bog sediments, the unusual shape of the ash deposit and the relative closeness of the ash deposit to the sediment surface raise further questions concerning the stratigraphy at the Ronald Bog coring site and the possibility of post-depositional disturbance of the sediments and ash deposit. These questions will be mentioned in the discussion of the results obtained from the bioturbated sediments model that follows and will be discussed in the comparison of the ^{14}C dates obtained for the Ronald Bog samples with the "consensus" ^{14}C age of the Mazama Ash layer in section 3.3.4.5.)

The expected differences between the ages of the *above* and *below* samples were calculated in the following manner: (1) The length of each core sample was expressed as a fraction of the bioturbation depth (12 cm) (i.e., it was expressed in generalized length units). This fraction was used to determine the number of model layers, either above or below the ash layer, that would be part of the core sample, assuming 25 model layers per generalized length unit. (For example, the length of a 5 cm *above* core sample would correspond to 0.417 generalized length units and, hence, to 10.41 model layers.) (2) The average relative age of the sediments within each sample (in generalized time units and relative to the time of ash layer deposition) was determined as the average of the relative ages of the model layers that had been included in the sample. (Linear interpolation between the age values obtained for discrete layers of the model was used to account for the fractions of layers that were calculated to be part of a sample.) (3) The average relative age of the sediments within each sample was converted from generalized units into cal years by multiplying the relative age from (2) by the bioturbation depth and then dividing by the sedimentation rate of the sediments in the sample (determined as described in the preceding paragraph). (4) The expected difference, $^{Biot}\Delta_{ex}$, between the ages of the *above* and *below* samples under this bioturbated sediments model was calculated as the difference between the relative ages of the *above* and *below* samples obtained in (3) for each core section. The $^{Biot}\Delta_{ex}$ values obtained from these calculations for the nine core sections sampled in this study are given in table 3.5, together with the expected $^{Cal}\Delta_{ex}$ values that were calculated above.

Before discussing these data in detail, there is one point about the $^{Biot}\Delta_{ex}$ calculations that should be mentioned. The constant relative age of the sediments within one bioturbation depth below the ash layer and the somewhat slow change in relative age with decreasing depth of the

sediments above, but close to, the upper surface of the ash layer combine to make the age differences in generalized units obtained from the model relatively insensitive to the length of the samples, provided that the samples are shorter than one bioturbation depth. For example, the expected age difference between *above* and *below* samples that are 0.17 generalized units long (i.e., 2 cm samples with a 12 cm bioturbation depth) is 1.53 generalized age units and the expected age difference between samples that are 0.50 generalized units long (i.e., 6 cm samples with a 12 cm bioturbation depth) is 1.63 generalized age units; thus, the expected age difference between the *above* and *below* samples in generalized time units changes by less than 7% over a range of sample sizes that encompasses all of the samples taken from the core sections in this study. Given this relative constancy of the expected age difference in generalized units for reasonable sample sizes and bioturbation depths, the ratio of the bioturbation depth to the sedimentation rate used in the conversion of generalized units to cal years is left as the predominant variable in the determination of the cal year expected age difference for samples from bioturbated sediments. Consequently, the validity of the assumptions made above concerning the bioturbation layer thickness and the calculation of the sedimentation rates is crucial to the accuracy of the $^{Biot}\Delta_{ex}$ values obtained from these calculations.

Notwithstanding the above, the main purpose in developing the bioturbated sediments model was not to explicitly prove that bioturbation was the cause of the larger-than-expected *above/below* ^{14}C age differences, but rather, was to demonstrate that, with reasonable assumptions, a mixing process in the surface sediments such as bioturbation could produce sufficiently large *above/below* ^{14}C age differences to account for the observed differences (which, in some cases, are a factor of three larger than the difference expected in unbioturbated sediments). Clearly, the lack of data pertaining to the state of the surface sediments at any of the coring site in this study implies that any quantitative conclusions drawn from calculated *above/below* ^{14}C age differences based on an assumed 12 cm thick bioturbation layer for all of the coring sites, must be treated with some caution. Further, even if data were obtained today on the current state of the surface sediments, forest clearance, farming, and/or European settlement in the watersheds of many of the lakes and bogs from which the cores used in this study were obtained has probably perturbed the transport and deposition of sedimentary materials within the lakes and bogs (e.g., the changes in sedimentation rate and sediment composition observed in the Crocker Lake core). Hence, the present state of the surface sediments at the coring site may not be representative of the conditions under which the sediments above and below the Mazama Ash layer were deposited. Thus, while the development of a quantitative computer model of the sedimentary process that accurately described the effects of both bioturbation and compaction

would seem to be possible, the collection of appropriate data to allow the model to be applied to the conditions under which sediments were deposited at the coring sites in this study some 7700 years ago would be a difficult undertaking. Since, as will be seen below, the bioturbated sediments model fulfilled its purpose in demonstrating that, with reasonable assumptions, bioturbation (or a similar mixing process in the surface sediments) could produce *above/below* ^{14}C age differences that were in qualitative agreement with the observed differences for several cores, the development and application of a detailed bioturbation/compaction model to the sediment cores used in this study was not undertaken.

3.3.4.3 Comparison of bioturbation model results to observed differences.

Examination of the $^{Biot}\Delta_{ex}$, $^{Cal}\Delta_{ex}$, and observed differences data in table 3.5 shows that neither the bioturbated sediments $^{Biot}\Delta_{ex}$ values nor the unbioturbated sediments $^{Cal}\Delta_{ex}$ values can account for the observed differences between the ages of all of the nine sets of *above* and *below* core samples. In fact, for one set of *above* and *below* samples (Dead Ice Pond), the $^{Biot}\Delta_{ex}$ and $^{Cal}\Delta_{ex}$ differences are both more than an order of magnitude larger than the observed difference. In the following paragraphs these data will be discussed in detail, with emphasis on observations of the physical state of the ash layer and the sediments in the cores, and the possible inappropriateness of the assumptions made in applying the bioturbated sediments model and deriving the $^{Biot}\Delta_{ex}$ differences for particular sets of *above* and *below* core samples.

Chase Lake, Heal Lake, and Rock Creek Pond.

The observed differences for three of the nine sets of *above* and *below* core samples (Chase Lake, Heal Lake, and Rock Creek) are in much better agreement with the $^{Biot}\Delta_{ex}$ values than the $^{Cal}\Delta_{ex}$ values derived for the samples (table 3.5). In these core sections the ash layer was 1-2 cm thick and formed a continuous layer that clearly separated the sediments below the layer from those above the layer; this suggests that the assumption that the ash layer formed a barrier that prevented bioturbative mixing of the above and below sediments was appropriate for these cores. As discussed above, examinations of the sediments in these cores and core sections, and other lines of indirect evidence, indicate that inaccuracies in the sedimentation rates determined from the core depth and age of the *above* core samples are probably ~15% or less, and hence, are not of significance in qualitative evaluation of the agreement (or disagreement) of the $^{Biot}\Delta_{ex}$ obtained for these cores with the observed *above/below* age differences. Given the significant uncertainties in the assumptions made in choosing the bioturbation depth and the sensitivity of the calculated $^{Biot}\Delta_{ex}$ values to this factor, the qualitative agreement of the observed

above/below differences with the $^{Biot}\Delta_{ex}$ values indicates that these differences could be largely attributed to the effects of bioturbation of the surface layers of the sediments.

Rhamnus Lake and Ronald Bog.

In two of the nine cores (Rhamnus Lake and Ronald Bog) the ash layer did not form a continuous layer across the width of the core. This suggests that the assumption that the ash layer formed a barrier that prevented bioturbative mixing of the above and below sediments was not appropriate for these cores.

In the Rhamnus Lake core the ash deposit appeared as a clumpy layer which spanned the core width but, because of the significant amounts of sediment between the ash clumps, did not isolate the sediments above the ash layer from those below. If some limited mixing through the ash layer occurred, then the age difference between the *above* and *below* samples would be expected to be somewhat less than if the ash layer had prevented such mixing. The observed difference for Rhamnus Lake is about midway between the $^{Cal}\Delta_{ex}$ and $^{Biot}\Delta_{ex}$ values (table 3.5) and is consistent with the premise that limited mixing of the sediments through the ash layer allowed sufficient exchange of pollen to have produced the intermediate observed difference. Hence, the observed differences for the Rhamnus Lake samples could be attributed to the effects of bioturbation of the surface layers of the sediments in combination with limited mixing of the sediments through the ash layer.

In the Ronald Bog core, the ash deposit appeared to be the edge of a lens that occupied about half of the width of the core and had a maximum thickness of 2.5 cm. There was no evidence of ash in the sediments in the other half of the core at the same depth. The presence of the ash as a discrete lump in the sediments, and the change in the physical appearance of the sediments above the ash layer at 15 cm core depth discussed above, imply that neither the assumption that the ash layer isolated the sediments above from those below nor the assumption that the sedimentation rate could be determined from the age and depth of the *above* sample is valid for the Ronald Bog core. In addition, the relative shallowness of the ash deposit in the Ronald Bog core (39 cm below the surface, compared to 1-6 m at the other sites) coupled with the current surface relief in the bog of 20-30 cm (caused by 30-100 cm diameter, very steep-walled "tussocks" of vegetation surrounded by 20-40 cm wide "water channels") raises concerns that, if similar conditions have prevailed at the coring for a significant period of time, erosion and deposition processes within the bog may have disturbed the sediment stratigraphy in the upper 39 cm of sediment at the coring site and/or allowed the movement of carbon-containing materials from other sediment layers into the sediments near the ash layer. In fact, the ^{14}C dates obtained

from the *above* and *below* samples from the Ronald Bog core (table 3.2), and the pollen fraction and β-prep ^{14}C dates obtained from one of the earlier samples from the core during the development of the pollen extraction procedure (labeled "Developmental Sample" under Ronald Bog in table 3.2), show that the ^{14}C ages of various components of the core vary considerably within the 5 cm diameter of the core at the ash layer core depth. Under these conditions, it is not possible to draw firm conclusions regarding the *above/below* differences and/or inconsistencies of the AMS ^{14}C dates obtained from the pollen fractions and β-prep samples from the Ronald Bog core samples.

Crocker Lake and Lizard Lake.

The observed differences for two other sets of *above* and *below* core samples (Crocker Lake and Lizard Lake) are in much better agreement with the $^{Cal}\Delta_{ex}$ values derived for the samples than with the $^{Biot}\Delta_{ex}$ values, which are much larger (table 3.5). In the Crocker Lake core, the ash layer was ~1 cm thick and formed a continuous, clearly defined layer, which appeared to have been an effective barrier that prevented bioturbative mixing of the *above* and *below* sediments. In the Lizard Lake core, the ash layer was a continuous, well defined ~42 cm thick layer that formed a massive barrier to bioturbative mixing of the above and below sediments. Hence, the assumption that the ash layer formed a barrier that prevented bioturbative mixing of the above and below sediments was appropriate for these cores. As was discussed above, the sediments in these cores and core sections (and other indirect evidence) indicate that inaccuracies in the sedimentation rates determined from the core depth and age of the *above* core samples are probably ~15% or less, and hence, are not of significance in qualitative evaluation of the (dis)agreement of the $^{Biot}\Delta_{ex}$ or the $^{Cal}\Delta_{ex}$ with the observed *above/below* age differences. The qualitative agreement of the observed differences from both of these cores with their respective $^{Cal}\Delta_{ex}$ values, and the clear disagreement with the much larger $^{Biot}\Delta_{ex}$ values, shows that bioturbative processes are not required to explain the observed differences. Hence, the observed differences between the ages of the *above* and *below* pollen fractions for these cores can be attributed to the lengths of the core samples and the sediment deposition rates and suggest that bioturbative processes did not mix the surface sediments significantly for periods of at least 200-300 years before and after the time of ash layer deposition at these sites.

It is worth mentioning that the ash layer in the Lizard Lake core was an order of magnitude thicker than in any other core in the study. This suggests that considerable amounts of the ash were transported to the coring site from within the lake (sediment focusing effects) and/or the watershed (surface wash, etc.) after the initial deposition of the ash. The fact that the 42 cm thick

ash layer was only 105 cm below the sediment/water interface at the coring site suggests that deposition and redistribution of the ash may have had a significant impact on environmental conditions that influenced the deposition and redistribution of sediments (and pollen) in the lake/watershed and, hence, that assumptions of constancy of process should be viewed with some caution for the period around the time of deposition of this very thick ash layer.

Dead Ice Pond and Kachess Bog.

The remaining two cores of the nine sampled in this study (Dead Ice Pond and Kachess Bog) were the only cores composed of coarse, matted peat (the others were composed of sediments that ranged from dry, compacted, organic-rich gyttia to clayey/silty gyttia). The observed *above/below* differences for these two sets of samples are smaller than both the $^{Biot}\Delta_{ex}$ and the $^{Cal}\Delta_{ex}$ values derived for the samples by more than the 1σ uncertainty in each difference, and neither of the observed differences is statistically different from zero at the 2σ level. In both of these cores the ash layer was 5-6 cm thick and formed a continuous layer that clearly separated the sediments below the layer from those above the layer. Both of the ash layers showed numerous horizontal and vertical brown streaks that suggested the presence of decomposed plant debris or roots within the ash layers. As discussed above, there were no apparent significant changes in the physical appearances of the sediments in the examined core sections suggesting that the sedimentation rate estimates derived from the core depths and ages of the sediments in the *above* samples from these cores were not inaccurate by more that ~15%. The fact that the observed differences from the only two cores in this study composed of coarse, matted peat are the only ones that show both of the statistical properties mentioned above confirms that the depositional environments for pollen in these peat bogs were indeed significantly different from the depositional environments at the other sites. Examination of the ^{14}C dates in table 3.2 shows that the dates obtained for the Dead Ice Pond and Kachess Bog pollen fractions and β-prep samples are distinctive, not only in terms of the observed differences between the dates obtained for the *above* and *below* core samples (i.e., ~zero), but also in terms of the absolute values of the dates (i.e., younger than expected). Several possible causes of this distinctiveness will be discussed below during comparisons of the ^{14}C ages obtained for the Mount Mazama eruption from the lake sediment and peat samples in this study to the ^{14}C ages obtained in previous studies.

3.3.4.4 Summary of the results of the internal consistency analyses.

The preceding analyses of the internal consistency of the dates obtained for the pollen fractions and β-prep samples from each lake sediment or peat core allow several conclusions to

be drawn.

First, there is no evidence of statistically significant differences between the ^{14}C dates obtained for the 20<<44 μm and 44<<88 μm pollen fractions from each core sample.

Second, there is evidence of statistically significant differences between the β-prep ^{14}C dates and the weighted-mean pollen fraction ^{14}C dates obtained for some core samples. In particular, for four of the nine *above* core samples (Chase Lake, Dead Ice Pond, Kachess Bog, and Ronald Bog) the ^{14}C dates obtained from the β-prep samples are significantly younger than those obtained from the pollen fractions. In addition, the ^{14}C dates obtained from the β-prep samples from the Crocker Lake core are both ~1000 years older than those obtained from the corresponding pollen fractions.

Third, for six of the nine cores (Chase Lake, Crocker Lake, Heal Lake, Lizard Lake, Rhamnus Lake, and Rock Creek) the observed differences between the dates obtained for the pollen fractions extracted from the *above* and *below* core samples are consistent with the expected differences for either unbioturbated sediments or bioturbated sediments (or for "partially" bioturbated sediments for which the assumptions made in applying the bioturbation model probably did not accurately represent the conditions under which the sediments and the ash layer were deposited).

Variations in the physical appearance of the sediments above the ash layer, and the "edge of a lens" shape of the ash deposit, in one of the other three cores (Ronald Bog) raise significant questions concerning potential large inaccuracies in the sedimentation rate estimates for this core and concerning the conditions under which the ash layer and surrounding sediments were deposited and preserved at the coring site. The uncertainties implied by these questions prevents firm conclusions from being drawn from the ^{14}C dates obtained from the samples from this core.

The observed *above/below* differences between the dates obtained for the remaining two cores (Dead Ice Pond and Kachess Bog), which were composed of coarse, matted peat, are small and are not consistent with expected differences obtained from either the bioturbated sediments model or the unbioturbated sediment model. The distinctiveness of the results obtained for the samples from these two peat cores shows that the differences between the depositional and/or post-depositional processes that effect the deposition of pollen in lakes and in peat bogs can have a significant effect on the average ^{14}C age of pollen in sediments associated with an ash layer in these types of deposits.

Altogether, these results and conclusions indicate that ^{14}C dates obtained from pollen extract fractions are more consistent than the ^{14}C dates obtained from samples prepared following the

traditional TOC procedure used to prepare samples for ^{14}C dating by either β-counting or AMS techniques. Further, the results suggest that depositional and/or post-depositional processes may have significant effects on the average ^{14}C ages of pollen (and other materials) in core samples associated with chronostratigraphic horizons, such as volcanic ash layers, and that the effects of such processes may have to be considered in the interpretation of ^{14}C dates obtained from such samples.

3.3.4.5 Comparison to previous ^{14}C dating of the Mazama Ash layer.

As described in the introduction to this study, a large number of ^{14}C dates pertaining to the age of the Mazama eruptive event/ash layer have been obtained in a multitude of previous studies. In the following, the ^{14}C dates obtained in this study will first be compared to the range of typical ^{14}C dates obtained in the previous studies; for the purposes of these initial comparisons, this range of typical ^{14}C dates will be defined as 6600 BP to 7100 BP since the ^{14}C dates obtained in previous studies have tended to group within these limits (see, for example, Sarna-Wojcicki *et al.* (1983)). Then, the accuracy and consistency of the ^{14}C dates obtained in this study will be evaluated by comparison to the "consensus" ^{14}C age of the climactic Mount Mazama eruption; for the purposes of these detailed comparisons, the 6840±50 BP ^{14}C date obtained by Bacon (1983) on burnt twigs found within pyroclastic flows near the eruptive site will be used as the "consensus" age of the eruption. (The uncertainties concerning this date mentioned above should be kept in mind during these comparisons.)

Most of the ^{14}C dates obtained from pollen fractions and β-prep samples in this study (table 3.2) are consistent with the 6600 BP to 7100 BP range mentioned above. However, there are three cases in which the dates obtained from particular cores (Ronald Bog, Rock Creek Pond and Chase Lake) are in obvious disagreement with the previously obtained dates. These cases of obvious disagreements will be discussed in the paragraphs immediately below before a detailed comparison of the remaining ^{14}C dates with the "consensus" age of the climactic eruption of Mount Mazama is presented.

Ronald Bog.

As was discussed above, the change in the physical appearance of the sediments above the ash layer, the clumpy nature of the ash deposit in the core, and the shallowness of the ash layer in the sediment column raise significant questions concerning the depositional and post-depositional processes under which the sediments associated with the ash deposit in the Ronald Bog core were deposited and preserved. The inconsistencies in the AMS ^{14}C dates obtained for the *above*, *below*, and Developmental samples from the Ronald Bog core (table 3.2) suggest that

sedimentary materials at the depth of the ash deposit contain significant amounts of materials with non-Mazama ^{14}C ages. In particular, the ^{14}C dates obtained for the four fractions from the Developmental Sample suggest the presence of a relatively large (>88 μm) and young (~1500 BP) material in the sediments at the depth of the ash deposit. In addition, the ^{14}C dates obtained for the *above* core sample are both significantly younger than the range of dates normally associated with the Mazama eruption/ash layer and are not consistent with the dates obtained for the Developmental Sample (which was taken from essentially the same core depth). These results suggest that, while the Ronald Bog core may (or may not) contain an interesting paleoclimatic record, the physical association of the sediments with the ash "clump" in the Ronald Bog core does not necessarily indicate a temporal association between the sedimentary materials and the Mazama eruption/ash layer deposition, and hence, that the Ronald Bog core is not an appropriate source of dating materials for a detailed study of the age of the ash layer. On this basis, the ^{14}C dates obtained from the Ronald Bog core samples have been excluded from further comparisons to Mazama eruption/ash layer ^{14}C dates obtained in previous studies.

Rock Creek Pond.

All of the ^{14}C dates obtained for the core samples from the Rock Creek Pond core (table 3.2) are significantly older than the range of dates normally associated with the Mazama eruption/ash layer. Apart from being ~1200 years older than expected, the Rock Creek Pond ^{14}C dates do not exhibit any distinguishing characteristics when compared to the sets of dates obtained for several of the other cores in this study. The Rock Creek Pond ^{14}C dates have internal consistency properties that are typical of the date sets obtained for the cores; i.e., the dates obtained for the 20<<44 μm and 44<<88 μm pollen fractions and the β-prep sample from each core sample are statistically indistinguishable, and the observed difference between the pollen fraction dates obtained for the *above* and *below* core samples is in qualitative agreement with the expected difference based on the bioturbated sediments model. As discussed above, the sediments in the core section from the Rock Creek Pond core which contained the ash layer did not show any significant changes in sediment type or color throughout the length of the core section. The ash layer in the Rock Creek Pond core was ~2.5 cm thick and formed a continuous layer across the core. The ash/sediment interface at the bottom of the layer was distinct and clearly defined; the top interface was somewhat diffuse and occupied about 1.5 cm of the 2.5 cm of total layer thickness. Taken together, these facts suggest that the Rock Creek Pond core is nearly ideal for the purposes of this study and provide no evidence of irregularities that could explain why the ^{14}C dates obtained for both the pollen fractions and the β-prep samples are ~1200 years older

than expected for samples associated with the Mazama Ash layer in a lake sediment core. The obvious (and perhaps correct) conclusion to draw from these observations is that the ash layer in the Rock Creek Pond core was not produced and deposited during the Mount Mazama eruption but rather that it was produced and deposited as a result of a volcanic eruption in the western United States some 1200 years before the Mount Mazama eruption, i.e., at ~8000 BP.

Review of the available literature on various aspects of the volcanic activity in the western United States during the latest Pleistocene and Holocene shows that very few currently recognized eruptive events are thought to have occurred in the areas relevant to the Rock Creek Pond site between ~11000 BP and ~7000 BP. In general, the events that did occur in this period are thought to have produced small to moderate amounts of ash and the dispersal of the ashes was limited to regions rather close to the eruptive sites (or, at least, distant from the Rock Creek Pond site). In an extensive review of volcanism in the western United States during the latest Pleistocene and Holocene, Sarna-Wojcicki *et al.* (1983) did not list any currently recognized "moderate to large" volume eruptive events that deposited significant ash layers in the Rock Creek Pond area between ~11000 BP and ~7000 BP; in fact, their map of the areal distribution of ash deposits from significant eruptive events since ~13000 BP showed that the only "moderate to large" events thought to have deposited ash in the Rock Creek Pond area during the entire Holocene were two eruptions from the Mono and Inyo Craters in east-central California that occurred within the last 2000 years.

The currently available information on the activity of the three known volcanic centers in the western United States that could be considered potential sources of the ash layer in the Rock Creek Pond sediments (Mount Mazama and the Mono and Inyo Craters) can be summarized as follows. (1) Bacon (1983) found no evidence of significant volcanic activity at Mount Mazama during the period from ~22000 BP to ~7200 BP. The Rock Creek Pond site is south of the mapped distribution of the Mazama Ash layer (Mullineaux, 1974; Sarna-Wojcicki *et al.*, 1983; Sarna-Wojcicki *et al.*, 1991) and the nearest published site at which a Mazama Ash layer has been identified is Osgood Swamp (Adam, 1967), which is just south of Lake Tahoe, California and is ~190 km north of the Rock Creek Pond site. (The occurrence of a Mazama Ash deposit at Mono Lake, ~70 km north of the Rock Creek Pond site, has been reported by Sarna-Wojcicki *et al.* (1991); unfortunately, this report is based on unpublished data from O. K. Davis and A. M. Sarna-Wojcicki). (2) The Mono and Inyo Craters volcanic areas are only ~50 km north of the Rock Creek Pond site and the available ages on Mono and Inyo Craters extrusive units and ash beds within the Mono Lake basin suggest that explosive volcanism must have been more or less continuous in the areas during the last ~40000 years and that there has been significant volcanic

activity in the areas over the period from ~12000 BP to ~500 BP (Sarna-Wojcicki *et al.*, 1983). In their review that is now more than ten years old, Sarna-Wojcicki *et al.* (1983) found no evidence of eruptive events at the Mono and Inyo Craters that produced widespread tephras in the early/mid Holocene but stated that the latest-Quaternary tephra deposits to the east and south of the Mono and Inyo Craters (the direction of the prevailing winds) had not been studied extensively and suggested that more widespread tephra units from these volcanic areas might be found in the future.

In the time since that review, Anderson (1987) has reported ^{14}C dates obtained from bulk sediment samples from immediately below an ash layer found in two cores from Barrett Lake of 8020±190 BP and 8235±105 BP; Barrett Lake is within the Mammoth Lakes district in California and is ~45 km south of Mono Lake and ~30 km northwest of the Rock Creek Pond site. This ash layer was attributed to an eruptive event in the Mono Craters area on the basis of the texture, color and chemical composition of the ash, but the exact source of the ash has not been identified. Anderson (1987) found no evidence of the Mazama Ash in the Barrett Lake cores nor in a set of cores from Tioga Pass Pond, which is located near Tioga Pass within Yosemite National Park, Mono County, California and is ~20 km west of Mono Lake (Tioga Pass Pond is ~70 km northwest of the Rock Creek Pond site). Thus, the currently available evidence on the activity of the nearby volcanic centers supports the ^{14}C dates obtained for the Rock Creek Pond core samples in this study and the conclusion that the ash layer in the Rock Creek Pond core was produced and deposited some 1200 years before the Mount Mazama eruption as a result of an eruptive event at ~8000 BP from an (as yet) unidentified source in the Mono Craters area.

In order to determine whether the ash in the Rock Creek Pond core can be distinguished from the Mount Mazama ash on the basis of its chemical composition, a subsample from the Rock Creek Pond ash was included in a set of six ash layer subsamples that have been submitted for electron microprobe (EMP) analysis to determine the concentrations of several chemical species, such as SiO_2, Al_2O_3, Fe_2O_3, and MgO, in the glass shards of the ashes. Four of the other five subsamples were from cores used in this study (Chase Lake, Heal Lake, Kachess Bog, and Lizard Lake) and the last was from an ash layer found in a lake sediment core from Lone Lake (which is about 8 km east of Chase lake on Whidbey Island). If the chemical composition of the Rock Creek Pond ash is similar to other ashes produced in other Mono Craters eruptive events (e.g., the "Tephra 2" ash that was produced in a Mono Craters eruptive event at ~1200 BP (Wood, 1977)), then based on EMP data in Anderson (1987) and Sarna-Wojcicki *et al.* (1983), the concentrations of SiO_2, Fe_2O_3, MgO, and CaO should allow the Rock Creek Pond ash to be clearly distinguished from the Mazama Ash. (This, in conjunction with the

results of other studies, might allow the source volcano to be identified unambiguously.) Unfortunately, the EMP data are not yet available.

Chase Lake.

In the final case in which the ^{14}C dates obtained from a set of core samples are in obvious disagreement with the 6600 BP to 7100 BP age range normally associated with the Mazama eruptive event/ash layer, the dates obtained for the core samples from the Chase Lake core are ~1300 years younger than expected (table 3.2). As in the case of the Rock Creek Pond dates, the Chase Lake ^{14}C dates do not exhibit any distinguishing characteristics compared to the other sets of dates obtained in this study other than being ~1300 years "too young"; i.e., the internal consistency properties of the Chase Lake ^{14}C dates are typical of the date sets obtained for the cores. As discussed above, the sediments in the core section from the Chase Lake core which contained the ash layer did not show any significant changes in sediment type or color throughout the length of the core section. The ash layer in the Chase Lake core was ~1 cm thick, and formed a continuous layer across the core, and the ash/sediment interfaces at the top and bottom of the layer were distinct and narrowly defined. There is no evidence in the above of irregularities that could explain why the ^{14}C dates obtained for both the pollen fractions and the β-prep samples are ~1300 years younger than expected for samples associated with the Mazama Ash layer in a lake sediment core. In this context it is significant to note that the Chase Lake core extended less than one meter below the ash layer and that extrapolation of the sedimentation rate determined from the age and depth of the sediments in the *above* core sample to the base of the core suggests that the initial deposition of sediments at the Chase Lake site occurred some time after the Mount Mazama eruption. Again, the obvious (and perhaps correct) conclusion to draw from these observations is that the ash layer was not produced and deposited during the Mount Mazama eruption but rather that the ash layer was deposited at the Chase Lake site as a result of a volcanic eruption in the Pacific Northwest ~1300 years after the Mount Mazama eruption, i.e., at ~5500 BP.

The available literature on volcanic activity in the western United States during the latest Pleistocene and Holocene shows that very few significant eruptive events are thought to have occurred in the Pacific Northwest between 5000 BP and 6000 BP, and that the events that did occur in this period are thought to have produced small to moderate amounts of ash whose dispersal was limited to regions rather close to and eastward from the eruptive sites. Sarna-Wojcicki *et al.* (1983) do not list any currently recognized "moderate to large" volume eruptive events that deposited significant ash layers in the Pacific Northwest between ~6500 BP and

~3500 BP and their map of the areal distribution of ash deposits from these "moderate to large" volume eruptive events shows the Mount Mazama climactic eruption to be the only known event to have deposited ash in the Whidbey Island area during the Holocene.

The available information on the activity of the four major volcanic centers in the Pacific Northwest (Mount Mazama, Mount Rainier, Glacier Peak and Mount Baker) during the period of interest can be summarized as follows. (1) The dispersal of significant amounts of ash from the Mount Mazama volcanic center ceased with the climactic eruption that formed Crater Lake at about 6850 BP (Bacon, 1983). (2) Evidence has been found for four ash-dispersing eruptive events at Mount Rainier within the 5000-6000 BP period (Mullineaux,1974). These events are thought to have produced small/moderate amounts of ash. The deposition patterns of the ash layers from these events within the Mount Rainier area suggest that the ashes were dispersed over relatively small areas that were generally limited to the vicinity of Mount Rainier and that the prevailing winds at the times of these eruptions carried the ashes eastward from the eruptive sites (rather than to the northwest towards the Chase Lake site). (3) In summaries of the current knowledge of the timing and extent of postglacial volcanic deposits from Glacier Peak, Beget (1982a; 1982b) reported evidence for the occurrence of several ash dispersing eruptive events at Glacier Peak between 5000 BP and 6000 BP. The layers deposited as a result of these events (designated Set D layers by Beget (1982a)) were reported to be ~15 cm thick on the flanks of Glacier Peak and were thought to extend eastward from the eruptive sites (rather than westward towards the Chase Lake site). These eruptive events produced many pyroclastic flows and lahars on the west and east sides of the volcano with some flows extending more than 100 km to the west. Beget (1982a) does not provide estimates of the areal distribution of the ash deposits that resulted from these eruptive events but suggests, based on modern meteorological data, that the probable dispersal direction for the ash layers would have been eastward. (4) In a review of the postglacial volcanic deposits from Mount Baker, Hyde and Crandell (1978) report that the thickest and most widely distributed tephra erupted by Mount Baker is a black, fine to coarse sand-sized ash that is thickest northeast of Mount Baker and overlies the Mazama Ash. At a site ~10 km to the northeast of the Mount Baker summit this ash occurs in 50 cm thick deposits. The age of the eruptive event that produced this ash is only known within limits defined by the fact that it overlies the Mazama Ash and a mudflow that is believed to be ~6000 years old and underlies another mudflow that is thought to be less than 500 years old. Hence, while the currently available evidence shows that there were several eruptive events in the Pacific Northwest region during the period between 5000 BP and 6000 BP, the small amounts of ash that these events are thought to have produced and the probable (or in some cases mapped)

dispersal patterns of the ashes imply that these events are unlikely to have been the source of the orange-brown ash layer in the Chase Lake core dated in this study at ~5500 BP.

While the available information on volcanic activity in the Pacific Northwest during the period between 5000 BP and 6000 BP indicates that none of the currently recognized eruptive events during that period is likely to have been the source of the ash layer found in the Chase Lake core, this lack of evidence does not exclude the possibility that a currently unknown eruptive event (or a currently recognized event whose magnitude has been underestimated in previous studies) at ~5500 BP may have been the source of the ash layer. In this regard, the fact that one of the volcanoes thought to have been the most active in the Pacific Northwest during the period between 5000 BP and 6000 BP, Glacier Peak, lies only 100 km to the east of the Chase Lake site raises the possibility that a relatively small, previously unrecognized eruption of Glacier Peak could have deposited an ash layer over a relatively small area that included the Chase Lake site. Alternatively, the possibility exists that, for reasons currently not known or understood, the ^{14}C dates obtained from the Chase Lake core samples do not accurately reflect the time at which the ash layer was deposited, and that the ash was actually produced in the Mount Mazama eruption and deposited in Chase lake at ~6850 BP. However, the overall internal consistency of the dates obtained from the Chase Lake core samples and the physical appearance of the ash layer in the sediments argue against the two most likely causes of such dating inaccuracies, post-depositional contamination of the samples with younger carbon-containing materials and significant disturbance and redeposition of the ash deposited within the watershed to form the ash layer found in the sediments. Clearly, further data will have to be obtained in order to determine whether the ash layer is from a previously unrecognized eruptive event in the Pacific Northwest or the Chase Lake ^{14}C dates do not accurately reflect the time of ash layer deposition.

Towards that end, a subsample from the Chase Lake ash was included in the set of six subsamples that have been submitted for electron microprobe (EMP) analysis. (As discussed above, the other subsamples are from the Heal Lake, Kachess Bog, Lizard Lake, Lone Lake, and Rock Creek Pond cores.) The chemical compositions of the glass shards from various ash layers in conjunction with previously obtained data on ash from identified deposits should allow the source volcano of the ash in the Chase Lake sediments to be identified (or, at least, show whether the Chase Lake ash can be distinguished from any of the other five submitted ash samples). For instance, the Set O ash produced in the Mount Mazama eruption can be distinguished from the Set G ash produced by Glacier Peak at ~12800 BP on the basis of the differences in the Al_2O_3, Fe_2O_3, and MgO concentrations in the two ashes (based on data summarized by Sarna-Wojcicki *et al.*, 1983). As stated above, the EMP data are, unfortunately,

not yet available.

Additionally, the accuracy and reliability of the ^{14}C dates obtained from the Chase Lake core samples could be evaluated by further dating of samples from the Chase lake core and/or samples from sediment cores from nearby sites. The fact that the Chase Lake core was split lengthwise before sampling and the samples used in this study were taken from one half, leaving the other half of the core intact and essentially undisturbed, assures that further measurements on core samples that are essentially identical to those used in this study are possible. In addition, the ash layer found in the sediment core from Lone Lake mentioned above shows considerable similarity to the layer found in the Chase Lake core; the close proximity of the two sites and the similarity of the ash layers suggests that the ^{14}C dating of materials in sediments associated with the ash layer in the Lone Lake core could be used to verify the ^{14}C dates obtained from the Chase Lake core samples.

Dead Ice Pond, Kachess Bog, and Crocker, Heal, Lizard, and Rhamnus Lakes.

Comparison to the 6600 BP to 7100 BP range of typical ^{14}C dates.

With the exclusion of the dates obtained for the samples from the three cores discussed above, the remaining six sets of ^{14}C dates obtained for the samples from the Crocker Lake, Dead Ice Pond, Heal Lake, Kachess Bog, Lizard Lake, and Rhamnus Lake cores are generally consistent with the 6600 BP to 7100 BP range normally associated with Mazama eruptive event/ash layer samples (figure 3.8). The ^{14}C dates obtained for the pollen fractions from the samples from the six cores are all consistent with the 6600 BP to 7100 BP age range. However, several of the ^{14}C dates obtained for the β-prep samples from these cores fall significantly outside the range. In the four cases in which the difference between the pollen fraction weighted mean date and the β-prep date for a core sample is more than twice the propagated uncertainty in that difference (i.e., $|z|>2$), the β-prep dates are outside the 6600–7100 BP range. In two of these cases (the *above* samples from the Dead Ice Pond and the Kachess Bog cores) the β-prep dates are significantly younger than the dates for the pollen fraction from the same samples and are younger than the lower limit of the normal Mazama eruption/ash layer range (6600 BP). In the other two cases, the β-prep dates for the *above* and *below* samples from the Crocker Lake core are both ~1000 years older than the dates for the pollen fraction from the same samples and the upper limit of the normal Mazama eruption/ash layer range (7100 BP). In addition, intercomparison of the sets of ^{14}C dates obtained for the six pairs of core samples indicates that the ^{14}C dates obtained from the pollen fractions are more consistent between cores than the dates obtained from the β-prep samples. Thus, the ^{14}C dates obtained for the samples from

these six cores demonstrate that the extraction and AMS ^{14}C dating of pollen from lake sediment and peat samples can significantly improve the consistency and reliability of ^{14}C dates obtained from core samples in comparison to the dates obtained from samples prepared following the methods normally used in preparing TOC samples for β-counting ^{14}C dating.

Comparison to the "consensus" ^{14}C age of the Mazama Ash layer.

As discussed in the introduction to this study, one of the main reasons for choosing to date samples associated with the Mazama Ash layer in these lake sediment and peat cores was that the accuracy of the ^{14}C dates obtained from the pollen fractions and the β-prep samples could be evaluated through comparisons with a "consensus" age of the Mazama Ash layer that was based on the numerous ^{14}C dates that have been obtained in previous studies. For the purposes of these comparisons the ^{14}C date for the climactic eruption of Mount Mazama obtained by Bacon (1983) of 6840±50 BP was used as the "consensus" age of the Mazama Ash layer. In the following, the ^{14}C dates obtained in this study and the "consensus" ^{14}C age of the Mazama Ash layer are compared directly rather than first converting the dates to cal years and then comparing the calibrated ages. The dates were compared in this manner for two reasons: (1) the minimal impact that calibration of the ^{14}C dates had in the previous discussions showed that the ^{14}C dates obtained in this study were not subject to significant nonlinearities in the ^{14}C/cal-year relationship, and hence, distortions of the temporal relationships between the ages of the samples due to the use of ^{14}C dates rather than cal years were expected to be insignificant, and (2) the use of ^{14}C dates throughout this discussion will facilitate comparison of the ^{14}C ages obtained for the Mazama Ash layer in this study with ^{14}C ages that have been obtained in previous studies without unwarranted concern about the ^{14}C/cal-year calibration complications introduced by the (often unspecified) characteristics of the particular samples dated in the previous studies. (To ensure that the effects of calibration on the temporal relationships between the samples were indeed insignificant, the cal year ages derived above for the pollen fraction ^{14}C dates (table 3.4) were considered in light of the discussion of the ^{14}C dates that follows. As expected, the impact of the conversion to cal years on the temporal relationships between the ages derived for the samples and the uncertainties in the ages was minimal and would not alter the conclusions reached in the following discussions.)

Calculation and comparison of the ^{14}C ages of the Mazama Ash layer.

The significant differences observed between the ^{14}C dates obtained for the pollen fractions from the *above* and *below* core samples in this study required that ^{14}C ages for the Mazama Ash layer be calculated from the pollen fraction dates in order to allow comparison of the results of

this study to the "consensus" age of the Mazama Ash layer. The form of these calculations for each set of core samples was based primarily on the results obtained from the bioturbation model in the preceding section concerning the internal consistency of the ^{14}C dates obtained for the pollen fractions. For the core samples from bioturbated sediments (Heal Lake and Rhamnus Lake), the observed difference between the *above* and *below* pollen fraction dates was scaled by the ratio of the modeled relative age of the sediments in the *above* core sample to the modeled total age difference between the *above* and *below* core samples (in generalized time units) and then added to the ^{14}C date obtained for the *above* core sample. (For example, for the Heal Lake core samples the observed difference was 330±65 ^{14}C years, the ratio of the modeled ages was 0.607/1.607 = 0.378, and the ^{14}C date for the pollen fractions from the *above* core sample was 6755±42 BP; hence, the calculated ^{14}C age for the Mazama Ash layer in the Heal lake core was (0.378 X 330)+6755 = 6880±49 BP.) The scaling of the observed difference between the *above* and *below* dates with the ratio of the modeled ages was necessary to account for the asymmetry of the effects of bioturbation on the apparent ages of the sediments above and below the ash layer (see figure 3.7). For the other two lake sediments cores (Crocker Lake and Lizard Lake), and the two coarse, matted peat cores (Dead Ice Pond and Kachess Bog), the results obtained from the bioturbation model indicated that bioturbation did not have a significant effect on the apparent ages of the core samples. For each of these cores the ^{14}C age for the Mazama Ash layer was calculated as the sum of the ^{14}C date obtained for the *above* core sample and one half of the observed difference between the pollen fraction ^{14}C dates obtained for the *above* and *below* core samples on the premise that the unbioturbated sediments model shown in figure 3.7 was the most reasonable (and simplest) model of the relationship between the age and depth of the sediments or peat in the cores. The ^{14}C ages obtained for the Mazama Ash layer from these calculations for the six cores under consideration here are shown in table 3.5. (Although the Chase Lake, Ronald Bog, and Rock Creek Pond cores were excluded from these considerations based on the discussions above, the ^{14}C ages obtained by these methods for the Mazama Ash layer in these cores are also shown in table 3.5 to facilitate comparison to the ^{14}C dates obtained for unknown ash layers in other sediment or peat cores.)

As expected, the ^{14}C ages for the Mazama Ash layer calculated from the pollen fraction dates obtained for the *above* and *below* samples from the six lake sediment and peat cores are generally consistent with the 6600 BP to 7100 BP age range of typical results in many of the previous studies. However, the ^{14}C ages calculated for the ash layer in the four lake sediment cores cluster around ~6900 BP and are distinct from those calculated for the ash layer in the two (and only) cores in this study that consisted of coarse, matted peat, which cluster around

~6660 BP. The weighted mean of the ^{14}C ages for the Mazama Ash layer obtained for the four lake sediment cores is 6898±35 BP which is statistically indistinguishable from the 6840±50 BP "consensus" ^{14}C age of the Mazama Ash layer. (The ±35 year uncertainty in the weighted mean is based on the scatter of the four ages rather than the individual uncertainties in those ages, which would have produced an uncertainty in the weighted mean of ±26 years.) The weighted mean of the ^{14}C ages obtained for the two peat cores is 6666±45 BP, which is significantly younger than the "consensus" age . (The ±45 year uncertainty in the weighted mean is based on the individual uncertainties in the two ages.)

The clustering of the ^{14}C ages from the two types of deposits into two statistically distinct groups indicates that the overall range of the dates is not merely due to random scatter of the ^{14}C dates, whose magnitude would have been inconsistent with the uncertainties in the dates, but rather reflects the influence of some systematic effect (or effects) that distinguish peats from lake sediments and have not been accounted for in the calculations of the ^{14}C ages for the Mazama Ash layer from the ^{14}C dates obtained from the *above* and *below* core samples. Consideration of the possible causes of the clustering of the ^{14}C ages into these two groups suggests that the systematic effects are related to differences between the depositional and/or post-depositional processes under which the ash and pollen were incorporated into the peat and lake sediment deposits. In the following sections, several depositional and post-depositional processes that occur in lake sediments or peats and are potential causes of the observed offset between the ^{14}C ages obtained for lake sediments and those obtained for peats will be discussed.

Depositional and post-depositional processes: lake sediments.

Bioturbation.

The results obtained above from the bioturbation model above clearly show that post-depositional bioturbation of the upper layers of the sediments could have a significant effect on the apparent ages of the bulk sediments (and pollen) in the layers above and below an ash layer in lake sediments. However, the bioturbation model results were used to correct for the post-depositional effects of bioturbation in the calculations of the ^{14}C ages for the Mazama Ash layer in those sediments which appeared to have been effected by bioturbation, and hence, the observed offset between the peat and the lake sediment Mazama Ash ^{14}C ages is probably not due to bioturbative effects.

Resuspension and redeposition of the surface sediments.

The post-depositional resuspension and redeposition of surface layer sediments caused by water circulation and turbulence under isothermal conditions within a lake is a second process that is known to cause mixing of the surface layers of lake sediments (Davis, 1968; Davis, 1973). Since no attempt was made to correct for the effects of this process in the calculations of Mazama Ash ^{14}C ages for the lake sediment cores, the resuspension and redeposition of surface layer sediments is a potential cause of the observed offset between the peat and lake sediment Mazama ages. However, results and discussions presented by Davis (1973) suggest that resuspension and redeposition are unlikely to affect more than the upper several millimeters of the sediments, and hence, are unlikely to affect sediments deposited more than 10–30 years previously. Thus, the post-depositional resuspension and redeposition of surface sediments is probably not the cause of the observed offset.

Post-depositional sinking of the ash layer.

Another post-depositional process that could have had an impact on the pollen fraction ^{14}C dates obtained in this study has been observed in studies of the incorporation of the ash produced in the 18 May 1980 eruption of Mount Saint Helens into the sediments of Williams Lake, Washington (Anderson *et al.*, 1984) and Moses Lake, Washington (Welch *et al.*, 1985). (Williams Lake is located near Cheney, Washington, and is ~600 km northeast of Mount Saint Helens. Moses Lake is located near Moses Lake, Washington, and is ~240 km northeast of Mount Saint Helens.) In these studies, the 1-2 cm thick ash layer at these sites was observed to have a tendency to sink into the uncompacted sediments that composed the surface layers of the sedimentary deposits; this tendency was attributed to the significantly higher bulk density of the ash layer compared to that of the uncompacted sediments (the bulk density of the ash layer was ~1.6 g/cm^3 while the bulk density of the sediments was just slightly greater than 1.0 g/cm^3).

At some locations in Williams Lake, the 1-2 cm thick ash layer appeared to have broken up into relatively small (typically 1-4 cm in diameter) tabular or irregularly shaped pieces, and these pieces had sunk in the uncompacted sediments to depths that ranged from ~15 cm to ~80 cm. Using sediment traps Anderson *et al.* (1984) measured the rate of sedimentation in the deepest part of Williams Lake and calculated that the observed stratigraphic displacement of the broken-up ash layer pieces corresponded to the pieces' being found in association with sediments that were 60-250 years older than the ash.

In many other locations in Williams Lake and the deeper water sites in Moses Lake (5 m and 10 m water depths), the ash layer appeared to continue to exist as an essentially continuous,

undeformed 1.5-2.5 cm thick layer (Welch *et al.*, 1985). At such locations in Williams Lake the ash layer did not appear to have sunk appreciably into the uncompacted sediments after two years, and at the 10 m water depth site in Moses Lake the ash layer had sunk only ~5 cm after three years. Descriptions in Welch *et al.* (1985) suggest that the ~5 cm of sediments overlying the ash layer were not from the uniform deposition of new sedimentary material, but rather, were composed of previously deposited uncompacted sediments that had effectively moved up through gaps in the ash layer and spread across the layer's upper surface as the denser ash layer sank into the uncompacted sediments.

These observations suggest that age differences between the ash layer and the surrounding sediments are not altered significantly if the ash layer has continued to exist as an essentially continuous, undeformed layer. The possibility that the above-described post-depositional process has introduced some bias towards older dates into the ^{14}C dates obtained in this study cannot be ruled out. However, the fact that the ash layers in the four lake sediment cores do not show any evidence of being pieces of a broken-up ash layer and that the ash in each of the layers occurs within a well-defined depth interval and forms an essentially continuous layer across the core suggests that any age differences introduced by the post-depositional sinking of the ash layers are probably insignificant in the context of these comparisons to the "consensus" ^{14}C age of the Mazama Ash layer. On this basis, the possible effects of this post-depositional process have been ignored in the above calculations of the ^{14}C ages for the Mazama Ash layer.

Depositional and post-depositional processes: peat deposits.

The basic structures of the ecosystems that form peat deposits are different from the structures of those that form lake sediment deposits. The majority of the organic material in a peat deposit was produced as a part of the surface layers of that deposit. In contrast, the majority of the organic material in the lake sediments was produced either on the surrounding landscape or within the lake waters above the sediments, but not in the sediments themselves. Hence, the depositional and/or post-depositional processes under which ash and pollen are incorporated into peat deposits would be expected to differ considerably from the processes in lake sediments. The basic structures within peat deposits that are of significance to palynological studies (and to this study) have been described by Moore *et al.* (1991) and can be summarized as follows. In general terms, peat deposits can be separated into two "layers"; the lower layer is the water saturated, permanently anaerobic region in which the stratified material of interest for most palynological purposes is preserved (referred to as the "catotelm"), and the upper layer is a region of active growth and decomposition of the vegetation that forms the peat (referred to as

the "acrotelm"). While there appears to be some very slow decay of organic matter within the catotelm, it is generally considered to be an essentially passive repository of the materials that enter the permanently anaerobic zone after being buried, decomposed, and compacted under successive layers of plant debris that are deposited on the surface of the acrotelm. The acrotelm, on the other hand, is the active zone of peat deposits and is the layer within which the depositional and post-depositional processes that are of interest in this context take place. In considering the possible effects of various processes in the acrotelm on the ^{14}C ages of the material above and below an ash layer that has since been incorporated into the catotelm, there are two post-depositional processes that appear to warrant attention.

The effects of "deep" root growth.

The fact that the roots of plants growing on the surface of the acrotelm commonly extent to depths of ~20 cm (and to depths of 60-100 cm for some plant species (Dickinson, 1983)) suggests that actively growing roots at about 20 cm depth could be surrounded by decomposing organic material that was deposited on the surface of the peat significantly earlier (For example, if we assume that the decomposition and compaction of the plant debris in the acrotelm results in a factor of 10 vertical compression of the peat by the time it becomes part of the catotelm (Clymo and Mackay, 1987), then the ~0.04 cm yr^{-1} accumulation rate of the Kachess Bog deposit implies an ~0.4 cm yr^{-1} accumulation rate at the surface in the acrotelm. If the acrotelm was 25 cm thick, then the (partially) decomposed material at the bottom of the acrotelm would have been deposited on the surface more than 50 years earlier.) This suggests that the continued growth of such roots during the time required to bury an ash layer under sufficient layers of litter and plant debris that the ash layer became incorporated into the catotelm would lead to the surrounding of the ash layer by sediments that contained significant quantities of relatively young organic carbon from the roots that had continued to grow below (and for that matter above) the ash layer while it was in the acrotelm.

The example above suggests that the growth of these "deep" roots could lead to ^{14}C ages for the organic matter surrounding the ash layer that are several tens of years younger than the actual age of ash deposition. Examination of the ^{14}C dates obtained for the β-prep samples from the two sets of peat core samples in this study (Dead Ice Pond and Kachess Bog) (table 3.2) shows that the dates obtained for both the *above* and *below* core samples are 300-400 years younger than the dates obtained for the corresponding β-prep samples from the Heal Lake, Lizard Lake and Rhamnus Lake cores; although larger than might be anticipated, the observed bias of the ^{14}C ages obtained for the β-prep samples from the peat cores towards younger ages

is consistent with what would be expected from such "deep root" effects. The ^{14}C dates obtained for the developmental sample from the Ronald Bog core (table 3.2) can also be interpreted as providing support for the occurrence and importance of this post-depositional effect: (1) the ~1510 BP date obtained for the >88 μm fraction reflects the average age of relatively intact plant fragments at the ash layer depth, and a significant fraction of these fragments are from relatively recent root growth at the sample depth; (2) the ~5550 BP date for the β-prep sample reflects the average age of a mixture of the relatively young root fragments with the decomposing remains of plant debris that was deposited on the surface of the peat deposit at the same time as the ash; and, finally, (3) the ~6730 BP dates for the pollen fractions reflect the age of the pollen that was deposited on the surface of the peat deposit at about the same time as the ash (at least, within the possible effects of other post-depositional processes that have not been considered in this discussion).

The effects of water movement in the acrotelm.

The second post-depositional process that appears to warrant consideration is the relatively free movement of water through the uncompacted acrotelm and the possibility that pollen (and other materials) may undergo significant horizontal and/or vertical displacement in response to such water movement. This could occur under natural flow conditions induced by processes such as evaporation from the peat surface and/or during events such as the often seasonal rising and lowering of the water table within the peat formation (see, for example, discussion in Moore *et al.* (1991)). In a series of laboratory measurements, Clymo and Mackay (1987) showed that pollen injected at various depths in the 10 cm deep *Sphagnum papillosum* columns used in their experiments had moved by about 1.5 cm and dispersed over about 3 cm by the end of the 36 day period of their experiment in response to reasonably natural water flow regimes through the peat. In considering these results, Clymo and Mackay (1987) pointed out that the extrapolation of laboratory measurements to natural deposits is fraught with difficulty and stated that the next step in their studies would be to determine if movement of pollen in response to water flow in the acrotelm can be observed in the field. Indeed, studies of fine-resolution (3 mm) pollen records from the upper 12 cm of the peat deposits in Bega Swamp, Australia (Green *et al.*, 1988), and of fine-resolution (~15 year) pollen and charcoal records from Mount Rainier, Washington (Sugita, 1990), have provided evidence that significant vertical migration of pollen did not occur in those deposits.

Discussion of these post-depositional effects.

While the question remains open as to whether the results obtained in either of these types of

studies are generally representative of the behavior of pollen within the acrotelm of peat deposits, or rather, represent special cases that are merely indicative of the range of possible behavior of pollen in the acrotelm, the evidence obtained by Clymo and Mackay (1987) suggests that pollen may move significant distances vertically within the acrotelm in response to water movement in at least some peat deposits. The fact that such vertical movement would probably occur along vertically oriented structures such as the stems and some roots of surface plants (Clymo and Mackay, 1987), combined with the fact that these stems and roots would, in all likelihood, pass through a 1-2 cm thick ash layer, suggests that stems and roots could provide pathways for the movement of pollen through the ash layer (from above to below or below to above, depending on the flow regime in the acrotelm). Clearly, under predominantly downflow regimes such post-depositional movement of pollen might cause the ^{14}C ages obtained for pollen fractions from both above and below an ash layer to be younger than the actual ^{14}C age of the ash layer.

However, the difference of ~150 years between the pollen fraction ^{14}C age for the *below* sample from the Kachess Bog core and the "consensus" Mount Mazama eruption date, and an estimated rate of accumulation in the acrotelm of the Kachess Bog peat deposit of ~0.4 cm yr^{-1} (derived from the 0.04 cm yr^{-1} sedimentation rate in the Kachess Bog core (table 3.3) and the factor of 10 decomposition/compaction factor mentioned above), imply that the observed age difference represents a movement of the pollen through the equivalent of at most ~60 cm of newly deposited material on the acrotelm surface. While such movement is not incompatible with the results obtained by Clymo and Mackay (1987), similar pollen movement in the Bega Swamp sediments would have completely smoothed the pollen percentage variations that were observed by Green *et al.* (1988). The fact that the apparent norm (10-30 years) of the time spans represented by the acrotelms in the deposits discussed by Clymo (1983) was much shorter than the ~150 year age difference between the pollen fraction ^{14}C age for the Kachess Bog *below* sample and the "consensus" Mazama eruption date suggests that sufficient movement of pollen within the acrotelm of Kachess Bog deposits to account for such an age difference is unlikely, unless the acrotelm represents a considerably longer time span than those discussed by Clymo (1983).

Summary of the results obtained for the six consistent cores.

The ^{14}C ages for the Mazama Ash layer calculated from the pollen fraction ^{14}C dates obtained for the core samples from the six cores under consideration show that generally consistent ages can be obtained by ^{14}C dating pollen fractions. However, the clustering of the

calculated Mazama Ash layer ^{14}C ages into two groups, one consisting of the samples from the two peat cores at ~6660 BP and the other of the samples from the four lake sediment cores at ~6900 BP, indicates that depositional and/or post-depositional processes can have a significant effect on the apparent ^{14}C age of the sedimentary material above and below an ash layer. For two of the lake sediment cores the effects of bioturbation on the *above* and *below* pollen fraction dates were found to be significant and were corrected for in the calculations of the ^{14}C ages of the Mazama Ash layer from the pollen fraction dates. The ^{14}C ages of the Mazama Ash layer calculated from the pollen fraction dates obtained for the four lake sediment cores are consistent with the "consensus" ^{14}C age of the Mazama Ash layer, demonstrating that the pollen fraction ^{14}C dates obtained from lake sediments in this study are accurate and reliable within the ±50–80 year uncertainties in the individual dates.

For the two peat cores the ^{14}C ages of the Mazama Ash layer calculated from the pollen fraction ^{14}C dates are statistically indistinguishable but are ~175 years younger than the "consensus" age of the Mazama Ash layer. The clustering of the pollen fraction ^{14}C dates from the peat core samples indicates that the ^{14}C dates obtained for the pollen fractions accurately reflect the ^{14}C content of the pollen in the peat above and below the ash layer and that the ~175 year differences are not due to inaccuracies in the pollen fraction ^{14}C dates. The ~230 year differences between the ^{14}C dates obtained for pollen fractions from the peat core samples and those obtained for the pollen fractions from the lake sediment samples indicates that the differences are due to the effects of depositional and/or post-depositional processes within the peat deposit (i.e., that such processes have redistributed the pollen within the peat deposit so that the pollen found above and below the ash layer was, on average, actually deposited on the surface of the peat deposit ~175–~230 years after the ash).

While the continuous growth of "deep" roots within the acrotelm of the peat deposits and the vertical displacement of pollen in response to the movement of water through the acrotelm could, in principle, be the source of the ~175–~230 year inconsistency, the lack of more than an essentially conceptual model of these processes and the lack of detailed information on the peat deposits at the Dead Ice Pond and Kachess Bog sites precludes the quantification of the effects of these post-depositional processes and, hence, does not allow corrections for these effects to be made during the calculation of the ^{14}C ages of the Mazama Ash layer from the pollen fraction ^{14}C dates obtained from the peat samples.

(For the sake of comparison, while the ^{14}C ages of the Mazama Ash layer calculated from the pollen fraction ^{14}C dates for the Dead Ice Pond and Kachess Bog core samples are ~175 years younger than the "consensus" ^{14}C age of the Mazama Ash layer and the differences

between the pollen fraction and "consensus" ^{14}C ages have |z| values of ~2.1, the ^{14}C ages calculated from the β-prep ^{14}C dates for the same core samples are ~300 years younger than the "consensus" ^{14}C age and the differences between the β-prep and "consensus" ^{14}C ages have |z| values of ~3.6.)

3.3.4.6 Discussion of the ^{14}C dates obtained for the Crocker Lake samples.

As mentioned above, the ~1000 year differences between the pollen fraction and β-prep sample ^{14}C dates obtained for the two Crocker Lake core samples are unique in the sets of dates obtained in this study. Comparison to the "consensus" ^{14}C age of the Mount Mazama eruption shows that the ^{14}C dates obtained for the pollen fractions from the Crocker Lake core samples are not statistically inconsistent with the "consensus" age and that the ^{14}C dates obtained for the β-prep samples are all ~1000 years older than expected. The β-prep sample dates are in reasonable agreement with a 7530±130 BP (Beta-60301) date obtained previously by β-counting ^{14}C dating of the TOC fraction from a 10 cm long, one-half cross-section sediment sample (~100 cm^3) taken from above the ash layer in the 5 cm diameter Crocker Lake core (between 601 cm and 611 cm depth) (L. B. Brubaker and J. S. McLachlan, personal communication, 1994)); this supports the premise that the β-prep sample dates do in fact reflect the average ^{14}C content of the total organic carbon in the sediments. Numerous previous studies of the sources of error in the radiocarbon dating of the total organic carbon from sediment and peat samples have shown that there are many potential causes of such unexpectedly (and often, as in this case, unacceptably) old ^{14}C dates (see, for example, references in the recent review by Hedges (1992)).

"Hard water" effects.

As discussed in the introduction, one relatively common cause of such dating errors is the inclusion of the remains of aquatic plants that had consumed ^{14}C depleted bicarbonate and dissolved CO_2 from lake or mire waters as a significant fraction of the TOC sample that was dated. The most common cause of the ^{14}C depletion of the lake or mire waters is that a significant fraction of the dissolved inorganic carbon in the lake or mire waters was derived from geological carbonate minerals, which are very ^{14}C depleted; the ^{14}C dating errors caused by this effect are commonly referred to as "hard water" dating errors. In the case of the Crocker Lake samples, the presence of carbonate mineral outcrops within the watershed of the lake (Tertiary period sedimentary rocks at high elevations in the nearby mountains (Tabor and Cady, 1978)) suggests that the β-prep samples and the bulk sediment β-counting sample suffered from such "hard water" dating errors.

The fact that the ^{14}C dates obtained for the pollen fractions from the Crocker Lake core samples are statistically consistent with the "consensus" ^{14}C age of the Mount Mazama eruption provides clear evidence of the effectiveness of pollen extraction procedure in eliminating the "hard water" affected plant remains from the pollen fractions to be AMS ^{14}C dated. The various steps in the pollen extraction procedure have isolated an essentially pure terrestrially-derived fraction from the core samples (pollen) and reduced the aquatic-derived content of the samples to be dated to insignificant levels. The elimination of such "hard water" effects as a potential source of dating errors, coupled with the fact that the pollen fraction ^{14}C dates were obtained from core samples that were almost an order of magnitude smaller than the sample required for the β-counting ^{14}C date, suggests that the general and routine use of the pollen extraction procedure could eliminate "hard water" effects as sources of error in ^{14}C dates obtained for lake sediment and peat samples and significantly improve the accuracy and reliability of ^{14}C chronologies established for lake sediment and peat cores in palynological (and other paleoclimatological) studies.

The ^{14}C date obtained for the macrofossil.

A second and equally significant aspect of the ^{14}C dates obtained for the Crocker Lake samples is the observed difference between the dates obtained for the pollen fraction and the macrofossil from the *above* core sample (table 3.2). The macrofossil was isolated from the >88 μm fraction produced in the pollen extraction procedure and was identified as a seed from the genus *Potamogeton* (F. S. Hu, personal communication, 1993). (While the identification of the seed to species level might have been possible, such identification would have had essentially no impact on the analysis of the ^{14}C dates that follows.). The genus *Potamogeton* consists of aquatic plants and includes both submerged and floating species (Prescott, 1980); the submerged species would incorporate bicarbonate and dissolved CO_2 from the surrounding waters while the floating species would incorporate CO_2 from the atmosphere (Wetzel, 1988). In view of these two groups of *Potamogeton* species, and the evidence discussed above of a "hard water" effect in Crocker Lake, the ^{14}C dating of this macrofossil from the Crocker Lake core was expected to yield one of two results: (1) if the seed was from a submerged species, the ^{14}C date obtained would suffer from the same "hard water" dating errors that had been observed for the β-prep and β-counting samples (i.e., would be significantly older than the "consensus" ^{14}C age of the Mount Mazama eruption), or (2) if the seed was from a floating species, the ^{14}C date obtained would reflect the atmospheric source of the plant carbon and be consistent with the ^{14}C dates obtained for the pollen fractions and with the "consensus" ^{14}C age of the Mount Mazama

eruption. Clearly, the ^{14}C date obtained for the macrofossil of 6560±100 BP is not consistent with either of these expectations.

Based on the calculated sedimentation rate in the Crocker Lake core of ~8.8 X 10^{-2} cm yr^{-1} (table 3.3), the ^{14}C age difference between the macrofossil and the "consensus" ^{14}C age of the Mount Mazama eruption is equivalent to a downward vertical displacement of the macrofossil in the sediments of 25±10 cm. Consideration of the mechanisms that could lead to such a displacement of the seed within the sediment column suggests several depositional and post-depositional processes that could contribute to the downward displacement of the seed. First, the resuspension and redeposition of the surface layer sediments could have caused the seed to be buried under a mixture of sedimentary material that contained some proportion of somewhat older sediments (Davis, 1968). However, as discussed above, results and discussions published by Davis (1973) suggest that resuspension and redeposition are unlikely to effect sediments deposited more than 10–30 years previously, and hence, are unlikely to have caused the ~400 year difference between the age of the macrofossil and the pollen from the *above* core sample. Second, bioturbation could have caused the seed to be transported to the bottom of the bioturbation zone relatively quickly and then left the seed at depth surrounded by significantly older sediments. However, the pollen fraction ^{14}C dates obtained for the *above* and *below* core samples suggest that bioturbative processes were not significant in the Crocker Lake sediments at the time of ash layer deposition. Third, because of its comparatively high density, the seed might have settled quickly through 10's of cm of unconsolidated sediments on the surface of the Crocker Lake deposits and stopped at some depth surrounded by significantly older sediments (15–30 cm thick layers of such unconsolidated sediment were observed at several of the sites in this study).

In considering the possibility that one or more of these (or other) processes are responsible for the macrofossil's being found in the significantly older sediments of the *above* core sample, it is interesting to note that the combination of bioturbation of the sediments and the sinking of a relatively intact "slab" of the ash layer to a depth of about 5 cm (as suggested by Welch *et al.* 's (1985) observations) would provide an alternative explanation for several aspects of the ^{14}C dates obtained for the Crocker Lake core. Under this scenario a relatively intact slab of the ash layer would sink into the sediment as the bioturbated sediments below the layer moved up through gaps at the edges of the slab and covered it to some depth, which will be assumed to be about 6 cm for this discussion. If the bioturbation layer is assumed to have been about 12 cm thick then, for some short period after the sinking, all of the sediments within about 6 cm above and below the sunken slab would have the same apparent age because all of these sediments

were part of the bioturbation layer that existed just before the ash was deposited at the site. Bioturbation would then mix subsequently deposited sedimentary material with the sediments from the old bioturbation layer that were on top of the ash layer.

The principal effect of this process would be to increase the apparent age of the sediments above the ash layer and, thereby, to reduce the difference between the apparent ages of the sediments above and below the ash layer relative to the expected difference from the bioturbated sediments model. If the reduction of the difference between the apparent ages of the sediments above and below the ash layer were sufficient, the difference would be found to be consistent with the expected difference for unbioturbated sediments and the conclusion reached that bioturbative processes were not significant in the sediments (as was concluded above for Crocker Lake and Lizard Lake). The increase in the apparent age of the sediments above the ash layer would also increase the age of ash layer deposition calculated from the *above* and *below* ages by (1) directly increasing the average of the *above* and *below* ages, and (2) reducing the difference between the *above* and *below* age, causing the erroneous conclusion to be reached that bioturbative processes were not active in the sediments. On the basis of this conclusion, the age of ash layer deposition would then be calculated as the midpoint between the *above* and *below* ages rather than correcting for the asymmetry introduced by bioturbation, which tends to make the calculated age of the ash layer younger than the midpoint between the *above* and *below* ages. In this context it is interesting to note that the calculated Mazama Ash layer deposition ages for the Crocker Lake and Lizard Lake cores (the two cores for which the *above* and *below* age differences were found to be consistent with the expectations for unbioturbated sediments) are both ~6960 BP and somewhat older than the ages of ~6850 BP obtained for the bioturbated sediments cores (Heal Lake and Rhamnus Lake).

Clearly, the data available from this study are not sufficient to allow quantitative predictions to be made on the basis of this scenario. It also is clear that the construction of a quantitative model of the sinking/bioturbation process is unlikely to become feasible, because such a model would require data concerning several parameters that would be difficult (if not impossible) to obtain, such as the depth of the bioturbated sediments layer that covered the ash layer after it sank. However, this scenario does provide a plausible post-depositional process that is, at least, not inconsistent with available data and provides an explanation of the smaller than expected differences between the *above* and *below* ages for the Crocker Lake and Lizard Lake samples while allowing significant bioturbative activity in the Crocker Lake and Lizard Lake sediments. In addition, this scenario provides an explanation for the age difference between the macrofossil and the pollen fractions from the *above* core sample: the sediments on top of the ash layer that

the seed was deposited in were composed, in part, of bioturbated "old" sedimentary material that had originally been below the ash layer and had moved onto the top of the layer as it sank. This scenario also raises the question of whether bioturbation in the Crocker Lake should be (or can be) ruled out as a post-depositional process that may have contributed to the downward displacement of the seed within the sediment column.

Conclusions regarding the macrofossil from the Crocker Lake core sample.

The presence of the seed in the *above* core sample from the Crocker Lake core can be attributed to the effects of at least one, and possibly two, post-depositional processes. The first is the settling of the seed through the unconsolidated surface sediments due to the higher density of the seed compared to that of the unconsolidated surface sediments, and the second is the relatively rapid transport of the seed to the bottom of the bioturbation layer as a result of bioturbation activity in the upper layers of the sediments. The fact that the ^{14}C age of the seed is significantly younger than the ^{14}C age of the pollen in the same sediment sample indicates that the transport of this macrofossil by post-depositional processes differed significantly from the transport of pollen deposited on the lake sediments at the same time as the macrofossil. The significant difference between the ^{14}C age obtained for the macrofossil and the "consensus" ^{14}C age of the Mount Mazama eruption indicates that, because of such post-depositional processes, AMS ^{14}C dates obtained for macrofossils found in lake sediment samples do not necessarily accurately reflect the ^{14}C age of the pollen or other sedimentary materials in the samples. In this case the ^{14}C date on the macrofossil was almost 300 years too young.

3.3.5 Summary of the results obtained in the Mazama Ash study.

The Mazama Ash study was undertaken to demonstrate the accuracy and reliability of AMS ^{14}C dates obtained from pollen fractions extracted from lake sediment and peat samples through the application of the pollen extraction procedure to samples associated with a well-known chronostratigraphic marker in lake sediment and peat cores. Several major conclusions can be drawn from the results of this study:

(1) ^{14}C dates obtained from pollen extract fractions are more consistent, accurate and reliable than ^{14}C dates obtained from β-prep samples (prepared following the traditional TOC procedure used to prepare samples for ^{14}C dating by β-counting techniques).

Analyses of the differences among the ^{14}C dates obtained for the pollen fractions and β-prep samples from each lake sediment or peat core sample, and among the ^{14}C dates obtained for the *above* and *below* samples from each core, show that the ^{14}C dates obtained for the pollen fractions are more consistent than the ^{14}C dates obtained for the β-prep samples.

Comparison of the pollen fraction ^{14}C dates obtained for the core samples to the 6600-7100 BP range of typical ^{14}C dates obtained for materials associated with the Mazama Ash layer in previous studies shows that all of the pollen fraction ^{14}C dates for the core samples from six of the nine cores in this study are consistent with the range, while several of the β-prep sample ^{14}C dates for these six cores fall significantly outside the range.

(The ^{14}C dates obtained for the pollen fractions and the β-prep samples from the other three cores are relatively consistent internally but are inconsistent with the 6600-7100 BP range. Other evidence suggests that these inconsistencies are not due to inaccuracies in the pollen fraction ^{14}C dates but, rather, are due to specific effects that are discussed in section 3.3.4.5 and will be mentioned below.)

Comparison of Mazama Ash ^{14}C ages calculated from the pollen fraction ^{14}C dates obtained for each of the same six cores to the 6840±50 BP "consensus" ^{14}C age of the Mount Mazama eruption shows that the Mazama ages obtained for the four cores of the six that were composed of lake sediments are consistent with the "consensus" age and have a weighted mean of 6898±35 BP. This demonstrates that the pollen fraction ^{14}C dates obtained for the lake sediments in this study are accurate and reliable within the ±50–80 year uncertainties in the individual dates.

Comparison of Mazama Ash ^{14}C ages calculated from the pollen fraction ^{14}C dates obtained for the remaining two of the six cores, which were composed of peat, to the 6840±50 BP "consensus" ^{14}C age of the Mount Mazama eruption shows that the Mazama ages obtained for the two peat cores are somewhat younger ($|z|=\sim 2.0$ for the difference between the peat core ages and the "consensus" age) and have a weighted mean of 6666±45 BP. The clustering of the Mazama ages obtained for the peat cores into this distinct but separate group suggests that the disagreement between the peat core Mazama ages and the "consensus" age does not reflect inaccuracies in the pollen fraction ^{14}C dates. Rather, it suggests that differences between depositional and/or post-depositional processes in the peat deposits and the lake sediments caused the ^{14}C ages of pollen adjacent to the ash layer in the peat deposits to differ from the ^{14}C ages of pollen in similar positions in the lake sediments. (These depositional and post-depositional processes are discussed in sections 3.3.4.1-5 and will be mentioned below.)

Altogether, the results described above demonstrate that pollen fraction AMS ^{14}C dates are more consistent, accurate and reliable than β-prep ^{14}C dates obtained from samples prepared following the traditional TOC sample preparation methods commonly used in preparing lake sediment and peat samples for β-counting and AMS ^{14}C dating.

(2) Depositional and post-depositional processes within lake sediments and peat deposits

can have significant effects on the ^{14}C dates obtained for pollen fractions and β-prep samples from lake sediment and peat samples.

The differences between the ^{14}C dates obtained for pollen fractions extracted from the *above* and *below* core samples from four of the nine cores in the Mazama Ash study are larger than expected under a simple linear model of the age/depth relationship in the sediments above and below the ash layer. However, the observed differences for these four cores are qualitatively consistent with the expected differences under a model of the age/depth relationship in the sediments that includes the effects of bioturbation. This suggests that post-depositional redistribution of the pollen in these sediments by bioturbative processes may have had a significant effect on the average age of the pollen in the sediments above and below the ash layer. The results obtained in the Mazama Ash study indicate that such effects can introduce 50-200 year shifts in ^{14}C ages of samples associated with an ash layer, and that the possibility of such effects must be taken into account during studies of relatively short-term events recorded in lake sediments and peats.

The differences between the ^{14}C dates obtained for pollen fractions extracted from the *above* and *below* core samples from the only two cores in the Mazama Ash study that were composed of peat are smaller than the results obtained from both the bioturbated sediments model and the simple linear model of the age/depth relationship in the sediments. As mentioned above, the clustering of the Mazama Ash ^{14}C ages obtained for these two cores at around ~6666 BP indicates that differences between the depositional and post-depositional processes within the peat bogs and the lakes have been the cause of a significant difference between the Mazama Ash ^{14}C ages obtained for the peat samples and those obtained for the lake sediments. Two such processes within the peat deposits that might have contributed to the ~200 year differences between the peat and the lake sediment Mazama Ash ^{14}C ages are the continuous growth of "deep" roots within the acrotelm and the vertical displacement of pollen in response to the movement of water through the acrotelm. Unfortunately, insufficient understanding of the effects of such post-depositional processes on pollen within peat deposits and a lack of detailed information on the peat deposits at the two sites precludes the application of corrections for such effects during the calculation of the Mazama Ash deposition ages from the pollen fraction ^{14}C dates obtained from the peat samples.

(3) For various reasons, three of the cores selected for the Mazama Ash study are not suitable for addressing the central goal of the study, i.e., the demonstration of the accuracy and reliability of ^{14}C dates obtained on pollen fractions through comparison of the known age of the Mazama Ash layer with ^{14}C dates obtained for pollen fractions and β-prep samples.

The ^{14}C dates obtained for the pollen fractions and β-prep samples from one of these three cores (Rock Creek Pond) are significantly older (~1200 years) than the range of typical ^{14}C dates for the Mazama Ash layer obtained in previous studies. The Rock Creek Pond ^{14}C dates center around ~8000 BP, and are in agreement with dates obtained for an ash layer found in a lake sediment core from a nearby site that has been attributed to an eruptive event in the Mono Craters area. On this basis, the ash layer found in the Rock Creek Pond core was attributed to a Mono Craters area eruption at ~8000 BP rather than the Mount Mazama eruptive event which occurred at ~6800 BP.

For the second of these three cores (Ronald Bog), the presence of a significant change in the physical appearance of the sediments between the ash deposit and the top of the core, and the "edge of a lens" shape of the ash deposit in the core, raise significant concerns that the sediments adjacent to the Mazama Ash "clump" may have been subjected to post-depositional process that disturbed the stratigraphy at the coring site and/or introduced carbon-containing materials whose ^{14}C ages differed significantly from the Mazama eruption age. The inconsistencies of the ^{14}C dates obtained for the pollen fractions and β-prep samples from three samples from the Ronald Bog core show that significant heterogeneity exists within the sediments adjacent to the ash deposit and, combined with the observations of the physical state of the ash deposit and the sediments, imply that reliable conclusions regarding the consistency, reliability, and accuracy of ^{14}C dates obtained from pollen fractions and/or β-prep samples cannot drawn from the ^{14}C dates obtained from these core samples.

The ^{14}C dates obtained for the pollen fractions and β-prep samples from the last of these three cores (Chase Lake) are significantly younger (~1300 years) than the range of typical ^{14}C dates for the Mazama Ash layer obtained in previous studies. The Chase Lake ^{14}C dates center around ~5500 BP and cannot be attributed to a known eruptive event at a particular volcano in the region at that time. The consistency of the ^{14}C dates obtained for the Chase Lake core samples and the appearance of the sediments in the core argue against common causes of dating errors that might have produced these ~5500 BP ^{14}C dates for the sediments immediately above and below an actual Mazama Ash layer. Electron microprobe analysis of the ash from the Chase Lake core and further AMS ^{14}C dating of pollen fractions from sediment cores from nearby lakes may allow the source of the ash to be identified. Until such data become available, the ^{14}C dates obtained for the Chase Lake core samples cannot be used as a basis for conclusions regarding the accuracy or reliability of pollen fraction AMS ^{14}C dates.

(4) The extraction and AMS ^{14}C dating of pollen fractions from lake sediment and peat cores eliminates the possibility of dating errors due to "hard water" effects.

The ^{14}C dates obtained for the pollen fractions from the Crocker Lake core samples are consistent with the "consensus" age of the Mount Mazama eruption but the ^{14}C dates obtained for β-prep samples from the same core samples are both ~1000 years older. The probable cause of this error in the β-prep sample dating is the inclusion of the remains of ^{14}C-depleted aquatic plants in the total organic carbon of the lake sediments, i.e., a "hard water" effect. The fact that the pollen fraction ^{14}C dates from the Crocker Lake core samples are consistent with the "consensus" age provides clear evidence that the isolation of essentially pure pollen fractions for AMS ^{14}C dating by the pollen extraction procedure developed in this research effectively eliminates possible dating errors due to "hard water" effects that are not uncommonly encountered in applying the traditional method of dating the TOC fraction from lake sediment and peat samples.

(5) ^{14}C dates obtained for macrofossils found in lake sediment samples do not necessarily accurately reflect the ^{14}C age of the pollen in the same lake sediment samples nor the ^{14}C age of associated materials in the lake sediments, such as a volcanic ash layer.

The 6560±100 BP ^{14}C date obtained for a macrofossil (*Potamogeton* seed) found in the *above* sample from the Crocker Lake core is 410±120 years younger than the ^{14}C date obtained for the pollen in the same sample and is 280±110 years younger than the "consensus" age of the Mount Mazama eruption. This suggests that depositional and/or post-depositional processes transported the macrofossil downwards in the sediments, relative to pollen that was produced at the same time as the macrofossil, to the depth of the ash layer. The magnitudes of the ^{14}C age differences given above show that such depositional and/or post-depositional processes can give rise to significant differences between the ^{14}C ages of macrofossils in a core sample and the ^{14}C age of the pollen in the same sample.

3.4 Lake Minakokosa Study

3.4.1 Introduction.

The Lake Minakokosa study was undertaken as an initial application of the pollen extraction and AMS ^{14}C dating procedures to samples from a lake sediment core that was being analyzed as part of an ongoing paleoclimatological research program. The goal of this study was to establish an accurate and reliable ^{14}C chronology for the palynological record from Lake Minakokosa, Alaska, currently under study by P. M. Anderson (UW, Quaternary Research Center). The Lake Minakokosa core was chosen for this initial application of the procedures for

the following reasons.

First, the Lake Minakokosa site is located in the upper Kobuk River drainage between two previously studied sites (figure 3.9). These previous studies suggested that alder (*Alnus*) had become established at the site to the east of Lake Minakokosa significantly later than at the site to the west and, conversely, that spruce (*Picea*) had become established at the site to the east of Lake Minakokosa significantly earlier than at the site to the west. The establishment of an accurate and reliable ^{14}C chronology for the Lake Minakokosa record was intended to allow the comparison of the timing of the appearance of pollen from these two taxa in the Lake Minakokosa pollen record with that of their appearance in the records from the other two sites.

Second, previous ^{14}C dating of lake sediment samples from the Lake Minakokosa core using total-organic-carbon (TOC) sample preparation methods and β-counting ^{14}C dating techniques had produced ^{14}C dates that were older than expected and were internally inconsistent. The inconsistencies of the TOC ^{14}C dates include a reversal in the age/depth relationship in the sediments at the core depths at which spruce and alder pollen first appear at significant percentages in the sediments.

And finally, the sediments in the Lake Minakokosa core were considered to be typical of sedimentary material commonly found in lake sediment cores from sites in Alaska. The Lake Minakokosa core consists predominantly of light brown/gray silts, which have a low organic carbon content. These light brown/gray silts are frequently interbedded with thin layers of darker brown (and perhaps higher organic content) silty sediments. The Lake Minakokosa sediments differ considerably from the relatively high-organic-carbon content lake sediment and peat cores from the Pacific Northwest that were utilized in the development of the pollen extraction procedure (described above). Since the further application of the pollen extraction and AMS ^{14}C dating procedures developed in this research to several lake sediment cores from similar sites in Alaska was planned, the application of the pollen extraction procedure to a representative core from an Alaskan site provided an opportunity to test the pollen extraction procedure on these low organic carbon content lake sediments (and, if need be, to develop further modifications to the procedure).

3.4.2 Study site, cores, and AMS ^{14}C dated samples.

Description of the Lake Minakokosa site.

The lake sediment cores used in this study were obtained from Lake Minakokosa by P. M. Anderson in June, 1985. The following site description is based on information provided by P. M. Anderson (personal communication, 1994). Lake Minakokosa (66° 55´ N, 155° 02´ W) is a large,

~300 ha, ~54 m deep, long and narrow lake located in the upper Kobuk River drainage in the south-central Brooks Range, Alaska, at an elevation of 122 m. The lake is morainely dammed behind Late Wisconsin moraines formed by a glacier that appears to have originated in several cirques ~6 km to the northwest of the current lake in the Angayucham Mountains. An ~5 m wide stream flows into the lake from the north and a somewhat wider, but shallower, stream flows out of the lake to the south. The lake is currently surrounded by an open spruce boreal forest with isolated pockets of poplar (*Populus*), and with alder and shrub birch (*Betula*) undergrowth.

Paleoecological context of the Lake Minakokosa site.

Palynological study of the Lake Minakokosa sediments has shown that the pattern of past vegetational changes over the last ~20 ka BP recorded in the cores is consistent with the variations found in other palynological records from north-central Alaska (P. M. Anderson, unpublished data, 1994). In general, pollen diagrams obtained from lake sediments cores from sites within north-central Alaska show three distinct zones: 1) a herb pollen zone that corresponds to the glacial period (before ~14 ka BP), 2) a birch pollen zone that corresponds to the late-glacial and early Holocene (~14 ka BP to ~8.5 ka BP), and 3) an alder pollen zone that corresponds to the middle and late Holocene (~8.5 ka BP to modern times) (see, for example, Brubaker *et al.*, 1983; Ager and Brubaker, 1985; Anderson, 1985). While these three pollen zones are common to pollen records from throughout the region, there are significant differences among sites as to the ages of the transitions between the zones and of particular vegetational changes within the zones.

One of the principal interests in the Lake Minakokosa record was the determination of the ages at which spruce and alder became established in the area near the lake. In a palynological study of lake sediment cores from Ruppert Lake (67° 04′ N, 154° 14′ W, the site which is to the east of Lake Minakokosa, near the headwaters of the Kobuk River drainage), Brubaker *et al.* (1983) found that spruce became established in the Ruppert Lake region at ~8.5 ka BP and alder somewhat later at ~7.5 ka BP. In a study of lake sediment cores from Joe Lake (66° 46′ N, 157° 13′ W, the site which is to the west of Lake Minakokosa, near the middle of the Kobuk River drainage), Anderson (1988) found that alder became established in the Joe Lake region at ~9 ka BP while spruce did not become established until much later at ~6 ka BP. (The birch, spruce, and alder sections of the pollen percentage diagrams for Joe Lake, Lake Minakokosa, and Ruppert Lake are shown in figure 3.10.) The Lake Minakokosa site was chosen for study, in part, because the pollen record obtained from the lake sediments would provide further information on the movement of spruce and alder through the Kobuk River drainage during the early Holocene and,

perhaps, contribute to an improved understanding of the causes of, and limitations on, these migrations.

Descriptions of the lake sediment cores and the AMS ^{14}C dating samples.

Three lake sediment cores were obtained by P. M. Anderson in 1985 from a small embayment in the southwest corner of Lake Minakokosa where the water depth was ~13.5 m using a 5-cm diameter modified Livingstone sampler. The first core obtained (designated 85–4–1) was ~7 m long; coring difficulties limited the two subsequent cores (85–4–2 and 85–4–3) to lengths of ~2 m. The two shorter cores and the upper ~2 m of the 85–4–1 core consisted of silty gyttia with some thin bands of darker, organic-rich material. The next 30 cm of the 85–4–1 core consisted of 10 cm of alternating layers of silt and woody trash (twigs and stems) followed by 20 cm of coarse sand with some gravel. Below the sand/gravel layer, the sediments throughout the remainder of the 85–4–1 core (5 m) consisted predominantly of silt with numerous thin bands of darker, organic-rich material and occasional thin layers of sandy silt.

A total of five samples were taken from the cores for pollen extraction and AMS ^{14}C dating. Each sample was 5 cm long, consisted of the entire core cross-section, and had a volume of ~100 cm^3. The samples were taken from near the core depths at which previous samples had been taken for TOC/β-counting ^{14}C dating to allow direct comparison of the AMS ^{14}C dates obtained in this study to the previously obtained dates. The uppermost sample, LM2, was taken from the 85-4-2 core between 160.5 cm and 165.5 cm core depth; the sample consisted of soft gray/brown silty gyttia. The remaining four samples, LM3, LM4, LM5 and LM1, were taken from the 85-4-1 core at core depths of 305-310 cm, 330-335 cm, 360-365 cm, and 485-490 cm, respectively. These samples consisted of hard, gray clayey silt.

The uppermost sample, LM2, was taken from the 85-4-2 core because the upper sections of the 85-4-1 core (~2 m) were not available. The position of the LM2 sample was correlated with the pollen diagram for the 85-4-1 core and the position of the sample taken previously from the 85-4-1 core for TOC/β-counting ^{14}C dating by reference to the recorded visual stratigraphy of the cores. In particular, a sandy layer occurred at a depth of 198 cm in core 85-4-1 and at a depth of 204 cm in core 85–4–2. After adjustments for the 8-15 cm thick flocculent layers at the surfaces of these cores (P. M. Anderson, 1985 Field Notes, personal communication, 1994), depth positions in the two core were correlated directly based on the sandy layers and the top of the consolidated sediments in each core. The sample LM2 was taken from the 85-4-2 core 40 cm above the sandy layer; this core depth corresponded to the ~160 cm depth at which a noticeable rise in spruce pollen was observed in the 85-4-1 core.

The particular core depths from which the samples for AMS ^{14}C dating were taken were chosen on the basis of the first appearances at significant percentages of birch, spruce and alder pollen in the sediments (figure 3.10). The lowermost core sample, LM1, was from the core depth (485-490 cm) at which birch pollen first rises to significant levels in the sediments, marking the beginning of the birch pollen zone. The next three samples going up the core, LM5, LM4 and LM3, spanned the core depths over which both spruce and alder pollen first rise to significant levels in the sediments (spruce pollen at ~340 cm and alder pollen at about ~310 cm (marking the beginning of the alder pollen zone)). The uppermost sample, LM2, was from the core depth (160.5-165.5 cm) at which spruce pollen percentage first rises from the 5-15% levels observed in the sediments between ~340 cm and ~165 cm to the 20-30% levels observed in the upper sections of the core.

Pollen extract fractions and β-prep samples were prepared from the five samples following the pollen extraction procedure given in figure 3.1. The β-prep samples were prepared to allow direct comparison of pollen fraction and β-prep AMS ^{14}C dates obtained for the sediment samples used in this study and to allow comparison of the ^{14}C dates obtained for the β-prep samples with those obtained previously by TOC/β-counting ^{14}C dating techniques (which involve essentially identical sample preparation procedures). As mentioned above, the sediments in the Lake Minakokosa samples differed considerably from the sedimentary material that had been used in developing the pollen extraction procedure. The main effect of the lower organic carbon contents of the Lake Minakokosa sediments on the processing of the samples was the requirement of several alterations to the established processing routines to accommodate the much larger (~100 cm^3 and 75-150 g) samples taken from the Lake Minakokosa cores compared to the relatively small (~20 cm^3 and 10-30 g) samples from the cores in the Mazama Ash study. For the most part, these alterations were related to the physical handling and efficient processing of the larger and heavier samples. The larger samples from the Lake Minakokosa core were required to obtain sufficient quantities of pollen from the low-organic-content silty sediments that comprised the core. One important alteration to the established procedures was the exercise of extreme care during the 29 N HF treatment step of the pollen extraction procedure because the silt/clay Lake Minakokosa samples reacted strongly to the addition of 29 N HF whereas the organic-rich samples from the Pacific Northwest had shown little or no reaction.

A second set of alterations to the pollen extraction procedure was required for the Lake Minakokosa samples because of the significantly different distribution of pollen types in the Lake Minakokosa samples compared to the samples from the Pacific Northwest cores. As mentioned above, the 20<<44 μm and 44<<88 μm size fractions were chosen for the preparation of pollen

fractions from the Pacific Northwest cores because these size fractions were particularly advantageous in isolating essentially pure pollen fractions from the sediments in those cores. The 20<<44 μm and 44<<88 μm size fractions were not appropriate for the preparation of pollen fractions from the Lake Minakokosa sediments because the pollen in these sediments consisted primarily of pollen types in the 20-40 μm size range (birch and alder) with relatively low amounts of spruce pollen at the core depths from which most of the samples for this study were taken. In order to allow the isolation of a 30<<88 μm pollen fraction that contained primarily birch and spruce pollen and a 10<<30 μm pollen fraction that contained primarily alder pollen, the smaller sieve sizes used in the pollen extraction procedure were changed to 10 μm and 30 μm. The effectiveness of these changes to the pollen extraction procedure will be discussed below in the context of the AMS ^{14}C dates obtained for the pollen fractions.

Processing of prepared samples for AMS ^{14}C dating.

The preparation of ion source targets from the Lake Minakokosa pollen fractions and β-prep samples followed the procedures given above for the samples in the Mazama Ash study (section 3.3.3). Data obtained during the processing of the Lake Minakokosa samples are given in table 3.6.

The % carbon values for the Lake Minakokosa β-prep samples range from 0.9% to 1.7%. These values are low compared to the β-prep samples from the cores in the Mazama Ash study because the Lake Minakokosa sediments were composed primarily of silt rather than the higher-organic-content gyttia and peat of the cores from the Pacific Northwest. These % carbon values imply that the 75-150 g Lake Minakokosa sediment samples used for the pollen extraction procedure study contained on the order of 1 g of organic carbon. Since the pollen fractions obtained from these samples contained only 1–4 mg of carbon, this implies that the pollen extraction procedure rejected ~99.999% of the initial sedimentary material and ~99.9% of the carbon containing materials in the sediments to produce the 10<<30 μm and 30<<88 μm pollen fractions used for AMS ^{14}C dating.

The % carbon values for the pollen fractions obtained from the Lake Minakokosa samples are, with only one exception, significantly lower than the 60-67% range expected for sporopollenin. This suggested that most of the 30<<88 μm and 10<<30 μm pollen fractions contained significant amounts of non-pollen material of lower carbon content. Microscopic examination of the portions of the pollen fractions remaining after the subsamples for AMS ^{14}C dating and $\delta^{13}C$ measurement were taken showed that many of the pollen fractions did indeed contain significant amounts of non-pollen materials. (The 30<<88 μm pollen fractions from the

LM3 and LM5 samples could not be examined because the entire fractions were taken for the ^{14}C measurements.)

In general, the 10<<30 μm pollen fractions contained considerable numbers of birch and alder pollen, many unidentifiable clear fragments, unidentifiable black fragments, and a multitude of 10 μm diameter clear globes (figure 3.11). These clear globes have been tentatively identified as bryozoan organisms (F.S. Hu, personal communication, 1994), invertebrates belonging to the phylum Bryozoa (cf. "brown bodies" of Bryozoa shown by Erdtman (1969)). These "bryozoan" globes were the predominant component of the 10<<30 μm pollen fractions from the four sediment samples from the upper sections of the core (LM2, LM3, LM4, and LM5). While significant numbers of the clear globes were evident in the 10<<30 μm pollen fraction from the sediment sample from the lower part of the core (LM1), the dominant components of that pollen fraction were the unidentifiable clear and black fragments (figure 3.12).

The 30<<88 μm pollen fractions from the LM2 and LM4 sediment samples consisted primarily of pollen with occasional unidentifiable clear fragments; there was no evidence of black fragments in these samples (figure 3.13). (The 10 μm diameter "bryozoan" globes were, of course, not present in these 30<<88 μm pollen fractions.) The 30<<88 μm pollen fraction from the LM1 sediment sample consisted of unidentifiable clear and black fragments; there appeared to be very few intact pollen, or fragments thereof, in the sample (figure 3.12).

These observations and the % carbon values obtained for the pollen fractions will also be discussed below in the context of the AMS ^{14}C dates obtained for the pollen fractions and the β-prep samples.

3.4.3 Results and discussion.

The AMS ^{14}C dates obtained for the β-prep samples and pollen fractions from the Lake Minakokosa samples in this study and the TOC/β-counting ^{14}C dates obtained previously are given in table 3.7 and are shown in figure 3.14. It is evident from these data that significant and systematic differences exist among the ^{14}C dates obtained for the different fractions and samples produced by the pollen extraction procedure.

The 10<<30 μm pollen fractions.

One of the most striking systematic features of the ^{14}C dates obtained for the Lake Minakokosa samples is that the 10<<30 μm pollen fractions are much older than the corresponding β-prep samples and most of the corresponding 30<<88 μm pollen fractions. The fact that the 10<<30 μm pollen fractions are ~3000 years older than three of the four

corresponding 30<<88 μm pollen fractions suggests that these fractions contain large amounts of a non-pollen contaminant that is significantly older than the "expected age" of the pollen. For example, if the contaminating carbon were of "infinite" ^{14}C age (i.e., contained no ^{14}C) then the non-pollen contaminant would have to contribute ~30% of the carbon in the fractions to cause the ~3000 year age difference. Since the observed ^{14}C age differences between the corresponding 10<<30 μm and 30<<88 μm pollen fractions for the LM2, LM3, and LM4 samples remain relatively constant at ~3000 years while the % carbon values for the pairs of fractions range from ~50% to ~33%, the amount of contaminating carbon present in the fractions is not simply related to the observed % carbon values obtained for the fractions.

Microscopic examination of the pollen fractions showed that the predominant component of the 10<<30 μm pollen fractions from the LM2, LM3, LM4, and LM5 samples was not pollen but was the "bryozoan" globes, and that these "bryozoan" globes were not present in the corresponding 30<<88 μm pollen fractions that could be examined (figures 3.11 and 3.13). This suggests that the "bryozoan" globes may be the "old" carbon contaminant.

Members of the phylum Bryozoa first appear in the geologic record about 500 million years ago (Ordovician, or possibly Cambrian, period) and continue to exist today (Bates and Jackson, 1984). The fact that Bryozoa organisms have existed for many millions of years implies that the "bryozoan" globes in the 10<<30 μm pollen fractions may, possibly, have been washed into Lake Minakokosa after being freed by erosion from the calcareous Devonian phyllite and recrystallized Devonian limestone exposures in the nearby mountains (Patton and Miller, 1966). Alternatively (and more probably), a significant "hard water" effect may exist in the waters of Lake Minakokosa due to erosion of such carbonate-containing rocks in the watershed and the ^{14}C content of "bryozoan" globes that grew at the time of the deposition of the sediments found in the samples would then be a reflection of the depleted ^{14}C content of the Lake Minakokosa waters. Under either of these scenarios, the "bryozoan" organisms could be the "old" carbon contaminant in the 10<<30 μm pollen fractions.

While the ^{14}C dates from this study do not provide sufficient information to reach a conclusion regarding the source of the "old" carbon contamination in the 10<<30 μm pollen fractions, the hypothesis that the "bryozoan" globes are the source is testable. The globes are all very close to 10 μm in diameter and sieving to select the 10<<15 μm size range could be very effective in producing a fraction that consisted almost exclusively of the "bryozoan" globes. The AMS ^{14}C dating of this 10<<15 μm fraction would provide clear evidence of the ^{14}C content of the "bryozoan" globes. Alternatively (and perhaps more productively), a new set of Lake Minakokosa sediment samples could be processed using 20 μm and 44 μm sieves in the pollen

extraction procedure to produce a 44<<88 μm pollen fraction that would isolate any spruce pollen in the sediments and a 20<<30 μm pollen fraction that would isolate any birch and alder pollen in the sediments and would not contain the "bryozoan" globes. In this context, it is clear that the original adjustment of the sieve sizes to produce 10<<30 μm and 30<<88 μm pollen fractions was not optimal in terms of the actual sizes of the pollen types that were to be isolated. Further, the AMS ^{14}C dates obtained for the 10<<30 μm pollen fractions and the observations from microscopic examination of these fractions show the importance of the selection of the appropriate sieve sizes in obtaining pollen fractions of the necessary purity from organic-poor lake sediment samples such as those from Lake Minakokosa. (It is also worth noting at this point, that while the identification of the 10 μm diameter clear globes as bryozoan organisms must be regarded as tentative and somewhat uncertain at this time, the significance of the globes is not that they may (or may not) be of "bryozoan" origin, but rather that the globes are a major, and clearly-indentifiable, nonpollen contaminant of the 10<<30 μm pollen fractions. While the globes are referred to as "bryozoan" in the above discussions, the arguments concerning the separation and measurement of a "globes" fraction are based on the clearly identifiable nature of the significant nonpollen contaminant rather than their identification as "bryozoan".)

As noted above, the dominant components of the 10<<30 μm pollen fraction from the LM1 sample were not "bryozoan" globes, but rather, were unidentifiable clear and black fragments (figure 3.12). Since the dominant components of the 30<<88 μm pollen fraction from the LM1 sample were also the unidentifiable clear and black fragments, the results obtained for the LM1 10<<30 μm pollen fraction will discussed below with the results obtained for the 30<<88 μm pollen fraction.

The β-prep samples.

Another systematic feature of the ^{14}C dates in figure 3.14 is the ~1000 year offset between the dates obtained for the β-prep samples from the Lake Minakokosa sediments and those obtained for most of the corresponding 30<<88 μm pollen fractions and most of the previous TOC/β-counting ^{14}C dates. The only exceptions to this offset are the 30<<88 μm pollen fraction from the LM1 sample (which will discussed further below) and the TOC date obtained previously from the 335–345 cm sediments. (The 335-345 cm ^{14}C date is older than the ^{14}C date obtained from sediments farther down in the core and is one of the dates that define the apparent age/depth reversal in the core observed in the previous dates.)

If these two anomalous ^{14}C dates are ignored, then the remaining ^{14}C dates show a consistent pattern with the β-prep samples' from the Lake Minakokosa sediments being

~1000 years older than the ^{14}C dates obtained for the corresponding 30<<88 μm pollen fractions and the previous TOC/β-counting ^{14}C dates. While the offset between the ^{14}C dates obtained for the Lake Minakokosa β-prep samples and 30<<88 μm pollen fractions can be attributed to any of a variety of possible causes (such as a "hard water" influence on the β-prep ^{14}C dates), the cause of the offset between the ^{14}C dates obtained for the Lake Minakokosa β-prep samples and the previous TOC/β-counting ^{14}C dates is unclear. The consistency of the relationships between the sets of ^{14}C dates and the lack of a reversal equivalent in either the 30<<88 μm pollen fraction ^{14}C dates or the Lake Minakokosa β-prep ^{14}C dates suggest that the TOC date obtained previously for the 335-345 cm sediment sample is erroneous, so that there is not, in fact, a reversal in the age/depth relationship in the Lake Minakokosa sediments between 305 cm and 365 cm depths.

One point that should be made here is that the nature of the β-prep samples and the TOC samples precludes meaningful microscopic examination of the materials in these samples (figure 3.15) and, hence, does not allow sufficiently informed discussion of the possible causes of observed ^{14}C dating inconsistencies. For instance, the offset between the ^{14}C dates obtained for the Lake Minakokosa β-prep samples and the previous TOC/β-counting ^{14}C dates may be due to differences in the procedures used to prepare the samples for ^{14}C dating, or it may be due to differences in the actual compositions of the sediment samples. But, because the carbon-containing materials in both of these sets of samples are basically uncharacterized and their association with the pollen in the sediments is known only in the sense that the pollen was found in the same sediments, there are no data on which a productive discussion of the causes of the offset between these two sets of ^{14}C dates can be based. (This situation can be contrasted with the discussion above concerning the causes of the ~3000 year offset between the ^{14}C dates for the 10<<30 μm pollen fractions and the corresponding β-prep samples and 30<<88 μm pollen fractions. In that case, microscopic examination provided clear evidence of non-pollen materials in the samples and allowed a useful discussion of the possible causes of the offset.)

The 30<<88 μm pollen fractions.

As can be seen in figure 3.14, the ^{14}C dates obtained for the 30<<88 μm pollen fractions from the LM2, LM3 and LM4 sediment samples are in general agreement with the core depth versus sediment ^{14}C age curve defined by the ^{14}C dates obtained previously from the TOC samples. The fact that microscopic examination of two of these 30<<88 μm pollen fractions (LM2 and LM4) showed that they were composed predominantly of identifiable pollen (and fragments thereof), with only a very few unidentifiable clear fragments (figure 3.13), supports the contention

that the ^{14}C dates obtained for these fractions provide accurate ^{14}C ages for the pollen in the sediments (as noted above, the LM3 and LM5 30<<88 µm pollen fractions could not be examined because the entire fractions were taken for the ^{14}C measurements). The fact that the TOC ^{14}C date for the 335–345 cm sample is ~1200 years older than the ^{14}C date obtained for the 30<<88 µm pollen fraction from the 330–335 cm sediment sample (LM4), and is ~800 years older than the TOC ^{14}C date for the 350–360 cm sample, indicates that the TOC ^{14}C date for the 335–345 cm sample probably does not accurately represent the age of the pollen in the sediments at that depth. On this basis the TOC ^{14}C date for the 335–345 cm sample will be assumed to be inaccurate and will not be considered in further discussions.

The LM1 30<<88 µm and 10<<30 µm pollen fractions.

The 30<<88 µm pollen fraction ^{14}C date obtained from the LM1 (485-490 cm) sediment sample is the only ^{14}C date obtained from a 30<<88 µm pollen fraction that is clearly inconsistent with the TOC ^{14}C dates obtained previously. As was mentioned above, microscopic examination of the 30<<88 µm pollen fraction from the LM1 sample showed that it consisted primarily of essentially unidentifiable clear and black fragments and was devoid of intact, clearly identifiable pollen grains (figure 3.12). The clear fragments appeared to be of organic origin and some appeared to be pieces of aquatic and/or terrestrial plants (i.e., fragments of *Pediastrum* colonies, etc.). The shape, angularity and complete blackness of some of the black fragments suggested that they might be charcoal or perhaps coal fragments. Microscopic examination also showed that the dominant components of 10<<30 µm pollen fraction from the LM1 sediment sample were similar unidentifiable clear and black fragments.

While the identification of the source materials of these fragments was not generally possible, it is clear that the fragments must have contained significant amounts of carbon because the % carbon value for the LM1 30<<88 µm and 10<<30 µm pollen fractions are both ~56%. The organic materials that are the likely sources of the clear fragments have % carbon contents that are in the 40-60% range (e.g., wood samples prepared in our system had % carbon values of ~55% and pure cellulose samples had % carbon values of ~43%). Since the fractions did not contain significant quantities of pollen (which is 60-67% carbon), then the unidentifiable black fragments, which made up a considerable fraction of these 30<<88 µm and 10<<30 µm fractions, must have had an average % carbon value of about 55-65%.

Given the similarities in the compositions of the LM1 30<<88 µm and 10<<30 µm pollen fractions, the fact that the ^{14}C dates obtained for the fractions are approximately equal is not surprising ($|z|=2.0$ for the ^{14}C dates obtained for these two fractions). However, the ^{14}C dates

obtained for the two LM1 pollen fractions are much older than both the TOC ^{14}C dates obtained previously and the ^{14}C date obtained for the β-prep sample from the LM1 sediments. If the TOC and β-prep ^{14}C dates are approximately correct estimates of the actual age of the sediments at that core depth, then the ~6000 year offset of the LM1 pollen fraction ^{14}C dates suggests that at least one component of the pollen fractions is significantly depleted in the ^{14}C. (For example, if the depleted component were of "infinite" ^{14}C age and the rest of the fraction had an age of ~15500 BP, then the depleted component would have to contribute ~50% of the carbon in the fractions to produce the ~21500 BP ^{14}C dates.) The apparent organic origin of the clear fragments, together with the ~15500 BP ^{14}C dates obtained on the TOC fraction of the sediment samples, suggests that the unidentifiable black fragments are the most likely source of the "old" carbon in the pollen fractions.

While the support for this explanation of the ~6000 year offset between the ^{14}C dates obtained for the LM1 30<<88 µm and 10<<30 µm pollen fractions and the β-prep sample is basically circumstantial, the primary fact in any consideration of the ^{14}C dates obtained for the pollen fractions is that microscopic examination showed that these fractions contained significant quantities of non-pollen materials and relatively little identifiable pollen. Under such circumstances, the association of the materials that are being ^{14}C dated with the actual age of the pollen of interest is uncertain, and, in relation to the age of the pollen in the sediment sample, the accuracy of any ^{14}C ages obtained from such contaminated "pollen" fractions is open to question.

The ^{14}C ages of the first establishment of spruce and alder.

As stated in the introduction to the Lake Minakokosa study, one of the principal interests in the pollen record in these lake sediments is the determination of the ages at which spruce and alder first became established in the Lake Minakokosa area. The LM3, LM4, and LM5 sediment samples were chosen to span the period during which these events took place and to allow the determination of the ^{14}C ages of the events by interpolation between the ^{14}C dates obtained for these pollen fractions. As mentioned above, microscopic examination of the 30<<88 µm pollen fractions from the LM2 and LM4 samples showed that they consisted primarily of pollen with occasional unidentifiable clear fragments, and that there were no black fragments in these samples (figure 3.13). The LM3 and LM5 30<<88 µm pollen fractions were too small to allow both microscopic examination and ^{14}C dating; the decision was made to date the fractions and infer the composition of the LM3 and LM5 30<<88 µm pollen fractions from the examinations of the LM2 and LM4 fractions. Unfortunately, the LM5 30<<88 µm pollen fraction was lost during CO_2

gas transfer steps after oxidation and it was not possible to obtain a ^{14}C date for this fraction. Hence, in order to derive estimates of the ages at which spruce and alder first became established in the Lake Minakokosa region by interpolation between measured ^{14}C dates, it was necessary to find a replacement for the missing LM5 pollen fraction ^{14}C date.

The only other set of ^{14}C dates that exists and is relevant to the ages of first establishment of spruce and alder in the region is the set of TOC/β-counting ^{14}C dates obtained previously (table 3.7 and figure 3.14). Given the general agreement between the ^{14}C dates obtained for the LM2, LM3 and LM4 30<<88 μm pollen fractions and the ^{14}C age/depth curve defined by the ^{14}C dates obtained previously from the TOC samples, the TOC ^{14}C dates for the 310-320 cm and 350-360 cm sediment samples provided a reasonable substitute for the missing LM5 pollen fraction ^{14}C date.

Therefore, the ^{14}C ages of the first appearance of spruce and alder in the Lake Minakokosa region were estimated from the core depths of the first significant rises in spruce and alder pollen percentages in the record (at 340 cm and 310 cm, respectively), and the ^{14}C dates obtained for the LM3 and LM4 30<<88 μm pollen fractions and for the 310-320 cm and 350-360 cm TOC samples, by interpolation of an uncertainty-weighted linear regression fit to the ^{14}C dates for these fractions and samples. The ^{14}C ages for the first appearance of spruce and alder in the Lake Minakokosa region derived in this manner are 9.4 ka BP and 8.5 ka BP, respectively. The uncertainty in these ^{14}C ages is about ±100 years based on the scatter of the four dates in the uncertainty-weighted linear regression about the regression line. Estimates of the ^{14}C ages of first establishment derived from just the two 30<<88 μm pollen fraction ^{14}C dates agree with the above ages within the ±100 year uncertainties. In consideration of the core depth separation of the palynology samples and the deposition rate of the sediments in the Lake Minakokosa core (~0.036 cm/yr), the uncertainties in the core depth of the first significant rises in spruce and alder pollen percentages are more probably about ±200 years, and this value will be used in subsequent discussions.

3.4.4 Alder migration.

The ^{14}C age of the first establishment of alder in the Lake Minakokosa area derived above (8.5±0.2 ka BP) is between the ages at which alder became established to the west at Joe lake (~9.0 ka BP)(Anderson, 1988) and to the east at Ruppert Lake (~7.5 ka BP)(Brubaker *et al.*, 1983). In attempting to evaluate the significance of the differences between these ages, the uncertainties in not only the Lake Minakokosa ^{14}C age but also the Joe Lake and Ruppert Lake ^{14}C ages must be considered.

Examination of the TOC ^{14}C dates upon which the chronology of the Ruppert Lake pollen record is based shows that there are disturbing inconsistencies in the dates (figure 3.10). In particular, the three ^{14}C dates between about 125 cm and 225 cm depth show an age/depth reversal: the upper sample (139-146 cm) was ^{14}C dated at 7690±60 BP, the middle sample (162-168 cm) at 7280±150 BP, and the lowest sample of the three (182-188 cm) at 7950±120 BP. These ^{14}C dates are of central importance to the establishment of the age/depth relationship in the Ruppert Lake core over the depths which encompass the first appearances at significant percentages of spruce and alder pollen in the sediments. Unfortunately, the inconsistencies of these TOC ^{14}C dates raise significant questions concerning the accuracy of the estimated ^{14}C age of the first arrival of alder in the Ruppert Lake area.

In a discussion of the importance of accurate and reliable chronological data in understanding the causes of past vegetational changes, Brubaker *et al.* (1983) point out that the ^{14}C ages assigned to the arrival of alder at the sites in their study range from 6860±100 BP to 8080±230 BP even though the relatively short distances between the sites would imply that the arrival of alder should be essentially synchronous at all of the sites. This range of ^{14}C ages for the first establishment of alder in their study region implies that the TOC ^{14}C dates they obtained for their sediment samples have a true uncertainty of at best ±500 years. In concluding their discussion of chronological control in palynological studies, Brubaker *et al.* (1983) comment that similar ~1000 year inconsistencies in ^{14}C dates have been observed in other studies and that such inconsistencies can introduce considerable uncertainty into the interpretation of vegetational changes that take place rapidly and/or over relatively short distances.

Examination of the available ^{14}C dates for the Joe Lake pollen record shows that ^{14}C dating inconsistencies are also the source of considerable uncertainty in the ^{14}C age at which alder became established in the Joe Lake area (figure 3.10). In a recent publication, Anderson *et al.* (1994) presented a study of the pollen record contained in the Joe Lake sediments that spans the period from the early Wisconsinan to the present. In this study, results from three cores (two of which were from the earlier study, Anderson (1988)) were combined to form a composite core and pollen record on the basis of the correlation of changes in particular pollen types in overlapping sections of the cores. Anderson *et al.* (1994) also presented a series of ^{14}C dates obtained on TOC samples and macrofossils from the newest of the three cores. Unfortunately, two inconsistencies that are significant to the purposes of this study exist between the new ^{14}C dates and the ^{14}C dates obtained in the previous study of the Joe Lake record (Anderson, 1988).

First, a new TOC ^{14}C date of 7860±70 BP was obtained for the sediments at the depth at which the spruce pollen percentage first rises above ~5%. In the previous study, two dates of

6050±90 BP and 5960±140 BP were obtained for samples from equivalent depths in the other cores. This ~1800 year discrepancy between the dates raises questions concerning the accuracy and reliability of any of the ^{14}C dates obtained for TOC samples from the Joe Lake sediments. On the basis of the above discrepancy, the ^{14}C date of 9440±100 BP that was obtained for a sample of the sediments in which alder pollen first rise to greater than ~10% could be in error by ~1800 years (and perhaps more). However, a ^{14}C date of 8890±160 BP obtained for the first appearance of alder in the pollen record from Niliq Lake (a lake that is somewhat distant from Joe Lake but has a similar pollen diagram (Anderson, 1988)) provides support for the 9440±100 BP date at Joe Lake and suggests that any inaccuracy in the Joe Lake date is probably ≤ ~500 years.

Second, new ^{14}C dates of 12655±85 BP and 13545±105 BP were obtained for macrofossils (insect and moss fragments identified as probably being of aquatic origin) from composite core depths of ~210 cm. In the previous study, a ^{14}C date of 10490±100 BP was obtained for a TOC sample from 220-230 cm depth. The 2000-3000 year older dates obtained for the aquatic insect and moss fragments indicate that aquatic plant/animal-derived components of the Joe Lake sediments may have been influenced by a significant "hard water" effect. While the contribution of such aquatic materials to the total organic carbon in the Joe Lake sediments cannot be estimated on the basis of available data, the occurrence of a "hard water" effect in the Joe Lake waters suggests that ^{14}C dates obtained for TOC samples from the lake sediments may be older than the actual ^{14}C age of the pollen in the sediment samples. The range of the ^{14}C dates obtained for the sediments from the depth at which the spruce pollen percentage first rises above ~10% suggests that ^{14}C dating errors causes by the "hard water" effects may be as large as ~1800 years.

In light of these uncertainties in the ^{14}C ages at which alder became established in the Ruppert Lake and Joe Lake areas, the ^{14}C age of 8.5±0.2 ka BP obtained in this study for the first establishment of alder in the Lake Minakokosa area can be regarded as consistent with the establishment of alder in the Lake Minakokosa area at the same time as, or slightly later than, in the Joe Lake area; i.e., at ~8.8-9.4 ka BP in the Joe Lake area and ~8.5 ka BP at Lake Minakokosa. In the case of Ruppert Lake, alder appears to have become established somewhat later than at Lake Minakokosa. Unfortunately, the inconsistencies in the TOC ^{14}C dates obtained for the Ruppert Lake core do not allow an age to be assigned to the first appearance of alder pollen in the lake sediments with any certainty better than sometime between ~7 and ~8 ka BP. However, the sequence of these ^{14}C ages is consistent with the west to east migration of alder from the lower Kobuk River drainage to the south-central Brooks Range between ~9.0 ka BP and

~7–8 ka BP (Anderson, 1985; Anderson and Brubaker, 1994).

3.4.5 Spruce migration.

The pollen diagram obtained by P. M. Anderson for the Lake Minakokosa sediment core shows two distinct changes in spruce pollen percentages over the late-Pleistocene and Holocene periods spanned by the pollen record (P. M. Anderson, unpublished data, 1994). The first change is the rise of spruce pollen to 5-10% levels at about 340 cm depth from the <2% levels found in the sediments at greater depths. The spruce pollen percentage then varies between ~5% and ~10% for the next 180 cm of sediments until the second change in the spruce pollen levels occurs at about 160 cm depth. There, the spruce pollen rises to 20-35% levels and remains within that range throughout the sediments in the upper sections of the core.

Similar patterns of variation of spruce pollen percentages have been observed in records from other sites both to the east and west of the Lake Minakokosa area (see, for example, Brubaker *et al.* (1983) and references therein). In some of these studies, measurements of the spruce grains were used to discriminate between white spruce (*Picea glauca*) and black spruce (*Picea mariana*) (e.g., Brubaker *et al.*, 1983). These studies showed that white spruce pollen were the predominant spruce pollen type during the period after the initial rise to ~5–10% levels. In the second spruce pollen percentage rise, black spruce pollen became the predominant spruce pollen type in the sediments and remained predominant throughout the upper sections of the record. While the separate appearances of these two species of spruce is of considerable significance in studies of the paleoecology of central Alaska (e.g., Brubaker *et al.*, 1983; Anderson *et al.*, 1988; Hu *et al.*, 1993), the significance of the white/black spruce distinction in relation to this study is that the two spruce pollen rises in the Lake Minakokosa pollen record (and in the records from Ruppert, Angal and Joe Lakes) represent separate paleovegetational events. For this reason, both of these pollen rises have been ^{14}C dated in this study, and distinctions will be made between these two events at Lake Minakokosa, and Joe and Ruppert Lakes, in the discussions below.

One point that complicates the interpretation of pollen percentages from the sedimentary records in terms of the paleovegetation in the region of the study site is the indirect relationship between pollen percentages and the actual vegetation in the region of study site. For the purposes of this study, the central difficulty raised by such complications is the determination of appropriate pollen percentages for spruce and alder to indicate that these particular species had actually become established in the Lake Minakokosa region (and the Joe Lake and Ruppert Lake regions).

In a recent study of modern pollen assemblages, Anderson and Brubaker (1986) showed that the modern range of alder in northern Alaska was reasonably well-matched to the 20% isopoll of modern alder pollen in surficial lake sediments. When coupled with the fact that alder pollen percentages in the three sedimentary records discussed here (and in most central Alaskan palynological records) show a single, relatively rapid rise from essentially 0% values to >40% values (figure 3.10), this 20% pollen percentage value provides a reasonably well constrained marker that indicates the establishment of alder in the study region. The ~20% pollen percentage level was used above in determining the core depth (310 cm) at which the pollen record indicated that alder had become established in the Lake Minakokosa region.

Unfortunately, the results obtained by Anderson and Brubaker (1986), and a more recent study by Hu *et al.* (1993), indicate that the relationship between spruce pollen percentages in sediments and the presence of white and black spruce species in the region is not as clearly defined. Anderson and Brubaker (1986) found that, while the modern range of spruce in north-central Alaska was reasonably well-matched to the 10% isopoll of modern spruce pollen in surficial lake sediments, spruce was relatively under-represented in the lower Kobuk and Noatak River drainages. They attributed the relatively low spruce pollen percentages in these regions to the transport of spruce pollen out of the region by the prevailing winds, which come from treeless regions to the west and northwest of these drainages. In an extensive study of a lake sediment record from Wien Lake in central Alaska, Hu *et al.* (1993) found that, at core depths with spruce pollen percentages below 10%, white spruce needles were present in the sediments indicating that white spruce was actually present in the drainage at that time. Together these results suggest that white spruce may, at least in some regions, have an established presence in a region without spruce pollen percentages rising above 10% in sedimentary records from the region.

Examination of the spruce pollen percentage diagrams for the lakes discussed here shows that the initial rises in spruce pollen percentages for Lake Minakokosa and Ruppert Lake are well-defined and are to >10% values (figure 3.10). In these two cases, the pollen percentage data provide a clear marker of the first establishment of (white) spruce in the regions of the lakes. Examination of the Joe Lake spruce pollen percentage diagram shows that, although the percentages are generally lower than in the Ruppert Lake and Lake Minakokosa diagrams, similar variations are evident in the three diagrams. In particular, all three diagrams show an initial spruce pollen percentage rise, followed by a period of several thousand years at somewhat lower values, and then an increase to substantially higher values with the establishment of essentially modern boreal forest some 5-6 thousand years ago. If the attribution of modern

under-representation of spruce pollen in surficial sediments in the lower Kobuk River drainage to prevailing westerly winds from treeless areas is coupled with General Circulation Model results which suggest that the prevailing winds in northwest Alaska at about 9 ka BP were also westerly from treeless areas (Barnosky *et al.*, 1987), then the use of a >10% spruce pollen percentage as the indicator of the presence of spruce in the Joe Lake region at about 9 ka BP is probably not appropriate (as was found by Hu *et al.* (1993) at Wien Lake). In the following discussions, the initial rise of spruce pollen percentages to ~3% values in the Joe Lake sediments will be interpreted as an indicator of the first establishment of white spruce within the Joe Lake drainage. Further, the period of somewhat lower percentages following the initial rise will be interpreted as indicating that white spruce remained as a part of the vegetation in the Joe Lake drainage throughout the period between the initial spruce pollen percentage rise and the later rise to 20–30% values.

In the above discussions, a ^{14}C age of 9.4±0.2 ka BP was derived for the pollen in the Lake Minakokosa sediments from the depth at which the spruce pollen percentage first rose into the ~5–10% range. Hence, the 9.4±0.2 ka BP ^{14}C age indicates the age of the first establishment of white spruce in the Lake Minakokosa area. The LM2 sediment sample was taken from the core depth at which the spruce pollen percentage first rose into the 20–30% range. Hence, the ^{14}C date of 5390±50 BP obtained for the 30<<88 µm pollen fraction from the LM2 samples indicates the age of the first establishment of black spruce in the Lake Minakokosa area. (Given that there is an uncertainty of ~2 cm in the correlation between the 85-4-1 and 85-4-2 cores at the depth of the LM2 sample, that there is an additional uncertainty of about ~±3 cm in the core depth at which the rise to 20-30% actually occurred (as discussed above), and that the deposition rate of the core is roughly 0.036 cm/year, an uncertainty of ±200 years would be a more appropriate estimate of the total uncertainty in the 5390 BP ^{14}C date and 5.4±0.2 ka BP will be used in the following discussions for the ^{14}C age of the first establishment of black spruce in the Lake Minakokosa area.)

Based on the chronology developed for the Ruppert Lake core, Brubaker *et al.* (1983) assigned a ^{14}C age of 8.0-8.5 ka BP to the first appearance of white spruce in the Ruppert Lake area. However, the age/depth reversal in the ^{14}C dates obtained for TOC samples from the Ruppert Lake core mentioned above occurs at about the core depths at which spruce pollen first appear at significant percentages in the sediments and raises significant questions concerning the accuracy of this ^{14}C age for the first arrival of white spruce in the Ruppert Lake area. The discussion above concerning the effect of the inconsistencies in the Ruppert Lake ^{14}C dates on the accuracy of the derived age of the first appearance of alder in the Ruppert Lake area

suggests that an uncertainty of at least ±500 years would provide a more realistic estimate of the true uncertainty in the derived ^{14}C age at which white spruce first became established in the Ruppert Lake area. In addition, linear interpolation between two ^{14}C dates obtained for Angal Lake, a nearby lake in Brubaker *et al.*'s (1983) study, provides an estimated age for the arrival of white spruce at that lake of ~9.2 ka BP. (Spruce pollen first appear in the Angal Lake record at ~140 cm depth, and the ^{14}C dates nearest to this core depth are 8080±230 BP at 123–132 cm depth and 13735±245 BP at 186–200 BP.) Consideration of this expanded uncertainty estimate (±500 years) and of the ~9.2 ka BP age of spruce arrival at Angal Lake suggests that white spruce may have become established in the Ruppert Lake area by 8–9 ka BP, i.e., perhaps earlier than suggested by the 8.0–8.5 ka BP ^{14}C age assigned by Brubaker *et al.* (1983).

In the case of black spruce, Brubaker *et al.* (1983) assigned a ^{14}C age of 5-6 ka BP to the rise of the spruce pollen percentage into the 20-30% range that indicated the appearance of black spruce in the area of Ruppert Lake. The ^{14}C dating inconsistencies discussed above appeared to occur at significantly greater core depths than the appearance of black spruce pollen in the Ruppert Lake record. Hence, the ^{14}C age assigned to the first arrival of black spruce in the Ruppert Lake is probably more reliable than the ^{14}C ages derived for the events that occurred in the 7-10 ka BP range (or, at least, the potential sources of inaccuracies in the black spruce ^{14}C age are less obvious than those in the ^{14}C ages derived for events that occur at somewhat greater core depths). However, a TOC ^{14}C date of 6540±290 BP was obtained for a sediment sample from the depth at which the spruce pollen percentage first rises above 10% in the Angal Lake record. Given the significant range of the 5-6 ka BP ^{14}C age assigned to the arrival of black spruce in the Ruppert Lake area by Brubaker *et al.* (1983) and the considerable uncertainty in the Angal Lake ^{14}C date, the available data suggest that the center of the 5-6 ka BP range may be slightly later than the actual ^{14}C age of black spruce arrival. However, there is little evidence to suggest that black spruce became established in the Ruppert Lake area significantly earlier than Brubaker *et al.*'s (1983) assigned age of 5–6 ka BP.

As discussed above, the pollen diagram obtained by Anderson *et al.* (1994) for the composite Joe Lake sediment core shows an initial rise in spruce pollen percentage to about 3% at a depth of 160 cm in the composite sediment core. After this rise, the spruce pollen percentage falls to 1-2% and remains at that level until it rises to >5% at ~75 cm and remains in the 5-12% range for the upper sections of the core (P. M. Anderson, personal communication, 1994). Although an analysis of the spruce pollen types in representative samples from the core has not been undertaken, the similarity of this pattern to the patterns of changes in the spruce pollen percentages observed in other cores (including the Lake Minakokosa and Ruppert Lake cores)

suggests that the initial small rise in spruce pollen indicates the appearance of white spruce in the Joe Lake area and the later rise to >5% levels indicates the appearance of black spruce in the area. Under this interpretation of the pollen percentage changes, white spruce first appeared in the Joe Lake area at ~9.7 ka BP and black spruce became established in the area at ~6.0 ka BP (these ages are based on the ^{14}C dates for the Joe Lake cores from Anderson (1988) and shown in figure 3.10).

In comparing these ^{14}C ages to the ages of first appearance of black and white spruce at other lakes, the considerable uncertainties in the ^{14}C dates that defined the chronology from which the ^{14}C ages of first appearances at Joe Lake have been derived must be considered. In particular, the inconsistencies of the three TOC ^{14}C dates obtained for sediments from the depth at which the first significant appearance of black spruce pollen occurs (viz., 6050±90 BP, 5960±140 BP and 7860±70 BP), and the evidence that the TOC ^{14}C dates from Joe Lake may suffer from significant "hard water" dating errors (discussed above in relation to alder), suggest that the Joe Lake ^{14}C dates obtained from TOC samples may be inaccurate by as much as ~1800 years. Under these circumstances, the uncertainty in the ^{14}C ages assigned to the appearance of black and white spruce in the Joe Lake area may be as great as ±1000 years and the magnitude of these uncertainties must be considered in any comparison of the assigned ^{14}C ages for Joe Lake to those from other lakes.

The considerable uncertainties in the ^{14}C ages assigned to the first appearances of white and black spruce in the Ruppert Lake and Joe Lake areas makes meaningful comparisons of these ages to the results from Lake Minakokosa difficult. The assigned ^{14}C ages for the first appearance of black spruce at Ruppert Lake (5-6 ka BP), Lake Minakokosa (5.4±0.2 ka BP), and at Joe Lake (~6.0 ka BP) are consistent with each other; thus, the possible inaccuracies in the Ruppert Lake and Joe Lake ^{14}C ages do not allow a direction of migration for black spruce to be established with any confidence.

The assigned ^{14}C ages for the first establishment of white spruce at Ruppert Lake (8–9 ka BP), Lake Minakokosa (9.4±0.2 ka BP), and at Joe Lake (~9.7 ka BP) suggest that white spruce may have migrated eastward from the Joe Lake area into the south-central Brooks Range area between 10 ka BP and 8-9 ka BP. But, as in the case of black spruce above, the inconsistencies in the ^{14}C dates for the Joe Lake and Ruppert Lake records do not provide sufficiently reliable estimates of the ^{14}C ages of the first appearance of white spruce in these areas to allow firm conclusions to be drawn from the presently available data.

3.4.6 Summary of the Lake Minakokosa study.

The results obtained from the application of the pollen extraction procedure to the Lake Minakokosa sediments demonstrate that essentially pure spruce pollen fractions can be isolated from these low-organic-carbon content sediments. The results also suggest that relatively pure alder/birch pollen fractions might be obtained from the sediments with only small adjustments of the sieve sizes used to determine the pollen size-fractions isolated from the sediments (i.e., the replacement of the 10 μm and 30 μm sieves with 20 μm and 44 μm sieves and, hence, the isolation of 20<<44 μm and 44<<88 μm pollen fractions rather than the 10<<30 μm and 30<<88 μm fractions used in the Lake Minakokosa study). Thus, these results indicate that the pollen extraction procedure developed during the Mazama Ash study should be sufficient (with, perhaps, minor alterations for the selection of particular size fractions) to allow the extraction and AMS ^{14}C dating of pollen fractions from the low-organic-carbon sediments that are expected to be encountered in the planned application of these procedures to the study of the migration of spruce and alder across Alaska during the early Holocene.

The AMS ^{14}C dates obtained in the Lake Minakokosa study for the three 30<<88 μm pollen fractions which consisted of essentially pure spruce pollen have provided a basis for the determination of the ^{14}C ages of the first arrivals of spruce and alder in the Lake Minakokosa area. The ^{14}C dates obtained for these 30<<88 μm spruce pollen fractions, combined with two of the TOC/β-counting ^{14}C dates obtained previously, show that the ^{14}C ages of the first establishment of white spruce, alder, and black spruce in the Lake Minakokosa area are 9.4±0.2 ka BP, 8.5±0.2 ka BP, and 5.4±0.2 ka BP, respectively.

Attempts to compare these ^{14}C ages with the ^{14}C ages obtained in studies of pollen records from sites to the east (Ruppert Lake) and west (Joe Lake) of Lake Minakokosa have not yielded firm conclusions regarding the timing or direction of the migrations of these species, mainly because of significant uncertainties in the ^{14}C ages of their first establishment at the other two sites. The available ^{14}C ages for the inferred first establishment of white spruce, alder and black spruce in the Ruppert Lake, Lake Minakokosa, and Joe Lake areas (and reasonable estimates of the uncertainties in these ^{14}C ages) allow the following conclusions to be drawn: (1) The ^{14}C ages obtained for the first appearances of white spruce at the three sites indicate that white spruce became established in these areas between ~8 ka BP and ~9.5 ka BP, but significant uncertainties in the Ruppert Lake and Joe Lake chronologies do not allow definitive statements to be made regarding the timing or direction of possible migrations of white spruce within this time period. (2) The ^{14}C ages obtained for the first appearances of alder at the three sites are consistent with the west to east migration of alder from the lower Kobuk River drainage to the

south-central Brooks Range between ~9.0 ka BP and ~7-8 ka BP. (3) The ^{14}C ages obtained for the first appearances of black spruce at the three sites are all consistent with the establishment of black spruce in these areas between ~5 ka BP and ~6 ka BP, but (as in the case of white spruce) the significant uncertainties in the Ruppert Lake and Joe Lake chronologies prevent definitive statements regarding the timing or direction of possible migrations of black spruce within this time period.

The difficulties encountered in this study in attempting to determine the timing and direction of possible migrations of these species through the Lake Minakokosa area in the early Holocene are a direct result of the inconsistencies of TOC/β-counting ^{14}C dates that have been used in defining ^{14}C chronologies for the Ruppert Lake and Joe Lake pollen records. Thus, the inability to reach firm conclusions regarding the migrations of these species through the Lake Minakokosa area in this study serves as a clear illustration of Brubaker *et al.*'s (1983) comments concerning the deleterious effects of such ~1000 year inconsistencies, which are frequently encountered in TOC/β-counting ^{14}C dates obtained from Alaskan and northwestern Canadian sediment samples, on the reconstruction of past vegetation changes in these regions.

As a part of the Lake Minakokosa study, AMS ^{14}C dates were also obtained for the 10<<30 μm pollen fractions produced routinely under the pollen extraction procedure for each of the Lake Minakokosa sediment samples. The AMS ^{14}C dates obtained for these fractions were significantly and systematically different from the ^{14}C dates obtained for the 30<<88 μm spruce pollen fractions and the TOC ^{14}C dates obtained previously (figure 3.14). Microscopic examination of the 10<<30 μm pollen fractions showed that these fractions consisted predominantly of various non-pollen materials. The identification of a particular non-pollen component of the 10<<30 μm pollen fractions as the probable cause of the ^{14}C age differences allowed the development of strategies to test whether that non-pollen component was indeed the cause of the differences, and to adjust the pollen extraction procedure to eliminate that non-pollen component from the smaller-size pollen fraction.

3.5 Summary of the Extraction and AMS ^{14}C Dating of Pollen.

The pollen extraction procedure (figure 3.1) developed as a part of the research described in this dissertation was designed to allow the isolation of essentially pure pollen fractions from high- and low-organic-content lake sediment samples and from peat samples. The procedure was also designed to be suitable for routine use in palynological laboratories in the preparation of pollen fractions for AMS ^{14}C dating.

The steps in the procedure are, for the most part, very similar to chemical treatments used in standard methods for the preparation of lake sediments and peat samples in palynological studies. Three steps in the procedure are extensions of the standard palynological methods. These steps are: (1) the physical selection of specific, appropriate size ranges from the samples, (2) the treatment of the samples with 2-3% NaOCl to deflocculate and oxidize finely-divided organic matter, and (3) the removal of cellulose through a two-step treatment of the samples with $H_2S O_4$. These extensions significantly improve the rejection of non-pollen materials by the procedure and do not appear to cause serious damage to pollen (at least, not to the pollen grains in the samples we have processed and examined to date).

Microscopic examination of the pollen fractions produced by the pollen extraction procedure shows that they are, in general, composed predominantly of pollen. The larger-sized pollen fractions (44<<88 μm or, in some cases, 30<<88 μm) almost always consist of essentially pure pollen. The smaller-sized fractions (20<<44 μm) from med- to high-organic-content core samples are usually composed predominantly of recognizable, intact pollen grains and fragments of larger pollen grains, but also tend to include small amounts of unidentified materials. The composition of the smaller-sized fractions (10<<30 μm) from low-organic-content core samples varies between samples, with most being composed of recognizable, intact pollen grains and fragments of larger pollen grains, together with significant amounts of unidentified materials, but one (LM1) was found to be composed almost entirely of unidentified materials and to be essentially devoid of recognizable, intact pollen grains or fragments of larger pollen grains.

The accuracy and reliability of AMS ^{14}C dates obtained from the pollen fractions produced by the pollen extraction procedure have been demonstrated through the extraction and AMS ^{14}C dating of pollen fractions from known age lake sediment and peat samples. In the Mazama Ash study, pollen fractions and β-prep (TOC equivalent) samples were obtained from core samples from above and below the ash layer deposited in lake sediments and peat deposits throughout the Pacific Northwest as a result of the climactic eruption of Mount Mazama, Oregon at about ~6800 BP. Overall, the results obtained from this study show that AMS ^{14}C dates obtained from the pollen fractions produced by the pollen extraction procedure are more consistent, accurate and reliable than ^{14}C dates obtained from "β-prep" samples that have been prepared following the traditional TOC procedures used routinely to prepare lake sediment and peat sample for β-counting ^{14}C dating (and often used to prepare such samples for AMS ^{14}C dating). The inconsistencies in the β-prep ^{14}C dates obtained in this study are similar to the ^{14}C dating inconsistencies that have been encountered in the application of traditional TOC/β-counting ^{14}C dating techniques in other studies.

The results obtained in the Mazama Ash study also show that: (1) The extraction and ^{14}C dating of pollen fractions eliminates "hard water" effects as potential sources of dating errors. (2) AMS ^{14}C dates obtained for macrofossils in lake sediment samples may not accurately reflect the ^{14}C age of the pollen in the same sediment samples nor the ^{14}C age of materials physically associated with the macrofossils in the sediments, such as a volcanic ash layers. (3) Depositional and post-depositional processes in lake sediments and peat deposits can have significant effects on the ^{14}C ages of pollen associated with particular chronostratigraphic markers, such as ash layers, in lake sediments and peats, and should be considered in evaluating AMS ^{14}C dates obtained on pollen fractions from core samples associated with such markers.

The results obtained from the application of the pollen extraction procedure to a low-organic-content lake sediment core from Lake Minakokosa, Alaska show that the procedure is sufficient to allow the isolation of essentially pure pollen fractions from samples from such cores. The AMS ^{14}C dating of pollen fractions obtained from the Lake Minakokosa core has allowed the ^{14}C ages at which white spruce, alder and black spruce first became established in the Lake Minakokosa area to be inferred. Attempts to determine the timing and direction of the migrations of these species across the Lake Minakokosa area through comparisons of the ^{14}C ages obtained in this study for these events at Lake Minakokosa with ^{14}C ages obtained for the events at sites to the east and west of Lake Minakokosa were frustrated (for the most part) by the large uncertainties in ^{14}C ages of the arrival of these species at the other sites. These uncertainties were caused by inconsistencies in the TOC ^{14}C dates obtained in previous studies at the other sites.

The analysis of the AMS ^{14}C dates obtained for the Lake Minakokosa sediment samples demonstrated that the ability to microscopically examine the pollen fractions produced by the pollen extraction procedure, thereby determining whether significant amounts of non-pollen materials were present in the fractions and unambiguously identifying the carbon-containing materials that were ^{14}C dated, provided an important method for evaluating the reliability of the AMS ^{14}C dates obtained for the Lake Minakokosa pollen fractions. This capability constitutes one of the significant advantages that the extraction and AMS ^{14}C dating of pollen has over the traditional methods of TOC/β-counting ^{14}C dating of bulk-carbon lake sediment and peat samples. While in the Lake Minakokosa study such microscopic examinations were used to "post-screen" the pollen fractions, they could be used more generally to "prescreen" pollen fractions before AMS ^{14}C dating and provide a basis for the determination of the purity of the pollen fractions to be ^{14}C dated and thereby avoid the time and expense incurred in the AMS ^{14}C dating of questionable materials.

Figure 3.1. Pollen Extraction Procedure.

The sequence of the major steps of the pollen extraction procedure developed as a part of the research presented in this dissertation is shown. The procedure is described in detail in the text (section 3.2). The single step procedure used in the total-organic-carbon (TOC) method that is traditionally (and routinely) used in the preparation of bulk lake sediment samples (and frequently in the preparation of peat samples) for β-counting ^{14}C dating is also shown. (This one-step procedure is also used by some to prepare such samples for AMS ^{14}C dating.)

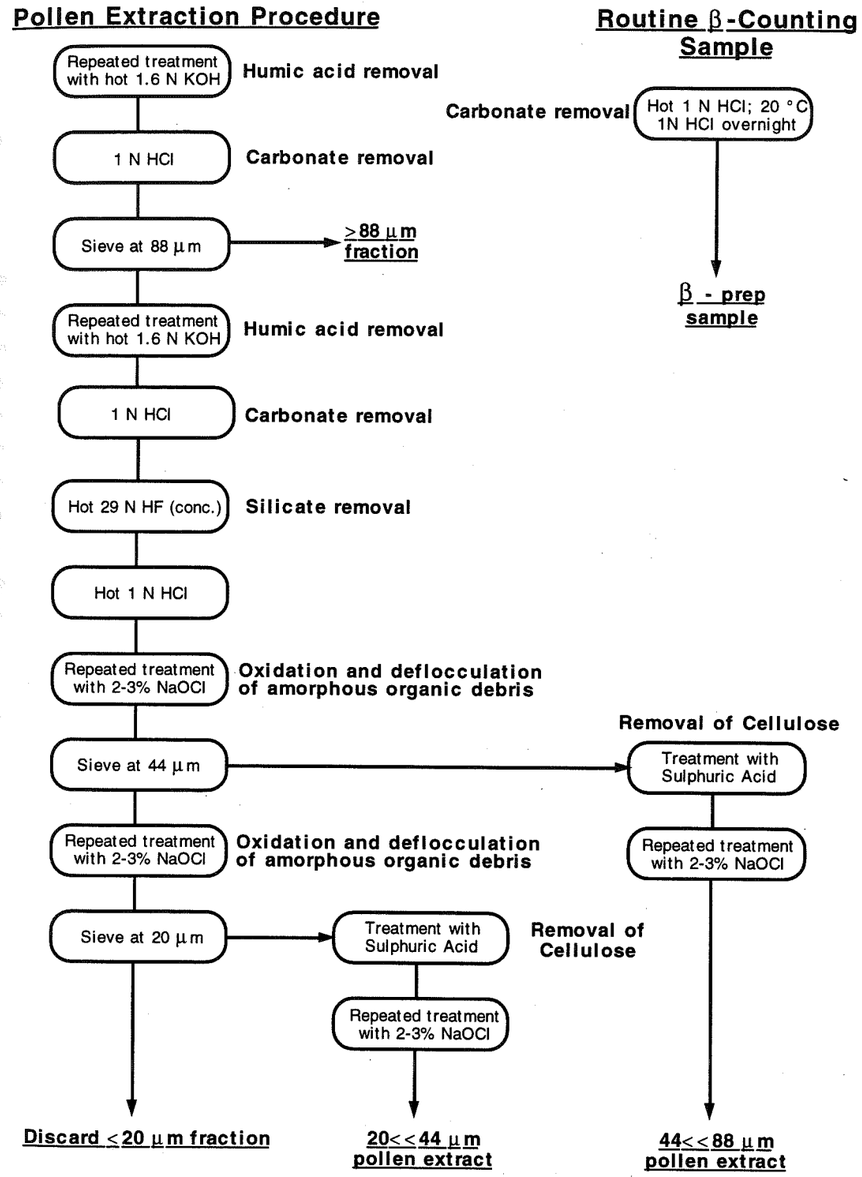

Figure 3.2. Microphotographs of Mazama Ash Study >88 μm Fractions.

Microphotographs of >88 μm fractions obtained from the application of the pollen extraction procedure (figure 3.1) to one peat sample and two lake sediment samples are shown. The peat sample was obtained from the Kachess Bog core (the sites from which the cores were obtained are discussed in the Mazama Ash study); the >88 μm fraction from this peat sample (shown in (a)) was composed predominantly of plant fragments and debris together with considerable numbers of amorphous lumps of organic material. One of the lake sediment samples was obtained from the Crocker Lake core; the >88 μm fraction from this sample (shown in (b)) was composed predominantly of crystalline minerals together with occasional organic fragments. The other lake sediment sample was obtained from the Rock Creek Pond core ; the >88 μm fraction from this sample (shown in (c)) was composed of a mixture of crystalline minerals, occasional well-defined organic fragments, and amorphous lumps of organic material. The carbon-containing components of these fractions would have been included in total-organic-carbon samples for β-counting ^{14}C dating but were rejected by the pollen extraction procedure.

(To allow comparison of the four fractions taken from a core sample, microphotographs of a >88 μm fraction, of 44<<88 μm, and 20<<44 μm pollen fractions, and of a β-prep sample from Rock Creek core samples are shown as (c) in figures 3.2 through 3.5.)

(a)

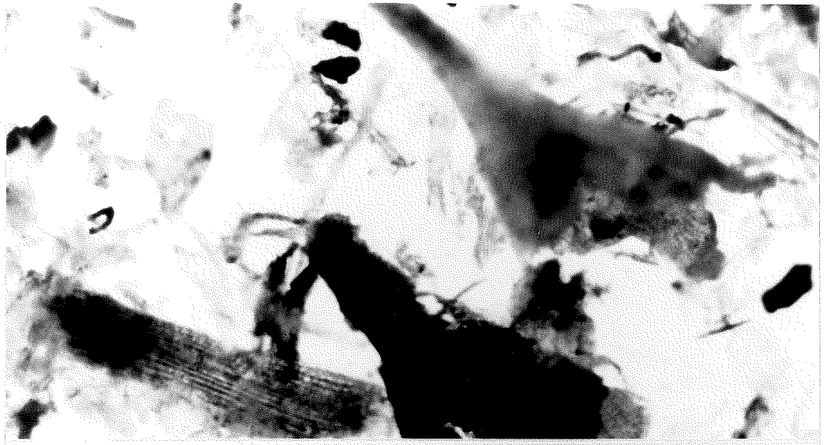

(b)

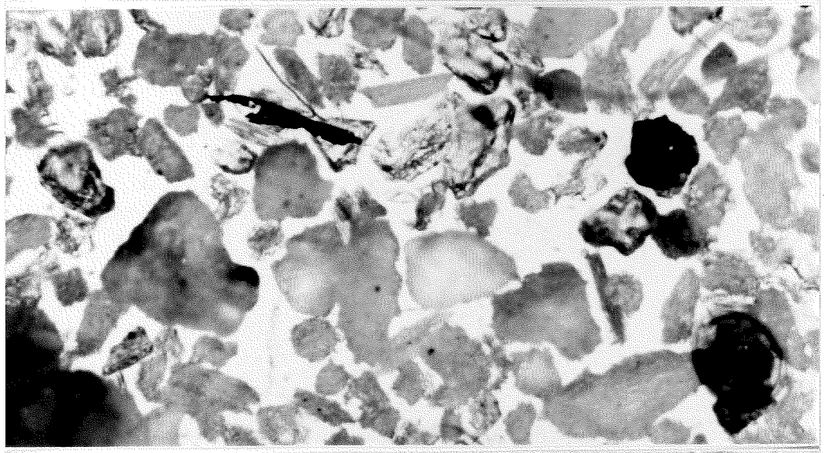

(c)

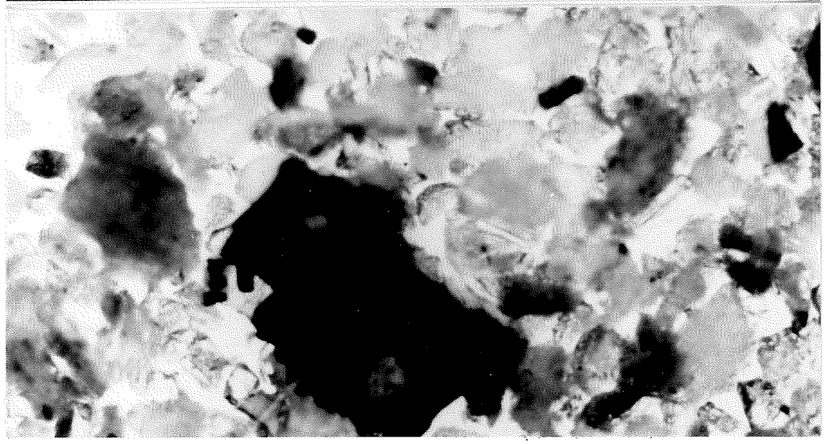

Figure 3.3. Microphotographs of Mazama Ash Study 44<<88 μm Fractions.

Microphotographs of 44<<88 μm fractions obtained from the application of the pollen extraction procedure (figure 3.1) to one peat sample and two lake sediment samples are shown. The peat sample (shown in (a)) was obtained from the Kachess Bog core (the sites from which the cores were obtained are discussed in the Mazama Ash study). One of the lake sediment samples was obtained from the Crocker Lake core (shown in (b)). The other lake sediment sample was obtained from the Rock Creek Pond core (shown in (c)). These 44<<88 μm fractions are composed almost completely of identifiable pollen grains (or fragments thereof). As discussed in the text, the particular pollen types (e.g., Douglas-fir, western hemlock, fir, pine, etc.) present in (or absent from) these 44<<88 μm fractions are in general agreement with the results of palynological studies of sites within the regions from which these cores were obtained.

(a)

(b)

(c)

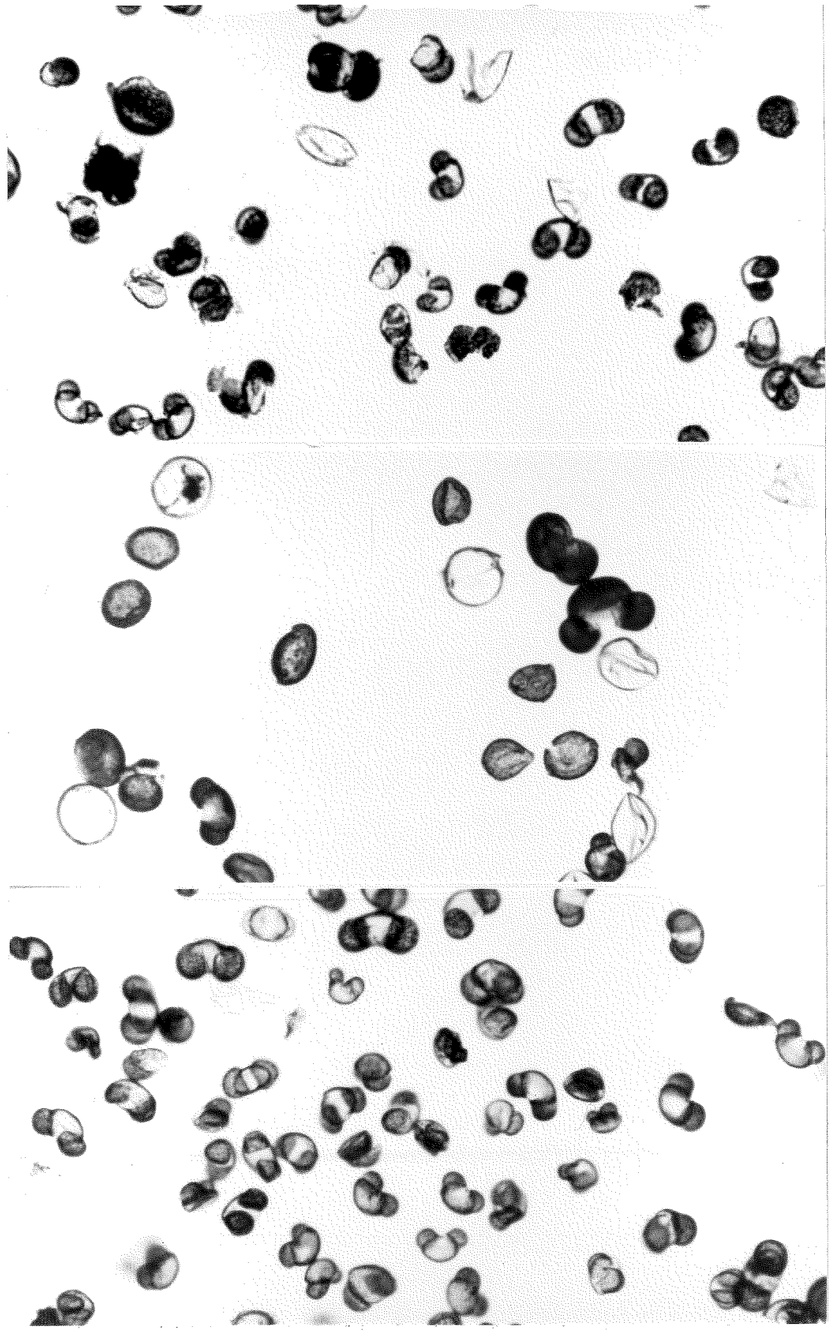

Figure 3.4. Microphotographs of Mazama Ash Study 20≪44 μm Fractions.

Microphotographs of 20≪44 μm fractions obtained from the application of the pollen extraction procedure (figure 3.1) to three lake sediment samples are shown. The first sample (shown in (a)) was obtained from the Ronald Bog core (the sites from which the cores were obtained are discussed in the Mazama Ash study). The second lake sediment sample was obtained from the Heal Lake core (shown in (b)). The third lake sediment sample was obtained from the Rock Creek Pond core (shown in (c)). These 20≪44 μm fractions are composed predominantly of identifiable pollen grains and fragments of larger pollen grains, but also contain small numbers of unidentifiable fragments. As discussed in the text, the presence in (or absence from) these fractions of particular pollen types (e.g., pine, alder, sedge, etc.) is in general agreement with the results of palynological studies of sites within the regions from which these cores were obtained.

(a)

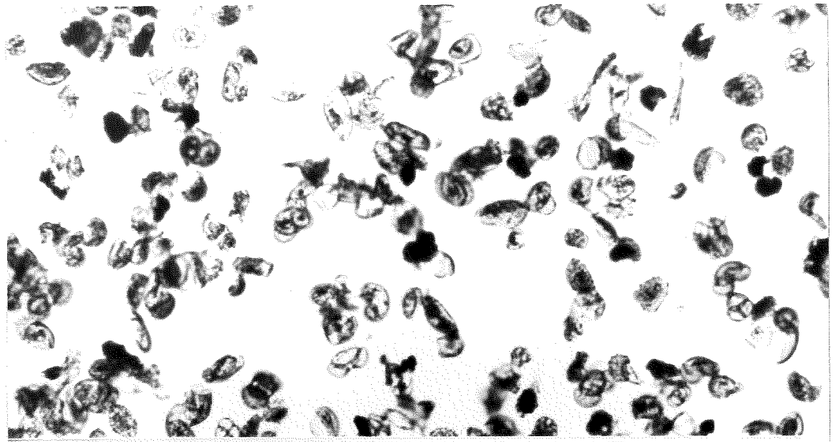

(b)

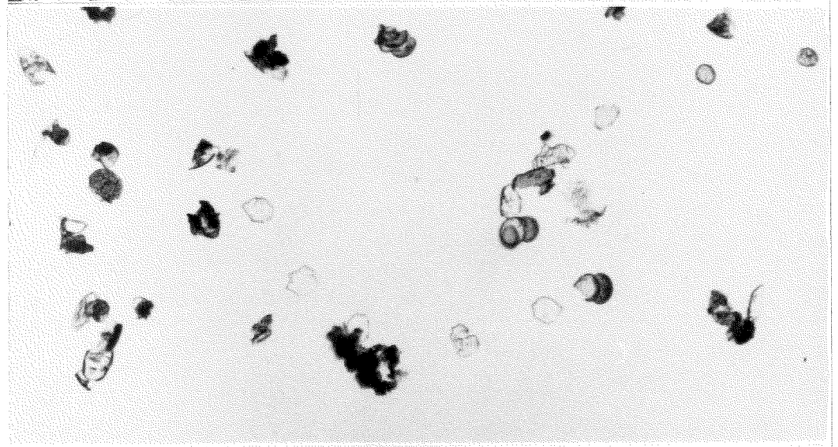

(c)

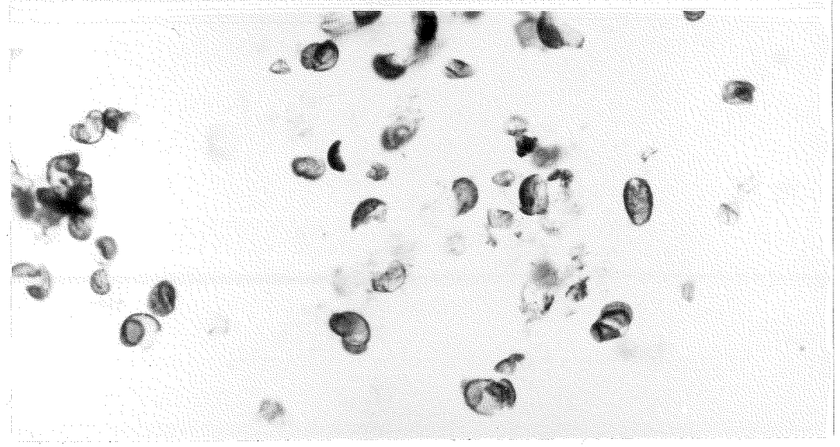

Figure 3.6. Locations of Mazama Ash Study Sites in British Columbia and Washington.

The locations of the eight sites in British Columbia and Washington from which cores were obtained for the Mazama Ash study are shown. The site numbers indicate the particular sites as follows: 1) Rhamnus Lake, 2) Heal Lake, 3) Crocker Lake, 4) Chase Lake, 5) Dead Ice Pond, 6) Lizard Lake, 7) Kachess Bog, and 8) Ronald Bog. The first four sites are from low elevation sites on southern Vancouver Island and in the Puget Lowlands. The other four sites are from higher elevation on the eastern side of the southern part of the North Cascade Range. The ninth core from which samples were obtained for the Mazama Ash study was obtained from the central Sierra Nevada, California and the location of this site is not shown. Figure was adapted from Heusser (1977) with permission from Quaternary Research.

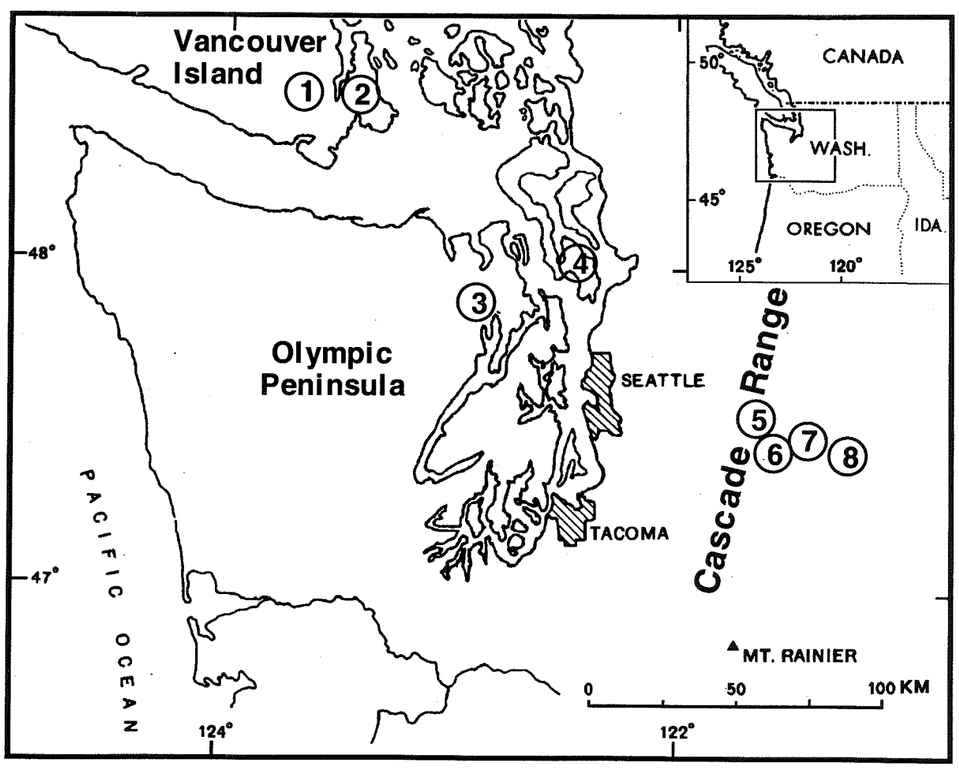

Table 3.1. % Carbon Values and Other Data for Mazama Ash Study Core Samples.

Data obtained during the processing of the pollen fraction and β-prep subsamples from the nine sediment cores in the Mazama Ash study are shown. Data obtained for the macrofossil found in the CR3 core sample, a *Potamogenton* seed, are also shown. The CO_2 obtained from the prepared subsamples was, in most cases, split into two subsamples, with one subsample being used for AMS ^{14}C measurements and the other for $\delta^{13}C$ measurements. The measured $\delta^{13}C$ values for the CO_2 subsamples were used in the calculation of ^{14}C ages for the samples following equation 2.32. The uncertainty in the $\delta^{13}C$ measurements was ±~0.2 per mil.

Core Sample	Prepared Fraction	Sample Designation	Initial dry weight (mg)	Carbon Yield (mg C as CO_2)	Carbon Yield (%of dry wt.)	Carbon for $\delta^{13}C$ (mg)	$\delta^{13}C$ (per mil wrt PDB)	Carbon for ^{14}C (mg)
Chase Lake:								
CL4	β-prep	TABRACL4	42.06	6.17	14.7	2.52	-27.63	3.65
from above	44<<88 μm	TAB8GCL4	4.35	2.68	61.6	0.57	-28.07	2.11
the ash layer	20<<44 μm	TAB2GCL4	2.32	1.38	59.5	0.56	-27.79	0.82
CL3	β-prep	TABRACL3	110.83	4.72	4.3	1.93	-	2.79
from below	44<<88 μm	TAB8GCL3	2.93	1.79	61.1	0.41	-27.94	1.38
the ash layer	20<<44 μm	TAB2GCL3	1.90	1.16	61.1	0.50	-27.59	0.66
Crocker Lake:								
CR3	β-prep	TABRACR3	46.46	1.12	2.4	0.33	-29.59	0.79
from above	44<<88 μm	TAB8GCR3	2.22	1.37	61.7	0.44	-28.84	0.93
the ash layer	20<<44 μm	TAB2GCR3	0.29	0.16	53.4	0.16	-31.42	-
Macrofossil	TABSDCR3	1.58	0.78	49.4	0.20	-24.91	0.58	
CR4	β-prep	TABRACR4	45.52	1.87	4.1	0.61	-30.10	1.26
from below	44<<88 μm	TAB8GCR4	2.18	1.32	60.6	0.44	-28.47	0.88
the ash layer	20<<44 μm	TAB2GCR4	0.37	0.20	54.9	0.20	-30.61	-
Dead Ice Pond:								
DP1	β-prep	TABRADP1	7.07	2.12	30.0	0.97	-29.01	1.15
from above	44<<88 μm	TAB8GDP1	2.95	1.88	63.7	0.73	-27.66	1.15
the ash layer	20<<44 μm	TAB2GDP1	1.32	0.84	63.6	0.29	-28.36	0.55
DP3	β-prep	TABRADP3	9.48	3.96	41.8	1.74	-25.71	2.22
from below	44<<88 μm	TAB8GDP3	1.75	1.07	61.1	0.25	-26.10	0.82
the ash layer	20<<44 μm	TAB2GDP3	2.26	1.41	62.4	0.64	-26.32	0.77

Table 3.1(Continued). % Carbon Values and Other Data for Mazama Ash Study Core Samples.

Data obtained during the processing of the pollen fraction and β-prep subsamples from the nine sediment cores in the Mazama Ash study are shown. Data obtained for the macrofossil found in the CR3 core sample, a *Potamogenton* seed, are also shown. The CO_2 obtained from the prepared subsamples was, in most cases, split into two subsamples, with one subsample being used for AMS ^{14}C measurements and the other for $\delta^{13}C$ measurements. The measured $\delta^{13}C$ values for the CO_2 subsamples were used in the calculation of ^{14}C ages for the samples following equation 2.32. The uncertainty in the $\delta^{13}C$ measurements was ±~0.2 per mil.

Core Sample	Prepared Fraction	Sample Designation	Initial dry weight (mg)	Carbon Yield (mg C as CO_2)	Carbon Yield (%of dry wt.)	Carbon for $\delta^{13}C$ (mg)	$\delta^{13}C$ (per mil wrt PDB)	Carbon for ^{14}C (mg)
Heal Lake:								
HL3	β-prep	TABRAHL3	23.53	4.29	18.2	2.02	-27.23	2.27
from above	44<<88 μm	TAB8GHL3	7.16	4.12	57.5	2.58	-29.09	1.54
the ash layer	20<<44 μm	TAB2GHL3	9.12	5.43	59.5	3.44	-29.32	1.99
HL4	β-prep	TABRAHL4	17.11	5.50	32.1	2.37	-27.43	3.13
from below	44<<88 μm	TAB8GHL4	6.81	4.36	64.0	2.03	-29.15	2.33
the ash layer	20<<44 μm	TAB2GHL4	5.00	3.26	65.2	1.04	-29.84	2.22
Kachess Bog:								
KB7	β-prep	TABRAKB7	69.95	6.28	9.0	2.69	-26.32	3.59
from above	44<<88 μm	TAB8GKB7	2.31	1.50	64.9	0.51	-27.69	0.99
the ash layer	20<<44 μm	TAB2GKB7	1.56	1.02	65.4	0.23	-28.97	0.79
KB8	β-prep	TABRAKB8	10.96	3.30	30.1	0.94	-26.10	2.36
from below	44<<88 μm	TAB8GKB8	1.23	0.81	65.9	-	-	0.81
the ash layer	20<<44 μm	TAB2GKB8	0.74	0.54	73.0	-	-	0.54
Lizard Lake:								
LZ1	β-prep	TABRALZ1	26.53	2.10	7.9	0.89	-25.05	1.21
from above	44<<88 μm	TAB8GLZ1	3.37	2.28	67.7	0.85	-26.41	1.43
the ash layer	20<<44 μm	TAB2GLZ1	4.23	2.90	68.6	1.24	-26.84	1.66
LZ2	β-prep	TABRALZ2	41.67	2.57	6.2	0.52	-25.17	2.05
from below	44<<88 μm	TAB8GLZ2	6.44	4.14	64.3	1.64	-26.27	2.50
the ash layer	20<<44 μm	TAB2GLZ2	2.96	2.07	69.9	0.92	-26.35	1.15

Table 3.1(Continued). % Carbon Values and Other Data for Mazama Ash Study Core Samples.

Data obtained during the processing of the pollen fraction and β-prep subsamples from the nine sediment cores in the Mazama Ash study are shown. Data obtained for the macrofossil found in the CR3 core sample, a *Potamogenton* seed, are also shown. The CO_2 obtained from the prepared subsamples was, in most cases, split into two subsamples, with one subsample being used for AMS ^{14}C measurements and the other for $\delta^{13}C$ measurements. The measured $\delta^{13}C$ values for the CO_2 subsamples were used in the calculation of ^{14}C ages for the samples following equation 2.32. The uncertainty in the $\delta^{13}C$ measurements was ±~0.2 per mil.

Core Sample	Prepared Fraction	Sample Designation	Initial dry weight (mg)	Carbon Yield (mg C as CO_2)	Carbon Yield (%of dry wt.)	Carbon for $\delta^{13}C$ (mg)	$\delta^{13}C$ (per mil wrt PDB)	Carbon for ^{14}C (mg)
Rhamnus Lake:								
RL4	β-prep	TABRARL4	12.46	2.89	23.2	1.54	-29.56	1.77
from above	44<<88 μm	TAB8GRL4	1.06	0.67	63.2	-	-	1.73
the ash layer	20<<44 μm	TAB2GRL4	3.52	2.31	65.6	1.16	-33.20	0.82
RL5	β-prep	TABRARL5	18.36	3.34	18.2	2.08	-29.37	2.50
from below	44<<88 μm	TAB8GRL5	4.07	2.64	64.9	1.43	-30.46	0.66
the ash layer	20<<44 μm	TAB2GRL5	4.29	2.86	66.7	1.26	-32.23	1.15
Rock Creek Pond:								
RC1	β-prep	TABRARC1	33.49	2.30	6.9	0.53	-23.31	1.77
from above	44<<88 μm	TAB8GRC1	3.58	2.22	62.0	0.49	-25.72	1.73
the ash layer	20<<44 μm	TAB2GRC1	1.51	0.96	63.8	0.14	-25.03	0.82
RC2	β-prep	TABRARC2	28.08	3.32	11.8	0.82	-22.87	2.50
from below	44<<88 μm	TAB8GRC2	1.22	0.76	62.0	0.10	-25.16	0.66
the ash layer	20<<44 μm	TAB2GRC2	2.55	1.45	56.9	0.30	-24.64	1.15
Ronald Bog:								
RB3	β-prep	TABRARB3	55.37	1.56	2.8	0.71	-28.78	0.85
from above	44<<88 μm	TAB8GRB3	3.19	2.04	63.9	0.94	-28.80	1.10
the ash layer	20<<44 μm	TAB2GRB3	1.04	0.68	65.4	-	-	0.68
RB4	β-prep	TABRARB4	49.94	2.93	5.9	1.36	-28.48	1.57
from below	44<<88 μm	TAB8GRB4	6.84	4.50	65.8	2.23	-28.22	2.27
the ash layer	20<<44 μm	TAB2GRB4	4.56	2.97	65.1	1.37	-29.46	1.60

Table 3.2. AMS ^{14}C Dates Obtained for the Mazama Ash Study Sample Fractions.

The AMS ^{14}C dates obtained for the pollen fractions and β-prep samples from the *above* and *below* samples from the nine sediment cores in the Mazama Ash study are shown. The dates are expressed in ^{14}C years before present (BP) with 1σ uncertainties, following the conventions of Stuiver and Polach (1977). The dates obtained for the macrofossil found in the CR3 core sample (a *Potamogenton* seed) and the Ronald Bog Developmental Sample are also shown. The weighted means of the ^{14}C dates obtained for the 20<<44 μm and 44<<88 μm pollen fractions from each core sample are given in the two rows labeled "Weighted Mean". The data in the $|z|_{pp}$ rows are the values of the normalized Gaussian statistic described in section 3.3.4.1 calculated for the ^{14}C dates obtained for the two pollen fractions from each core sample. The data in the $|z|_{pb}$ rows are the values of the same normalized Gaussian statistic calculated, in this case, from the weighted mean ^{14}C date obtained for the pollen fractions and the ^{14}C date obtained for the β-prep sample from each core sample. The data in the $|z|_{ab}$ row are the values of the normalized Gaussian statistic calculated from the weighted mean ^{14}C dates obtained for the pollen fractions from the *above* and *below* core samples. (The differences between the weighted mean ^{14}C dates obtained for the pollen fractions from the *above* and *below* core samples are also given.) The $|z|_{mpa}$ value is the normalized Gaussian statistic calculated from the ^{14}C date obtained for the macrofossil found in the CR3 core sample and the weighted mean ^{14}C date obtained for the pollen fractions from the CR3 core sample.

AMS ^{14}C dated Fraction	Crocker Lake	Heal Lake	Lizard Lake	Rhamnus Lake	Dead Ice Pond	Kachess Bog	Ronald Bog	Rock Creek Pond	Chase Lake
From the *above* core sample:									
20<<44 μm	-	6690±60	6770±60	6820±60	6720±220	6590±60	9430±70	8010±110	5350±70
$\|z\|_{pp}$	-	1.53	0.51	2.12	0.30	0.71	-	0.91	0.51
44<<88 μm	6970±60	6820±60	6810±50	6640±60	6650±70	6650±60	5950±60	7880±90	5300±70
Weighted Mean	6970±60	6755±42	6794±38	6730±42	6656±67	6620±42	5950±60	7932±70	5325±49
β-prep Sample	7940±70	6790±60	6770±70	6840±60	6430±50	6470±60	5750±70	8060±90	5080±60
$\|z\|_{pb}$	10.5	0.54	0.30	1.50	2.70	2.05	2.17	1.12	3.16
From the *below* core sample:									
20<<44 μm	-	7130±70	7120±70	7020±60	6680±60	6690±250	7220±70	8160±120	5850±100
$\|z\|_{pp}$	-	0.91	0.28	0.90	0.00	0.08	1.30	0.32	0.00
44<<88 μm	6960±60	7040±70	7150±80	6930±70	6680±70	6710±60	7100±60	8110±100	5850±70
Weighted Mean	6960±60	7085±49	7133±56	6982±46	6680±46	6710±58	7151±46	8130±77	5850±57
β-prep Sample	8150±70	7110±60	7050±80	7070±70	6700±50	6590±60	7160±60	8100±90	5850±60
$\|z\|_{pb}$	12.9	0.32	0.86	1.05	0.29	1.44	0.12	0.25	0.00
above/below age difference	-10±85	330±64	339±65	252±62	24±81	90±72	1201±76	198±104	525±75
z_{ab}	0.12	-5.11	-5.20	-4.05	-0.30	-1.26	-15.9	-1.90	-6.98

Macrofossil

6560±100

$|z|_{mpa}$=3.52

Ronald Bog Developmental Sample

β-prep sample 5550±80

>88 μm fraction 1510±90

44<<88 μm 6690±100

20<<44 μm 6770±100

Table 3.3. Calculation of $^{C14}\Delta_{ex}$ Values and Comparison to Observed Differences.

The data used in calculating the relatively crude $^{C14}\Delta_{ex}$ estimates of the expected difference between the ^{14}C dates obtained for the *above* and *below* core samples following the expression given in section 3.3.4.1 are shown for each of the nine sediment cores in the Mazama Ash study. The weighted mean ^{14}C dates for the *above* core samples were calculated in table 3.2. The uncertainties in the core depth of the ash layer and the lengths of the *above* and *below* core samples were based on operational observations during coring and sample selection. The uncertainties in the $^{C14}\Delta_{ex}$ values from these sources are insignificant compared to the uncertainties in the observed differences between the *above* and *below* ^{14}C dates.

Lake Sediment or Peat Core	Wt. Mean ^{14}C date of Above Pollen Fractions (BP)	Ash Layer Core Depth (cm) (± larger of 1 cm or 1%)	Length of Above Core Sample (l_a) (±0.2 cm)	Length of Below Core Sample (l_b) (±0.2 cm)	Sedimentation Rate (d) ($X10^{-2}$ cm yr^{-1})	$^{C14}\Delta_{ex}$ (^{14}C years)	Observed Above/Below Difference (^{14}C years)
Crocker Lake	6970±70	611±6.1	2.5	2.5	8.77±0.12	28.5±1.7	-10±85
Heal Lake	6755±42	367±3.8	5	5	5.43±0.06	92.1±2.8	330±64
Lizard Lake	6794±38	105±1.1	4	3	1.55±0.02	226±9.6	339±65
Rhamnus Lake	6730±42	417±4.2	5	5	6.20±0.07	80.6±2.5	252±62
Dead Ice Pond	6656±67	112±1.1	3.8	3.8	1.68±0.02	226±8.8	24±81
Kachess Bog	6620±42	256±2.6	5	5	3.87±0.05	129±4.0	90±72
Ronald Bog	5950±60	39±1.0	5	5	0.66±0.09	763±30	1201±76
Rock Creek Pond	7932±70	539±5.4	5	3.8	6.80±0.07	64.7±2.3	198±104
Chase Lake	5325±49	291±2.9	5	5	5.46±0.07	91.4±2.8	525±75

Table 3.4. Calculation of $^{Cal}\Delta_{ex}$ Values and Comparison to Observed Differences.

The data used in calculating the $^{Cal}\Delta_{ex}$ estimates of the expected calendar year differences for the *above* and *below* core samples are shown. The calibrated ages (Method A) and age ranges (Method B) were determined using the standard ^{14}C-to-calendar year calibration program, Calib 3.0.3 (Stuiver and Reimer, 1993), as described in section 3.3.4.1. The weighted mean ^{14}C dates for the *above* and *below* core samples were calculated in table 3.2. The calibrated observed differences obtained by Method B (the final column) were calculated as the difference between the midpoints of the 1σ calendar year age ranges obtained for each pair of *above* and *below* core samples. The uncertainties in these calibrated observed differences were calculated by using one half of the span of the calibrated age range for each date as a pseudo-1σ uncertainty in the midpoint of the age range, and then combining the pseudo-1σ uncertainties for the *above* and *below* core samples in standard error-propagation equations. Although these uncertainty estimates are not normal "Gaussian 1σ" uncertainties (because of nonlinearities in the ^{14}C-to-calendar year calibration curve), they do provide reasonable estimates of the uncertainties in the calibrated observed differences obtained by Method B.

Lake Sediment or Peat Core	Sample Position Relative to Ash Layer	Wt. Mean ^{14}C Age of Pollen Fraction (BP)	Moving-average Time Span (years)	Calib 3.0.3 Method A Intercept (cal BP)	Calib 3.0.3 Method B 68% Prob. Range (cal BP)	Calibrated Observed Difference Method A (calendar years)	Calibrated Observed Difference Method B (midpoint±span/2) (calendar years)
Crocker Lake	above	6970±60	40	7736	7811-7676	-13	-7±94
	below	6960±60	40	7723	7803-7671		
Heal Lake	above	6755±42	100	7556	7590-7537	333	315±56
	below	7085±49	100	7889	7927-7829		
Lizard Lake	above	6794±38	280	7591	7620-7560	355	348±56
	below	7133±53	220	7946	7985-7891		
Rhamnus Lake	above	6730±42	100	7545	7577-7523	213	207±62
	below	6982±46	100	7758	7812-7701		
Dead Ice Pond	above	6656±67	260	7490	7542-7440	13	15±60
	below	6680±46	260	7503	7538-7473		
Kachess Bog	above	6620±42	140	7454	7500-7434	82	68±55
	below	6710±58	140	7536	7579-7491		
Ronald Bog	above	5950±60	300	6766	6844-6718	1201	1185±73
	below	7151±46	300	7967	8002-7930		
Rock Creek Pond	above	7932±70	80	8680	8925-8597	306	318±198
	below	8130±77	60	8986	9190-8968		
Chase Lake	above	5325±49	100	6129	6174-6031	562	572±100
	below	5850±57	100	6691	6745-6604		

Table 3.5. Comparison of $^{C14}\Delta_{ex}$, $^{Cal}\Delta_{ex}$, and $^{Biot}\Delta_{ex}$, and Calculation of Mazama Ages.

The $^{C14}\Delta_{ex}$, $^{Cal}\Delta_{ex}$, and $^{Biot}\Delta_{ex}$ values of the expected differences between the ages of the *above* and *below* core samples obtained (as described in sections 3.3.4.1 and 3.3.4.2) for the nine sediment cores in the Mazama Ash study are shown along with the observed ^{14}C year and in calendar year age differences for the *above* and *below* core samples. These results are discussed in detail in section 3.3.4.3. The calibrated ages for the *above* and *below* core samples (columns 1 and 2) were calculated as the midpoints of the 1σ calendar year age ranges obtained for each pair of *above* and *below* core samples (table 3.4) and the uncertainties were calculated as one half of the span of the calibrated age range for each date. (As discussed above, these uncertainty estimates are not normal "Gaussian 1σ" uncertainties, but the consistency between these uncertainties and those given for the observed age differences in ^{14}C years suggests that they do provide reasonable uncertainty estimates for the calibrated observed differences.)

In addition, the calculated ages of the Mazama Ash layer obtained for each core are given in ^{14}C years (BP) and in calendar years (cal BP). These results are discussed in detail in section 3.3.4.5.

Lake Sediment or Peat Core	Calibrated Ages of Above Core Samples (derived from Method B data in table 3.4)	Below	Observed Age Differences Calibrated (calendar years) (as derived in tables 3.3 and 3.4)	^{14}C Dates (^{14}C years)	$^{C14}\Delta_{ex}$ (^{14}C years)	$^{Cal}\Delta_{ex}$ (calendar years)	$^{Biot}\Delta_{ex}$	Calculated Age of Ash Layer (Calibrated) (cal BP)	(^{14}C) (BP)	Sediment Type
Crocker Lake	7744±68	7737±66	-7±94	-10±85	28.5±1.7	31.6±1.3	234±4	7740±80	6965±74	Silty gyttia
Heal Lake	7564±27	7878±49	315±56	330±64	92.1±2.8	103±3	396±6	7680±34	6880±49	dry, compacted gyttia
Lizard Lake	7590±30	7938±47	348±56	339±65	226±9.6	254±10	1375±17	7764±41	6963±50	gyttia
Rhamnus Lake	7550±27	7757±56	207±62	252±62	80.6±2.5	90.6±2.7	348±5	7628±36	6825±48	gyttia
Dead Ice Pond	7491±51	7506±33	15±60	24±81	226±8.8	253±10	1261±21	7500±60	6668±78	coarse peat
Kachess Bog	7467±33	7535±44	68±55	90±72	129±4.0	146±5	562±9	7500±43	6665±55	coarse peat
Ronald Bog	6781±63	7966±36	1185±73	1201±76	763±30	870±35	3349±127	7374±73	6551±71	silty gyttia
Rock Creek Pond	8761±164	9079±111	318±198	198±104	64.7±2.3	71.5±2.8	310±7	8881±180	8007±80	gyttia
Chase Lake	6103±72	6675±71	572±100	525±75	91.4±2.8	105±3	406±7	6320±80	5523±57	clayey gyttia

Figure 3.7. Bioturbation Model: Age Versus Core Depth.

The apparent ages of sediments above and below an ash layer produced by the bioturbated sediments model discussed in the text (section 3.3.4.2) are shown as a function of core depth (heavy solid line). The sediment ages and core depths are expressed in the generalized length and time units of the bioturbated sediments model. The apparent ages of sediments above and below an ash layer for unbioturbated sediment are also shown (heavy dashed line). The thickness of the ash layer is arbitrary, and was chosen to be one-half of one bioturbation layer thick (i.e., $0.5D_{biot}$) in this case for plotting convenience. The horizontal dot-dashed lines mark the ends of core samples taken from above and below the ash layer that are one-half of one bioturbation layer long (i.e., $0.5D_{biot}$ long). The average ages of unbioturbated sediments in the $0.5D_{biot}$ long core samples from above and below the ash layer are marked by the two thin solid vertical lines which define the age difference denoted by "A". This age difference, A, is the 0.5 generalized time unit age difference expected between a pair of such above and below core samples from unbioturbated sediments. The average ages of bioturbated sediments in the $0.5D_{biot}$ long core samples from above and below the ash layer are marked by the two thin solid vertical lines which define the age difference denoted by "B". This age difference, B, is the 1.63 generalized time unit age difference expected between a pair of such above and below core samples from bioturbated sediments.

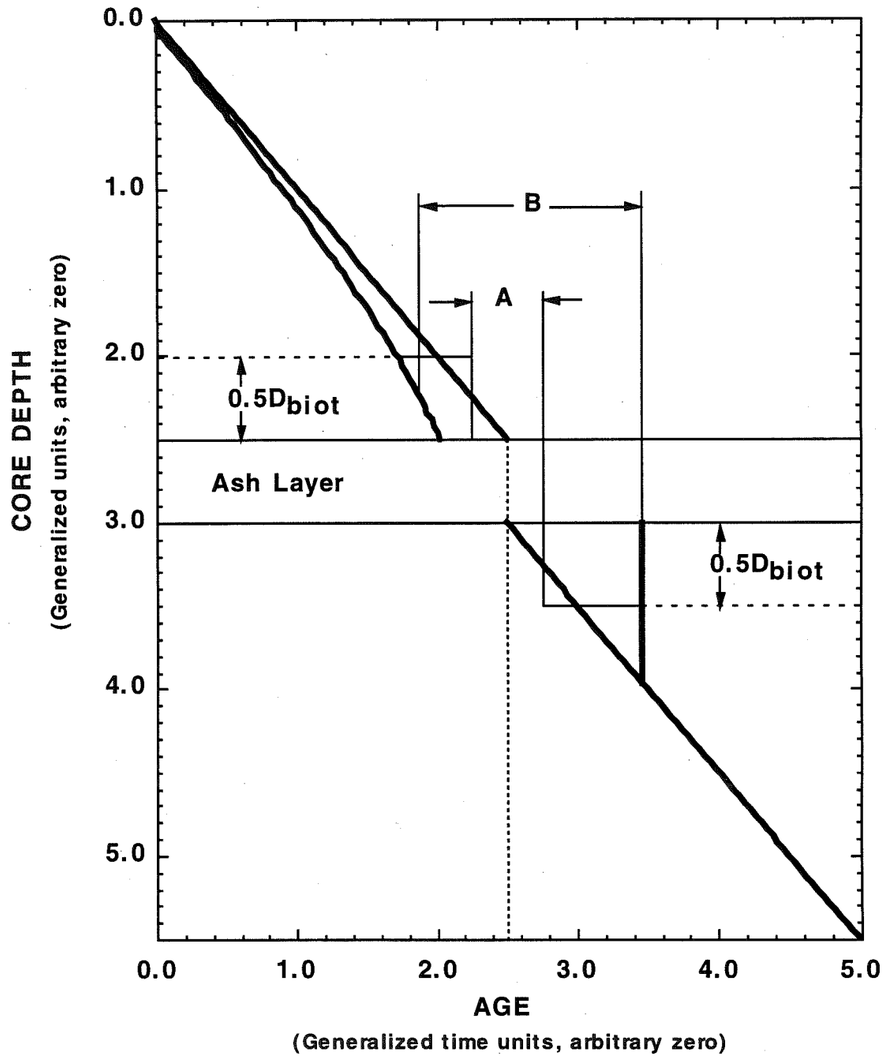

Figure 3.8. ^{14}C Dates Obtained for Six of the Mazama Study Cores.

The AMS ^{14}C dates obtained for the pollen fractions and β-prep samples from the *above* and b*elow* core samples from the six "consistent" cores are shown. The pollen fraction and the β-prep dates for the *above* core samples are indicated by open squares and closed squares, respectively. The pollen fraction and the β-prep dates for the *below* core samples are indicated by open circles and closed circles, respectively. The AMS ^{14}C date obtained for the macrofossil found in the *above* core sample from the Crocker Lake core is indicated by the crossed diamond. The vertical error bars indicate the 1σ uncertainty in the ^{14}C dates. The dashed horizontal lines indicate the limits of the 6600-7100 BP range of typical ^{14}C dates obtained in previous dating of materials associated with the Mazama Ash layer.

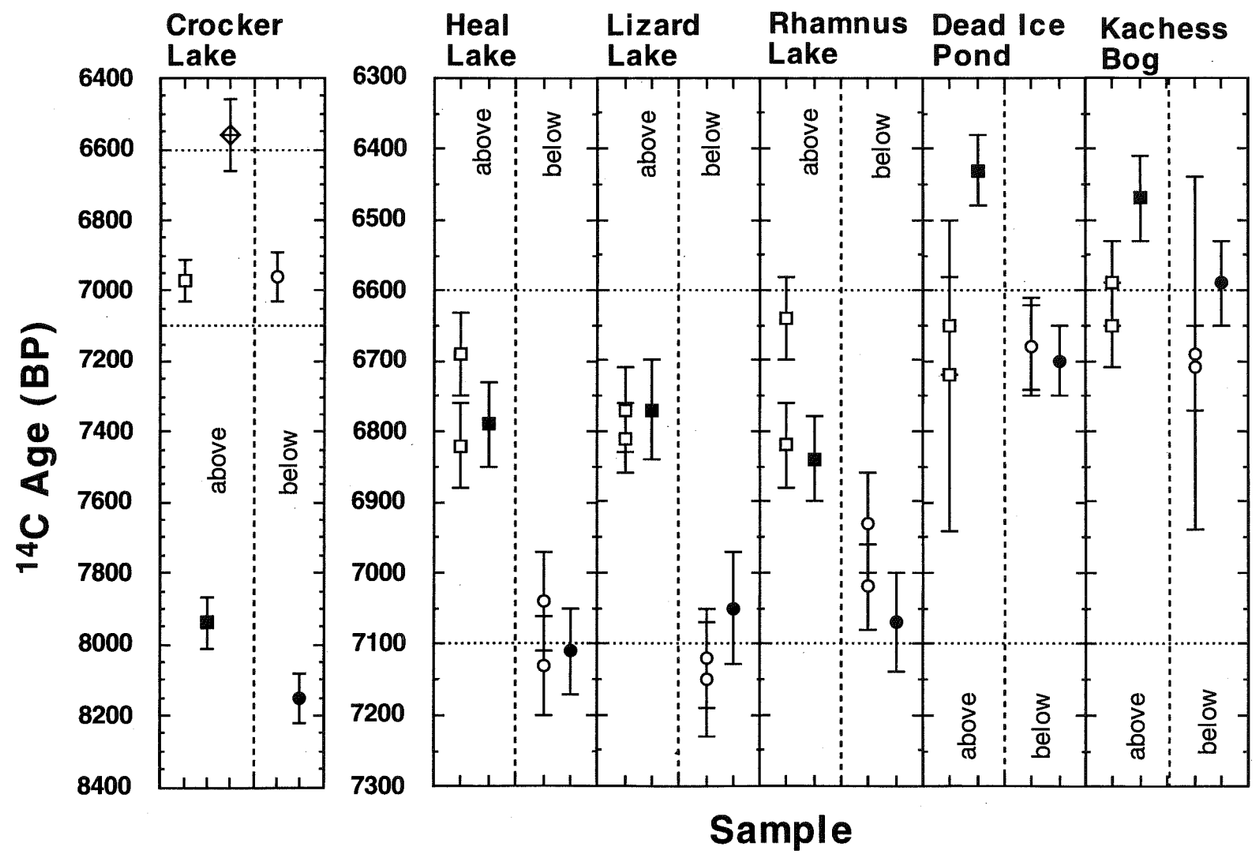

Figure 3.9. Locations of Alaskan Study Sites.

The locations of the three Alaskan sites discussed in the Lake Minakokosa study are shown. The site numbers indicate the particular sites as follows: 1) Ruppert Lake, 2) Lake Minakokosa, and 3) Joe Lake. The sediment core from the Ruppert Lake site was studied by Brubaker *et al.* (1983) and the sediment cores from the Joe Lake site were studied by Anderson (1988) and Anderson *et al.* (1994). Results from these studies are discussed in relation to the results obtained in the Lake Minakokosa study in sections 3.4.3, 3.4.4, and 3.4.5. Figure was adapted from Anderson (1988) with permission from Quaternary Research.

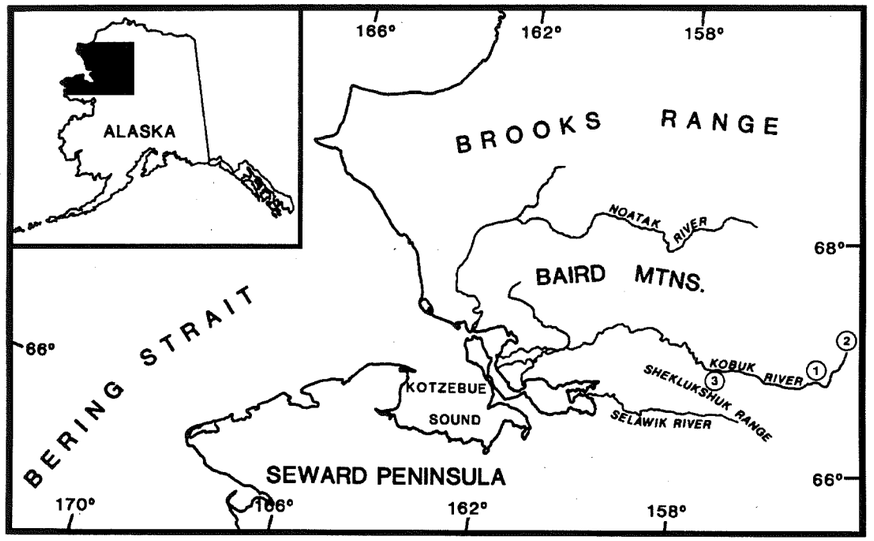

Figure 3.10. Spruce, Birch and Alder Pollen Percentages for the Alaskan Cores.

The spruce, birch and alder sections of the pollen percentages diagrams for the three Alaskan sites discussed in the Lake Minakokosa study are shown with the western site (Joe Lake) on the left and the eastern site (Ruppert Lake) on the right. The pollen percentage data and the ^{14}C dates for Ruppert Lake were provided by L. B. Brubaker (personal communication, 1994) and have been published (Brubaker *et al.*, 1983). The pollen percentage data and the ^{14}C dates for Joe Lake were provided by P. M. Anderson (personal communication, 1994) and have been published (Anderson, 1988; Anderson *et al.*, 1994). The pollen percentage data and the ^{14}C dates for Lake Minakokosa have not been published and were provided by P. M. Anderson (personal communication, 1994).

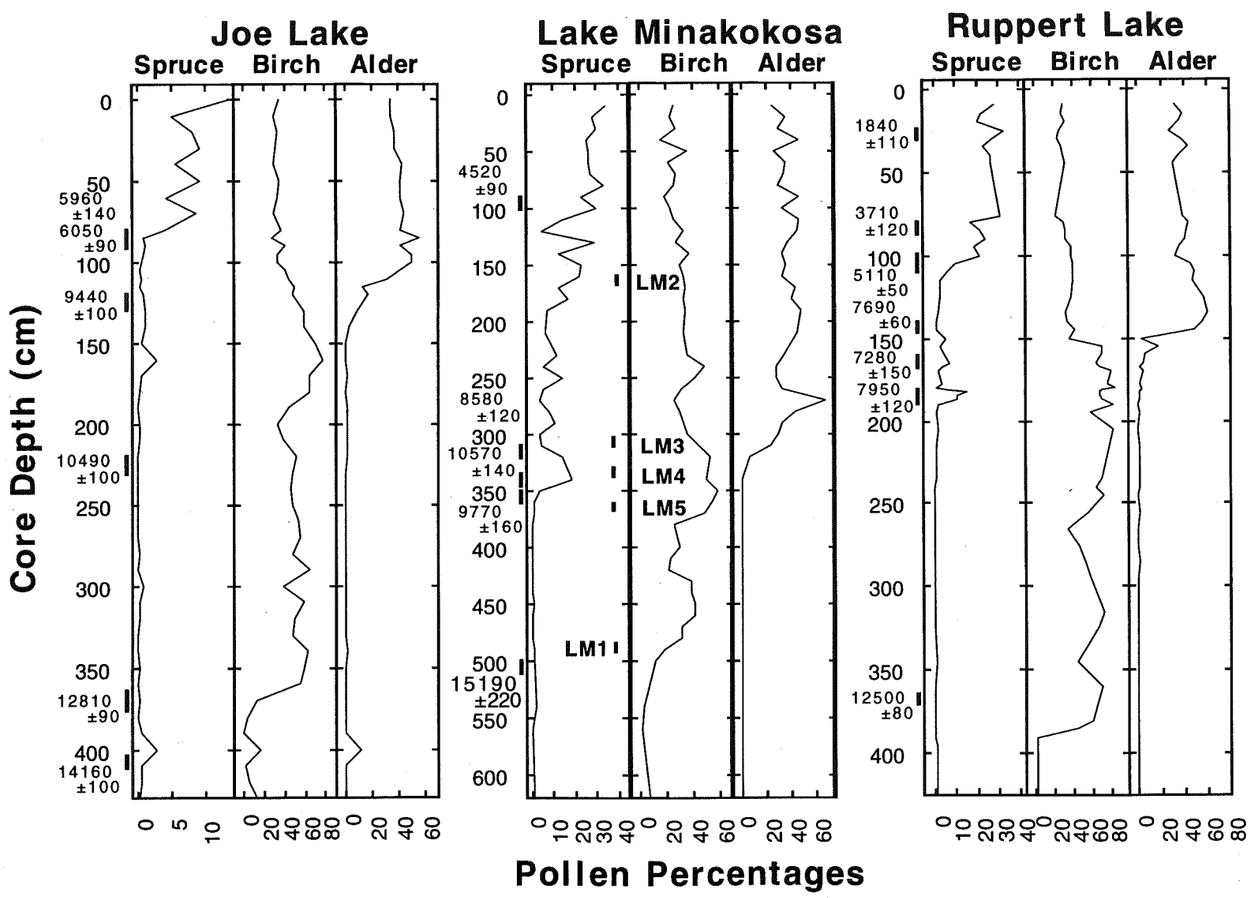

Table 3.6. % Carbon Values and Other Data for Lake Minakokosa Study Samples.

Data obtained during the processing of the pollen fraction and β-prep subsamples from the five samples from the Lake Minakokosa sediment core are shown. The CO_2 obtained from the prepared subsamples was, in most cases, split into two subsamples, with one subsample being used for AMS ^{14}C measurements and the other for $\delta^{13}C$ measurements. The measured $\delta^{13}C$ values for the CO_2 subsamples were used in the calculation of ^{14}C ages for the samples following equation 2.32. The uncertainty in the $\delta^{13}C$ measurements was ±~0.2 per mil. For the LM3, LM4, and LM5 core samples, the amount of CO_2 obtained from the 30<<88 μm pollen fractions were too small to allow both $\delta^{13}C$ and AMS ^{14}C measurements; in these cases the entire CO_2 sample was used for AMS ^{14}C measurement. In the calculation of ^{14}C ages, the $\delta^{13}C$ values for these samples were assumed to be equal to the $\delta^{13}C$ values obtained for the 10<<30 μm pollen fractions from the same core samples.

Core Sample (depth in cm)	Prepared Fraction	Sample Designation	Initial dry weight (mg)	Carbon Yield (mg C as CO_2)	Carbon Yield (%of dry wt.)	Carbon for $\delta^{13}C$ (mg)	$\delta^{13}C$ (per mil wrt PDB)	Carbon for ^{14}C (mg)
LM2	β-prep	TABRALM2	152.67	2.66	1.7	0.78	-27.08	1.88
160.5-165.5	30<<88 μm	TAB8GLM2	2.65	1.39	52.5	0.40	-26.46	0.99
	10<<30 μm	TAB1GLM2	3.92	1.94	49.5	0.59	-29.40	1.35
LM3	β-prep	TABRALM3	178.71	2.54	1.4	0.77	-27.55	1.77
305-310	30<<88 μm	TAB8GLM3	0.77	0.46	59.7	-	-	0.46
	10<<30 μm	TAB1GLM3	3.72	1.93	51.9	0.55	-29.87	1.38
LM4	β-prep	TABRALM4	117.56	1.78	1.5	0.57	-28.35	1.21
330-335	30<<88 μm	TAB8GLM4	1.49	0.49	32.9	-	-	0.49
	10<<30 μm	TAB1GLM4	6.08	2.14	35.2	0.54	-29.80	1.60
LM5	β-prep	TABRALM5	168.85	2.56	1.5	1.07	-28.42	1.49
360-365	30<<88 μm	TAB8GLM5	1.08	0.48	44.4	-	-	-
	10<<30 μm	TAB1GLM5	2.78	1.33	47.8	0.40	-30.81	0.93
LM1	β-prep	TABRALM1	183.43	1.74	0.9	0.59	-26.75	1.26
485-490	30<<88 μm	TAB8GLM1	1.42	0.81	57.0	0.25	-25.62	0.56
	10<<30 μm	TAB1GLM1	1.77	0.99	55.9	0.33	-25.86	0.66

Figure 3.11. Microphotographs of Lake Minakokosa 10<<30 µm Fractions.

Microphotographs of 10<<30 µm fractions obtained from the application of the pollen extraction procedure (figure 3.1) to Lake Minakokosa core samples are shown. These fractions were obtained from the (a) LM3, (b) LM4, and (c) LM5 core samples. The multitude of 10 µm diameter clear "bryozoan" globes in these 10<<30 µm fractions is evident in the microphotographs (discussed in sections 3.4.2 and 3.4.3). The microphotgraphs also show the presence of many unidentifiable clear and black fragments in these fractions. Microscopic examination of the 10<<30 µm fractions showed the presence of considerable numbers of birch and alder pollen in the fractions.

(a)

(b)

(c)



Figure 3.11. (Continued) Microphotographs of Lake Minakokosa 10<<30 μm Fractions.

Higher magnification microphotographs of 10<<30 μm fractions obtained from the application of the pollen extraction procedure (figure 3.1) to Lake Minakokosa core samples are shown. These fractions were obtained from the (a) LM2 and (b) LM5 core samples. The 10 μm diameter clear "bryozoan" globes, the unidentifiable clear and black fragments, and various pollen grains are evident in the microphotographs.

(a)

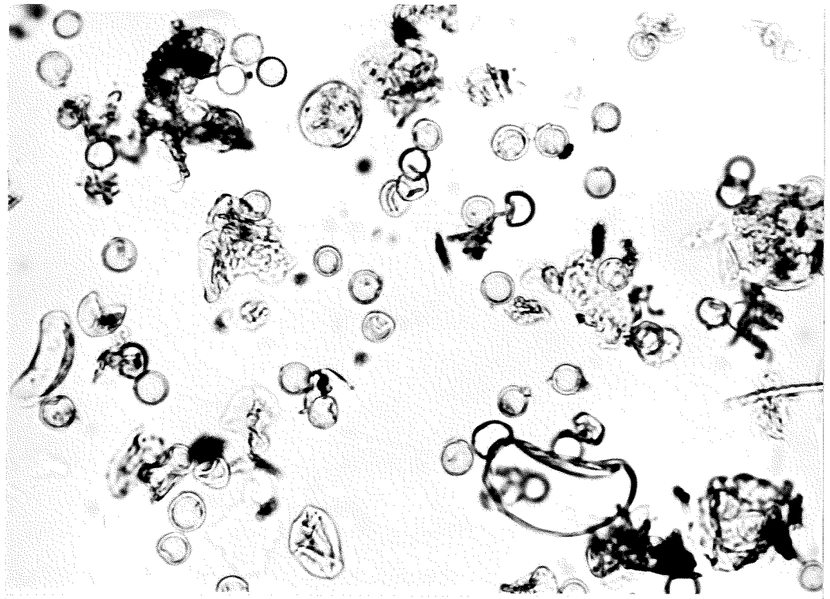

(b)

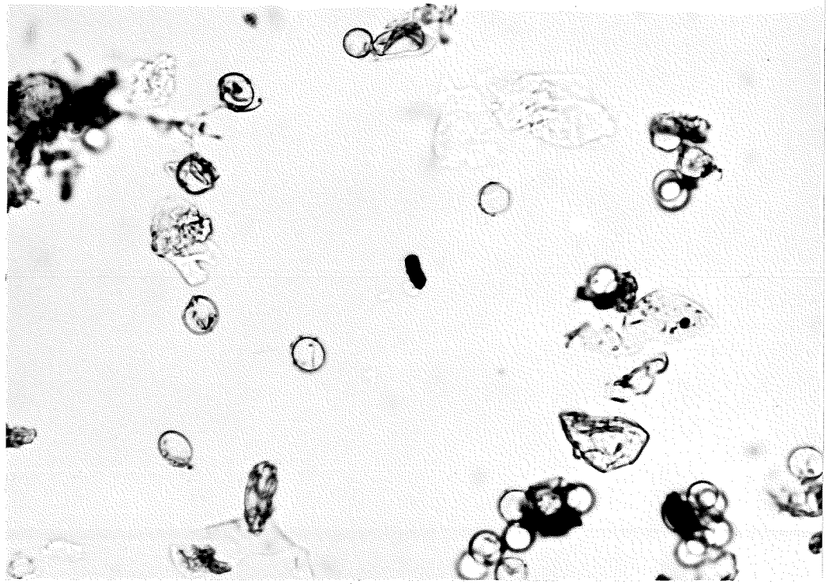

Figure 3.12. Microphotographs of LM1 10<<30 μm and 30<<88 μm Fractions.

Microphotographs of the 10<<30 μm and 30<<88 μm fractions obtained from the application of the pollen extraction procedure (figure 3.1) to the Lake Minakokosa core sample LM1 are shown. The microphotograph of the 30<<88 μm fraction (a) was taken at a relatively low magnification (~40X) so that the field of view would show a reasonable representation of the types of materials in the fraction. The dominance of the unidentifiable clear and black fragments in these fractions and the lack of intact pollen or fragments thereof is evident in the microphotograph. The microphotograph of the 10<<30 μm fraction (b) was taken at a relatively high magnification (~500X) and shows the large number of unidentifiable clear and black fragments in these fractions, the presence of numerous 10 μm diameter clear "bryozoan" globes, and the paucity of intact pollen, or fragments thereof.

(a)



(b))

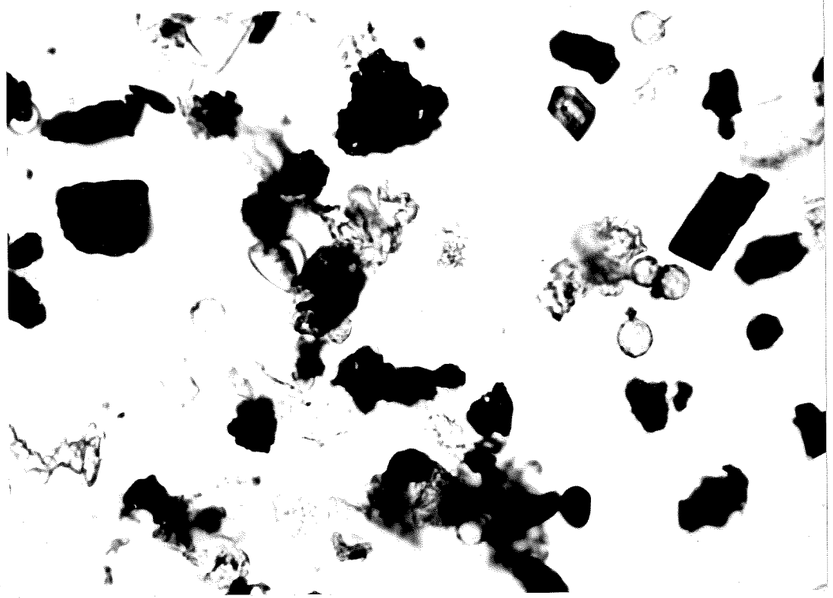

Figure 3.13. Microphotographs of Lake Minakokosa 30<<88 μm Fractions.

Microphotographs of 30<<88 μm fractions obtained from the application of the pollen extraction procedure (figure 3.1) to Lake Minakokosa core samples are shown. These fractions were obtained from the (a) LM2 and (b) LM4 core samples. The microphotgraphs show that the fractions are composed essentially entirely of identifiable spruce pollen, or fragments thereof, and demonstrate the effectiveness of the pollen extraction procedure in rejecting non-pollen materials while retaining the spruce pollen. As discussed in sections 3.4.2 and 3.4.3, the 30<<88 μm fractions from the LM3 and LM5 core samples were too small to allow microphotography, $\delta^{13}C$ measurement, and AMS ^{14}C measurement. The entire LM3 and LM5 30<<88 μm fractions were used for AMS ^{14}C measurement.

(a)



(b)

Table 3.7. AMS ^{14}C Dates Obtained for Lake Minakokosa Study Sample Fractions.

The AMS ^{14}C dates obtained in this study for the pollen fractions and β-prep subsamples from five Lake Minakokosa core samples are shown. The TOC ^{14}C dates previously obtained for other Lake Minakokosa core samples are also shown.

		AMS ^{14}C Dates Obtained in This Study			TOC ^{14}C Dates Obtained Previously	
Core Sample	Core Depth (cm)	Prepared Fraction	Sample Designation	^{14}C Date (BP)	Core Depth (cm)	^{14}C Date (BP)
					90-100	4520±90
LM2	160.5-165.5	β-prep	TABRALM2	6730±70		
		30<<88 μm	TAB8GLM2	5390±50		
		10<<30 μm	TAB1GLM2	8740±60		
LM3	305-310	β-prep	TABRALM3	9350±80		
		30<<88 μm	TAB8GLM3	8480±80		
		10<<30 μm	TAB1GLM3	11050±70		
					310-320	8580±120
LM4	330-335	β-prep	TABRALM4	9960±170		
		30<<88 μm	TAB8GLM4	9300±80		
		10<<30 μm	TAB1GLM4	12490±80		
					335-345	10570±140
					350-360	9770±160
LM5	360-365	β-prep	TABRALM5	11150±90		
		30<<88 μm	TAB8GLM5	-		
		10<<30 μm	TAB1GLM5	15100±390		
LM1	485-490	β-prep	TABRALM1	15660±170		
		30<<88 μm	TAB8GLM1	21810±180		
		10<<30 μm	TAB1GLM1	21280±180		
					500-510	15190±220

Figure 3.14. ^{14}C Dates Obtained for the Lake Minakokosa Study Samples.

The AMS ^{14}C dates obtained for the pollen fractions and β-prep samples from the Lake Minakokosa core samples are shown. The dates obtained for the 30<<88 μm pollen fractions are denoted by open circles connected by a thick solid line. The dates obtained for the 10<<30 μm pollen fractions are denoted by open squares connected by a thick solid line. The dates obtained for the β-prep samples are denoted by open diamonds connected by a thick solid line. The dates obtained previously (Anderson, unpublished data, 1994) for total-organic-carbon samples by β-counting ^{14}C dating are denoted by filled diamonds connected by the thin solid line. The lines connecting the ^{14}C dates from a particular set of samples are shown merely to aid in the identification of the ^{14}C dates in each set; the drawn lines are not intended to indicate the (possible) variation of sediment age with depth between the measured ^{14}C dates. In almost all cases the 1σ uncertainties in the ^{14}C dates are smaller than the datum symbols; in the one case where the uncertainty is larger, the 1σ uncertainty is indicated by horizontal error bars.

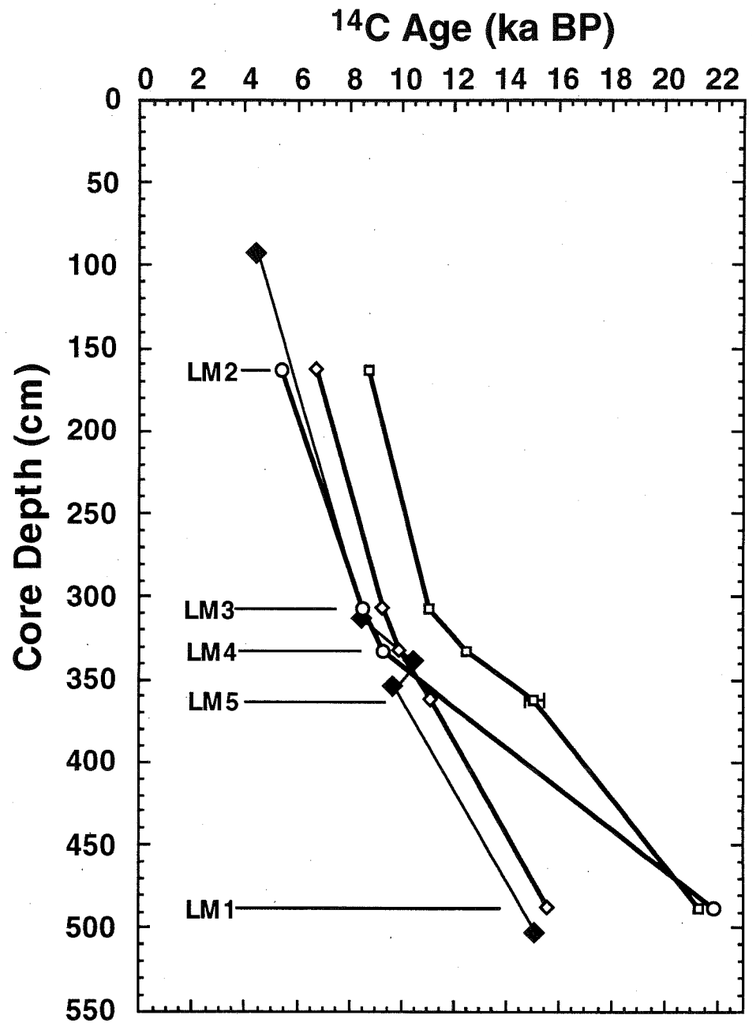

Figure 3.15. Microphotographs of Lake Minakokosa β-prep Samples.

Microphotographs of β-prep samples obtained from the application of the one-step β-prep procedure (figure 3.1) to Lake Minakokosa core samples are shown. These fractions were obtained from the (a) LM2, (b) LM4, and (c) LM1 core samples. The microphotgraphs show the generally amorphous and uncharacterizable nature of the β-prep samples that are produced by the application of the β-prep procedure to the low-organic-content lake sediments from the Lake Minakokosa core.

(a)

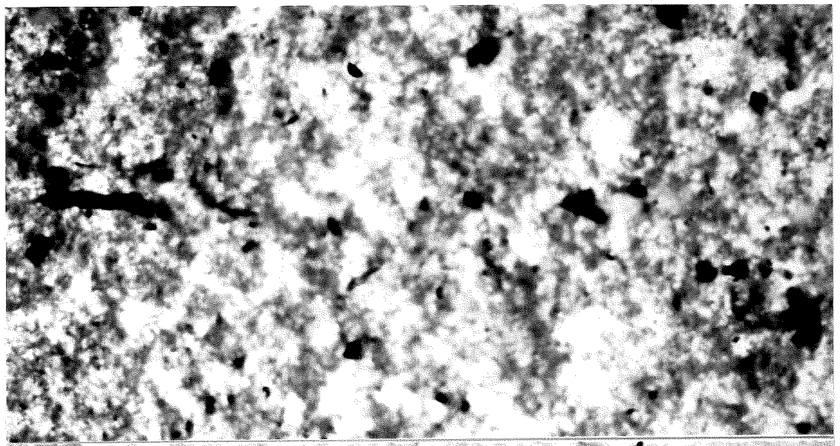

(b)

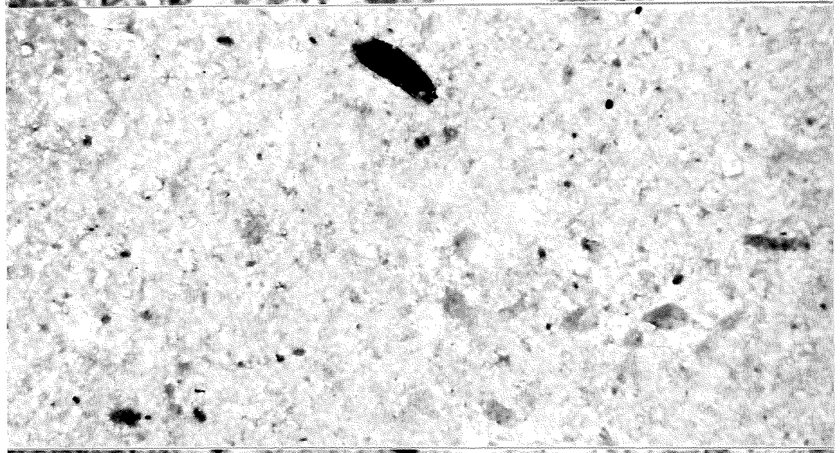

(c)

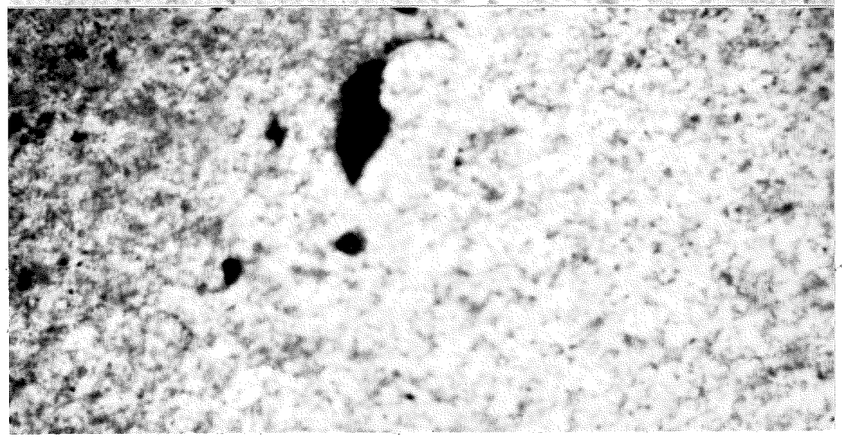

Chapter 4: Conclusions.

The first part of the research undertaken for this dissertation centered on the improvement of the UW AMS ^{14}C measurement system to allow the measurement of the pollen fractions that were isolated from lake sediment and peat samples.

The equipment and procedures used to produce ion source targets for ^{14}C measurement in the UW AMS system were modified extensively (with many components being replaced) to allow samples containing ~1 mg (or less) of carbon to be processed and measured. These modifications reduced the diameter of the ion source targets to 0.7 mm from the ~1.5 mm diameter targets that had been produced with the previous equipment. (This reduction in target diameter was possible because of modifications to the ion source which reduced the diameter of the Cs^+ ion sputtering spot and improved the reproducibility of the position of that spot on ion source targets.) The ion source target Ta-encapsulation equipment and procedures developed in this research now allow the routine preparation of consistent and reliable targets which contain ~300 μg of carbon and produce 15–25 μA of $^{12}C^-$ current for ~1 hr under our normal ion source operating conditions and have produced ~80 μA $^{12}C^-$ when tested under high-output operating conditions. (These targets produced ~250 μA of $^{12}C^-$ current when measured in the high intensity ion source at CAMS, Lawrence Livermore National Laboratory.)

The critical components of the UW AMS ^{14}C measurement system were studied in detail, and many were either modified or replaced, in order to improve the precision and accuracy of our ^{14}C measurements. The three sets of modifications made to the AMS system which appear to have been the most significant in this regard are: (1) modifications to the ion source and several associated power supplies which improved the vacuum in the ion source, the stability of the voltages on several focussing and accelerating elements of the source, and the consistency of the internal alignment of the source elements resulted in increased C^- current output and improved long-term reliability, (2) the removal of a LE beamline aperture and the entrance gridded-lens of the accelerator, coupled with significant adjustments of the focussing and steering elements of the LE ion beam transport system, increased the transmission of C^- ions from the ion source through the accelerator by 50% and reduced the sensitivity of the measurement system to differences between ion source targets, and (3) realignment of the object slits of the analysing magent, adjustments of the variable slits and focussing/steering elements of the HE ion beam transport system, and the introduction of a "wide acceptance" ΔE-E $^{14}C^{4+}$ detector resulted in a 32 kV wide transmission plateau for $^{14}C^{4+}$ ions at the detector, and significantly improved the transmission of C^{4+} ion beams through the HE beamline section while reducing the sensitivity of the measurement system to small drifts in any of the HE beamline

components.

These modifications resulted in significant improvements in the accuracy and precision uncertainties of ^{14}C measurements made using the UW AMS system. Hundreds of measurements of standards, secondary standards, and samples show that: (1) the non-Poisson contribution to the observed scatter of unnormalized $^{14}C/^{13}C$ ratios with ~0.6% counting statistics uncertainties is ≤0.3%, (2) there is no evidence of a significant (i.e., a non-zero) non-Poisson contribution to the observed scatter of normalized $^{14}C/^{13}C$ ratios, (3) the normalized $^{14}C/^{13}C$ ratios are accurate within the uncertainties of the measurements, and (4) any systematic inaccuracies in the normalized $^{14}C/^{13}C$ ratios are ≤~0.3%. On the basis of these results, the UW AMS ^{14}C system is capable of measuring ^{14}C concentrations in samples with precision and accuracy that rival (or exceed) the capabilities of presently operating dedicated AMS ^{14}C facilities.

The improved measurement accuracy and precision that resulted from the modifications to the UW AMS ^{14}C system allowed the ^{14}C ages of the extracted pollen fractions to be determined to the levels of accuracy and precision required for the Mazama Ash study and the Lake Minakokosa study during routine measurements (i.e., with total accuracy and precision uncertainties of 0.5-0.8%, which is equivalent to ±40-60 years).

The second part of the research undertaken for this dissertation consisted of the development, validation, and application of techniques and procedures to isolate and AMS ^{14}C date essentially pure pollen fractions from lake sediment and peat samples. The pollen extraction procedure that has been developed involves several steps that are routinely used in preparing samples for palynological analysis and three steps that are not. Two of the non-routine steps, sieving to select particular size fractions and treatment with weak NaOCl, were part of the original procedure used in the extraction of pollen from lake sediments for AMS ^{14}C dating (Brown *et al.*, 1989). The third of these steps, a two-stage treatment with H_2SO_4, was developed during the course of the Mazama Ash study to remove cellulosic materials from the pollen fractions. The effectiveness of this H_2SO_4 treatment in removing cellulose-based materials, and its apparent lack of significant effect on pollen grains, suggest that the treatment would be a significant improvement on the traditional acetolysis treatment used in routine palynological sample preparation procedures. The application of the pollen extraction procedure to various sedimentary materials over the course of this research showed that the procedure is capable of extracting datable pollen fractions from sediments ranging from high-organic-content gyttia or peat to very low-organic-content silty and/or clayey lake sediments.

Microscopic examination of the pollen fractions extracted from relatively high-organic-content

Pacific Northwest lake sediment and peat samples showed that the pollen extraction procedure was effective in producing essentially pure 44< <88 μm pollen fractions, which consisted almost entirely of coniferous pollen types. Examination of the 20< <44 μm pollen fractions extracted from the same lake sediment and peat samples showed the presence of small numbers of unidentifiable nonpollen fragments among the pine, alder and sedge pollen which were the predominant components of typical fractions. In the case of a low-organic-content lake sediment core from Alaska, all but one of the extracted 30< <88 μm pollen fractions were composed of essentially pure spruce pollen, or fragments thereof. (Based on previous pollen analyses on samples from the core, there was no expectation that spruce pollen would be found in that one nonpollen sample.) The extracted 10< <30 μm pollen fractions from the Alaskan core samples contained significant amounts of nonpollen materials, most of which appeared to be 10 μm diameter clear globes, and the ^{14}C dates obtained from these fractions were much older than expected. The presence of the nonpollen materials in the 10< <30 μm pollen fractions from the low-organic-content Alaskan core samples implies that some modifications of the pollen extraction procedure may be required to allow the routine extraction of essentially pure, small-sized pollen fractions from such lake sediment samples.

The accuracy and reliability of AMS ^{14}C dates obtained from extracted pollen fractions were studied through the extraction and ^{14}C dating of pollen fractions from sedimentary materials associated with Mazama Ash layer in nine lake sediment or peat cores from Pacific Northwest deposits. The internal consistency of the AMS ^{14}C dates obtained for the pollen fractions, and the inconsistencies between the pollen fraction and β-prep sample dates, showed that ^{14}C dates obtained from pollen fractions are more reliable than dates obtained from samples prepared following the traditional TOC/β-counting ^{14}C dating method.

Comparison of the ^{14}C dates obtained for pollen fractions extracted from the lake sediment and peat samples from the nine cores with ^{14}C dates that have been obtained for materials associated with the Mazama Ash layer in previous studies showed that the dates obtained for six of the cores were consistent with the ~6600 BP to ~7100 BP range of previous dates. For two of the cores whose pollen fraction ^{14}C dates fell outside this range, the ^{14}C dates indicate that the ash layers in these cores were not from the climactic Mazama eruption but rather were produced in eruptive events that occurred at other volcanoes on different dates. For the third of these cores, the inconsistencies were attributed to variations in environmental/depositional conditions at the coring site at some time after the deposition of the Mazama Ash layer, and possible disturbance of the sedimentary stratigraphy.

Detailed comparisons of the precise AMS ^{14}C dates obtained for the pollen fractions and β-

prep samples from the six "consistent" cores with the 6840±50 BP "consensus" ^{14}C age of the Mount Mazama eruption allowed the following conclusions to be drawn: (1) The Mazama Ash layer ^{14}C ages derived for the samples from the lake sediment cores showed that the pollen fraction ^{14}C dates obtained for the lake sediment samples were accurate and reliable within the ±50–80 year uncertainties in the ^{14}C dates. (2) The ^{14}C dates obtained on pollen fractions and β-prep samples from one lake sediment core showed that the AMS ^{14}C dating of pollen fractions eliminated the "hard water" effect as a cause of ^{14}C dating errors. (3) The larger-than-expected differences between pollen fraction ^{14}C dates obtained for lake sediment core samples from above and below the ash layer showed that depositional and/or post-depositional processes, such as bioturbation, had introduced significant biases into the ^{14}C ages of the pollen (and other materials) associated with the ash layer in the lake sediment deposits. (4) The ~180 years younger-than-expected Mazama Ash layer ^{14}C ages derived from ^{14}C pollen fraction dates obtained for peat core samples showed that depositional and/or post-depositional processes within the upper layers of the peats (i.e., "deep" root growth and/or vertical displacement of pollen by water movement) had a significant effect on the ^{14}C ages of pollen (and other materials) associated with the ash layer in the peat deposits. (5) The ^{14}C dates obtained for the pollen fraction and a macrofossil from one of the lake sediment samples showed that significant differences can exist between the ^{14}C ages of macrofossils and pollen within a sediment sample, and hence, that ^{14}C dates obtained from macrofossils in lake sediment samples do not necessarily reflect the ^{14}C age of pollen in the same sediment sample.

One implication of these results is that while ^{14}C dates obtained for extracted pollen fractions accurately reflect the ^{14}C age of pollen in lake sediment and peat samples, the effects of depositional and post-depositional processes in both lake sediment and peat deposits can cause significant differences between the average ^{14}C age of the pollen in a lake sediment or peat sample that is associated with a particular chronostratigraphic marker in the deposit and the ^{14}C age of that chronostratigraphic marker as determined in independent measurements of other types of materials in different types of deposits, such as burnt twigs in proximal ash flows. Hence, in order to determine the ^{14}C ages of chronostratigraphic markers, such as the Mazama Ash layer, to better than about ±150 year accuracies from pollen fraction ^{14}C dates (or ^{14}C dates on any other components of the lake sediments or peats), appropriate corrections must be made for the redistribution effects of depositional and post-depositional processes on the pollen (or the other components) within the lake sediment or peat deposits.

In the final section of the research undertaken for this dissertation, the pollen extraction procedure was applied to samples from a low-organic-content Alaskan lake sediment core. The

results obtained in this study demonstrated that essentially pure spruce pollen fractions could be isolated from the low-organic-content sediments, and suggested that, with minor modifications to the method, relatively pure fractions of smaller-sized pollen could also be obtained.

The ^{14}C dates obtained for the 30< <88 μm spruce pollen fractions, combined with two TOC/β-counting ^{14}C dates from a previous study, allowed the ^{14}C ages of the first establishment of white spruce, alder and black spruce in the Lake Minakokosa area to be determined as 9.4±0.2 ka BP, 8.5±0.2 ka BP, and 5.4±0.2 ka BP, respectively (within assumed correlations between particular rises in pollen percentages and the arrival of particular spruce species in the Lake Minakokosa area). While significant uncertainties in the ^{14}C ages of the first establishment of these species in adjacent areas from two previous studies prevented firm conclusions being drawn concerning the timing or direction of migrations through the Lake Minakokosa area, the ^{14}C ages for the first establishment of these species obtained in this study and in the previous studies suggest that white spruce arrived in all three areas during the period between ~8 ka BP and 9.5 ka BP, that alder migrated from the lower Kobuk River drainage to the south-central Brooks Range (from the west to the east) between ~9.0 ka BP and 7-8 ka BP, and that black spruce arrived in these three areas in the period between ~5 ka BP and ~6 ka BP.

During the course of the Lake Minakokosa study, one of the advantages of the pollen extraction and AMS ^{14}C dating method was instrumental in allowing the interpretation of the unexpectedly old ^{14}C dates obtained for the 10< <30 μm pollen fractions (in most cases, the ^{14}C dates obtained for the 10< <30 μm pollen fractions were ~3000 years older than the dates obtained for the 30< <88 μm pollen fractions from the same core samples). Microscopic examination showed the presence of large amounts of nonpollen materials in the 10< <30 μm pollen fractions; the predominant component of the fractions was not pollen but, rather, was 10 μm diameter clear globes. The ability to microscopically examine the ^{14}C dated samples and determine that significant amounts of nonpollen contaminants were present in the 10< <30 μm pollen fractions, but not in the 30< <88 μm pollen fractions, provided clear evidence that the ^{14}C dates obtained for the 10< <30 μm pollen fractions were erroneous.

The results obtained during the research undertaken for this dissertation show that the extraction and AMS ^{14}C dating of pollen fractions produces ^{14}C dates for lake sediment and peat samples that are significantly more accurate and reliable than ^{14}C dates obtained using the traditional TOC/β-counting ^{14}C dating method. The pollen extraction procedure developed in this research is relatively simple, is very similar to the sample preparation methods used routinely in palynological studies, and is intended to be used routinely by palynologists (and by other paleoclimatologists) in preparing pollen samples for ^{14}C AMS dating. It is hoped that the general

utilization of these pollen extraction and AMS ^{14}C dating methods in palynological (and other paleoclimatological) studies will significantly improve the accuracy and reliability of ^{14}C dates that are routinely obtained for lake sediment and peat samples, and hence, will improve the accuracy and reliability of the chronologies that allow meaningful intercomparison of paleoclimate records obtained from different sites. Such improvements in the chronologies obtained for paleoclimatic records derived from lake sediment and peat deposits should allow the detailed study of environmental/climatic variations that are difficult, if not impossible, to study at present because of ongoing problems caused by inconsistencies and uncertainties in the presently available chronologies.

List of References

Adam, D.P. (1967) Late-Pleistocene and recent palynology in the central Sierra Nevada, California. *In* "Quaternary Paleoecology." (E.J. Cushing and H.E. Wright, Jr., Eds.), 275-301. Yale University Press, New Haven.

Ager, T.A. and Brubaker, L.B. (1985) Quaternary palynology and vegetational history of Alaska. *In* "Pollen Records of Late-Quaternary North American Sediments." (V.M. Bryant, Jr. and R.G. Holloway, Eds.), 353-384. American Association of Stratigraphic Palynologists Foundation.

Allen, G.B. and Hebda, R.J. (1993) Forest history of South Vancouver Island since deglaciation. *In* "Program with abstracts and field guide: CANQUA93." Canadian Quaternary Association Annual Meeting, April 18-21, 1993, Victoria, B.C. Canada.

Anderson, P.M. (1985) Late Quaternary vegetational change in the Kotzebue Sound area, northwestern Alaska. *Quaternary Research* **24**, 307-321.

Anderson, P.M. (1988) Late Quaternary pollen records from the Kobuk and Noatak River drainages, northwestern Alaska. *Quaternary Research* **29**, 263-276.

Anderson, P.M., Reanier, R.E., and Brubaker, L.B. (1988) Late Quaternary vegetational history of the Black River region in northeastern Alaska. *Canadian Journal of Earth Sciences* **25**, 84-94.

Anderson, P.M. and Brubaker, L.B. (1994) Vegetation history of northcentral Alaska: a mapped summary of Lake-quaternary pollen data. *Quaternary Science Reviews*, in press.

Anderson, P.M., Bartlein, P.J., and Brubaker, L.B. (1994) An early Wisconsinan to present history of tundra vegetation in northwest Alaska. *Quaternary Research*, in press.

Anderson, R.S. (1987) "Late-Quaternary environments of the Sierra Nevada, California." Ph.D. dissertation, Department of Geosciences, University of Arizona, Arizona.

Anderson, R.S. (1990) Holocene forest development and paleoclimates within the central Sierra Nevada, California. *Journal of ecology* **78**, 470-489.

Anderson, R.Y., Nuhfer, E.B., and Dean, W.E. (1984) Sinking of volcanic ash in uncompacted sediment in Williams Lake, Washington. *Science* **225**, 505-508.

Andree, M., Oeschger, H., Siegenthaler, U., Riesen. T., Moell, M., Ammann, B., and Tobolski, K. (1986) ^{14}C dating of plant macrofossils in lake sediment. *Radiocarbon* **28**, 411-416.

Arnold, J.R. and Libby, W.F. (1951) Radiocarbon dates. *Science* **113**, 111-120.

Bacon, C.R. (1983) Eruptive history of Mount Mazama and Crater Lake caldera, Cascade

Range, U.S.A. *Journal of Volcanology and Geothermal Research.* **18**, 57-115.

Balsley, D.R., Farwell, G.W., Grootes, P.M., and Schmidt, F.H. (1987) Ion source sample preparation techniques for carbon-14 AMS measurements. *Nuclear Instruments and Methods in Physics Research* **B29**, 37-40.

Barnosky, C.W. (1981) A record of Late Quaternary vegetation from Davis Lake, southern Puget Lowland, Washington. *Quaternary Research.* **16**, 221-239.

Barnosky, C.W. (1985a) Late Quaternary vegetation near Battle Ground Lake, southern Puget Trough, Washington. *Geological Society of America Bulletin.* **96**, 263-271.

Barnosky, C.W. (1985b) Late Quaternary vegetation in the Southwestern Columbia Basin, Washington. *Quaternary Research.* **23**, 109-122.

Barnosky, C.W., Anderson, P.M., and Bartlein, P.J. (1987) The northwestern U.S. during deglaciation; vegetational history and paleoclimatic implications. *In* "North America and adjacent oceans during the last deglaciation, The Geology of North America, vol. K 3." (W.F. Ruddiman and H.E. Wright, Jr., Eds.), 289-321. Geological Society of America, Boulder, Colorado.

Bates, R.L. and Jackson, J.A., Eds. (1984) "Dictionary of Geological Terms." Anchor Press/Doubleday, New York.

Beget, J.E. (1982a) Postglacial volcanic deposits at Glacier Peak, Washington, and potential hazards from future eruptions. *United States Geological Survey Open-file Report* **82-830**, p.77.

Beget, J.E. (1982b) Recent volcanic activity at Glacier Peak. *Science* **215**, 1389–1390.

Bennett, C.L., Beukens, R.P., Clover, M.R., Gove, H.E., Lievert, R.B., Litherland, A.E., Purser, K.H., and Sondheim, W.E. (1977) Radiocarbon dating using electrostatic accelerators: negative ions provide the key. *Science* **198**, 508-510.

Berger, W.H. and Heath, G.R. (1968) Vertical mixing in pelagic sediments. *Journal of Marine Research* **26**, 134-143.

Bevington, P.R. (1969) "Data reduction and error analysis for the physical sciences." McGraw-Hill, New York.

Birman, J.H. (1964) Glacial geology across the crest of the Sierra Nevada, California. *Geological society of America Special Paper* **75**, p.79.

Broecker, W.S., Kulp, J.L., and Tucek, C.S. (1956) Lamont natural radiocarbon measurements III. *Science* **124**, 154-165.

University, Burnaby, British Columbia, Canada.

Farwell, G.W., Schmidt, F.H., and Grootes, P.M. (1981) Accelerator mass spectrometry at the University of Washington. *In* "Proceedings of the Symposium on Accelerator Mass Spectrometry" (W. Kutschera, Ed.) held May 11-13, 1981, 100-119. Argonne National Laboratory, Illinois. ANL/PHY-81-1.

Farwell, G.W., Grootes, P.M., Leach, D.D., and Schmidt, F.H. (1984) The accelerator mass spectrometry facility at the University of Washington: current status and an application to the ^{14}C profile of a tree ring. *Nuclear Instruments and Methods in Physics Research* **B5**, 144-149.

Faure, G. (1986) "Principles of Isotope Geology, 2nd Ed." John Wiley and Sons, New York.

Fowler, A.J., Gillespie, R., and Hedges, R.E.M. (1986) Radiocarbon dating of sediments. *Radiocarbon* **28**, 441-450.

Fryxell, R. (1965) Mazama and Glacier Peak volcanic ash layers: relative ages. *Science* **147**, 1288-1290.

Gillespie, R. and Hedges, R.E.M. (1984) Laboratory contamination in radiocarbon accelerator mass spectrometry. *Nuclear Instruments and Methods in Physics Research* **B5**, 294-296.

Gove, H.E., Litherland, A.E., and Elmore, D., Eds. (1987) Proceedings of the Fourth International Symposium on Accelerator Mass Spectrometry. *Nuclear Instruments and Methods in Physics Research* **B29**, p. 455.

Green, D., Singh, G., Polach, H., Moss, D., Banks, J., and Geissler, E.A. (1988) A fine-resolution palaeoecology and palaeoclimatology from south-eastern Australia. *Journal of Ecology* **76**, 790-806.

Grootes, P.M., Stuiver, M., Farwell, G.W., Leach, D.D., and Schmidt, F.H. (1986) Radiocarbon dating with the University of Washington accelerator mass spectrometry system. *Radiocarbon* **28**, 237-245.

Grootes, P.M., Farwell, G.W., Schmidt, F.H., Leach, D.D., and Stuiver, M. (1989) Importance of biospheric CO_2 in a subcanopy atmosphere deduced from ^{14}C AMS measurements. *Radiocarbon* **31**, 475-480.

Guinasso, Jr., N.L. and Schink, D.R. (1975) Quantitative estimates of biological mixing rates in abyssal sediments. *Journal of Geophysical Research* **80**, 3032-3043.

Hansen, H.P. (1947) Postglacial forest succession, climate, and chronology in the Pacific Northwest. *Transactions of the American Philosophical Society* **37**, 1-130.

Hansen, J.E. and Takahashi, T., Eds. (1984) "Climate Processes and Climate Sensitivity." *Geophysical Monograph* 29, American Geophysical Union, Washington, D.C.

Hebda, R.J. (1993) Climate history, Heal Lake, Vancouver Island, British Columbia. *In* "Program with abstracts and field guide: CANQUA93." Canadian Quaternary Association Annual Meeting, April 18-21, 1993, Victoria, B.C. Canada.

Hedges, R.E.M. (1992) Sample treatment strategies in radiocarbon dating. *In* "Radiocarbon After Four Decades." (R.E. Taylor, A. Long, and R.S. Kra, Eds.), 165–183. Springer-Verlag, New York.

Heslop-Harrison, J. (1968) Pollen wall development. *Science* **161**, 230-237.

Heusser, C.J. (1977) Quaternary Palynology of the Pacific Slope of Washington. *Quaternary Research* **8**, 282–306.

Hu, F.S., Brubaker, L.B., and Anderson, P.M. (1993) A 12000 year record of vegetation change and soil development from Wien Lake, central Alaska. *Canadian Journal of Botany* **71**, 1133-1142.

Hyde, J.H. and Crandell, D.R. (1978) Postglacial volcanic deposits at Mount Baker, Washington, and potential hazards from future eruptions. *United States Geological Survey Professional Paper* **1022-C**, p.17.

Jull, A.J.T., Wilson, A.E., Burr, G.S., Toolin, L.J., and Donahue, D.J. (1992) Measurements of cosmogenic ^{14}C produced by spallation in high-altitude rocks. *Radiocarbon* **34**, 737-744.

Kittleman, L.R. (1973) Mineralogy, correlation, and grain-size distributions of Mazama tephra and other postglacial pyroclastic layers, Pacific Northwest. *Geological Society of America Bulletin.* **84**, 2957-2980.

Krajina, V.J. (1978) Biogeoclimatic zones of British Columbia. *British Columbia Ecological Reserves Committee*, Department of Lands, Forest, and Water Resources, British Columbia, Canada.

Leopold, E.B., Nickmann, R., Hedges, J.I., and Ertel, J.R. (1982) Pollen and lignin records of Late Quaternary vegetation, Lake Washington. *Science.* **218**, 1305-1307.

Libby, W.F. (1952) "Radiocarbon Dating." University of Chicago Press, Chicago.

Lowe, J.J. and Walker, M.J.C. (1980) Problems associated with radiocarbon dating the close of the Lateglacial Period in the Rannoch Moor area, Scotland. *In* "Studies in the Lateglacial of North-west Europe." (J.J. Lowe, J.M. Gray, and J.E. Robinson, Eds.), 123–138. Pergamon Press, Oxford.

Lowe, J.J., Lowe, S., Fowler, A.J., Hedges, R.E.M., and Austin, T.J.F. (1988) Comparison of accelerator and radiometric radiocarbon measurements obtained from Late Devensian Lateglacial lake sediments from Llyn Gwernan, North Wales, UK. *Boreas* **17**, 355-369.

MacDonald, G.M., Beukens, R.P., Kieser, W.E., and Vitt, D.H. (1987) Comparative radiocarbon dating of terrestrial plant macrofossils and aquatic moss from the "ice-free corridor" of western Canada. *Geology* **15**, 837-840.

MacDonald, G.M., Beukens, R.P., and Kieser, W.E. (1991) Radiocarbon dating of limnic sediments: a comparative analysis and discussion. *Ecology* **72**, 1150-1155.

Mack, R.N., Okazaki, R., and Valastro, S. (1979) Bracketing dates for two ash falls from Mount Mazama. *Nature* **279**, 228-229.

Mathewes, R.W. (1973) A palynological study of postglacial vegetation changes in the University Research Forest, southwestern British Columbia. *Canadian Journal of Botany* **51**, 2085-2103.

Mathewes, R.W. and Heusser, L.E. (1981) A 12000 year palynological record of temperature and precipitation trends in southwestern British Columbia. *Canadian Journal of Botany* **59**, 707-710.

McLachlan, J.S. (1994) "Local and regional vegetation change on the northeastern Olympic Peninsula during the Holocene." M.Sc. thesis, College of Forest Resources, University of Washington, Washington.

Mehringer, Jr., P.J., Blinman, E., and Petersen, K.L. (1977) Pollen influx and volcanic ash. *Science* **198**, 257-261.

Moore, P.D., Webb, J.A., and Collinson, M.E. (1991) "Pollen Analysis, 2nd ed." Blackwell Scientific, Oxford.

Mullineaux, D.R. (1974) Pumice and other pyroclastic deposits in Mount Rainier National Park, Washington. *United States Geological Survey Bulletin* **1326**, p.83.

Nambudiri, E.M.V., Teller, J.T., and Last, W.M. (1980) Pre-quaternary microfossils - a guide to errors in radiocarbon dating. *Geology* **8**, 123-126.

Nelson, D.E. (1991) A new method for carbon isotopic analysis of protein. *Science* **251**, 552-554.

Nelson, D.E., Korteling, R.G., and Stott, W.R. (1977) Carbon-14: Direct detection at natural concentrations. *Science* **198**, 507-508.

Olsson, I.U. (1979) A warning against radiocarbon dating of samples containing little carbon. *Boreas* **8**, 203-207.

Olsson, I.U. (1991) Accuracy and precision in sediment chronology. *Hydrobiologia* **214**, 25-34.

Patton, Jr., W.W. and Miller, T.P. (1966) Regional geologic map of the Hughes quadrangle, Alaska. *Miscellaneous Geologic Investigations* Map I-459, U.S. Geological Survey, Washington D.C.

Peng, T.-H., Broecker, W.S., and Berger, W.H. (1979) Rates of benthic mixing in deep-sea sediment as determined by radioactive tracers. *Quaternary Research* **11**, 141–149.

Porter, S.C. (1976) Pleistocene glaciation in the southern part of the North Cascade Range, Washington. *Geological Society of America Bulletin* **87**, 61-75.

Prescott, G.W. (1980) "How to know the aquatic plants, 2nd ed." Wm. C. Brown, Iowa.

Regnell, J. (1992) Preparing pollen concentrates for AMS dating - a methodological study from a hard-water lake in southern Sweden. *Boreas* **21**, 373-377.

Robbins, J.A. and Edgington, D.N. (1975) Determination of recent sedimentation rates in Lake Michigan using Pb-210 and Cs-137. *Geochimica et Cosmochimica Acta* **39**, 285-304.

Robbins, J.A., Krezoski, J.R., and Mozley, S.C. (1977) Radioactivity in sediments of the Great Lakes: post-depositional redistribution by deposit-feeding organisms. *Earth and Planetary Science Letters* **36**, 325-333.

Robbins, J.A., McCall, P.L., Fisher, J.B., and Krezoski, J.R. (1979) Effect of deposit feeders on migration of ^{137}Cs in lake sediments. *Earth and Planetary Science Letters* **42**, 277-287.

Rozanski, K., Stichler, W., Gonfiantini, R., Scott, E.M., Beukens, R.P., Kromer, B., and Van der Plicht, J. (1992) The IAEA ^{14}C intercomparison exercise 1990. *Radiocarbon* **34**, 506-519.

Rubin, M. and Alexander, C. (1960) U.S. Geological Survey radiocarbon dates V. *Am. J. Sci. Radiocarbon Supplement* **2**, 129-185.

Ruddiman, W.F. and Wright, H.E., Jr., Eds. (1987) "North America and adjacent oceans during the last deglaciation, The Geology of North America, vol. K 3." Geological Society of America, Boulder, Colorado.

Sarna-Wojcicki, A.M., Champion, D.E., and Davis, J.O. (1983) Holocene volcanism in the conterminous United States and the role of silicic volcanic ash layers in correlation of latest-Pleistocene and Holocene deposits. *In* "Late-Quaternary Environments of the United States" (H.E. Wright, Jr., Ed.), 53-77. University of Minnesota Press, Minnesota.

Sarna-Wojcicki, A.M. and Davis, J.O. (1991) Quaternary tephrochronology. *In* "The Geology of North America Vol. K-2 Quaternary nonglacial geology: conterminous U.S." (R.B. Morrison, Ed.), 93-116. Geological Society of America, Boulder.

Schmidt, F.H. and Farwell, G.W. (1979) An effective reflection-type geometry for sputter ion sources. *Bull. Am. Phys. Soc.* **24**, 540.

Schmidt, F.H., Brown, T.A.,Farwell, G.W., and Grootes, P.M. (1990) The University of Washington AMS system: a six year technical update. *Nuclear Instruments and Methods in Physics Research* **B52**, 229-232.

Shackleton, N.J., Duplessy, J.C., Arnold, M., Maurice, P., Hall, M., and Cartlidge, J. (1988) Radiocarbon age of last glacial Pacific deep water. *Nature* **335**, 708-711.

Stuiver, M. (1983) International agreements and the use of the new oxalic acid standard. *Radiocarbon* **25**, 793-795.

Stuiver, M. and Polach, H.A. (1977) Discussion: reporting of ^{14}C data. *Radiocarbon* **19**, 355-363.

Stuiver, M., Heusser, C.J., and Yang, I.C. (1978) North American glacial history extended to 75,000 years ago. *Science* **200**, 16-21.

Stuiver, M., Burk, R.L., and Quay, P.D. (1984) ^{13}C /^{12}C ratios in tree rings and the transfer of biospheric carbon to the atmosphere. *Journal of Geophysical Research* **89**, 11731-11748.

Stuiver, M., Long, A., and Kra, R.S., Eds. (1993) Calibration 1993. *Radiocarbon* **35**, p. 244.

Stuiver, M. and Reimer, P.J. (1993) Extended ^{14}C data base and revised CALIB 3.0 ^{14}C age calibration program. *Radiocarbon* **35**, 215-230.

Stuiver, M. and Becker, B. (1993) High-precision decadal calibration of the radiocarbon time scale, AD 1950-6000 BC. *Radiocarbon* **35**, 35-66.

Sugita, S. (1990) "Palynological records of forest disturbance and development in the Mountain Meadows watershed, Mt. Rainier, Washington." Ph.D. dissertation, Department of Botany, University of Washington, Washington.

Sundquist, E.T. and Broecker, W.S., Eds. (1985) "The Carbon Cycle and Atmospheric CO_2: Natural Variations Archean to Present." *Geophysical Monograph* 32, American Geophysical Union, Washington, D.C.

Sutherland, D.G. (1980) Problems of radiocarbon dating in newly deglaciated terrain: examples from the Scottish Lateglacial. *In* "Studies in the Lateglacial of North-west Europe." (J.J. Lowe, J.M. Gray, and J.E. Robinson, Eds.), 139–149. Pergamon Press, Oxford.

Swart, P.K., Lohmann, K.C., McKenzie, J., and Savin, S., Eds. (1993) "Climate Change in continental Isotopic Records." *Geophysical Monograph* 78, American Geophysical Union, Washington, D.C.

Tabor, R.W. and Cady, W.M. (1978) Geologic map of the Olympic Peninsula, Washington. *Miscellaneous Geologic Investigations* Map I-994 (East Half), U.S. Geological Survey, Washington D.C.

Thomsen, M.S. (1990). "Accelerator mass spectrometry applied to the radio-isotopes ^{14}C and ^{32}Si." Ph.D. dissertation, Institute of Physics, University of Aarhus, Denmark.

Tornqvist, T.E., de Jong, A.F.M., Oosterbaan, W.A., and van der Borg, K. (1992) Accurate dating of organic deposits by AMS ^{14}C measurement of macrofossils. *Radiocarbon* **34**, 566-577.

Trainor, T.A. (1989) Tandem Belt Charge System. Nuclear Physics Laboratory Annual Report, Nuclear Physics Laboratory, University of Washington, 84.

Tuskada, M., Sugita, S., and Hibbert, D.M. (1981) Paleoecology in the Pacific Northwest I. Late Quaternary vegetation and climate. *Verh. Internat. Verein. Limnol.* **21**, 730–737.

van Klinken, G.J. and Hedges, R.E.M. (1992) Experiments on ^{14}C dating of contaminated bone using peptides resulting from enzymatic cleavage of collagen. *Radiocarbon* **34**, 292-295.

Vogel, J.S., Southon, J.R., Nelson, D.E., and Brown, T.A. (1984) Performance of catalytically condensed carbon for use in accelerator mass spectrometry. *Nuclear Instruments and Methods in Physics Research* **B5**, 289-293.

Vogel, J.S., Nelson, D.E., and Southon, J.R. (1986) Contamination of small carbon samples during graphite preparation by catalytic reduction, *In* "Proceedings of the Workshop on Techniques in Accelerator Mass Spectrometry" (R.E.M. Hedges and E.T. Hall, Eds.) held June 30-July 1, 1986, 8-13. Oxford Radiocarbon Accelerator Unit, Oxford.

Vogel, J.S., Southon, J.R., and Nelson, D.E. (1987a) Catalyst and binder effects in the use of filamentous graphite for AMS. *Nuclear Instruments and Methods in Physics Research* **B29**, 50-57.

Vogel, J.S., Nelson, D.E., and Southon, J.R. (1987b) ^{14}C background levels in an accelerator mass spectrometry system. *Radiocarbon* **29**, 323-333.

Wainman, N. and Mathewes, R.W. (1987) Forest history of the last 12000 years based on plant macrofossil analysis of sediment from Marion Lake, southwestern British Columbia. *Canadian Journal of Botany* **65**, 2179–2187.

Welch, E.B., Tomasek, M.D., and Spyridakis, D.E. (1985) Instability of the Mount St. Helen's ashlayer in Moses Lake. *Journal of Freshwater Ecology* **3**, 103-112.

Wetzel, R.G. (1988) Water as an environment for plant life. *In* "Handbook of Vegetation Vol 15/1: Vegetation of Inland Waters." (J.J. Symons, Ed.), 1-30. Kluwer Academic, Dordrecht.

Wood, S.H. (1977) Distribution, correlation, and radiocarbon dating of late Holocene tephra, Mono and Inyo Craters, eastern California. *Geological Society of America Bulletin* **88**, 89-95.

Wright, HE, Jr. (1967) A square-rod piston sampler for lake sediments. *Journal of Sedimentary Petrology* **37**, 975-976.

Wright, H.E., Jr., Ed. (1983) "Late-Quaternary Environments of the United States." University of Minnesota Press, Minnesota.

Yiou, F. and Raisbeck, G.M., Eds. (1990) Proceedings of the Fifth International Conference on Accelerator Mass Spectrometry. *Nuclear Instruments and Methods in Physics Research* **B52**, p. 630.

Vita

Thomas Alexander Brown

Advanced Degrees:

1980 B.Sc. (Honours Chemical-Physics), Simon Fraser University, Burnaby, B.C., Canada

1985 M.Sc. (Physics), Simon Fraser University, Burnaby, B.C., Canada
Thesis: ^{10}Be production rate variations as recorded in a mid-latitude lake sediment.
M.Sc. Supervisor: Professor D.E. Nelson
Department of Archeology

Publications:

Huntley, D.J., Berger, G.W., Divigalpitiya, W.M.R., and Brown, T.A. (1983) Thermoluminescence dating of sediments. *PACT* **9**, 607-618.

Brown, T.A., Nelson, D.E., Vogel, J.S., and Southon, J.R. (1984) ^{10}Be production rate variations over the last 20 ky b.p. as given by ^{10}Be concentration variations in lake sediments. *In* "Proceedings of the First Users Workshop: A Proposed AMS Laboratory for the Northwest Coast" (D.E. Nelson, Ed.) held September 28-29, 1984, 51-67. Simon Fraser University, Burnaby, British Columbia, Canada.

Vogel, J.S., Southon, J.R., Nelson, D.E., and Brown, T.A. (1984) Performance of catalytically condensed carbon for use in accelerator mass spectrometry. *Nuclear Instruments and Methods in Physics Research* **B5**, 289-293.

Brown, T.A., Nelson, D.E., Vogel, J.S., and Southon, J.R. (1985) The extraction of ^{10}Be from lake sediments: leashing versus total dissolution. *Chemical Geology (Isotope Geoscience Section)* **52**, 375-378.

Nelson, D.E., Vogel, J.S., Southon, J.R., and Brown, T.A. (1986) Accelerator radiocarbon dating at SFU. *Radiocarbon* **28**, 215-222.

Brown, T.A., Nelson, D.E., Southon, J.R., and Vogel, J.S. (1987) ^{10}Be production rate variations as recorded in a mid-latitude lake sediment. *Nuclear Instruments and Methods in Physics Research* **B29**, 232-237.

Brown, T.A., Nelson, D.E., Vogel, J.S., and Southon, J.R. (1988) Improved collagen extraction by modified Longin method. *Radiocarbon* **30**, 171-177.

Brown, T.A., Nelson, D.E., Mathewes, R.W., Vogel, J.S., and Southon, J.R. (1989) Radiocarbon dating of pollen by accelerator mass spectrometry. *Quaternary Research* **32**, 205-212.

Brown, T.A., Farwell, G.W., Grootes, P.M., Quay, P.D., and Schmidt, F.H. (1990) ^{14}C AMS at the University of Washington: measurements in a shared facility at the 1% level on 0.4 mg samples. *Nuclear Instruments and Methods in Physics Research* **B52**, 351-356.

Schmidt, F.H., Brown, T.A.,Farwell, G.W., and Grootes, P.M. (1990) The University of Washington AMS system: a six year technical update. *Nuclear Instruments and Methods in Physics Research* **B52**, 229-232.

Morlan, R.E., Nelson, D.E., Brown, T.A., Vogel, J.S., and Southon, J.R. (1990) Accelerator mass spectrometry dates on bones from Old Crow Basin, Northern Yukon Territory. *Canadian Journal of Archeology* **14**, 75-92.

Quay, P.D., King, S.L., Stutsman, J., Wilbur, D.O., Steele, L.P., Fung, I., Gammon, R.H., Grootes, P.M., Farwell, G.W., Schmidt, F.H., and Brown, T.A. (1990) Carbon isotopic composition of atmospheric CH_4: fossil and biomass burning source strengths. *Global Biogeochemical Cycles* 5, 25-47.

Vogel, J.S., Brown, T.A., Southon, J.R., and Nelson, D.E. (1991) Accelerator radiocarbon dates from the NOGAP archaeology project. *Canadian Archaeological Association Occasional Paper* **1**, 143-147.

Brown, T.A., Farwell, G.W., Grootes, P.M., and Schmidt, F.H. (1992) Radiocarbon AMS dating of pollen extracted from peat samples. *Radiocarbon* **34**, 550-556.

Brown, T.A., Farwell, G.W., Grootes, P.M., Schmidt, F.H., and Stuiver, M. (1993) Intra-annual variability of the radiocarbon content of corals from the Galapagos Islands. *Radiocarbon* **35**, 245-251.

Brown, T.A., Farwell, G.W., and Grootes, P.M. (1994) Current status of the ^{14}C AMS program at the University of Washington. *Nuclear Instruments and Methods in Physics Research*, in press.

2 718WWI TH 1083
9/94 31365-179